Queen Mary
University of London

Investigating Cell Senescence in Basal Cell Carcinoma

Pirzado, Muhammad Suleman

The copyright of this thesis rests with the author and no quotation from it or information derived from it may be published without the prior written consent of the author

For additional information about this publication click this link.
http://qmro.qmul.ac.uk/jspui/handle/123456789/8633

Information about this research object was correct at the time of download; we occasionally make corrections to records, please therefore check the published record when citing. For more information contact scholarlycommunications@qmul.ac.uk

Investigating Cell Senescence in Basal Cell Carcinoma

Muhammad Suleman Pirzado

2012

Thesis submitted in accordance with the regulations for

The degree of Doctorate of Philosophy (PhD)

Centre for Cutaneous Research

Blizard Institute

Barts and The London School of Medicine and Dentistry

Queen Mary University of London

Declaration of Originality of This Research

I hereby declare that the work presented in this thesis is entirely my own.

Muhammad Suleman Pirzado

2012

Abstract

The Aim of the project was to investigate cell senescence in basal cell carcinoma (BCC). Although the concept of oncogene-induced senescence (OIS) was originally confined to cultured cells, it is now well established that this mechanism has an important role in tumour biology. OIS represents a physiological response that restricts the progression of benign tumours into their malignant counterparts e.g. nevi to melanoma or adenoma to adenocarcinoma. Full malignancy is associated with the loss of important tumour suppressor genes including RETINOBLASTOMA and/or *TP53*. BCC of the skin is the most common skin tumour and is associated with mutational inactivation of the *PTCH*1 tumour suppressor gene (and less frequently oncogenic activation of SMOOTHENED). Although BCC does not appear to stem from precursor lesions - though mouse models of BCC display areas of basaloid hyperproliferation - and it is relatively stable at the genomic level, we sought to determine if these unique tumours display any characteristics of OIS. Human BCCs were positive for Senescence-associated β-galactosidase (SA-β-gal) activity (pH 6.0) and expressed known markers of senescence including DCR2, DEC1 (SHARP2) as well as the cell cycle inhibitors $p15^{INK4b}$ and $p16^{INK4a}$. Interestingly, SA-β-gal activity was observed in stromal cells surrounding the tumour islands and this may account for why BCCs are difficult to culture in vitro as senescent cells are known to express increased levels of growth factors, cytokines and ECM proteins. To determine if OIS is associated with Hedgehog signalling in BCC, I employed a novel in vitro model of BCC created through *PTCH1* suppression in human immortalised NEB1 keratinocytes. NEB1-sh*PTCH*1 cells are viable and proliferative (albeit more slowly than control NEB1-shCON cells) and do not display SA-β-gal activity but they express higher levels of several senescent markers including DCR2 and $p21^{WAF1}$. I also investigated senescence in a Mouse model of BCC in which one allele of *Ptch1* is mutated and which on x-ray irradiation results in BCC formation. The expression of known markers of senescence including DCR2, DEC1 (SHARP2) as well as the cell cycle inhibitors $p15^{INK4b}$, $p16^{INK4a}$ and p53 were all with the exception of $p21^{WAF1}$ detected in these tumours. Together these data suggest that senescence is a characteristic of BCC and may explain why these tumours rarely metastasise.

Table of Contents

INDEX OF FIGURES

INDEX OF TABLES

ABBREVIATIONS

ACTH	Adernocorticotropic Hormone
BCC	Basal Cell Carcinoma
BCNS	Basal Cell Nevous Syndrome
bHLH	Basic helix loop helix
BSA	Bovine Serum Albumin
CCPDMA	Complete Circumferential Peripheral and Deep Margin Assessment.
CAFs	Cancer Associated Fibroblasts
CCND1	Cyclin D1
CDKIs	Cyclin-dependent Kinase Inhibitors
DAB	3,3'-Diaminobenzidine
DAPI	6-Diamidino-2-Phenylindole
DCR2	Decoy Receptor
DEC1	Deferentially embryo-chondrocyte Expressed gene
DEPC	Diethylpyrocarbonate
DHH	Desert Hedgehog
DMSO	Dimethyl sulfoxide
DP	Dermal Papilla
DEJZ	Dermo-epidermal Junction Zone

ECM	Extracellular Cellular Matrix
EDTA	Ethylenediaminetetraacetic Acid
EGF	Epidermal Growth Factor
FBS	Foetal Bovine Serum
FDA	Food and Drug Administration
FDG	Fluorescein-di-β-D-galactopyranoside
FOXM1	Forkhead box protein M1
FU	Fused
HH	Hedgehog
HHIP	Hedgehog Interacting Protein
HPV	Human Papillomavirus
IFE	Inter Follicular Epidermis
IF	Immunofluorescence
IF	Intermediate Filament
IFT	Intraflagellar proteins
IHH	Indian Hedgehog
IRS	Inner Root Sheath
KGM	Keratinocyte Growth Medium
αMEM	Minimum Essential Medium Eagle Alpha Modifications

MMPs	Metalloproteinase
MSH	Melanocyte Stimulating Hormone
NBCCS	Nevoid Basal Cell Carcinoma Syndrome
NMSC	Non Melanoma Skin Cancer
OIS	Oncogene Induced Senescence
ORS	Outer Root Sheath
PBS	Phosphate Buffer Saline
PCR	Polymerase Chain Reaction
PDGF	Platelet-derived Growth Factor
PDGFRA	Alpha-type Platelet-derived Growth Factor Receptor
PDT	Photodynamic Therapy
PTCH	Patched
qPCR	Quantitative Real Time-Polymerase Chain Reaction
RB	Retinoblastoma
SFRP1	Secreted Frizzled-related Protein 1
SHH	Sonic hedgehog
SHARP2	Enhancer of split and Hairy related protein
SMO	Smoothened
Stra13	Stimulated with retinoic acid 13
SuFu	Suppressor of Fused

TAC	Transit-amplifying Cells
TGF-β	Transforming Growth Factor
TRAIL	Tumour necrosis related apoptosis-Inducing ligand
UV	Ultraviolet

PUBLICATIONS AND PRESENTATIONS

Work described in this thesis has also been presented at the following scientific conferences:

• William Harvey Day Programme (2010), Queen Mary University of London, UK, Senescence in Basal Cell Carcinoma (poster presentation).

• British Society for Investigative Dermatology, Annual Meeting (2011), Manchester, UK, (poster presentation).

• Society of Investigative Dermatology's 71st Annual Meeting (2011), Phoenix, Arizona, USA, Senescence in Human Basal Cell Carcinoma (poster presentation).

• Hedgehog 2012 Signalling in Development Evolution and Disease Date, Singapore, Senescence in Basal Cell Carcinoma (poster presentation).

ACKNOWLEDGEMENTS

I gratefully acknowledge the many people who have helped me develop as a research scientist and who helped me to produce this thesis. In particular I am indebted to my supervisors Professor Mike Philpott and Professor Rino Cerio for providing me with this outstanding opportunity to undertake this rather challenging and inspiring project and without their help, guidance and patience I would not have made it this far. I would also like to acknowledge my sincere thanks to Dr. Graham Neil who always helped me to cope with experimental problems with this project. For the provision of BCC samples I would like to thank Professor Rino Cerio, Department of Dermatology and Dermatopathology, Royal London Hospital. I am grateful to the Liaquat University of Medical and Health Sciences, Jamshoro, Sindh, Pakistan for their funding and also my supervisor Professor Mike Philpott who provide me funding for last year to complete my work. A special thanks to my colleague Dr. Muhammad Mahmudur Rahman for helping me in finishing off my project. I would also like to thank the people in my group Jane Elliott, Gopinath Damodaran and Lucia Bianchi and also Dr. Sahira Khalif, for their valuable support during my entire PhD. I would like to thank people in Dermatopathology, Royal London Hospital who provided me space and guidance in the laboratory for doing experiments. Last but not the least this PhD would not have been possible without the support of Centre for Cutaneous Research, Queen Mary University of London. I would like to thank everyone at the Centre for Cutaneous Research, past and present, for making it such an enjoyable place to work and for their assistance at every stage of my PhD studentship.

Finally I would like to thank my Father, Mother, Wife, my lovely Sisters and specially my brother Muhammad Daud Pirzado and his wife and all my friends for their support and love, and to whom this thesis is dedicated.

Chapter 1: Introduction

1.1 Structure of normal skin

The skin is the largest organ of the body, making up 16% of body weight, with a an average surface area of 1.8m^2 (Gawkrodger, 2002). Skin performs many vital functions as both a barrier and regulating influence between the outside world and the controlled environment within our bodies. It protects internal tissues from exposure to trauma, ultraviolet (UV) radiation, temperature extremes, toxins, and bacteria. Other important functions include sensory perception, immunologic surveillance, thermoregulation, and control of fluid loss. Structurally skin consists of three mutually dependent layers the epidermis, dermis and subcutis (***Figure 1.1***) (McGrath et al., 2008). The epidermis is derived from surface ectoderm but is colonized by pigment-containing melanocytes of neural crest origin, antigen-processing langerhans cells of bone marrow origin, and pressure-sensing merkel cells of neural crest origin. The dermis is derived from mesoderm and contains collagen, elastic fibres, blood vessels, sensory structures, and fibroblasts (Rinn et al., 2006). During the fourth week of embryologic development, the single cell thick ectoderm and underlying mesoderm begin to proliferate and differentiate. The specialized structures formed by the skin, including teeth, hair follicles, fingernails, toenails, sebaceous glands, sweat glands, apocrine glands, and mammary glands also begin to appear during this period of development. Teeth, hair, and hair follicles are formed by the epidermis and dermis in concert, while fingernails and toenails are formed by the epidermis alone. Hair follicles, sebaceous glands, sweat glands, apocrine glands, and mammary glands are considered epidermal glands or epidermal appendages, because they develop as down growths or diverticula of the epidermis into the dermis (Gawkrodger, 2002*)*.

The skin is a dynamic organ that undergoes continuous changes throughout life as outer layers are shed and replaced by inner layers. It also varies in thickness among anatomic location, sex, and age of the individual. This varying thickness primarily represents a difference in dermal thickness, as epidermal thickness is rather constant throughout life and from one anatomic location to another. Skin is thickest on the palms and soles of the feet (1.5 mm thick), while the thinnest skin is found on the

eyelids and in the post-auricular region (0.05 mm thick). Skin exposed to sunlight is the main site of synthesis of vitamin D, which is essential for the growth and maintenance of our bones (Farage et al., 2010). Much importance is attached to the appearance of skin, especially in our modern society. Medical conditions affecting the skin can have marked effects, not only on our state of well being but also on the ways we interact with other people, on our suitability for certain occupations and on the sorts of pastimes we can enjoy. Some of the consequences of skin disease, such as rashes and itching, may be obvious and others, such as the psychological impact, can be more subtle although just as important.

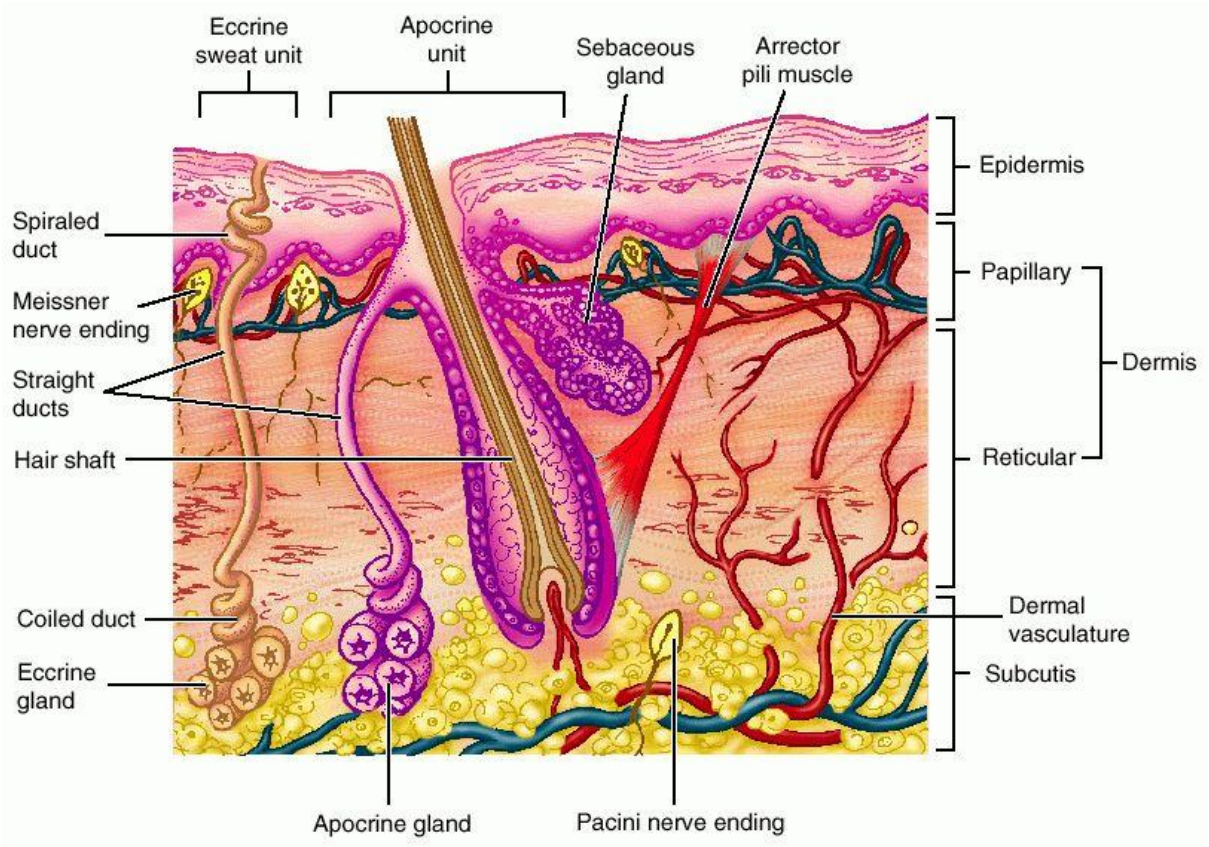

Figure 1.1: Structure of Normal Skin. Normal skin consists of the three layers, epidermis, dermis and subcutis. Within the skin a number of glands and appendages are found including the hair follicle, sebaceous and apocrine gland and eccrine sweat glands (http://medical-dictionary.thefreedictionary.com/lax+skin).

1.1.1 Epidermis

The epidermis is the thin, tough, outermost layer or epithelial layer of the skin (**see Figure 1.2**). It consists of stratified squamous epithelium that is composed primarily of keratinocytes. The epidermis contains no blood vessels and is entirely dependent on the underlying dermis for nutrient delivery and waste disposal via diffusion through the dermoepidermal junction. Its thickness varies according to body site and in most parts of the body the epidermis is about 0.1 mm thick, but on the soles of the feet and the palms of the hands it can be 1mm thick or more. It provides a protective barrier against mechanical, thermal and physical injury and hazardous substances. The epidermis is also important in preventing loss of moisture, it reduces the harmful effects of UV radiation and acts as a sensory organ (touch, detects temperature), the epidermis helps regulate temperature and immune organ to detect infections and preventing entry of substances and organisms into the body. In certain areas of the body that require greater protection (such as the palms of the hands and the soles of the feet), the outer keratinised layer of the epidermis (stratum corneum) is much thicker .

Most of the cells in the epidermis are **keratinocytes**, named because they produce a tough intermediate filament (IF) protein called keratin. Keratin is also the protein from which nails and hair are formed. Keratin gives skin much of its resistance to physical wear and tear and makes skin waterproof. Keratinocytes arise in the deepest level of the epidermis and new cells are constantly being produced and slowly migrate up toward the surface of the epidermis. Once the keratinocytes reach the skin surface, they are gradually shed and are replaced by younger cells pushed up from below. On average it takes about 60 days for a new keratinocyte to migrate to the surface and to be shed. As keratinocytes divide and differentiate, they move from this deeper layer to the more superficial layers. Once they reach the stratum corneum, they are fully differentiated keratinocytes or corneocytes, devoid of nuclei and are subsequently shed in the process of epidermal turnover. Cells of the stratum corneum are the largest and most abundant of the epidermis. The stratum corneum ranges in thickness from between 15-100 or more cells depending on anatomic location and is the primary

protective barrier from the external environment (McGrath et al., 2008, Farage et al., 2010, Fuchs, 1990).

Melanocytes (pigment-producing cells): Melanocytes, are the second most abundant cells type found in the epidermis and are derived from neural crest cells and are found in the basal layer of the epidermis as well as in hair follicles, the retina, uveal tract, and leptomeninges (McGrath et al., 2008). Melanocytes produce pigment called melanin, which is responsible for different skin colour. The amount of melanin pigment in the skin determines an individual's skin color (skin phototype). Skin pigment can be inherited genetically or can be acquired through various diseases. Hormonal changes during pregnancy can also vary the amount of pigmentation. The Fitzpatrick Scale is used to classify skin complexion and response to UV exposure (**See Table 1.1 below**). This classification is used clinically for evaluation of facial skin pigmentation before resurfacing procedures and is important for predicting outcomes and adverse effects. Melanin's primary function, however, is to filter out ultraviolet radiation from sunlight, which can damage DNA, resulting in numerous harmful effects, including skin cancer. Melanin is packaged into small parcels (or melanosomes), which are then transferred to keratinocytes, where they absorbs radiant energy from the sun and protects the skin from the harmful effects of UV radiation. Melanocytes are the cells of origin of melanoma. In areas exposed to the sun, the ratio of melanocytes to keratinocytes is approximately 1:4. In areas not exposed to solar radiation, the ratio may be as small as 1:30. Absolute numbers of melanosomes are the same among the sexes and various races. Differing pigmentation among individuals is related to melanosome size rather than cell number. Sun exposure, melanocyte-stimulating hormone (MSH), adrenocorticotropic hormone (ACTH), estrogens, and progesterones stimulate melanin production. With aging, a decline is observed in the number of melanocytes populating the skin of an individual. Since these cells are of neural crest origin, they have no ability to reproduce.

Table 1.1: Skin types.

Skin Types	Colour	Features
I.	White or freckled skin	Always burns, never tans
II.	White skin	Burns easily, tans poorly
III.	Olive skin	Mild burn, gradually tans
IV.	Light brown skin	Burns minimally, tans easily
V.	Dark brown skin	Rarely burns, tans easily
VI.	Black skin	Never burns, always tans

The epidermis also contains **Langerhans' cells (immune cells),** which are part of the skin's immune system and found in the epidermis. Langerhan's cells are responsible for helping the body learn and later recognise new 'allergens' (material foreign to the body). Although these cells help detect foreign substances and defend the body against infection, they also play a role in the development of skin allergies. Langerhans cells originate from the bone marrow and are found in the basal, spinous, and granular layers of the epidermis (Farage et al., 2010).

Merkel cells are a fourth, epidermal cell and are less visible. These cells are found in the basal layer of the epidermis. Their exact role and function of these cells is not well understood. Special immunohistochemical stains are needed to visualise Merkel cells. These cells are derived from neural crest cells, are found on the volar aspect of digits, in nail beds, on the genitalia, and in other areas of the skin. These cells are specialized in the perception of light touch (Farage et al., 2010).

The epidermis contains four distinct layers, described below from the most superficial to the deepest. These layers include stratum basale, stratum spinosum, stratum granulosum and stratum corneum. In addition, the **stratum lucidum** is a thin layer of translucent cells seen in thick epidermis. The stratum lucidum represents a transition from the stratum granulosum and stratum corneum and is not usually seen in thin epidermis. Together, the stratum spinosum and stratum granulosum are sometimes referred to as the Malphigian layer.

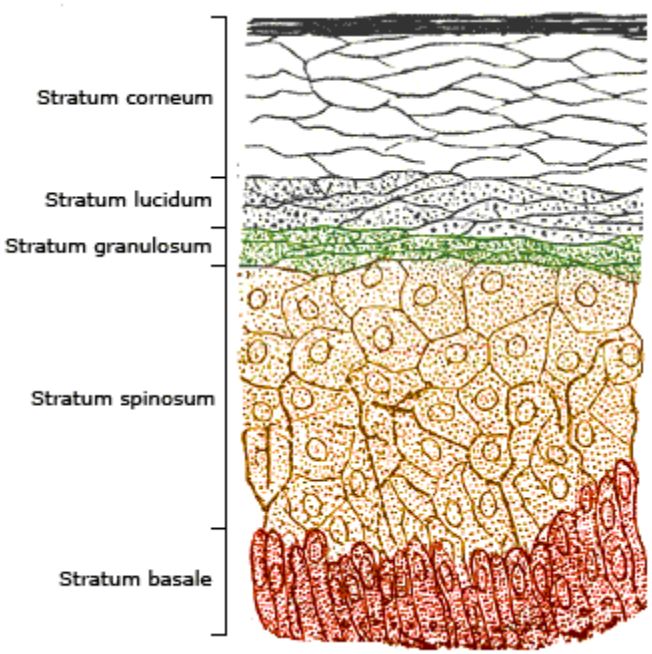

Figure 1.2: Showing epidermal layers. The epidermis consists of five different layers of keratinocytes, stratum basale, stratum spinosum, stratum granulosum, stratum lucidum and stratum corneum (http://www.youthful-you-wisdom.com/structure-of-human-skin.html) .

1.1.1.1 Stratum basale (basal layer): The innermost layer of the epidermis which lies adjacent to the dermis comprises mainly dividing and non-dividing keratinocytes, which are attached to the basement membrane by hemidesmosomes. This layer is responsible for constantly renewing epidermal cells. It is a continuous layer that is generally one cell thick although it can be two or three cells thick in glabrous skin. The basal cells are small, 10-14 nm, and cuboidal in shape (McGrath et al., 2008). These undifferentiated, proliferative cells are mitotically active and differentiate outward to form the distinctive supra-basal layers of the differentiated tissues. As well as keratinocytes, about 25% of the cells found in the basal layer are the melanocytes, they produce the melanin that provides pigmentation to skin and hair. Keratinocytes of the basal layer synthesize keratins K5 and K14 forming cytoskeleton filaments (keratin intermediate filaments) that aggregate into thin bundles (tonofilaments) (Fuchs, 1990, Blanpain and Fuchs, 2006). Whilst keratinocytes differentiate and progress to the skin surface, some cells of the basal layer remain undifferentiated and self-renew. These are the stem cells of the basal layer, being so defined as they do not terminally differentiate and with each division a daughter cell is produced which can commit to differentiate (McGrath et al., 2008) (Fenderson, 2008). The purpose of these cells is to maintain homeostasis regenerating hair and repairing the epidermis after injury. These stem cells are located in the basal inter follicular epidermis (IFE) and the bulge region of the hair follicle (Alonso and Fuchs, 2003). The stem cells in the hair follicle can give rise to the eight differentiated cell types within the hair follicle or either sebocytes of the sebaceous glands and under wound healing conditions IFE. The hair follicle cell types are as follow; outer root sheath (ORS), companion layers of the ORS, Henle, Huxley layers of the Inner Root Sheath (IRS) plus the IRS Cuticle, Cortex of the hair fiber and hair fiber cuticle and finally hair follicle germinative epithelium (that will give rise to above). Whereas the stem cells of the IFE can also be induced to give rise to hair and sebocyte lineages as long as they have the correct mesenchymal signals (Owens and Watt, 2003, Youssef et al., 2010). Epidermal stem cells strongly adhere to their underlying basement membrane and maintain the homeostasis of the IFE by replenishing the suprabasl terminally differentiated cells (Blanpain and Fuchs, 2006, McGrath et al., 2008). Compared to differentiated keratinocytes the undifferentiated keratinocyte stem cells have a greater life span, are slow cycling and divide to give rise

to cell that will remain in the basal layer as a stem cell and to daughter cell, known as a transit-amplifying cell (TAC). TA cells, initially undergo a few rounds of division increasing the number of cells and from there cells will go on to undergo an irreversible withdrawal from the cell cycle (Potten and Booth, 2002, Owens and Watt, 2003). During this there is a loss of adhesiveness, and the cells are pushed up through the layers of the epidermis, undergoing gradual differentiation until they will reach the stratum corneum (Owens and Watt, 2003, Youssef et al., 2010).

1.1.1.2 Stratum spinulosum (spinous, spiny or prickle cell layer): As basal cells divide and mature, they move towards the outer layer of skin, initially forming the stratum spinosum. Intercellular bridges, the desmosomes, which appear as `prickles' at a microscopic level, connect the cells (McGrath et al., 2008). The stratum spinosum is a multilayered (4-8 layered) arrangement of cuboidal cells and is the first layer of the differentiation compartment formed by the migration of the cells from the basal layer (Fuchs, 1990). The basal cells progressively weaken their attachment to the basement membrane and those of their neighbors and are pushed up into the spinous layer. Although, cells of stratum spinosum are normally post-mitotic, they are still metabolically active and synthesize keratins K1 and K10 forming cytoskeletal filaments that aggregate to form tonofibrillar bundles which are thicker than tonofilament bundles in basal cells (Blanpain and Fuchs, 2006, Fuchs, 1990). These keratin intermediate filament are anchored to the desmosomes, which are abundant in spinous cells than in the basal cells, joining adjacent cells to provide extra structural support, helping the skin resists the abrasion (Blanpain and Fuchs, 2006, Fuchs, 1990). As cells move upwards within the spinal layer they synthesize lamellar granules which contain lipids that are to be released into the intercellular spaces of the granular and stratum corneum cells. These lamellar granules are responsible for the barrier properties of the stratum granulosum and stratum corneum through avoidance of transepidermal water loss (Fuchs, 1990).

1.1.1.3 Stratum granulosum (granular layer): Succeeding the stratum spinosum is the stratum granulosum or granular layer which typically contains 3 to 5 layers of squamous cells. Continuing their transition to the surface the cells continue to flatten, lose their nuclei and their cytoplasm appears granular at this level. Keratohyalin forms

dense cytoplasmic granules that contain profilaggrin-the precursor of the interfilamentous protein fillagrin. Additional structural proteins of the cornified envelope including loricrin and involucrin are further synthesize by granular cells and deposited just beneath the plasma membrane to reinforce the cornified envelope (Fuchs, 1990, McGrath et al., 2008).

1.1.1.4 Stratum corneum (horny layer): This layer is the outermost portion of the epidermis, known as the stratum corneum and is relatively waterproof and, when undamaged, prevents most bacteria, viruses, and other foreign substances from entering the body. The cells of this layer, now referred to as corneocytes or squames, are flattened cells that have lost their nuclei and their cytoplasmic organelles (McGrath et al., 2008). As the dead cells slough off, they are continuously replaced by new cells. During the transition of granular cells to cornified keratinocytes profilaggrin is converted to filaggrin which aggregates the keratin filaments into tight bundles (conversion of bundling tonfibrils into macrofirillar cables) (Candi et al., 2001, Whitfield James and Chakravarthy, 2001). This promotes the collapse of the cell into a flattened shape, which is characteristic of the corneocytes of the cornified layer (Fuchs, 1990, McGrath et al., 2008). Therefore, corneocytes mostly consist of keratin intermediate filament embedded in a filaggrin matrix and surrounded by insoluble lipids (Candi et al., 2001).

1.1.2 Dermoepidermal junction/ Basement Membrane:

The dermoepidermal junction is an undulating basement membrane and has an important role in making sure the epidermis adheres to the underlying dermis. The dermo-epidermal junction zone (DEJZ) connects the epidermis and dermis (Villone et al., 2008). It is composed of a network of structural proteins, which provides a firm connection between the basal keratinocytes and the dermis. This structural network is made up of: hemidesmosome-anchoring filament complex, basement membrane with two layers (the lamina lucida and the lamina densa) and anchoring fibrils (Villone et al., 2008).

1.1.3 Dermis

The dermis is the fibrous connective tissue or supportive layer of the skin. It lies immediately underneath the epidermis and is about four times thicker. It varies in thickness, ranging from 0.6 mm on the eyelids to 3 mm on the back, palms and soles. The primary function of the dermis is to sustain and support the epidermis. Two layers comprise the dermis: a thin **papillary layer** and a thicker **reticular layer** (**see Figure 1.3**). The papillary dermis lies below and connects with the epidermis. It contains thin loosely arranged collagen fibres. Thicker bundles of collagen run parallel to the skin surface in the deeper reticular layer, which extends from the base of the papillary layer to the subcutis tissue. The dermis contains nerve endings, sweat glands and oil (sebaceous) glands, hair follicles, and blood vessels (**see Figure 1.3**). **Fibroblasts** are the major cell type of the dermis and secrete procollagen and elastic fibers. Procollagen is terminally cleaved by proteolytic enzymes into collagen that aggregates and becomes cross-linked. These tightly cross-linked collagen fibers provide tensile strength and resistance to shear and other mechanical forces. Collagen makes up 70% of the weight of the dermis, primarily Type I (85% of the total collagen) and Type III (15% of the total collagen) (Farage et al., 2010, Bremnes et al., 2011). Elastic fibers constitute less than 1% of the weight of the dermis, but they play an enormous functional role by resisting deformational forces and returning the skin to its resting shape.

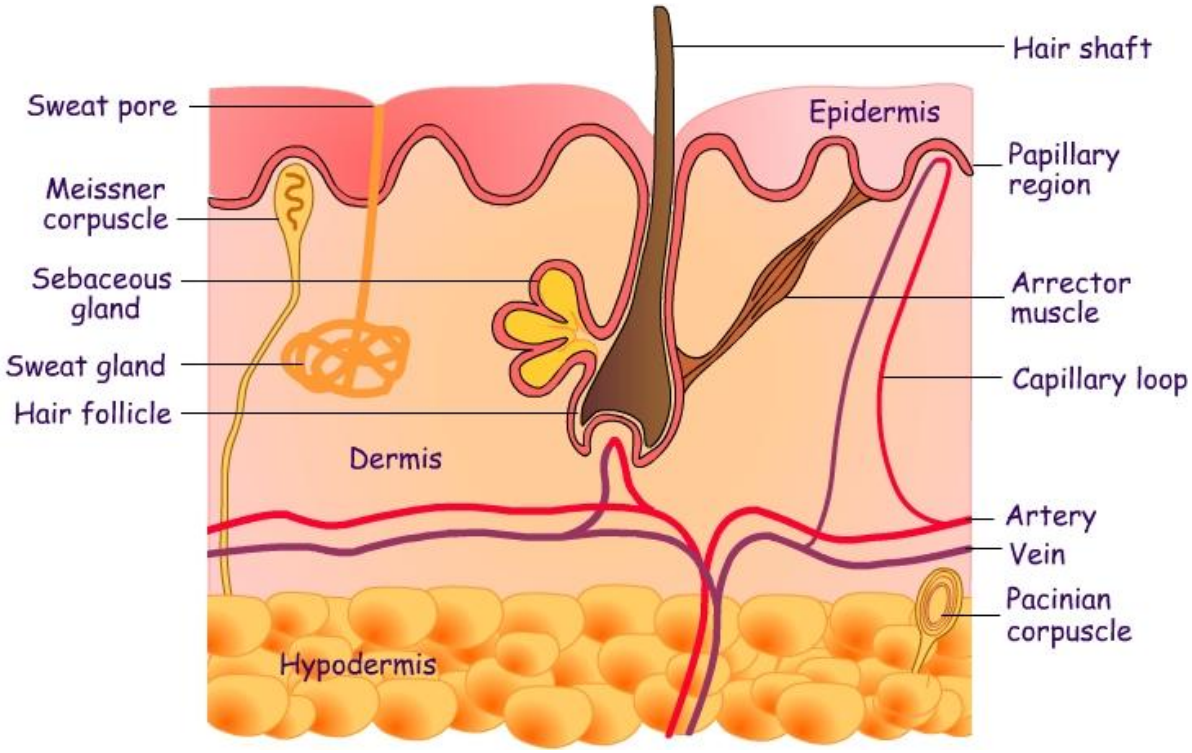

Figure 1.3: The dermis including derivative structures of skin.

1.1.4 Subcutis

The subcutis is the fatty layer immediately below the dermis and epidermis (**see Figure 1.3**). It is also called subcutaneous tissue, hypodermis or panniculus. It mainly consists of fat cells (adipocytes), nerves and blood vessels. It can vary considerably in thickness from person to person depending mostly on whether they are overweight.

1.2 Derivative structures of the skin

Hair: Hair (**see Figure 1.3**) can be found in varying densities of growth over the entire surface of the body, exceptions being on the palms, soles and glans penis, clitoris, labia minora, mucocutaneous junction, and portions of the fingers and toes (McGrath et al., 2008). Hair follicles are most dense on the scalp and face and are derived from the epidermis and the dermis (Gawkrodger, 2002). The development of the hair follicle is dependent on a series of epithelial-mesenchymal interaction. To begin the dermis signals the epidermis to make an appendage, this forms a hair placode in which the basal epithelium becomes elongated. In response to this the epidermis signals the dermal cells causing them to consolidate and form the dermal papilla (DP) (Blanpain and Fuchs, 2009, Widelitz, 2008). Subsequently the DP signals back promoting differentiation and proliferation to form the appendage. The developing follicle extends down and encloses the DP, whilst the cells at the base still maintain a high proliferative state (the matrix cells). Thereafter as the follicle matures the cells begin to differentiate into the IRS and the outer layer of the cells differentiates into the ORS. The ORS is continuous with the epidermis and has an external basement membrane (Fuchs and Raghavan, 2002). Whereas the IRS degenerates near the skin surface which enable the hair to protrude on its own. The hair is comprised of terminally differentiated keratinocytes from the matrix. Hair follicles also contains sebaceous glands to ensure the hair is impermeable to water. Also attach to the follicle is tiny bundle of muscle fibre called errector pili, which is responsible for causing the follicle lissis to become more perpendicular to the surface of the skin, and causing the follicle to protrude slightly above the surrounding skin (Blanpain and Fuchs, 2006, Fuchs, 1990). The body generates a constant supply of new hair throughout the lifetime although the purpose of this is unknown. To produce new hairs, existing follicles

undergo cycles of growth (anagen), regression (catagen), rest (telogen) and shedding (exogen). During each angen phase, follicles produce an entire hair shaft, while during catagen and telogen, follicles rest and prepare their stem cells so that they can receive the signal to start the next growth phase and make the new hair shaft (Fellous et al., 2009, Fuchs and Raghavan, 2002). As well as the IFE, stem cell niches have also been implicated and reported in the upper regions of the ORS including the bulge region and in the germinal epithelium or matrix (Fuchs, 1990). These bulge stem cells are multipotent and can differentiate into all epidermal lineages. It is believed that these stem cells are also involved in IFE repair and contribute to wound healing (Blanpain and Fuchs, 2006, Fuchs, 1990, Gawkrodger, 2002, Potten and Booth, 2002, Youssef et al., 2010).

Nails: These consist of a dense plate of hardened keratin between 0.3 and 0.5mm thick. Fingernails function to protect the tip of the fingers and to aid grasping. The nail is made up of a nail bed, nail matrix and a nail plate. The thickened epidermis which underlies the free margin of the nail at the proximal end is called the hyponychium. Fingernails grow at 0.1 mm per day; the toenails more slowly (Gawkrodger, 2002, McGrath et al., 2008).

Sebaceous glands: Sebaceous glands (**see Figure 1.3**) or holocrine glands are found over the entire surface of the body except the palms, soles, and dorsum of the feet. They are largest and most concentrated in the face and scalp where they are the sites of origin of acne. The normal function of sebaceous glands is to produce and secrete sebum, a group of complex oils that include triglycerides and fatty acid breakdown products, wax esters, squalene, cholesterol esters, and cholesterol. Sebum lubricates the skin to protect it against friction and makes the skin more impervious to moisture (Gawkrodger, 2002).

Sweat glands: Sweat glands (**see Figure 1.3**) or eccrine glands are found over the entire surface of the body except the vermillion border of the lips, the external ear canal, the nail beds, the labia minora, and the glans penis and the inner aspect of the prepuce. They are most concentrated in the palms and soles and the axillae. Each gland consists of a coiled secretory intradermal portion that connects to the epidermis

via a relatively straight distal duct. The normal function of the sweat gland is to produce sweat, which cools the body by evaporation. The thermoregulatory center in the hypothalamus controls sweat gland activity through sympathetic nerve fibers that innervate the sweat glands. Sweat excretion is triggered when core body temperature reaches or exceeds a set point (Gawkrodger, 2002).

1.3 Introduction to Basal Cell Carcinoma (BCC)

Melanoma and Non melanoma skin cancer (NMSC) are the most common skin cancers and NMSC is more common in the caucasian population (Czarnecki et al., 1994). Basal cell carcinoma of the skin is a form of non melanoma skin cancer also known as the basalioma, basal cell epithelioma, rodent ulcer and Jacobs ulcer; and is the commonest tumour affecting humans worldwide. According to the American Cancer Society, 75% of all skin cancers are basal cell carcinomas. BCC was first describe in 1824 by Jacobs and mainly arises from keratinocytes.BCC is a slow growing tumour and painless (Lo et al., 1991). BCC is a form of malignant tumour but it rarely metastasis (Domarus and Stevens, 1984). BCC is a treatable cancer but if left untreated it can cause huge destruction of surrounding tissues and causes a huge burden on cost of the health treatment worldwide. BCC mostly occurs on sun exposed areas and is common on the head & neck region and also occurs on trunk and limbs. Although the anatomical distribution varies between different types of BCC, nodular basal cell carcinoma mainly occurs on the head and neck and superficial is common on the trunk (Bastiaens et al., 1998).

1.4 Incidence of BCC

BCC can occur at any age but it is more prevalent over 40 years of age, and rarely occurs at an earlier age. BCC is very rare in dark skin people because of increase in pigmentation and due to this have less effect of UV rays of sun. The incidence of BCC shows marked difference in geographical variation. In UK around 100,000 people were diagnosed with non-melanoma skin cancer in 2010. In the USA more than 1million cases occur every year. In Australia the incidence is much higher at 726 per 100,000 (Marks et al., 1993). Comparative studies from Australia and the UK shows that this tumour is more common in men than in women (Diepgen and Mahler, 2002).

1.5 Aetiology/Risk factors of Basal Cell Carcinoma

The main reason for developing BCC is exposure to ultraviolet radiations (UV) and this radiation mostly comes from sun exposure (Zanetti et al., 1996). Other risk factors for developing BCC include skin colour, with light coloured hair and eyes, also those more likely to burn than tan, are more at risk of sun damage than dark skinned people (Lear et al., 1997). Other risk factors for developing skin cancer include, age (Mithoefer et al., 2002), if you have had skin cancer before, having a family history of skin cancer (Vitasa et al., 1990), having had certain other skin conditions or previous radiotherapy (Yamada et al., 1996), having been exposed to certain chemicals (such as arsenic) (Maloney, 1996) and having a weakened immune system (Hartevelt et al., 1990).

BCC can develop either sporadically or by hereditary means (Jemal et al., 2001, Kricker et al., 1995). Hereditary BCC develops as a result of basal cell nevous syndrome (BCNS), also called Nevoid Basal Cell Carcinoma Syndrome (NBCCS), or Gorlin Syndrome (Gorlin, 1995). Gorlin syndrome is an autosomal dominant condition. The reason for this syndrome is a mutation in the patched (*PTCH1*) tumour suppressor gene which is located on 9q22.3 (Hahn et al., 1996, Johnson et al., 1996). Approximately one half of 1% of BCC cases are attributable to the nevoid basal cell carcinoma syndrome (NBCCS), an autosomal dominant disorder characterized by multiple BCCs. Other tumors associated with the syndrome include medulloblastoma, ovarian fibroma, cardiac fibroma, fibrosarcoma, rhabdomyosarcoma, and meningioma. Congenital malformations are also features of this syndrome and include pits of the palms and soles of the feet, keratocysts and other dental malformations, midline brain malformations, strabismus, spine and rib abnormalities, ectopic calcification, mesenteric cysts, macrocephaly with characteristic coarse facies, and generalized overgrowth.

BCC can also develop in patients with Xeroderma pigmentosum (autosomal recessive disease), Bazex Syndrome also called as Bazex-Dupre-Christol Syndrome (x-linked dominant condition) and Rombo Syndrome (autosomal dominant condition). PUVA (psoralens plus ultraviolet A) treatment for psoriasis can increase chances of developing BCC (Stern and Lange, 1988). There is also an association between infection

with the monogenic types of human papillomavirus (HPV) and development of BCC (Pfister and Schegget, Barr et al., 1989).

1.6 Types of Basal Cell Carcinoma and clinical presentation

Basal cell carcinoma (BCC) is the most common type of skin cancer and the least dangerous. It is locally invasive, slowly eating away at the surrounding tissue, and may eventually become an ulcerated, bleeding sore. BCC are commonly divided on the basis of clinical and histological appearances (Rippey, 1998) Each has a distinct clinical presentation as discussed below. More than twenty five different types of BCC can be recognised. These different types of BCC are mainly divided into aggressive and non aggressive types. The more common types of BCC include nodular, superficial and morphoeic BCC.

1.6.1 Nodular Basal Cell Carcinoma

Nodular BCC is the most common form of BCC and accounts for about 60% of all BCC cases (Jacobs et al., 1982). These types of BCC mostly occur on the sun exposed areas especially on the face and ears but can involve other parts of body. Nodular BCCs typically present as a shiny, pearly, raised spot or nodule. Recurrent ulceration is frequent and this may lead to a depressed area in the central part of the lesion with a more raised, rolled edge. Sensory symptoms are uncommon. Unlike superficial BCCs though, nodular lesions will repeatedly ulcerate and bleed (**see Figure 1.4 A**). Histological this tumour is characterised by rounded mass of neoplastic cells with peripheral (**see Figure 1.4 B**).

1.6.2 Superficial Basal Cell Carcinoma

The second most common type of BCC (25%) (Jacobs et al., 1982) usually appears on the trunk but also on the head & neck or extremities. Clinically it appears as a Superficial BCC and presents as a bright pink, shiny, usually well-defined patch on the skin. The degree of redness may fluctuate greatly, and it may be more obvious when the skin is warm or the spot is rubbed, e.g. after a shower. Superficial BCC may sometimes be pigmented, as may all BCCs. It is not usually symptomatic, although it may sometimes be slightly itchy. Though these lesions are readily eroded by minor

trauma, they seldom bleed. Superficial BCC progressively enlarges over months to years. With time, areas of nodular or even morphoeic growth pattern may supervene within the original superficial BCC (**see Figure 1.4 C**). Histologically it is defined as one or more tumour foci extending from epidermis into the papillary dermis with peripheral palisading cells (**see Figure 1.4 D**) .

1.6.3 Morphoeic Basal Cell Carcinoma

This type of BCC also called sclerosing (resemble scar) BCC. This type of tumour is less common (2%) but is an aggressive type of BCC (Jacobs et al., 1982). It is often found on the head and neck, much like nodular BCC. Morphoeic BCCs are usually long standing and tend to be deeply invasive and have the appearance of a pale scar (**see Figure 1.4 E**). They can be difficult to detect and sometimes the patient is unaware of it, or may have simply thought it was an old scar that hadn't healed very well. They are quite firm to touch. Morphoeic BCCs constitute an aggressive growth pattern and are often associated with significant tissue destruction. Their finger-like processes often extend much more widely and deeply than it seems on inspection. Morphoeic BCCs are frequently asymptomatic, and may remain undetected for many years before being treated. Histologically it is defined as one or more tumour island in deep dermis with peripheral palisading cells (**see Figure 1.4 D**).

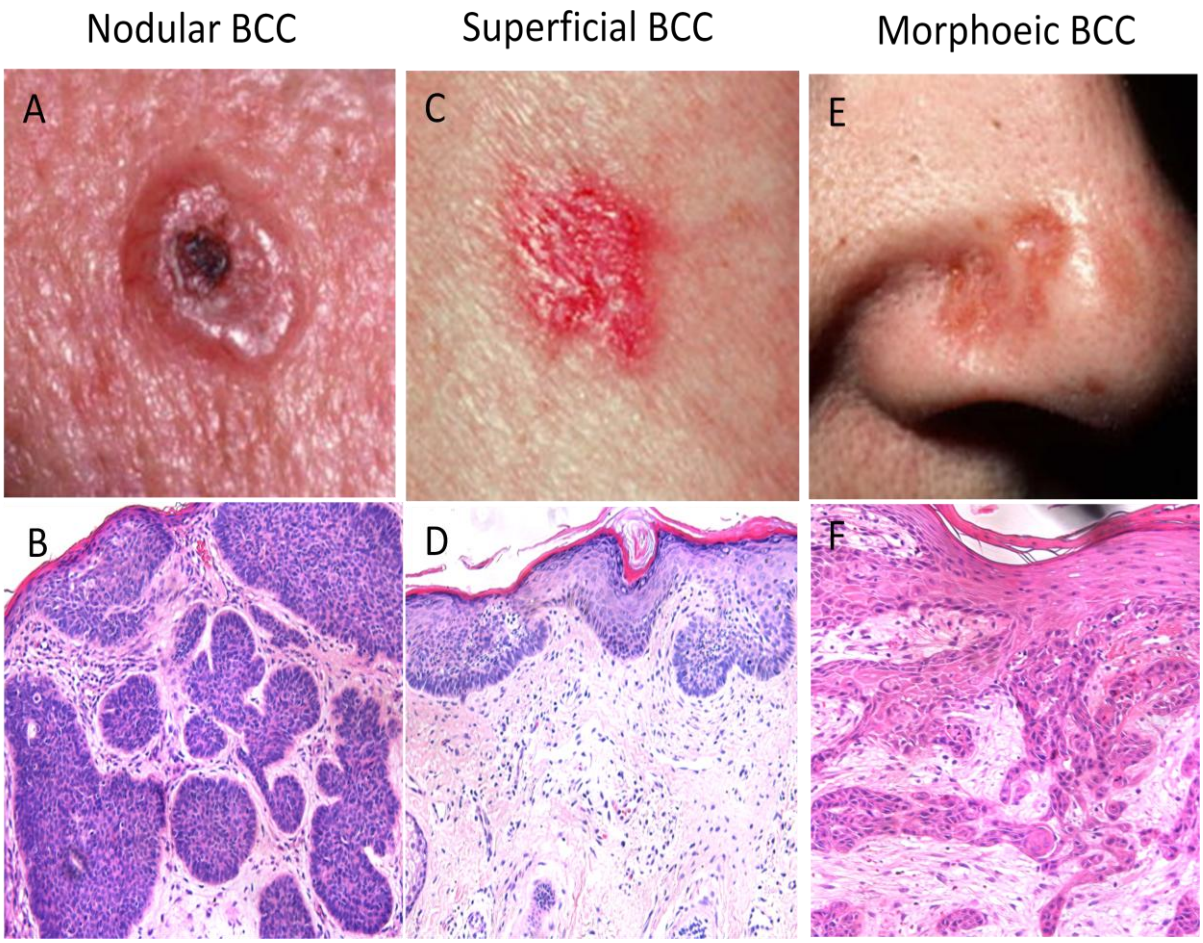

Figure 1.4: Showing clinical and histological images of BCC (A) Nodular BCC (B) Shows histology of Nodular BCC (C) Superficial BCC (D) Shows histology of Superficial BCC (E) Morphoeic BCC (F) Shows histology of Morphoeic BCC. Figure A, C and E were taken from http://www.skincancerclinic.md/skin-cancer/bcc/. Other pictures taken from BCC used in this study**.**

1.7 Treatment of Basal Cell Carcinoma

BCC is a treatable cancer but if left untreated it can cause huge disfigurement of surrounding tissue. There are different treatment options available for this disease and choice of treatment is based on the type, size, location, and depth of penetration of the tumour, the patient's age and general health, and the likely cosmetic effect.

Standard surgical excisions. This is the preferred method for removing BCC. This method involves the removal of the whole tumour mass and surrounding normal tissues. After removal of the tumour tissues the wound is closed by stitching. Standard surgical excision is not as good and efficient than Mohs but still has cure rate near 90%. The basic disadvantage of this procedure is the high reoccurrence of BCC of the face, especially around eyelids and nose (Sigurdsson and Agnarsson, 1998, Farhi et al., 2007).

Mohs surgery (or Mohs micrographic surgery). This type of treatment is normally done in the outpatient department or clinic of doctor. By using this method anaesthetic is applied on the surgical area of the patient. The tumour is excised and immediately examined under the microscope thoroughly. If the tumour is still present the procedure is repeated until the last layer of tumour examined under the microscope is tumour free. This method of surgery is a form of pathology processing called CCPDMA (complete circumferential peripheral and deep margin assessment) and has the highest rate of cure generally 98% or better(Rowe et al., 1989a). This method of treatment is generally used for recurring tumours, poorly demarcated tumours, or in critical areas around eyes, nose, lips and ears (Rowe et al., 1989b).

Chemotherapy/Topical Medication. Some superficial cancers can be treated with local therapy such as 5-flurouracil and 5% Imiquimoid cream five times a week for a few weeks. These are chemotherapy agents and are approved by the FDA for superficial BCC. The success rate of treatment is near about 70% to 90% (Romagosa et al., 2000, Love W, 2009).

Immunotherapy. Treatment using Euphorbia peplus, a common garden weed has been used as an immunotherapy agent in Australia for treating BCC. This is now commercially available in the UK and has the trade name 'Picato'.

Radiation. In this method x-ray beams are directed towards the tumour. This treatment is repeated several times per week for few weeks. This form of treatment is recommended for tumours that are hard to manage surgically and for elderly patients and those in poor health and also recommended for sites where surgical excision can cause disfigurement. The cure rate of this treatment is around 95% for small tumours and 80% for large tumours. This treatment can cause long term cosmetic problems, radiation risk and involve multiple visits to the clinic.

Photodynamic therapy (PDT). This type of treatment is useful when the patient has more than one BCC. In this treatment a photosensitizing agent such as Methyl aminolevulinate is applied on the tumour after which the area of treatment is activated by strong light. The cure rate ranges from 70% to 90%.

Cryosurgery. In this technique liquid nitrogen is used to destroy the tumour by freezing. The procedure may be repeated during the same session to remove all tumour tissues. It is an effective form of treatment for all forms of tumours and treatment of choice for patients with bleeding disorders or intolerance to anaesthesia. The cure rate for this treatment is less effective than excision and ranging from 80% to 90%. The disadvantages of this treatment include lack of margin control, tissue necrosis, over and under treatment of tumour and long recovery time.

Electrodessication and curettage. In this method the doctor uses a curette to remove the cancerous growth and then skin is burned with an electric current to soften the area for further cancer removal. This technique is repeated to ensure tumour is fully removed. The cure rate of this technique is less effective than surgical excision. This technique is not recommended for treating aggressive BCC and those on high risk and difficult sites.

Hedgehog Pathway Inhibitors. Vismodegib (Erivedge) is the first FDA-approved drug for advanced forms of basal cell carcinoma (Keating, 2012). It selectively inhibits

Smoothened (SMO), a key transmembrane protein involved in hedgehog signal transduction of cancerous epithelial cells. In a phase I dose-ranging study by Von Hoff et al (2011), 18 of 33 patients showed an objective response. Two of the 18 had complete response, and the remaining 16 showed a partial response. FDA-approval was based on a single, international, open-label trial (n=104). Of the 104 participants, 96 were evaluable. Of those with metastatic BCC (n=33), 30.3% had partial response, but none had complete response. With locally advanced BCC (n=63), 22% showed a partial response and 20% showed complete response (Keating, 2012).[1]

1.8 Hedgehog Signalling Pathway

The Hedgehog (HH) family of secreted signalling proteins play a crucial role in the development of animal organisms from Drosophila to humans, regulating the morphogenesis of various tissues and organs. HH plays a major role in patterning of tissues including growth of digits in limbs (Towers and Tickle, 2009), spinal cord and organization of brain (Weedon et al., 2008). Recent studies show the HH family also plays an important role in adult life including maintenance of the stem cell population to regulate maintenance and regeneration of adult tissues (Huangfu and Anderson, 2006). HH pathway is also involved in the development of cancers especially of lung, mammary glands, prostate and skin (BCC) (Velcheti and Govindan, 2007, Huang et al., 2011, Hatsell and Frost, 2007, Li et al., 2011, Datta and Datta, 2006).

HH was originally identified as a determinant of segment polarity in Drosophila melanogaster, the fruit fly (Rubin et al., 2005, Hooper and Scott, 2005). Drosophila have one hedgehog gene (*Hh*) whereas vertebrates have a more complex signalling system (Dennler et al., 2007, Hooper and Scott, 2005). HH proteins are glycoproteins that activate a membrane-receptor complex (**see Figure 1.5**) and consist of three family members; Sonic Hedgehog (SHH), Indian Hedgehog (IHH) and Desert Hedgehog (DHH) (Lauth and Toftgard, 2007, Hooper and Scott, 2005). HH precursors are cleaved at the C- and N- terminal regions for cholesteroylation, (a cholesterol molecule is covalently attached to the COOH-terminal glycine); and palmitoylation, (a palmitoyl moiety found on the NH_2 terminal cysteine). Subsequently mature HH proteins are

transported to the cell surface (Katoh and Katoh, 2008, Hooper and Scott, 2005, Couve-Privat et al., 2004, Yang et al., 2010). The best characterised is SHH as it is the most commonly expressed and potent of all the HH ligands although the binding affinities of all three are similar (Ruiz i Altaba et al., 2002c, Lauth and Toftgard, 2007, Daya-Grosjean and Couvé-Privat, 2005). The N terminal domain of SHH is responsible for the signalling activities whilst the C terminal domain is responsible for the intramolecular precursor processing of the protein (Couve-Privat et al., 2004). HH signalling is mediated through incompletely described balances between activating and repressive forms of GLI (Bishop et al., 2010).

HH ligand can be transported by diffusion through extracellular spaces or a concentration gradient. HH can also enter the cell via endocytosis which can be receptor mediated (Ryan and Chiang, 2012). Heparin sulphate proteoglycans (HSPG) have been shown to control a number of signalling pathways such as HH, Wnt, TGF-β and FGF signalling pathways. HSPGs are capable of retaining and stabilising HH ligands by facilitating ligand-receptor interactions (Ryan and Chiang, 2012). For HH to be released from the cell, a 12-pass transmembrane protein Dispatched (DISP) is required. DISP has a significant sequence similarity to *PTCH* in particular, the sterol sensing region that is implicated in lipid transport or secretion of lipid modified proteins (Lum and Beachy, 2004). Lipid modified HH is not secreted from cells if there is an absence of DISP. In *D. melanogaster*, DISP releases lipid modified HH from the cell compared to mammalian DISP which is thought to be involved in HH multimer formation (Daya-Grosjean and Couvé-Privat, 2005). HH signalling is controlled by the tumour suppressor protein *PTCH*1 and the G-protein coupled receptor SMO (Taipale and Beachy, 2001). *PTCH*1 contains twelve transmembrane domains and two extracellular loops that bind to HH ligands (Marigo et al., 1996). Mutations of *PTCH1* are associated with various birth defects as the HH pathway is heavily involved in embryonic development (Hahn et al., 1996). PTCH2 was discovered in vertebrates shares a 54% sequence homology to PTCH1 however the amino and carboxylic regions differ which confers a different protein function (Carpenter et al., 1998). Not only does PTCH1 function as the HH receptor, PTCH1 is a negative regulator of the HH pathway by inhibiting SMO. SMO has been described as a proto-oncogene (Beachy et al., 2004, Couve-Privat et al., 2004,

Daya-Grosjean and Couvé-Privat, 2005) and is 7-transmembrane 115 kDa protein with structural similarity to serpentine, G-protein coupled receptors (van den Heuvel and Ingham, 1996, Alcedo et al., 1996). Smoothened is responsible for triggering intracellular signalling and the subsequent activation of HH target genes. There is one known human smoothened gene (*SMO*) and is homologous with members of the 'frizzled' (WNT receptor) family. SMO comprises of a cytoplasmic tail with a domain that binds to a multi-molecular series of interacting proteins which also includes suppressor of fused (SuFu), fused (Fu) and GLI (Beachy et al., 2004, Epstein, 2008, Lauth and Toftgard, 2007). In the absence of a HH signal, PTCH1 localises to the primary cilium and maintains SMO in an inactive form thus preventing its translocation to the cilia (Rohatgi et al., 2007a). Early studies of PTCH1 would suggest that it binds directly with SMO (Murone et al., 1999), however more recent studies indicate that the two proteins do not physically bind to each other (Taipale and Beachy, 2001).

The key components of the HH signalling pathway are shown in **Figure 1.5** and discussed in more detail in **sections 1.8.1**, **1.8.2 and 1.8.3**. The HH receptor **(see Figure 1.5**), patched (PTCH), represses HH signalling by inhibiting the signalling effecter smoothened (SMO). PTCH mutational inactivation leads to over expression of downstream HH-responsive genes, such as GLI-1 and GLI-2, which results in BCC development (Denef et al., 2000). Downstream of SMO, the GLI-1 transcription factors are activated resulting in the induction of transforming growth factor (TGF-β) (Heberlein et al., 1993) and platelet-derived growth factor alpha (PDGF) (Xie et al., 2001).

As the HH signalling pathway plays an important role in development, it is not surprising that dysregulation of the pathway is associated with disease including cancer (di Magliano and Hebrok, 2003, Ruiz i Altaba et al., 2002a, Taipale and Beachy, 2001). HH signalling has also been shown to be required for the maintenance of cancers such as lung and prostate cancer despite the tumours arising from the dysregulation of other signalling pathways (Karhadkar et al., 2004, Watkins et al., 2003). HH signalling was implicated In BCC biology after the observation that Gorlin syndrome patients are predisposed to developing BCCs (Johnson et al., 1996). Gorlin syndrome patients are born with a defective PTCH1 allele and upon the loss of

function of the remaining allele (loss of heterozygosity, LOH) BCCs develop (Gailani and Bale, 1997). As a result Gorlin patients are more likely to acquire the LOH mutation of PTCH1 and develop BCCs at an earlier age than non-Gorlin patients. Non-Gorlin patients develop tumours later in life because loss of function mutations to both PTCH1 alleles takes longer to occur for BCCs to form (Gailani et al., 1996). *PTCH1* LOH mutations have been observed sporadic BCCs ranging between 11-67% in various studies (Saran, 2010). It has been reported that approximately 90% of sporadic BCCs harbour loss of function mutations of *PTCH1* and 10% activating mutations of *SMO* (Youssef et al., 2010). 50% of sporadic BCCs have been shown to carry mutations of *PTCH1* that are caused by UVB radiation (Gailani and Bale, 1997). In contrast one study has shown that out of the BCCs examined, *PTCH* mRNA was over expressed in all samples. *PTCH* protein expression was found in all tumour cells and stronger in palisading cells but not in normal epidermal cells. Downstream of *PTCH*1, activating mutations of *SMO* have been described in sporadic BCCs as Arg-562-Gln in *SMO-mutant 1* (M1) and Trp-535-Leu in *SMO-mutant 2* (M2). Of the two identified mutations the *SMO-M2* mutation was found in nearly all BCCs where *PTCH1* remained intact. Mice over expressing wild type SMO do not develop any abnormalities whereas SMO-M2 over expressing mice display BCC like characteristics (Xie et al., 1998). A number of mouse models of BCC have been developed to help understand how BCCs may form. As *Ptch -/-* mice are not viable, *Ptch +/-* mice were developed with a single allele mutation of *Ptch* as seen in Gorlin patients. An *in-vivo* study has shown that loss of *Ptch1* function in mouse skin is capable of inducing BCC formation (Daya-Grosjean and Couvé-Privat, 2005, Donovan, 2009). Further downstream of the HH pathway, mice over expressing GLI1 were able to develop tumours that share a resemblance to BCCs (Nilsson et al., 2000a). Interestingly, mice over expressing an activated mutant form of GLI2 which is a positive regulator of GLI1 developed multiple BCCs (Grachtchouk et al., 2000, Sheng et al., 2002). GLI2 studies in mice show that over expression of the protein in hair follicle stem cells leads to nodular BCC formation compared to GLI2 over expression in the IFE which leads to a more superficial BCC phenotype (Grachtchouk et al., 2000).

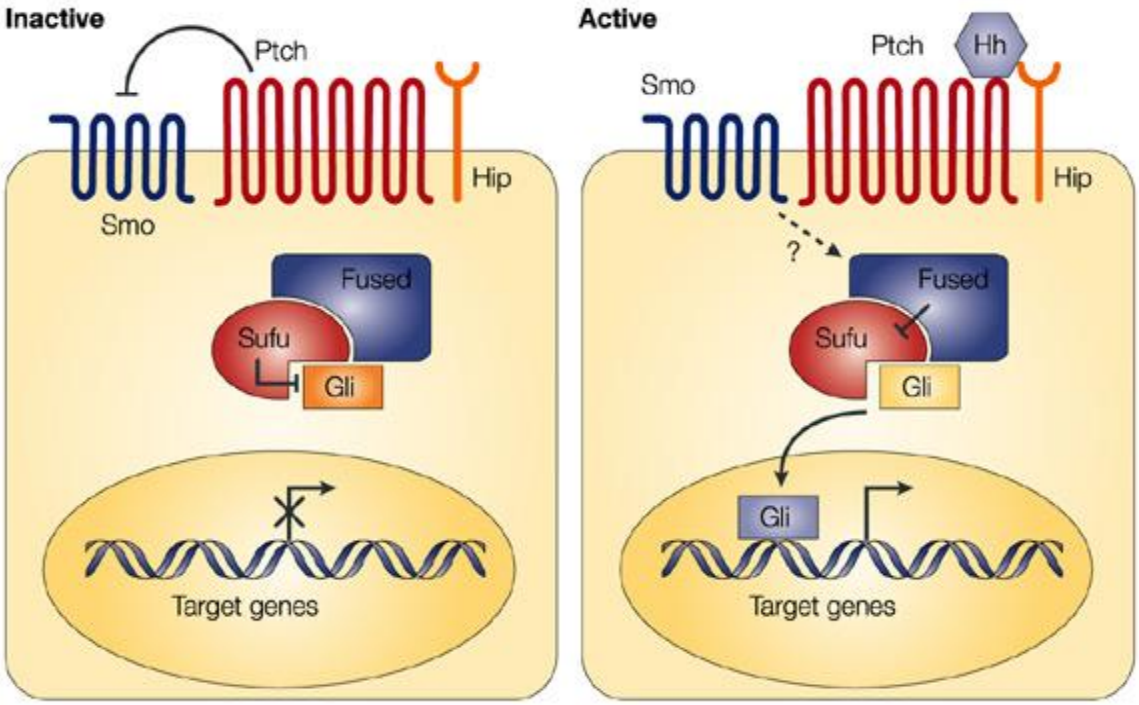

Figure 1.5: Overview of Sonic Hedgehog Signalling. In the absence of ligand, the HH signalling pathway is inactive (left). In this case, the transmembrane protein receptor Patched (PTCH) inhibits the activity of Smoothened (SMO), a seven transmembrane protein. The transcription factor GLI-1 a downstream component of HH signalling, is prevented from entering the nucleus. As a consequence, transcriptional activation of HH target genes is repressed. Activation of the pathway (right) is initiated through binding of any of the three mammalian ligands — Sonic hedgehog, Desert hedgehog or Indian hedgehog (all are represented as HH in the figure) — to PTCH. Ligand binding results in de-repression of SMO, thereby activating a cascade that leads to the translocation of the active form of the transcription factor GLI to the nucleus. Nuclear GLI activates target gene expression, including PTCH and GLI-1 itself, as well as Hip, a HH binding protein that attenuates ligand diffusion (di Magliano and Hebrok, 2003).

1.8.1 Patched (*PTCH*)

PTCH is the component that specifically binds hedgehog (Stone et al., 1996), is 1500 amino acids glycoprotein with 12- pass transmembrane receptor and two large extracellular loops that are needed for binding with hedgehog (Hooper and Scott, 1989, Nakano et al., 1989). *PTCH*, a tumour suppressor gene is located on chromosome 9 q22-q31 and encodes for the protein *PTCH*, a 12-transmembrane receptor (Ruiz i Altaba et al., 2002c, Asplund et al., 2008). There are two *PTCH* genes, *PTCH1* and *PTCH2* which have similar affinities for SHH (Couve-Privat et al., 2004). PTCH1 is a transmembrane protein that together with Smoothened forms a receptor complex for SHH. This protein is expressed in the cell membrane of target tissues, where it represses Smoothened signalling. Binding of SHH to *PTCH1* (physiological activation) or mutational inactivation of *PTCH1* (pathological activation) suspends the inhibition of Smoothened, which results in the activation of the hedgehog pathway. Mutations in *PTCH* can cause tumours including BCC, medulloblastoma, meningioma, breast carcinoma and neuroectodermal tumours (Hahn et al., 1996, Johnson et al., 1996).

1.8.2 Smoothened (SMO)

SMO has been described as a proto-oncogene (Beachy et al., 2004, Couve-Privat et al., 2004, Daya-Grosjean and Couvé-Privat, 2005) and is 7-transmembrane 115 kDa protein with structural similarity to serpentine, G-protein coupled receptors (van den Heuvel and Ingham, 1996, Alcedo et al., 1996). Smoothened is responsible for triggering intracellular signalling and the subsequent activation of HH target genes. There is one known human smoothened gene (*SMO*) and is homologous with members of the 'frizzled' (WNT receptor) family. SMO comprises of a cytoplasmic tail with a domain that binds to a multi-molecular series of interacting proteins which also includes suppressor of fused (SuFu), fused (Fu) and GLI (Beachy et al., 2004, Epstein, 2008, Lauth and Toftgard, 2007). The multi-molecular complex is a key regulator in shuttling GLI proteins between the cytoplasm and the nucleus. In the absence of hedgehog, patched interacts at the membrane with smoothened, rendering it inactive. When inactive the multi-molecule complex is bound to microtubules/ cytoskeleton and retains the GLI in the cytoplasm though phosphorylation of the carboxy-terminus or

full length GLI, which represses the translocation of GLI to the nucleus (Lauth and Toftgard, 2007) However, when hedgehog binds to patched, the inhibition of smoothened signalling is released and downstream genes are transcriptionally unregulated.

1.8.3 GLI Proteins

GLI proteins are large multifunctional transcription proteins, initially isolated from glial cell tumours (Fischer et al., 1995), present either in the nucleus and in cytoplasm. There are three different forms of GLI. GLI-1 only occurs as a full length transcriptional activator and GLI-2 and GLI-3 can be processed as truncated repressors (Wang et al., 2000, Pan et al., 2006). The over expression of GLI-1 and GLI-2 can induce spontaneous skin tumorigenesis (Nilsson et al., 2000b). In the presence of HH ligand **(Figure 1.6)** the pathway is activated. This can occur on binding to any of the HH ligands, SHH, DHH or IHH to the PTCH receptor. This results in the inhibition of PTCH action on SMO. Consequently SMO is activated and transduces a signal from the plasma membrane to the cytoplasm. SuFu is inhibited by SMO and through an unknown mechanism this triggers the dissociation of GLI from the SuFu/Fu complex. This regulates between the full length forms and the truncated, repressive forms of GLI (Bishop et al., 2010). GLI then translocates to the nucleus and subsequently binds to the DNA of HH-target genes with a consensus-binding site (5'-tgggtggtc-3') (Yang et al., 2010). GLI zinc finger proteins are large multifunctional transcription factors that are the transcriptional target genes of SHH signalling (Ruiz i Altaba et al., 2002c, Lauth and Toftgard, 2007). They were first identified as a gene unregulated in Glioblastoma (Epstein, 2008). There are three members of the GLI family named GLI 1, 2 and 3 which have a highly conserved DNA-binding domain with a zinc finger that binds with a consensus sequence although each has an independent role (Dennler et al., 2007, Fernandez-Zapico, 2008). GLI is inherent in both the nucleus and the cytoplasm and are part of a multi-molecular complex as previously mentioned (**Figure 1.6**) (Ruiz i Altaba et al., 2002c, Lauth and Toftgard, 2007, Ruiz i Altaba et al., 2002b). Both GLI 2 and 3 have C-terminus activator domains and N-terminus repressor domains and therefore can act as either activators or suppressors, whereas GLI1 only has a C-terminus domain, functioning only as an activator (Epstein, 2008, Katoh and Katoh,

2008, Hooper and Scott, 2005, Tojo et al., 2003). Activators GLI 2/3 function upstream of GLI-1 and induces the transcription of the *GLI-1* gene and *PTCH* via direct binding to their promoter regions (Dennler et al., 2007, Lauth and Toftgard, 2007). PTCH then negatively feeds back inhibiting the membrane signal, whereas GLI-1 positively feeds back inducing GLI-1 specific genes (Katoh and Katoh, 2008, Lauth and Toftgard, 2007, Hooper and Scott, 2005, Bonifas et al., 2001). HH-interacting protein (HIP) participates in a negative feedback loop by sequestering hedgehog ligands, but unlike PTCH, it has no effect on the activity of SMO (Hooper and Scott, 2005, Yang et al., 2010). The SHH signalling cascade is believed to activate several genes including Transforming Growth factor β (TGFβ)/ Bone Morphogenetic Protein (BMP), and Wnt family proteins (Couve-Privat et al., 2004, Bonifas et al., 2001). Other transcription targets of GLI are reported target genes such as *FOXM1, CCND1, SFRP1* and *PDGFRA* (Katoh and Katoh, 2008, Asplund et al., 2008).

1.8.4. Primary Cilia

The primary cilium is a microtubule-based organelle which projects from the surface of virtually all cells in the mammalian body but is predominantly seen in stromal and epithelial cells (Michaud and Yoder, 2006, Hoey et al., 2011). They are immotile and anchored to the cell by the basal body just beneath the plasma membrane, which develops from the centriole of the centrosome by turning microtubules into a structure called the axoneme (Simpson et al., 2009, Michaud and Yoder, 2006, Rohatgi et al., 2007b). The development of the cilia is regulated by the cell cycle, as such primary cilia are found in cells within the G_0 phase of the cell cycle. The cilium forms a continuous membrane with the cell although the transport of proteins into the cilium is regulated (Michaud and Yoder, 2006, Hoey et al., 2011). The function of the primary cilium is as a sensory organelle which receives both mechanical and chemical signals from other cells and the environment, and transmits these signals to the nucleus to elicit a cellular response (Hoey et al., 2011).

The mechanism for the signal transduction cascade from SMO to GLI-1 is not fully defined, although increasing data suggest that the primary cilium provides a platform for relaying the signal from the cell membrane to the nucleus (Kasper et al., 2009).

The discovery that the protein components of the primary cilia are required for HH signalling led to the suggestion that sub cellular localisation is important in HH signalling (Rohatgi et al., 2007b). Recent studies revealed that multiple components of the SHH, but also the platelet derived growth factor receptor-A signal transduction pathway is localize to the primary cilium (Michaud and Yoder, 2006, Kasper et al., 2009). As well as PTCH and SMO, the GLI proteins and Sufu have been shown to reside in the dorsal tip of the primary cilium (Michaud and Yoder, 2006, Simpson et al., 2009). SMO localizes to the primary cilia in response to SHH which appears to be a crucial step in its activation. Rohatgi et al, 2007 showed that after stimulation of cells with SHH, endogenous SMO was enriched in the primary cilia. Total levels of SMO were not altered, but localised to the cilia (Rohatgi et al., 2007b). Furthermore SHH triggered the removal of PTCH from the primary cilium, thereby allowing the binding and movement of SMO within the cilia (Rohatgi et al., 2007b). The loss of the cilium blocks ligand-induced signalling by the SHH pathway (Michaud and Yoder, 2006, Fendrich et al., 2011).

Intraflagellar transport (IFT) function in the cilia is also believed to be required for SMO activity as well as modulation of GLI protein activity (see **Figure 1.11**) (Michaud and Yoder, 2006, Simpson et al., 2009, Kasper et al., 2006b). As IFT proteins do not play a role in Drosophila HH signalling, Kasper et al, 2006 speculate that cilia are involved in the relay of the mammalian HH-signal and that IFT proteins organise a structure that may facilitate the interaction of other HH-signalling components with latent GLI transcription factors (Kasper et al., 2006b).

Genetic mutations that disrupt the function of primary cilia result in a broad spectrum of disorders, including cystic kidneys, hepatic and pancreatic abnormalities, skeletal malformations, obesity, and severe developmental defects (Michaud and Yoder, 2006). Defects and function mutations in IFT result in severe patterning defects of the neural tube similar to observations made in SHH and SMO mutated embryos (Kasper et al., 2006b).

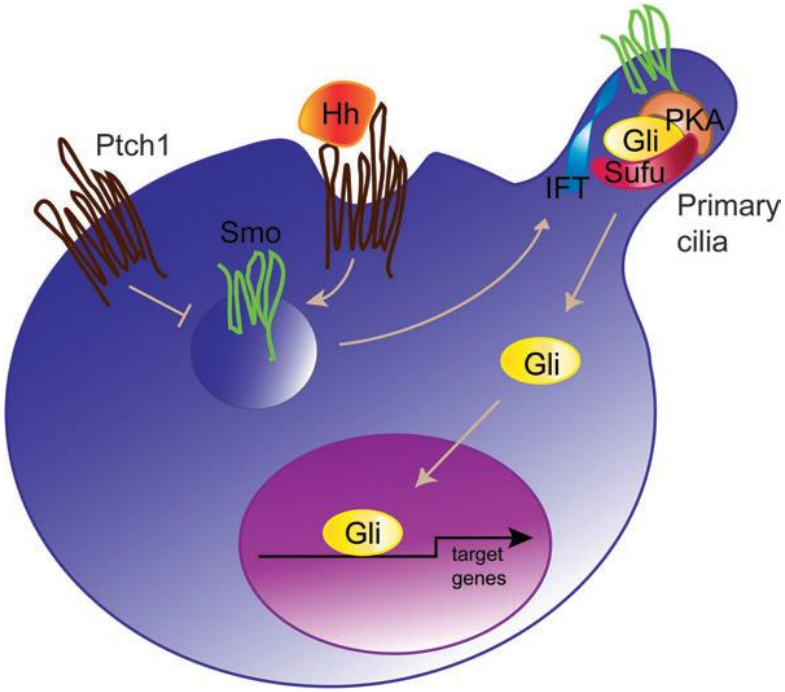

Figure 1.6: **Hedgehog Signalling Through Primary Cilia** An illustrative representation of HH signalling through the primary cilium. Activation of the pathway is initiated upon HH binding to PTCH1, which leads to de-repression of SMO. Therefore the HH signalling cascade involving a multi-protein complex with the primary cilium acting as a processing platform, leads to the translocation of the active GLI transcription factors to the nucleus. Abbreviations: Intraflagellar proteins (IFT); Protein kinase A (PKA); Suppressor of fused (SuFu). Modified from Kasper et al, 2009 (Kasper et al., 2009)

1.9 Hedgehog Signalling in Cancer

It has been well documented that the aberrant activation of the HH signalling pathway can lead to a number of cancers. As the HH signalling pathway plays an important role in development, it is not surprising that dysregulation of the pathway is associated with disease including cancer (di Magliano and Hebrok, 2003, Ruiz i Altaba et al., 2002a, Taipale and Beachy, 2001, Lee and Frederic, 2006). HH signalling has also been shown to be required for the maintenance of cancers such as lung and prostate cancer despite the tumours arising from the dysregulation of other signalling pathways (Walsh, 2005). HH signalling was implicated in BCC after the observation that Gorlin syndrome patients are predisposed to developing BCCs. Patients with this syndrome are born with a defective *PTCH1* allele and upon the loss of function of the remaining allele (loss of heterozygosity, LOH) BCCs develop (Gailani and Bale, 1997). As a result these patients are more likely to acquire the LOH mutation of *PTCH1* and develop BCCs at an earlier age than non-Gorlins patients. Non-Gorlins patients develop tumours later in life because loss of function mutations to both *PTCH1* alleles takes longer to occur for BCCs to form. *PTCH1* LOH mutations have been observed sporadic BCCs ranging between 11-67% in various studies (Lee and Frederic, 2006). It has been reported that approximately 90% of sporadic BCCs harbour loss of function mutations of *PTCH1* and 10% activating mutations of *SMO* (Youssef et al., 2010).

SHH signalling is often activated in solid tumours including BCC, but also Gastric Carcinoma, Melanoma, Medulloblastomas, Gliomas in brain, pancreatic and small cell lung cancer to name a few and are reported to have increased levels of SHH (Snijders et al., 2009, Yauch et al., 2008, Katoh and Katoh, 2008, Yoo et al., 2008, Daya-Grosjean and Couvé-Privat, 2005, Walter et al., 2010). Activation of the pathway can be either by over expression of the ligand or by the alteration of the downstream signalling pathway within the tumour epithelium (**Figure 1.7**) (Snijders et al., 2009, Yauch et al., 2008). Predominantly mouse models have been used to study BCCs. Over expression of HH in the skin of transgenic mice results in skeletal and skin anomalies and the development of tumour like BCCs (Daya-Grosjean and Couvé-Privat, 2005). In mice over expressing GLI-1 and GLI-2, BCC like tumours also develop.

Perturbations in the SHH pathway can occur through the mutation or deletion of *PTCH* or *SMO*. (Crowson, 2006) Mutations in the *PTCH* gene produces a truncated form of the protein which is unable to bind to and inactivate *SMO* (Crowson, 2006). Heterozygous mutations in *PTCH1* were first noticed in Gorlin syndrome as previously mentioned (**Section 1.2.1**) (Wong et al., 2003, Crowson, 2006). Sporadic mutations in other forms of cancer such as medulloblastoma, oesophageal SCC and transitional cell carcinoma of the bladder have also been reported with the loss of *PTCH* function (Beachy et al., 2004, Dennler et al., 2007). Downstream of PTCH1, activating mutations of *SMO* have been described in sporadic BCCs as Arg-562-Gln in *SMO-mutant 1* (M1) and Trp-535-Leu in *SMO-mutant 2* (M2). Of the two identified mutations the *SMO-M2* mutation was found in nearly all BCCs where *PTCH1* remained intact. The mice over expressing wild type *SMO* do not develop any abnormalities whereas *SMO-M2* over expressing mice display BCC like characteristics. *SMO* gain of function mutations have been documented in a subset of small cell lung carcinoma (Dennler et al., 2007). Non-canonical activation of the HH pathway i.e. the pathway is stimulated by another factor, may also contribute to BCC development. Transforming growth factor-β (TGF-β) has been reported to induce both GLI1 and GLI2 expression in keratinocytes (Javelaud et al., 2011).

The results of these sporadic mutations leads to SHH-independent constitutive activation by the target genes *GLI-1* and *PTCH1* itself (Valin et al., 2009). Consequently, there is consistent up-regulation of the transcription target family GLI. Studies of the HH signalling pathway are usually performed by the activation, inhibition and expression of downstream targets including SMO and GLI.

Up-regulation of GLI-1 has been seen in BCC and is thought to play a role in the development of BCC by activating BCL2 which therefore decreases apoptosis. (Crowson, 2006) The up regulation of *GLI-1* and *GLI2* has also been reported in mRNA extractions from micro-dissected BCC cells (Asplund et al., 2008, Daya-Grosjean and Couvé-Privat, 2005). PTCH1 expression was not up-regulated in their study. Work with mice has shown that GLI can induce BCC like tumour formation (Ruiz i Altaba et al., 2002c) indicating that activation of the SHH pathway and thereby the activation of a single transcription factor can cause tumour formation. Furthermore sporadic BCCs

frequently have GLI-1 expression unlike sporadic SCCs which show no expression (Ruiz i Altaba et al., 2002c). More recently work on Oesophageal SCC has shown the HH signalling pathway to be active. High levels of SHH and SMO were detected in SCC whereas *PTCH*1 levels were low. GLI1 showed varied expression with 50% of SCC expressing high levels of GLI1 (Leovic et al., 2011). It has also been reported that GLI-1 expression is not always associated with a loss of the receptor *PTCH* suggesting that GLI-1 may have a more aggressive role in development of BCC (Micke et al., 2007). Furthermore recent work has shown that SHH responsive tumours have activated canonical pathways in the tumour stroma and in some cases this is restricted to the stroma (Chen et al., 2011).

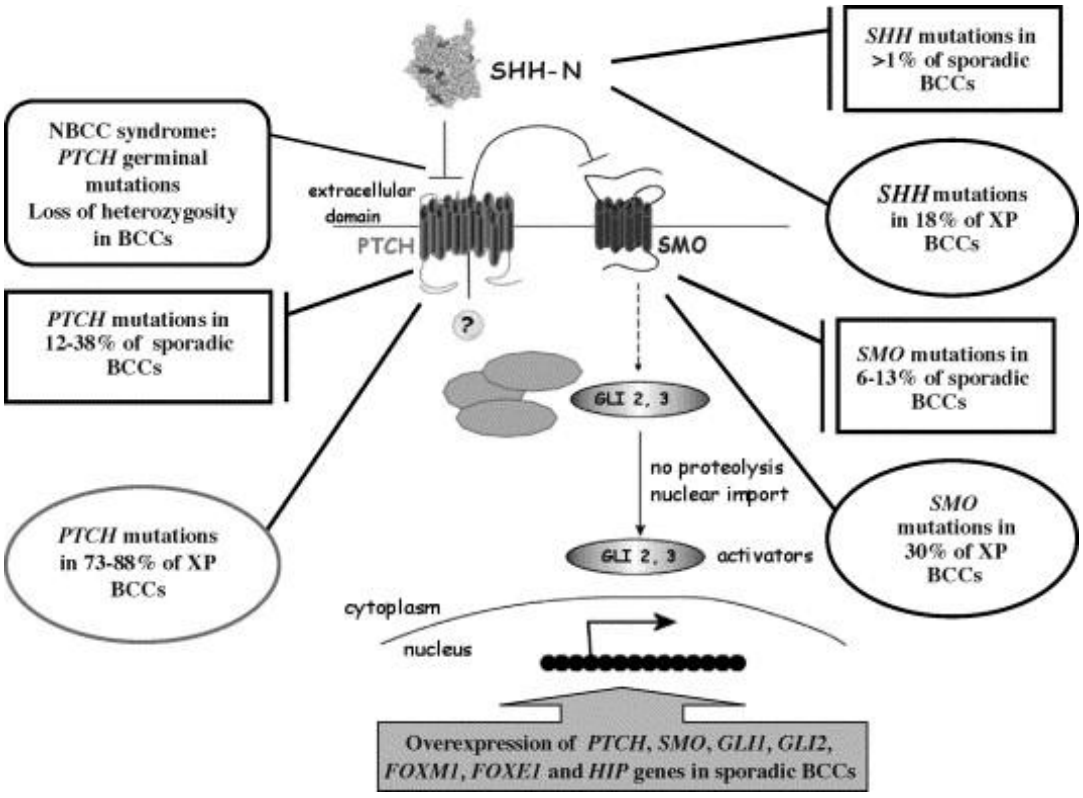

Figure 1.7: SHH Signalling Pathway Mutations in BCC Mutations of the tumour suppressor gene *PTCH* are found in the nevoid basal cell carcinoma (NBCC) patients, sporadic and Xeroderma Pigmentosum (XP). BCCs present mutations of *PTCH* as well as the proto-oncogenes *SHH* and *SMO*. Over expression of downstream target genes such as *GLI-1* is also implicated in BCC development. Modified from (Daya-Grosjean and Couvé-Privat, 2005)**.**

1.10 Mouse Models of Basal Cell Carcinoma

Basal cell carcinomas, the commonest human skin cancers, consistently have abnormalities of the hedgehog signalling pathway and often have *PTCH* gene mutations (Undén et al., 1997). There are so many mouse models of BCC have been developed to help understand how BCCs may form (Aszterbaum et al., 1999). The *Ptch* mutant mice provide the first mouse model, to our knowledge, of ultraviolet and ionizing radiation-induced basal cell carcinoma-like tumours, and also demonstrate that *PTCH* inactivation and hedgehog target gene activation are essential for basal cell carcinoma tumorigenesis (Aszterbaum et al., 1999)**.** In one study $Ptch^{+/-}$ mice develop primordial follicular neoplasms resembling human trichoblastomas, and when they expose to ultraviolet radiation or ionizing radiation results in an increase in the number and size of these tumours and a shift in their histologic features so that they more closely resemble human basal cell carcinoma (Mancuso et al., 2004). Like human BCCs, mouse trichoblastoma and BCC-like tumours are composed of nests of basaloid cells with large nuclei, scant cytoplasm and few mitotic figures (Mancuso et al., 2004). Some of the mouse BCC and trichoblastoma tumour nests also have peripheral palisading and small cysts lined by cornified cells reminiscent of hair follicle structures (Mancuso et al., 2004). An *in vivo* study has shown that loss of *Ptch1* function in mouse skin is capable of inducing BCC formation (Adolphe et al., 2006). An inducible *Ptch1* knockout mouse system has demonstrated that the loss of *Ptch1* function from the basal cell population is sufficient to induce skin tumour formation that resembles BCC. This system differs to $Ptch^{+/-}$ mouse models that are UV irradiated to tumours therefore there may be non-specific effects of the UV radiation (Donovan, 2009, Daya-Grosjean and Couvé-Privat, 2005). The Adolphe model shows that the targeted deletion of both *PTCH1* alleles is sufficient to induce BCC-like tumour formation which implies that specifically the loss of *PTCH1* is function is important for tumour formation.

Further downstream of the HH pathway, mice over expressing GLI1 were able to develop tumours that share a resemblance to BCCs (Nilsson et al., 2000a). Interestingly, mice over expressing an activated mutant form of GLI2 which is a positive regulator of GLI1 developed multiple BCCs (Sheng et al., 2002, Grachtchouk et

al., 2000). GLI2 studies in mice show that over expression of the protein in hair follicle stem cells leads to nodular BCC formation compared to GLI2 over expression in the IFE which leads to a more superficial BCC phenotype (Grachtchouk et al., 2000). Other components of the HH pathway have been investigated including SUFU. SUFU knockdown in mice results in embryonic death but *SUFU+/-* mice develop characteristics that can be found in Gorlins patients such as jaw keratocysts. Fibroblasts derived from *SUFU-/-* mice were shown to have elevated levels of GLI1 mediated HH signalling which implies that loss of SUFU function leads to ligand independent HH activity (Svärd et al., 2006). Mouse studies where GLI2 is over expressed reveals the development of multiple BCCs which suggests that GLI2 is a potent oncogene. These tumours strongly resemble human BCCs in their histology and express various BCC markers. HH components such as *PTCH*1, GLI1 and GLI2 were increased at the mRNA level in the tumours but not the epidermis. As HH ligand is not detected in human BCCs, this suggests that tumours can arise independently of the HH ligand (Grachtchouk et al., 2000).

1.11 Cell Senescence and Basal Cell Carcinoma

1.11.1 Cell senescence

Cell senescence is defined as the physiological process of terminal cell growth arrest, it can be due to alteration of telomeres or by different forms of stress causing DNA damage. This process is also called replicative senescence, it is thought to be tumour suppressive mechanism and underlying cause of aging and Longevity. This process is also known as the Hayflick Phenomena or Hayflick limit in honour of Dr. Leonard Hayflick. In 1961 Dr.Leonard Hayflick and his colleague Dr.Paul Morehead, discovered that many human cells particularly fibroblasts had a limited capacity to divide in culture (Hayflick and Moorhead, 1961). They found that these and many other normal human cells derived from fetal, embryonic or newborn tissues can divide for 40-60 division and after that they stop growing (Dimri et al., 1995b). Senescent cells are characterised by an enlarged cell size, flattened morphology, inability to synthesize DNA and expression of the biomarker senescence associated β-galctosidase (Dimri et

al., 1995b). Hayflick also pointed out that there are two types of cells normal mortal cells and immortal cancer cells. Dr Hayflick and his colleagues only worked with fibroblast, a cell type found in connective tissues, but replicative senescence can be found in other cells of the body includes, keratinocytes, endothelial cells, lymphocytes, adrenocortical cells, vascular smooth muscle cells, chondrocytes cells etc. The exception exists in certain cancer cell lines where the cells never reach replicative senescence, these are said to be`` immortal cells'' and include embryonic germ cells and most cell lines derived from tumours, such as HeLa Cells. The reason for appearance of β-Galactosidase staining during replicative senescence is increase in the level of Lysosomal enzyme (Kurz et al., 2000).

Another type of senescence is called oncogene induced senescence (OIS). This is a form of cellular senescence that represents a physiological response that restricts the progression of benign tumours into their malignant counterparts e.g. nevi to melanoma or adenoma to adenocarcinoma. This mechanism is very crucial for protection against cancer development (Serrano et al., 1997, Lowe et al., 2004). The two main pathways of OIS mostly involve p16INK4a-RB (retinoblastoma) and ARF-p53 (Campisi, 2005). These two pathways are very crucial for tumour suppression and are often mutated in tumours (Hollstein et al., 1991, Ruas and Peters, 1998b, Sharpless and DePinho, 1999a). The tumour-suppressor pathway formed by the *Cdkn2a* locus (Arf) and by p53 (also called Trp53) plays a central part in the detection and elimination of cellular damage, and this constitutes the basis of its potent cancer protection activity (Ander et al., 2007). Arf was originally identified as an alternative transcript of the Ink4a tumour suppressor locus (Jes et al., 2006). Its expression levels are normally low, but transcription of Arf is highly induced when oncogenes are introduced into normal cells. On this basis, Arf is regarded as a protein specialized in communicating to p53 what has been called "oncogenic stress," a term that encompasses the array of cell perturbations produced by oncogenes (Matheu et al., 2008). The Arf/p53 pathway protects cells against several types of damage and this is the basis of its tumour suppressor activity. Interestingly, aging is a process associated with the accumulation of damage derived from chronic stresses of small magnitude. In agreement with its damage protection role, it has been recently described that the

Arf/p53 pathway not only protects mammalian organisms from cancer but also from aging. The ability of p53 to induce cell growth arrest and apoptosis is relatively well-understood, and its importance in tumour suppression is firmly established. The activities of pRb and p53 are dramatically increased during cellular senescence and inactivation of these proteins in senescent mouse embryonic fibroblasts (MEFs) results in reversal of the senescent phenotype leading to cell-cycle re-entry, suggesting that pRb and p53 are required not only for the onset of cellular senescence, but also for the maintenance of the senescence programme in murine cells (Takahashi et al., 2007). In human cells, once pRb is fully engaged, particularly by its activator, p16INK4a, senescent growth arrest becomes irreversible and is no longer revoked by subsequent inactivation of pRb and p53 (Takahashi et al., 2007). The p16INK4a tumour suppressor protein functions as an inhibitor of CDK4 and CDK6, the D-type cyclin-dependent kinases that initiate the phosphorylation of the retinoblastoma tumour suppressor protein, RB (Ohtani et al., 2004). Thus, p16INK4a has the capacity to arrest cells in the G1-phase of the cell cycle and its probable physiological role is in the implementation of irreversible growth arrest termed cellular senescence (Ohtani et al., 2004). In contrast to normal cells, the function of the p16INK4a gene or its downstream mediators is frequently deregulated in many types of human cancers, illustrating the importance of cellular senescence in tumour suppression. The $p16^{INK4a}$ cyclin-dependent kinase inhibitor has a key role in establishing stable G1 cell-cycle arrest through activating the retinoblastoma (Rb) tumour suppressor protein pRb in cellular senescence. Akiko Takahashi et.al. (2007) shows the $p16^{INK4a}$/Rb-pathway also cooperates with mitogenic signals to induce elevated intracellular levels of reactive oxygen species (ROS), thereby activating protein kinase Cδ (PKCδ) in human senescent cells (Takahashi, 2007). This irreversible cytokinetic block is likely to act as a second barrier to cellular immortalization ensuring stable cell-cycle arrest in human senescent cells (Takahashi, 2007).

1.10.2 What causes cell senescence

Cellular senescence (**see Figure 1.8**) is a state of irreversible growth arrest and altered function of normal somatic cells after finite number of cell division normally after 50 cell divisions (Dimri et al., 1995b). It's basically a general process that occurs as

response to stress and DNA damage (d'Adda di Fagagna et al., 2004). The first major cause of senescence was telomere shortening leading to telomere dysfunction (Campisi, 2005, Shay and Wright, 2005, Zglinicki et al., 2005). Recent studies show that other stress signals cause senescence and these include oxidative stress, oncogene activation (Serrano et al., 1997, Lowe et al., 2004), cytotoxic drugs (Roninson, 2003, Schmitt, 2003) and DNA damage (Prescott and Blackburn, 1999, Ventura et al., 2007).

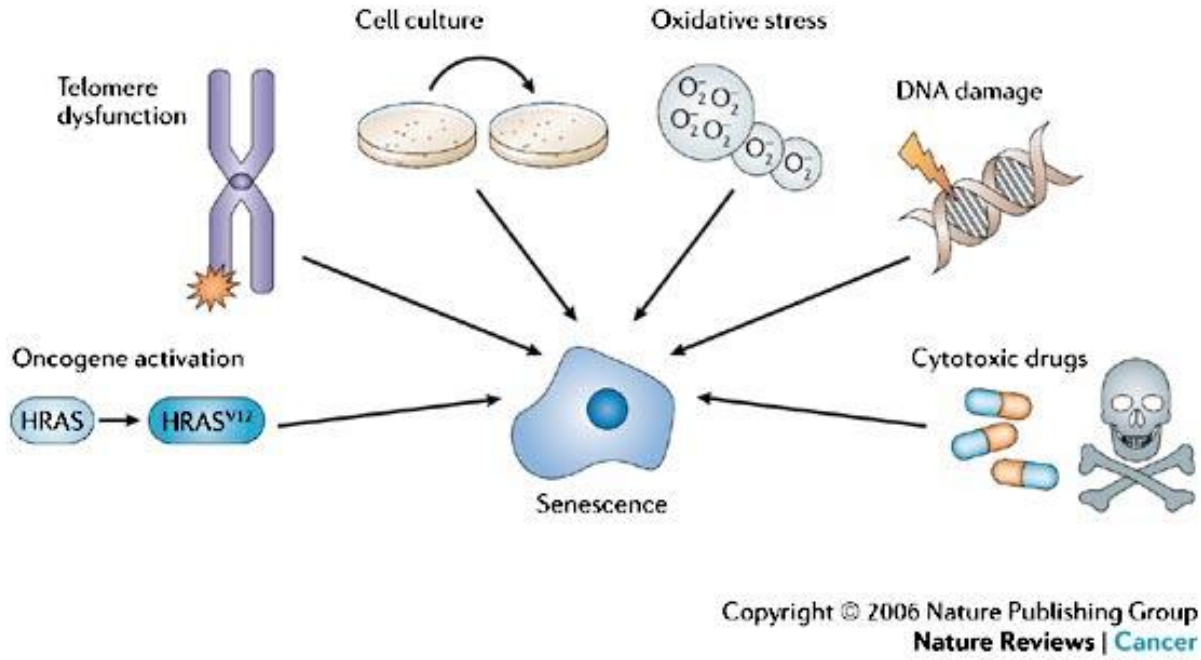

Copyright © 2006 Nature Publishing Group
Nature Reviews | Cancer

Figure 1.8: Showing the various factors that are known to cause Cell Senescence (Collado and Serrano, 2006).

1.11.3 Markers of cell senescence

Collado and Serrano 2006 haven identified a number of cell markers that are associated with cell senescence (**Table 1.2**) (Collado and Serrano, 2006).

Table: 1.2: Summary of best established Markers of Cell Senescence. Collado et al.(2006).

Marker	Assay
SA-β-Gal	Immunohistochemistry (IHC)
$p16^{INK4a}$	Western Blot (WB), IHC
$p15^{INK4b}$	WB, IHC
p53	WB, IHC
ARF	WB, IHC
$p21^{WAF1}$	WB, IHC
SAHFSs	Immunofluorescence (IF)
DEC1	WB, IHC
DCR2	WB, IHC

1.11.3.1 Decoy Receptor 2(DcR2)

DcR2 (decoy receptor) also known as TRAIL-4 and TNFRSF10D is one of the tumour necrosis factor related apoptosis-inducing ligand (TRAIL) receptors and suppresses TRAIL inducing apoptosis and also has a role regulating chemosensitivity (Liu et al., 2005). It's expression like other TRAIL receptors including DR4, DR5 and DcR1 is regulated by p53.

1.11.3.2 Differentially Embryo-chondrocyte Expressed Gene (DEC1)

DEC1 (differentially embryo-chondrocyte expressed gene) in humans; also known as SHARP2 (enhancer of split and hairy related protein) in rat, BHLHB2 and Stra13 (stimulated with retinoic acid) in mouse is a basic helix-loop helix (bHLH) transcription factor (Yamada and Miyamoto, 2005). It is a member of subfamily of basic helix-loop-helix transcription factors along with DEC2.These BHLH transcription factors are proteins functionally associated with development events such as cell proliferation, differentiation, myogenesis, neurogenesis (Villares and Cabrera, 1987), sex determination (Cronmiller et al., 1988), regulation of immunoglobulin genes (Beckmann et al., 1990), phospholipids metabolism (Nikoloff et al., 1992), xenobiotic response (Hirose et al., 1996) and lineage commitment (Yamada and Miyamoto, 2005). DEC1 functions as transcription repressor by directly binding to class B E-boxes (Li et al., 2003). The human DEC1 is highly expressed in many tissues including some tumour tissues and tumour derived cell lines (Fujimoto et al., 2001, Ivanova et al., 2001, Zawel et al., 2002). Yuxin et al. (2002) has shown that DEC1 is expressed in colon cancer but not in the surrounding normal tissues (Li et al., 2002a).

1.11.3.3 $p16^{INK4a}$

$p16^{INK4a}$ is a member of cyclin-dependent kinase inhibitors (CDKIs) also known as CDKN2A and is tumour suppressor gene. $p16^{INK4a}$ is an inhibitor of CDK4 and CDK6 and prevents phosphorylation of pRB protein and cell-cycle arrest in the G1 phase. $p16^{INK4a}$ is an important tumour suppressor among the four INK4 family members and is inactivated in many human tumours. The CDK4 gene is also mutated in gliomas, mesotheliomas, nasopharyngeal, pancreatic, biliary tract tumours and acute lymphoblastic leukaemia's (Boukamp, 2005), melanomas and breast cancer (Borg et al., 2000). The main factor which distinguishes $p16^{INK4a}$ from other members of INK4 family is its capacity to be unregulated in response to senescence and oncogene stress.

1.11.3.4 $p15^{INK4b}$

$p15^{INK4b}$ is a member of cyclin-dependent kinase inhibitor and encoded in humans by CDKN2 locus on chromosome 9p21.2. $P15^{INK4b}$ is highly homologous with $p16^{INK4a}$. Along with $p16^{INK4a}$ it play major role in the regulation of cell cycle. By inhibiting the activity of CDK4 and CDK6 to inactivate the retinoblastoma (Rb) family of tumour suppressors. The expression of this gene is induced by TGF beta, which suggest a role in TGF beta induced growth inhibition.

1.11.3.5 $p21^{WAF1}$

p21 is a member of CIP/KIP family of cyclin-dependent kinase inhibitors which also include INK4. It was first member of this family that was simultaneously cloned from different sources. These CDKIs commonly negatively regulate cell cycle. The members of this family of proteins are found in complex with the cyclin D, cyclin E and cyclin A-dependent kinases.

1.11.3.6 p53

p53 is a tumour suppressor protein that in humans is encoded by the TP53 gene located on the short arm of chromosome 17 (17p 13.1). p53 regulates cell cycle and functions as tumour suppressor and is involved in the prevention of cancer. p53 plays an important role in transcription, DNA repair, genomic stability, apoptosis and cell senescence (Prives and Hall, 1999, Ko and Prives, 1996). Due to this quality, this protein is also known as the guardian of the genome and also the master watchman. p53 is the most commonly mutated or deleted gene in human cancer and has typical ultraviolet induced changes (C---T and CC—TT nucleotide changes) (Ziegler et al., 1993). p53 has a dual role in regulating cell growth because it can induce cell cycle arrest and apoptosis as well.

1.11.3.7 β-galactosidase.

The most widely used assay for senescence is the cytochemical detection of β-galactosidase activity at pH 6.0, termed senescence-associated β-galactosidase (SA-β-Gal) (Dimri et al., 1995a). This is derived from the increased lysosomal content of

senescent cells, which enables the detection of lysosomal β-galactosidase at a suboptimal pH, pH 6.0 (pH 4.0 is optimal) (Kurz et al., 2000). β-Galactosidase activity is generally accepted as a marker of senescence both *in vitro* and *in vivo*, although its biochemical basis is still unknown and there is evidence for a positive SA-β-Gal reaction in settings of cellular stress that are unrelated to senescence, such as serum withdrawal or high confluence in cell culture (Yang and Hu, 2004). Its activity is normally assayed in cultured cells or tissue sections using the chromogenic substrate 5-bromo-4-chloro-3-indolyl β-D-galactopyranoside (X-Gal), or the fluorescent analogue fluorescein-di-β-D-galactopyranoside (FDG) (Severino et al., 2000).

1.8 Aims of Study

Background:

BCCs are relatively stable at the genomic level and although, a number of BCC subtypes are recognised and these can be grouped into benign and aggressive tumours very little is known about the molecular differences between these subtypes. OIS is known to play an important role in tumorigenesis and is a characteristic of pre-malignant lesions of many cancers. Although pre-malignant lesions have not been described for BCC it is possible that OIS may be a key feature of more benign BCCs and that loss of OIS may explain the more aggressive subtypes.

Hypothesis:

That over-expression of the HH signalling pathway in BCC results in OIS and that loss or down regulation of OIS may characterise more aggressive from benign BCC subtypes.

Aim:

The aim of the work in my thesis is to determine the expression pattern of senescent markers in non-aggressive and aggressive subtypes and using in vitro cell culture see whether this is associated with up regulation of HH signalling

Chapter 2: Materials and Methods

2.1 Tissues collection and Sectioning

2.1.1 Paraffin Embedded Human BCC and Normal Human Skin Tissue Blocks

BCC tumour and normal human facial skin sample blocks were taken from the tissue archive of the Department of Dermatology, Royal London Hospital and ethical permission for this study was obtained from the East London and The City Local Research Ethics Committee (Ethics NO: 08/H0704/65) with informed consent from all patients. The average age of the patients was 63.5 and out of this 7 patients were male and 8 were female (**SEE Appendix 1**). The blocks were randomly selected from the archive. The diagnosis of these blocks was checked by looking at the histopathological report of the patients and this was carried out by a qualified dermatopathologist Professor Rino Cerio. The inclusion criteria for this project was to include only nodular (non aggressive) and morphoeic (aggressive) BCC subtypes. The tumour and normal skin sections were cut by the Pathology core facility Blizard Institute, Queen Mary University of London on a Shandon Finesse E+ microtome (Thermo Scientific, Germany). 3µm sections were cut and placed on superfast plus glass slides (VWR).

2.1.2 Fresh Frozen BCC Samples

Fresh biopsies of BCC tissues were taken from department of dermatology of Royal London Hospital from patients being treated for excisional surgery to remove BCC. The patients were contacted before surgery for donation of their tissues for this project. After excisional surgery biopsy specimens were snap frozen in liquid nitrogen for better preservation and then kept at -80Ċ until required for use. The average age of the patients was 63 and out of this 11 patients were male and 10 were female (**SEE Appendix 2**). Before cutting the tissues, embedding was performed using a Bright Cryospray 134 (Bright Instrument, Huntingdon, UK). The sections were cut by the Pathology core facility Blizard Institute of Cell and Molecular Sciences, Queen Mary University of London on a Shandon cryotome E product number 0620E(Thermo Scientific). 4µm sections were placed on superfast plus glass slides (VWR).

2.1.3 Mouse BCC, wild type *Ptch* +/+ Skin and *Ptch* +/- Skin

Mouse BCC tumour and *Ptch*1 Mouse +/+ and +/- skin sample blocks were provided by Mariateresa Mancuso from Biotechnology Unit and Radiation Protection Unit, ENEA-Ente per le Nuove Tecnologie, l'Energia e l'Ambiente, Centro Ricerche, Casaccia, Rome, Italy. This group have generated Mice lacking one *Ptch*1 allele, through targeted disruption of exons 6 and 7 in 129/SV ES cells and maintained on CD1 background (Mancuso et al., 2004). Mancuso et al performed X-ray irradiation **(HVL _ 1.6 mmCu)** on these mice using a Gilardoni CHF 320G X-ray generator (Gilardoni S.p.A.; Mandello de Lario Lecco, Italy) operated at 250 kVp, 15 mA, with filters of 2.0 mm of A1 and 0.5 mm of Cu. *PTCH*1$^{neo67/+}$ mice and wild-type littermates of both sexes were whole-body irradiated with 3 Gy of X-rays as newborns (4 days of age) or adults (90 days of age). In addition, 2-month-old mice were subjected to local irradiation of the dorsal skin with a single dose of 4 Gy of X-rays. Briefly, anesthetized mice were radially positioned on a lead plate, and shaped lead shields were placed on each mouse to provide protection to the body parts to be spared. A dorsal skin area of 3 cm^2 was irradiated through a central trapezoidal window of a lead shield (4-mm thickness, 60 mm in length). The shield was accurately positioned on the anesthetized mouse using its tail insertion as reference. Mice were inspected daily and at the first sign of morbidity or when tumours were visible were sacrificed and complete autopsies performed. A piece of grossly normal appearing dorsal skin with an area of 5 cm^2, corresponding to the site of local irradiation or an equivalent area of macroscopic-tumour-bearing skin, was fixed in 4% buffered formalin. Normally tumours appear in irradiated mice 60 to 90 weeks post irradiation. Skin biopsies from these mice were sent to the Centre for Cutaneous Research for use in this project and sections were cut by Pathology core facility Blizard Institute, Queen Mary University of London on a Shandon Finesse E+ (Thermo Scientific, Germany). 3µm sections were placed on superfast plus glass slides (VWR).

2.2 β -Galactosidase Assay

β-galactosidase assay was carried out using either a commercial kit supplied by cell signalling technology (Senescence β-Galactosidase Staining Kit Cell SignallingTechnology, 166B Cumming Center, Beverly, MA 01915). In addition to the commercial kit we also carried out β-galactosidase assay using individual reagents. The reason for carrying out the β-galactosidase assay using individual reagents was one of cost. The β-galactosidase assay is a simple assay but the kits are expensive. In contrast the individual reagents are more cost effective and as a result most groups within my Institute prepare their own reagents.

2.2.1 β-Galactosidase assay for cell senescence carried out using the commercial β-galactosidase Staining Kit

β-galactosidase staining using the commercial kit (**Appendix 3**) was carried out according to the manufacturers instruction as follows:-

Frozen tissue sections on glass slides were taken from -80c freezer and kept at room temperature for 15 minutes. Then the slides were put in cold acetone for 15 minutes. After this slides were fixed in 1X Fixative Solution for 10-15 minutes at room temperature. Then the slides were washed for two times with 1X PBS. After that β-Galactosidase Staining Solution was placed on the tissue sections and the slides were incubated at 37°C overnight in a dry incubator (no CO2). While the β-Galactosidase Staining Solution is still on the tissue sections, the slides were checked under a microscope for the development of blue colour. Once blue colour was seen the slides were washed in PBS to remove the β-Galactosidase Staining Solution and then counter stained with haematoxylin after which the slides were kept at room temperature.

2.2.2 β-galactosidase assay using individual laboratory reagents.

The basis of the β-galactosidase assay is straightforward. β-Gal is an essential enzyme that catalysis β-galactosidase into monosaccharides. When it is expressed it reacts with X-gal which forms a blue precipitate. When β-Gal activity is observed at pH 6 it is characteristic of senescent cells and is not found in pre-senescent, quiescent or immortal cells. To save cost we therefore decided to use commercially available

reagents to develop our town β-galactosidase assay. The reagents used are shown in **Appendix 4**.

8µM frozen sections were cut by the pathology core facility Blizard Institute and kept in the -80 freezer until required for future work. The sections were taken out from the -80c freezer and left at room temperature for 15 minutes. Sections were fixed with 0.2% (v/v) glutaraldehyde (1ml of 25% (v/v) glutaraldehyde) mixed with PBS (125ml) (PAA Laboratories GmbH) for 5 minutes at room temperature. Slides were then washed with PBS (PAA Laboratories GmbH) for 5 minutes. After that tissue sections were incubated with x-gal solution for 24-72 hr at 37°c without CO_2. Tissues were checked every 6hr to detect any blue staining of the tissues. In senescent tissues blue staining normally appears after 24 hr. When the blue staining appeared the X-Gal solution was removed and sections washed in PBS. After that tissues were counterstained with Haematoxylin mounted with glass cover slips.

2.3 Immunohistochemistry (IHC) for Human and Mouse BCC tissues.

2.3.1 Immunohistochemistry Protocol

Reagents used for immunohistochemistry are shown in **Table 3.1.** Tissue sections were washed in Xylene twice (2X) for two minutes for dewaxing. After that tissue sections were washed in Alcohol (Industrial Methylated Spirits (IMS) 2X for two minutes. Then the tissue sections were washed in tap water for five minutes. Antigen retrieval (**see Table 2.2**) was carried out using the Antigen Unmasking solution (VECTOR Laboratories) at pH 6.0 in microwave oven at different times for different antibodies, as follows GLI-1, DEC1, p53 (35 minutes microwave oven) and for $p15^{INK4b}$ the pH was 9.0 (35 minutes in microwave oven) and $p16^{INK4b}$, $p21^{WAF1}$ (35 and 30 minutes in microwave oven respectively).

After antigen retrieval tissue sections were washed in tap water for 5 minutes. Endogenous peroxidise was blocked with Hydrogen Peroxide 3% (v/v) for 15 minutes in distilled water. Tissue sections were then washed in tap water for 5 minutes and then further washed with wash buffer (Dako wash buffer 10x,Dako) for 5 minutes. Normal Horse Serum R.T.U. VECTASTAIN Universal Elite ABC KIT (VECTOR Laboratories) was used for blocking tissue sections and was applied to the slides for 20 minutes. Primary antibodies for human skin sections (**see Table 2.3**) and mouse skin sections (**see Table 2.4**) were then applied to the slides and incubated at room temperature for 1 hour.

Tissue sections were then washed in wash buffer (Dako wash buffer 10x, Dako) twice (2X) for two minutes. Secondary antibodies were then applied to the slides as shown in **Table 2.3** for human skin sections and **Table 2.4** for mouse skin sections and incubated for 45 minutes at room temperature. Tissue section were then washed with Dako wash buffer 10x (Dako) twice (2X) for two minutes. ABC Reagent R.T.U. VECTASTAIN Universal Elite ABC KIT (VECTOR Laboratories) was applied to the slides for 30 minutes at room temperature. Tissue sections were then washed with Dako wash buffer for 2X for two minutes. Liquid DAB substrate was added to the slides (1ml substrate buffer + 1 drop of DAB chromogen) for DAB staining for 5 minutes. Slides were washed in tap water for 5 minutes. Sections were counter stain with Haematoxylin on immuno

program in staining machine (Thermo Scientific Shandon Varistain® Gemini ES) (running tap water 2 minutes, Gills HX 2 minutes, running tap water 5 minutes, acid alcohol 10 seconds, running tap water 5 minutes, IMS 2 minutes 3X and Xylene 2 minutes for 3X). Cover slips were then placed on the slides and sections observed using light microscopy.

Table 2.1: Reagents used for the immunohistochemistry

1	Xylene 100%
2	Alcohol 100%
3	Antigen Unmasking Solution H-3300 and H-3301, Vector Laboratories, UK
4	Tris Citrate EDTA Buffer PH8.1 (**See Appendix-5**)
5	Pap PEN
6	3% Hydrogen Peroxide, Product VWR-BDH Prolabo, UK
7	Dako Real™ Antibody Diluent, Code S2022
8	R.T.U Vectastain® Universal Elite ABC Kit, PK-7200, Vector Laboratories, UK
9	Dak Wash Buffer 10X, S3006 Immunohistochemistry, Dako UK Ltd
10	Liquid DAB Substrate, HK130-5K, HK542-XAK, BioGenex, U.S.A.

Table 2.2: Antigen Retrieval Solution and Conditions

Proteins	**Antigen Retrieval Solution and Conditions**
GLI-1	Antigen Unmasking Solution H-3300 Vector Laboratories, UK, 35min MW.
DcR2	Antigen Unmasking Solution H-3300 Vector Laboratories, UK, 20 minMW.
DEC1 (SHARP2)	Antigen Unmasking Solution H-3300 Vector Laboratories, UK, 35min MW.
p53	Human Tissues: Tris Citrate EDTA Buffer PH8.1, 35min MW. Mouse Tissues: The section were incubated in 0.1% trypsin in 0.1% $CaCl_2$ (pH 7.8) for 10 minutes at 37°C.
$p16^{INK4a}$	Antigen Unmasking Solution H-3300 Vector Laboratories, U.S.A, 30min MW.
$p15^{INK4a}$	Antigen Unmasking Solution, H-3301 Vector Laboratories, U.S.A, 35min MW.
$p21^{WAF1}$	Antigen Unmasking Solution H-3300 Vector Laboratories, U.S.A, 30min MW

Table 2.3: Primary and Secondary Antibodies used for Immunohistochemistry on Human BCC and Human Skin.

Proteins	**Primary Antibody and Dilution**	**Secondary Antibody and Dilution**
GLI-1	GLI-1 , rabbit polyclonal IgG, 200 µg/ml, (H-300): sc-20687, Santa Cruz, U.S.A, 1:500 overnight incubation	Prediluted Biotinylated Universal Secondary Antibody (recognize mouse and rabbit), Vector Laboratories, U.S.A.
DcR2	DcR2 rabbit polyclonal antibody, AAP-371, Assay Designs, U.S.A, 1:50 1hour incubation.	Prediluted Biotinylated Universal Secondary Antibody (recognize mouse and rabbit), Vector Laboratories, U.S.A.
DEC1(SHARP2)	Anti-SHARP2 Rabbit, S 8443, S-8443, Sigma Aldrich, U.S.A, 1:100 1hour incubation.	Prediluted Biotinylated Universal Secondary Antibody (recognize mouse and rabbit), Vector Laboratories, U.S.A.
p53	Anti-p53(Ab-6)(Pantropic) Mouse mAb (DO1), OP43, Merck4Biosciences, UK, 1:50 1hour incubation.	Prediluted Biotinylated Universal Secondary Antibody (recognize mouse and rabbit), Vector Laboratories, U.S.A.
$p16^{INK4a}$	$p16^{INK4a}$ (C-20)Rabbit Polyclonal Antibody, sc-468, Santa Cruz, U.S.A, 1:100 1hour incubation.	Prediluted Biotinylated Universal Secondary Antibody (recognize mouse and rabbit), Vector Laboratories, U.S.A.
$p15^{INK4b}$	$p15^{INK4b}$ Polyclonal Antibody, 4822, Cell Signalling, U.S.A, 1:100 1hour incubation	Prediluted Biotinylated Universal Secondary Antibody (recognize mouse and rabbit), Vector Laboratories, U.S.A.
$p21^{WAF1}$	Purified Mouse Anti-Human, $p21^{WAF1}$ BD Pharmingen™ 1:100 dilution, 1 hour incubation	Prediluted Biotinylated Universal Secondary Antibody (recognize mouse and rabbit), Vector Laboratories, U.S.A.

Table 2.4: Primary and Secondary Antibodies use for Immunohistochemistry on Mouse BCC and Mouse *Ptch*1 +/+ and +/- Skin**.**

Proteins	**Primary Antibody and Dilution**	**Secondary Antibody and Dilution**
GLI-1	GLI-1 rabbit polyclonal IgG, 200 µg/ml, (H-300): sc-20687, Santa Cruz, U.S.A, 1:500 overnight incubation	Biotinylated Anti-Rabbit IgG (H+L) Goat , Catalog Number BA-1000, Vector Laboratories, 1:200 1 hour incubation
DcR2	DcR2 rabbit polyclonal antibody, AAP-371, Assay Designs, U.S.A, 1:50 1hour incubation.	Biotinylated Anti-Rabbit IgG (H+L) Goat , Catalog Number BA-1000, Vector Laboratories, 1:200 1 hour incubation
DEC1(SHARP2)	Anti-SHARP2 Rabbit, S 8443, S-8443, Sigma Aldrich, U.S.A, 1:100 1hour incubation.	Biotinylated Anti-Rabbit IgG (H+L) Goat , Catalog Number BA-1000, Vector Laboratories, 1:200 1 hour incubation
p53	Rabbit Polyclonal Antibody p53 Protein (CM5), NCL-p53-CM5p, Leica Microsystem, UK, 1:100 1hour incubation.	Biotinylated Anti-Rabbit IgG (H+L) Goat , Catalog Number BA-1000, Vector Laboratories, 1:200 1 hour incubation
$p16^{INK4a}$	$p16^{INK4a}$ (C-20)Rabbit Polyclonal Antibody, sc-468, Santa Cruz, U.S.A, 1:100 1hour incubation.	Biotinylated Anti-Rabbit IgG (H+L) Goat , Catalog Number BA-1000, Vector Laboratories, 1:200 1 hour incubation
$p15^{INK4b}$	$p15^{INK4b}$ Polyclonal Antibody, 4822, Cell Signalling, U.S.A, 1:100 1hour incubation	Biotinylated Anti-Rabbit IgG (H+L) Goat , Catalog Number BA-1000, Vector Laboratories, 1:200 1 hour incubation
$p21^{WAF1}$	$p21^{WAF1}$ (DCS60) Mouse mAb, Cell Signalling, U.S.A, 1:100 1hour incubation	Prediluted Biotinylated Universal Secondary Antibody (recognize mouse and rabbit), Vector Laboratories, U.S.A.

2.3.2 Visual Analogue Score

The intensity of staining was analysed by visual analogue score which is normal practice of histopathologists (**see Table 2.5 and 2.6**) (Harvey et al., 1999). The scoring was carried out blind by Professor Rino Cerio (Dermatopathologist) of Royal London Hospital. Statistical analysis of this score was carried out using GraphPad Prism Software (La Jolla, CA 92037 USA) and data was plotted on excel sheet to compare Morphoeic with Nodular BCC. The same criteria were used for visual analogue scoring between mouse and human samples. Scoring was carried out as follows 0 is no staining, 1 is up to 30% staining (weak), 2 is between 30% to 60% (moderate) 3 is staining greater than 60% (strong).

Table 2.5 Visual Analogue Scoring of Immunohistochemical staining for human tissues.

0	No Staining
1	Weak Staining
2	Moderate Staining
3	Strong Staining

Table 2.6 Visual Analogue Scoring of Immunohistochemical staining for mouse tissues.

No Staining	0
Weak Staining	1
Moderate Staining	2
Strong Staining	3

2.4 NEB-1 Cell Culture

2.4.1 Cell Culture

All cell culture was performed in a laminar flow cabinet hood under aseptic conditions in accordance with standard tissue culture technique. All sterile disposable tissue culture flasks, plates and dishes were purchased from thermo fisher scientific (NY, USA). For tissue culture all centrifuge steps were using an IEC Centra-3C Centrifuge (International Equipment Company, Dunstable, U.K). Reagents used for the culture of NEB-1 keratinocytes are shown in **Table 2.7.**

NEB1 immortalised keratinocytes were used to generate the *in vitro* BCC model. NEB1 cells originate from early epidermal keratinocytes and are immortalised using HPV16 (Morley et al., 2003). NEB1 cells were retrovirally transduced with *PTCH* shRNA construct 189A that targets exon 24 of *PTCH* mRNA. A scramble control vector was used as a control. NEB1 GLI-1 cells were generated using the pBabePuro retrovirus, with NEB1 pBP cells used as an empty vector control. All cell lines were made by Muhammad Rahman PhD Student Center for Cutaneous Research.

NEB1 cells were cultured in keratinocyte growth medium (KGM) consisting of Alpha MEM (450ml) and heat inactivated foetal bovine serum 10% (Lonza, Slough, UK), L-glutamine (7ml) and penicillin/streptomycin (5ml) (PAA Laboratories, Somerset, UK). The KGM supplement was made up of epidermal growth factor (EGF) 10µg/ml, hydrocortisone 0.5µg/ml, insulin (bovine pancreas) 5µg/ml, adenine (5ml) and cholera toxin (0.5mls) (Sigma, Poole, UK). Cells were incubated at 37°c in an atmosphere 5% CO2/95% air. For growing these cells the tissue culture media was changed after the 3rd or 4th day. When the cells reached 70% confluence they were washed once with sterilised PBS. After washing with the PBS the cells were trypsinised to count and split for other procedures or frozen down for future work. For trypsinisation 3ml trypsin/EDTA (PAA Laboratories) was added to each flask which was left in the 37^{0}c incubator to detached the cells from flask. When cells were detached, 5ml KGM media was added to inhibit the trypsinisation. After that cells were transferred to a falcon tube and centrifuged at 1300rpm for 5 minutes at room temperature, then supernatant was discarded and the cell pellet was re-suspended in PBS and cells were

counted and divided for different experimental procedures including, cell staining, qPCR while remaining cells were frozen down in freezing media (10% (v/v) DMSO in FBS) for future work.

Table 2.7: Reagents used for the culture of NEB-1 keratinocytes.

Materials used for cell culture	Company
αMEM	Lonza, Switzerland
KGM Supplement (**See Appendix 6**)	
Penicillin, Streptomycin and L-Glutamine	Sigma-Aldrich, St. Louis, MO
Trypsin-EDTA	PAA, Dartmouth, MA
Foetal Bovine Serum (FBS)	Lonza, Switzerland
Haemocytometer	Kisker Biotech GmbH, Germany
Inverted semi confocal Microscope	Nikon, Japan
6 well plates, pipettes, T75 and T25 flasks	Thermo Fisher scientific, NY,USA
NEB1 Keratinocytes Cells	1. Cancer Research UK Cell Structure Research Group, Dundee University School of Life Sciences and 2. Centre for Cutaneous Research, Bart's and the London Queen Mary's School of Medicine and Dentistry, UK
All plastic ware and culture flasks	Nunc/Thermo Fisher scientific, NY, USA

2.4.2 Cell Counting

After trypsinisation cells (10µl of cell suspension) were counted using a haemocytometer. The Haemocytometer 4x4 grid and each square contains sixteen squares. The cells within these squares were counted. The formula used for counting cells per ml is to multiply the number of cells counted by 10^4.

2.5 Immunofluorescence (IF) Microscopy.

2.5.1 Protocol for Immunofluorescence Microscopy

Reagents used for immunofluorescence are shown in **Table 2.8.** Cells were washed in PBS for 2X for 5 minutes. Then the cells were fixed in 4% (v/v) Para formaldehyde for 15 minutes. The cells were washed for 3X for 5 minutes with PBS. Cells were then permiablised in PBS-Triton (0.1% (v/v) triton x 100) for 10 minutes. After that cells were blocked with 3% (v/v) BSA at room temperature for 30 minutes. Primary and secondary antibodies used for immunofluorescence are shown in **Table 2.9**. All these antibodies (dilution 1:1000 in 3% (v/v BSA) were applied and the control was left in 3% (v/v) BSA in cold room for overnight. The cells were washed in PBS three times for 5 minutes. Secondary antibody was applied (dilution 1:1000) and left at room temperature for 1 hour and kept in dark. The cells were washed with PBS three times for 5 minutes and kept in dark. Cells were counter stained with DAPI (dilution 1ul of DAPI with 5 ml of dH_2O) for 5 minutes. The cells were washed once with PBS. Slides were mounted and cover slips applied. Analysis was carried out using a confocal microscope.

Images were quantified using Image J software. Cells were selected and analysed based on the intensity of pixels taking into account the size of the cell. The relative density was then calculated which indicates the intensity of staining.

Table 2.8: Reagents Used for IF are shown below.

1	PBS
2	4% Paraformaldehyde
3	Triton (0.1% Triton X100) permiablised in PBS
4	3% BSA
5	DAPI
6	Mount Medium

Table 2.9: Primary and Secondary Antibodies for Immunofluorescence Microscopy.

Proteins	**Primary Antibody and Dilution**	**Secondary Antibody and Dilution**
GLI-1	GLI-1 Goat Polyclonal Antibody, (H-300): sc-20687, Santa Cruz, U.S.A, 1:500 overnight incubation	Alexa Fluor® 488 Rabbit anti-goat A-11078, Invitrogen, UK, 1:1000 1hour dilution
DcR2	DcR2 rabbit polyclonal antibody, AAP-371, Assay Designs, U.S.A, 1:500 overnight incubation.	Alexa Fluor® 488 Goat anti-rabbit A-11008, Invitrogen, UK, 1:800 1hour incubation.
DEC1(SHARP2)	Anti-SHARP2 Rabbit, S 8443, S-8443, Sigma Aldrich, U.S.A, 1:500 overnight incubation.	Alexa Fluor® 488 Goat anti-rabbit A-11008, Invitrogen, UK, 1:800 1hour incubation.
p53	Anti-p53(Ab-6)(Pantropic) Mouse mAb (DO1), OP43, Merck4Biosciences, UK, 1:500 overnight incubation.	Alexa Fluor® 488 goat anti-mouse $IgG_{2b,}$ Invitrogen, UK, 1:800, 1 hour incubation.
$p16^{INK4a}$	$p16^{INK4a}$ (C-20)Rabbit Polyclonal Antibody, sc-468, Santa Cruz, U.S.A, 1:500 overnight incubation.	Alexa Fluor® 488 Goat anti-rabbit A-11008, Invitrogen, UK, 1:800 1hour incubation.
$p15^{INK4b}$	$p15^{INK4b}$ Polyclonal Antibody, 4822, Cell Signalling, U.S.A, 1:500 overnight incubation	Alexa Fluor® 488 Goat anti-rabbit A-11008, Invitrogen, UK, 1:800 1hour incubation.
$p21^{WAF1}$	Purified Mouse Anti- Human $p21^{WAF1}$, BD Pharmingen™, UK, 1:500 overnight dilution.	Alexa Fluor® 488 goat anti-mouse $IgG_{2b,}$ Invitrogen, UK, 1:800, 1 hour incubation.

2.6 RNA Extraction and cDNA Synthesis

2.6.1 RNA Extraction

Reagents for RNA extraction are shown in **Table 2.10**. For total RNA extraction cells were grown in 6cm dishes. When the cells had reached enough (75% confluence), the medium was removed and cells were washed with PBS (PAA Laboratories GmbH). After that 350 µl of RLT buffer from RNeasy Plus mini kit (QIAGEN) & Beta-mercaptoethanol (10µl) were added, to lyse the cells. The cells and supernatant were removed from dish and placed in the QIAshredder spin column (QIAGEN) and centrifuged for 2 minutes at maximum speed. The lysate was transferred to a gDNA eliminator spin column (QIAGEN), and centrifuged for 30sec at 10,000rpm. After that the column was discarded and the flow through saved and added to 1 volume (350µl) of 70% (v/v) ethanol. I transferred 700 µl of this flow through to an RNeasy spin column and centrifuged at 10,000rpm for 15seconds. The flow through was discarded and the RNeasy spin column saved I then added 700µl of buffer RW1 to the column and centrifuged at 10,000rpm for 15seconds. The flow through was discarded and I saved the RNeasy spin column and added 500µl of buffer RPE to the column and centrifuged it for 2 minutes at 10,000rpm speed to wash the spin column. Finally, the RNeasy spin column was put in a new 1.5ml collection tube and I added 50µl of RNease free water and centrifuged it for 1minute at 10,000rpm to recover the RNA.

The concentration of RNA was quantified using a Nanodrop Spectrophotometer ND 1000 (Labtech International Ltd, East Sussex, UK). First of all I used 1 µl RNAse DNA free water to clean and take a standard blank reading. After that 1µl RNA was used to measure the concentration (ng/µl) of RNA.

2.6.2 cDNA synthesis

Reagents for cDNA synthesis are shown in **Table 2.10**. For making cDNA a SuperScript® VILO™ cDNA synthesis kit (Invitrogene™)was used. This kit contains 5X VILO Reaction mix (4µl), 10X Superscript Enzyme mix (2µl). The other reagents needed for making cDNA included RNA (up to 2.5µg) and DEPC treated water. The total reaction volume for making cDNA was 20µl. The following protocol was employed using a thermal cycler (PTC-100 Peltier-Effect Cycling, MJ Research Inc, USA) shown below (**see Table: 2.11**).

Table 2.10: Reagents for RNA extraction and cDNA synthesis are shown below.

1	RNeasy Mini kit QIAGEN, WS, UK
2	RNase free-DNase kit QIAGEN, WS, UK
3	NanoDrop® UV spectrophotometer Thermo-Scientific, DE, USA
4	SuperScript® VILO™ cDNA Synthesis kit Invitrogen, Paisley, UK
5	DNA engine PCR machine MJ Research(Bio-Rad),Hercules, CA

Table 2.11: Conditions for cDNA reaction.

Temperature (Ċ)	**Time (minutes)**
25 Ċ (initial heating)	10
42 Ċ (cDNA synthesis)	1 hrs
85 Ċ (RT inactivation)	5

2.7 Quantitative real time-polymerase chain Reaction (qPCR)

2.7.1 qPCR Protocol

Quantitative Real Time-Polymerase Chain Reaction (qPCR) is a method based upon the principles of the Polymerase Chain Reaction (PCR). The primers were designed by using the primer 3 online tool (**Table 2.12**) (Rozen and Skaletsky, 1999). For qPCR a fluorescent dye is used, such as SYBR Green. The master mix used for the reaction is bought from Sigma (SYBER® Green JumpStart™ Taq Ready Mix Cat# S4438) and protocol performed using guidelines provided by the manufacturer of the kit. . For all the qPCR experiments the master mix was prepared using the following components tabulated in **Appendix 7**. The program for all the PCR varied only with the annealing and extension times all the other parameters are the same.

1. 95 ^{0}C for 15min (Enzyme activation).

2. 95 ^{0}C for 15sec (Denaturation).

3. X ^{0}C for 20 sec (X-varies according to primers. (Tm Annealing step).

4. 72 ^{0}C for Xsec (X-varies depending on the product size (extension step- For normal PCR a final extension step at 72 ^{0}C for 10min was used) b, c and d steps were repeated for 40times.

5. For qPCR melting curve parameters was set from 55 ^{0}C to 95 ^{0}C at a 1 sec rampage.

Each sample or standard was performed in triplicate. An amplification curve for each sample is obtained based on the levels of fluorescence present in each amplification cycle. The software detects the fluorescence threshold cycle (Ct) during the PCR when the level of fluorescence provides a signal over the background and is in the linear portion of the amplified curve. This Ct value is responsible for the accurate quantification of qPCR. The final stage of the run is a dissociation curve, which is used to assess the homogeneity of the PCR products, including the presence of primer dimers, thereby determining the specificity of the PCR reaction. During the melting analysis the green fluorescence signal is acquired continuously as the samples are melted at 95^{o}C, cooled to 60^{o}C and then quickly heated again to 95^{o}C. As a result of

the melting, SYBR Green molecules are released from the denatured DNA, drastically decreasing fluorescence signal. In order to visualise the dissociation curve as a peak, the negative first derivatives are also plotted.

2.7.2 Primers

The mRNA sequences were taken from the NCBI Gene database for the human variant. If there are multiple isoforms for a single gene, all sequences were analysed using the Clustal W program (http://www.ebi.ac.uk/Tools/msa/clustalw2/) which is a sequence alignment tool. Primers would then be designed for an area where mRNA sequences match between all the isoforms. The sequence is then put into the Primer 3 software (http://frodo.wi.mit.edu/) which generates a number of primer pairs. These primer sequences were then checked manually with the mRNA sequence and also via a nucleotide BLAST search (http://blast.ncbi.nlm.nih.gov/) to determine if the primers are specific to gene of interest. Primers used are shown in **Table 2.12**.

Table 2.12: Primers and their sequences

Gene	Forward	Reverse	Temperature	Product Size
GAPDH	GTGAACCATGAGAAGTATGACA	CATGAGTCCTTCCACGATACC	60	123
DcR2	AGCTGAAGGGTGTCAGAGGA	GACTGTTTCTTCCAGGCTGC	63	254
DEC1	CTCTTCAGTTTGGGAGCTGG	AACCACTACCGTGCTATGCC	63	194
$p16^{INK4a}$	TGCCTTTTCACTGTGTTGGA	GCCATTTGCTAGCAGTGTGA	60	184
$p21^{INK4b}$	TTAGCAGCGGAACAAGGAGT	GCCGAGAGAAAACAGTCCAG	58	1296
p53	GTCACTGCCATGGAGGAGCCGCA	GACGCACACCTATTGCAAGCAAGGGTTC	58	225

2.8 Statistical Analysis

Statistical analysis was performed using Excel and GraphPad Prism and calculated as a Student's t-test and Two-way Analysis of Variance (ANOVA) for three independent Variants. The significance level was assessed as a probability value of $P<0.05$ (95% confidence).

Chapter 3: Expression of senescence markers and their quantification in normal human skin and in BCC.

3.1 Expression of β-Galactosidase in normal human skin and BCC.

β-galactosidase staining was carried out on frozen tissue sections of basal cell carcinoma (BCC) collected from the dermatology clinics at The Royal London Hospital. Frozen sections were used for β-galactosidase assay as formalin fixation denatures the β-galactosidase enzyme and as a result the colorimetric assay would not work. When cells undergo senescence they normally change their morphology and β-galactosidase staining at pH6, is widely recognized as an accepted marker of senescent cells (Dimri et al., 1995a). BCCs have a number of different morphological sub-types (see introduction) and I have attempted to investigate β-galactosidase staining on these different types of BCC to determine whether senescence is characteristic of all BCC types or perhaps only restricted to specific groups. One aspect of my hypothesis being that the more benign BCC subtypes would exhibit senescence and that this is lost in more aggressive subtypes. To investigate this I used a panel of 21 BCC samples of different BCC types; these are summarised in **Table 3.1** and full demographics shown in **Appendix 2**, in addition I used 7 normal skin biopsies in order to enable me to compare β-galactosidase staining between normal skin and BCC. The staining when present took 24 hours to develop. Results of these experiments are shown in **Figure 3.1** which shows β-galactosidase staining in normal skin (including epidermis and hair follicle), Nodular BCC (**see Figure 3.2**), Morphoeic BCC (**see Figure 3.2**) and Infiltrative BCC (**see Figure 3.2**). The staining protocol was the same for all BCC samples. The slides were visually analysed to observe the pattern of staining. The staining for β-galactosidase was observed in most of BCC samples investigated but in normal skin was mainly restricted to the hair follicles and especially the outer root sheath (ORS). Staining for β-galactosidase was also observed in the sebaceous and eccrine sweat glands of normal skin. In BCC sections the staining was mostly seen in the stroma of BCC when compared to the epithelium and this was the same for the different types of BCC. However, in nodular BCC the β-galactosidase staining was also seen in the epithelial palisading cells when compared to morphoeic and infiltrative BCC types in which the tumour epithelium was mainly negative for β-galactosidase.

Table 3.1: Summary of BCC Samples used for β-Galactosidase Staining

BCC Type	Numbers of Tumours
Nodular BCC	10
Morphoeic BCC	3
Infiltrative BCC	3
Superficial BCC	3
Micronodular BCC	1
Nodular/Micro Nodular BCC	1
Normal Skin	7

β-galactosidase assay was carried out on frozen section of different BCC types as shown above. The demographic details of the individual patients are shown in **Appendix 2**. Normal skin was redundant from cosmetic surgery and as far as we are aware the patients had no skin disease.

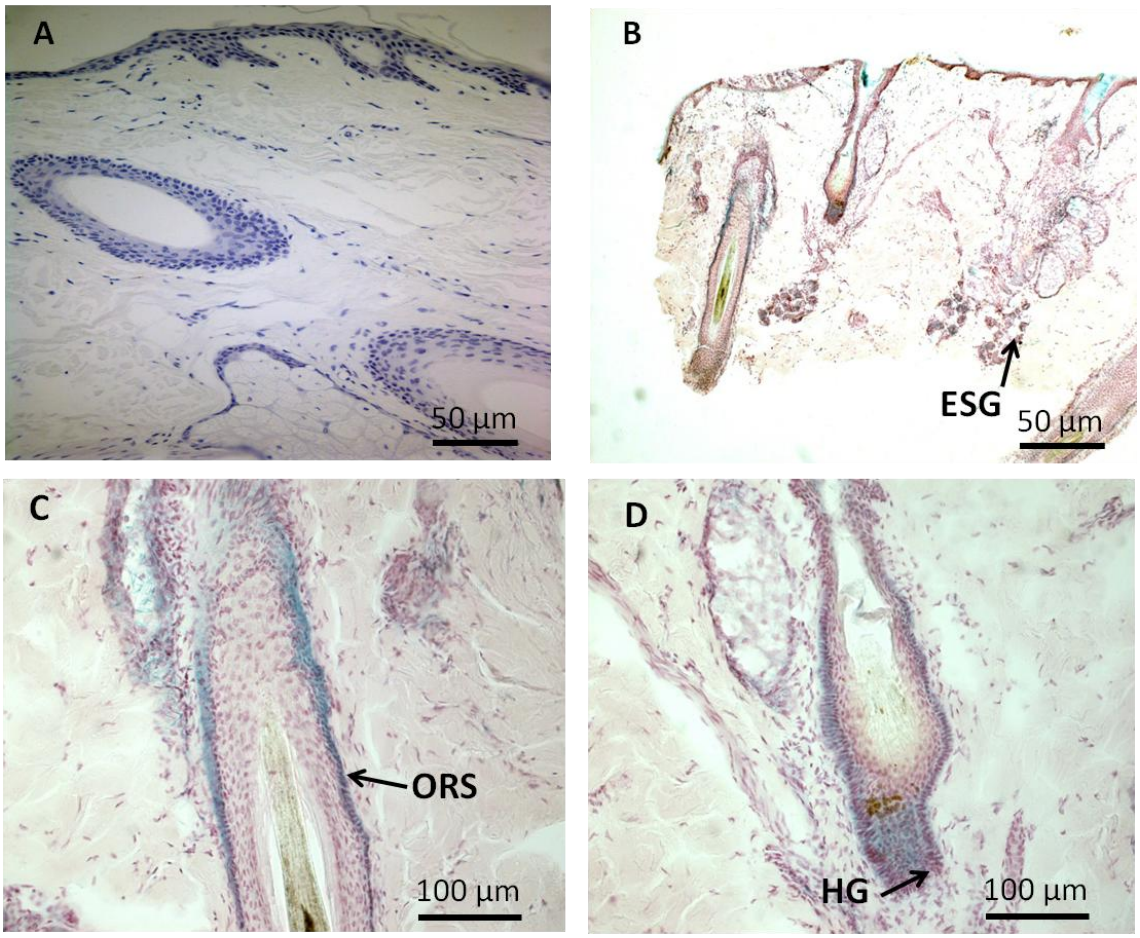

Figure 3.1: Expression of β-Galactosidase in normal human skin. (A) is Negative control (B) Normal human skin. β-galactosidase staining is seen mostly in hair follicles and eccrine sweat gland (ESG). In the hair follicle β-galactosidase staining is restricted to the outer root sheath (ORS) of the hair follicle and secondary hair germ (HG) of the resting telogen hair follicle.

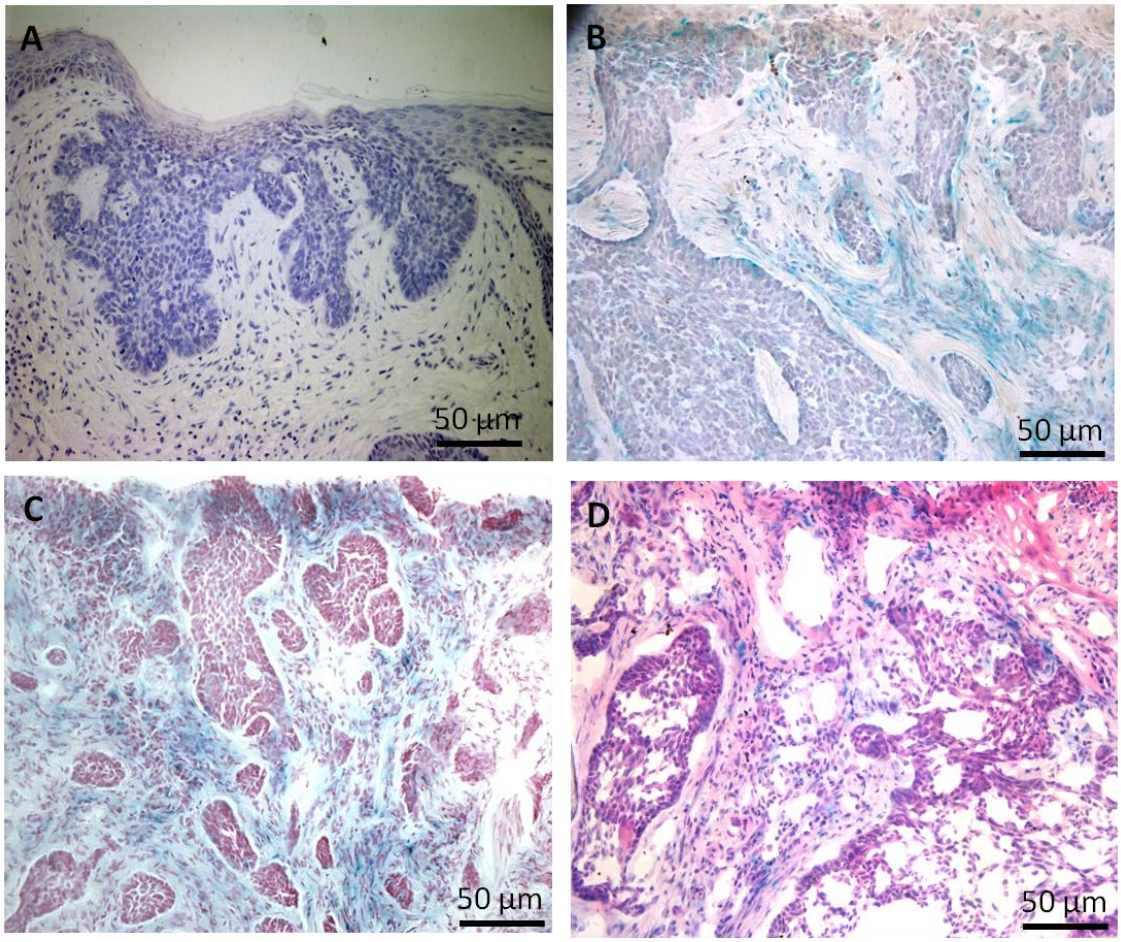

Figure 3.2: Representative images showing β-galactosidase staining in different BCC subtypes including (A) Negative Control (B) Nodular BCC (C) Morphoeic BCC and (D) Infiltrative BCC. Results show that β-galactosidase staining appears to be restricted to the stroma of different BCC subtypes and only occasionally expressed in tumour epithelium.

3.2 Immunohistochemical Analysis of Senescence Markers in Basal Cell Carcinoma of Skin.

Using β-galactosidase assay on frozen sections of different BCC types I observed that staining for β-galactosidase was mainly restricted to the stroma. To investigate this further immunohistochemical analysis of senescence markers was carried out on paraffin wax embedded BCC. I chose to investigate two of different types of BCC, Nodular BCC is non aggressive and whereas, Morphoeic BCC is considered an aggressive sub-type of BCC. To determine whether these BCC subtypes shows expression of cell senescence and also whether senescence may be more characteristic of either benign or aggressive BCC subtypes. The senescence markers used for this study-included $p16^{INK4a}$, $p15^{INK4b}$, $p21^{WAF1}$, p53, DcR2 and DEC1 as they have previously been reported to be good markers of senescence in tumours (Collado et al., 2005).

For the staining of BCC tissue I collected 15 different samples of nodular and morphoeic BCC and 7 normal skin. Expression of markers in BCC was also compared with normal human skin. Data was analysed by visual analogue scoring and was carried out blind by Professor Rino Cerio (**see section 2.3.4**). Data was plotted on an excel spreadsheet, Statistical analysis was carried out using GraphPad Prism Software (La Jolla, CA 92037 USA) with 95% confidence interval calculated as a Student's t-test (two variants) and Two-way Analysis of Variance (ANOVA) for three independent Variants. Raw data for visual analogue scoring of human BCC is shown in Appendix 8

3.2.1 GLI-1 Expression in BCC types

Initially I carried out staining for GLI-1 on these tissue sections. The results for GLI-1 are shown in **Figure 3.3**. GLI-1 staining was quite strong on the BCC samples. GLI-1 was detected on both the tumour epithelium and in the stroma of both nodular and morphoeic BCC subtypes. I have used normal skin as a control and that shows staining in epidermis and hair follicles.

Visual analogue scoring of the staining for GLI-1 in these tumours was carried out and the data analysed as mentioned in **chapter 2 (section 2.3.2)** by plotting the mean staining results with 95% confidence limits by subtype. **Figure 3.3 E** shows the results of data analysis comparing nodular with morphoeic BCC and as can be seen from this figure there was no significant difference between GLI-1 expression in nodular and morphoeic BCC subtypes.

I also compared differences in nuclear and cytoplasmic expression and epithelial with stroma staining for both Morphoeic (**see Figure 3.4**) and Nodular (**see Figure 3.5**) BCC subtypes. As can be seen from **Figure 3.4** there was no significant difference between nuclear and cytoplasmic GLI-1 in morphoeic BCC (**see Figure3.4A**) and from **Figure 3.4B** there was also no difference between epithelial and stromal expression of GLI-1.

Comparison between nuclear and cytoplasmic expression and epithelial with stroma for nodular BCC (**see Figure 3.5**) also showed no significant difference between nuclear and cytoplasmic expression of GLI-1 (**see Figure 3.5A**) or between epithelial and stroma staining in nodular BCC (**see Figure 3.5B**).

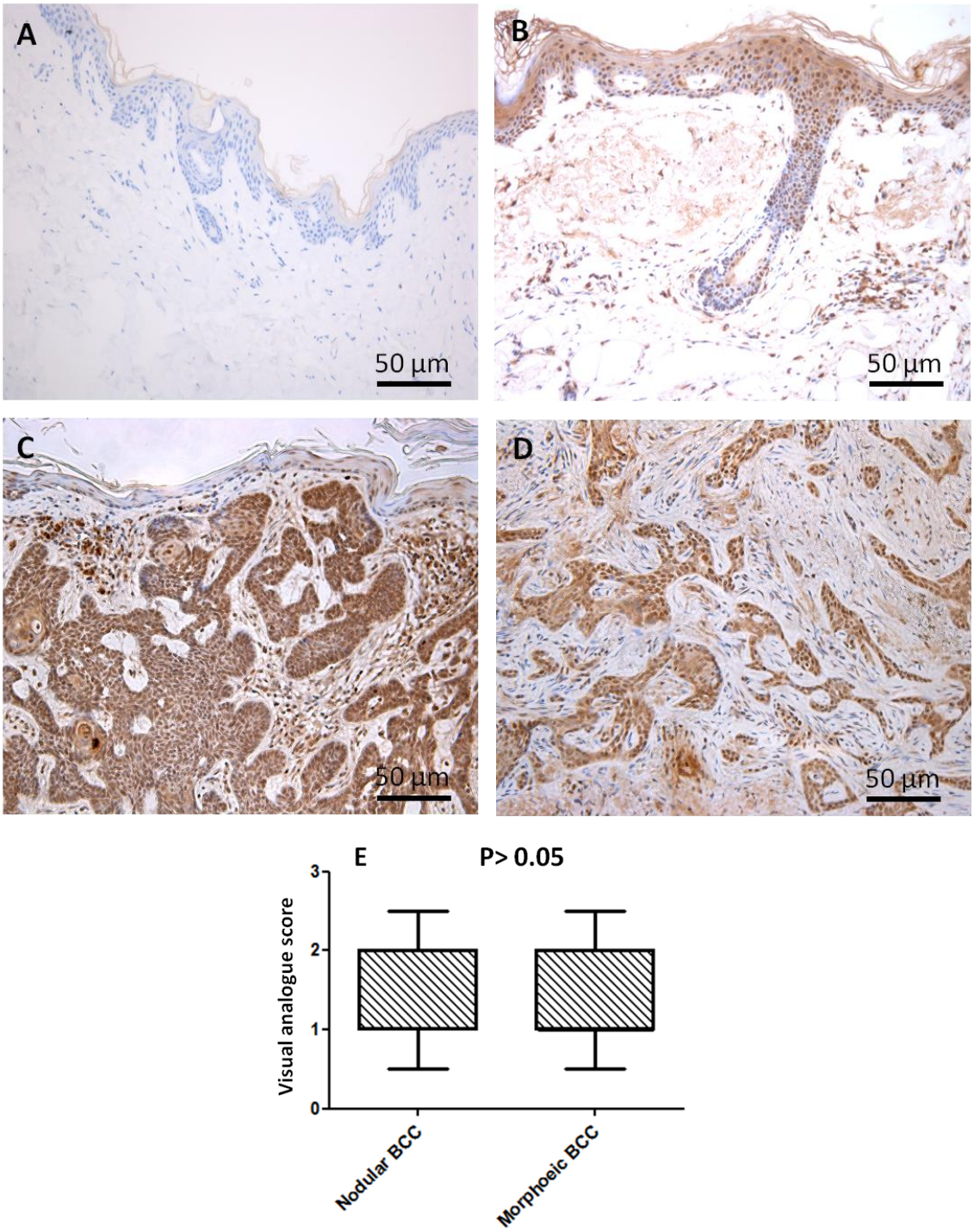

Figure 3.3: Representative images showing GLI-1 expression in (A) Negative Control (B) Normal skin (C) Nodular BCC (D) Morphoeic BCC. Visual analogue (E) scoring of total GLI-1 staining between nodular and morphoeic BCC showed no significant difference in GLI-1 expression between nodular and morphoeic BCC. Visual analogue scoring was carried out n=15 nodular and n=15 morphoeic BCC. Statistical analysis was carried out using student's t-test.

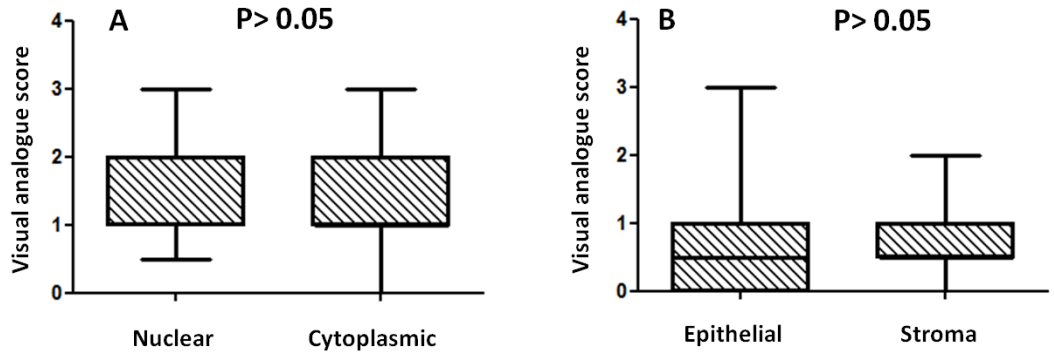

GLI-1 Staining in Morphoeic BCC

Figure 3.4: GLI-1 visual analogue scoring comparing (A) Nuclear versus Cytoplasm and (B) Epithelial versus Stroma expression of GLI-1 in Morphoeic BCC. The analysis shows no significant difference between nuclear and cytoplasmic GLI-1 and also no difference between epithelia and stroma. Statistical analysis was carried out using student's t-test (n=15 Morphoeic, n=15 Nodular).

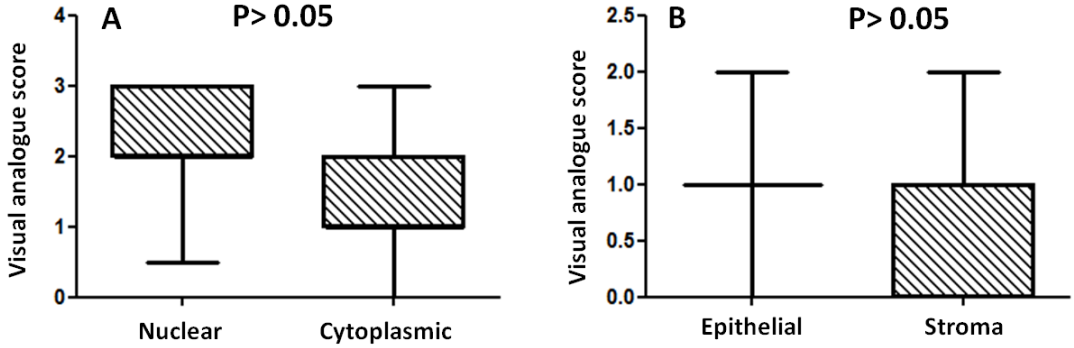

GLI-1 Staining in Nodular BCC

Figure 3.5: GLI-1 visual analogue scoring comparing (A) Nuclear versus Cytoplasm and (B) Epithelial versus Stroma expression of GLI-1 in Morphoeic BCC. The analysis shows no significant difference between nuclear and cytoplasmic also no difference between epithelial and stromal GLI-1. Statistical analysis was carried out using student's t-test (n=15 Morphoeic, n=15 Nodular).

3.2.2 Expression of DCR2 in normal skin and BCC

DcR2 (Decoy Receptor 2) stained positive on all BCC tissue sections of nodular and morphoeic BCC **(see Figure 3.6 C and D**) when compared with normal skin and negative control (**see Figure 3.6 A and B**). In both nodular and morphoeic BCC DcR2 staining is quite clearly seen in both the tumour epithelium of morphoeic BCC and in particular the palisading cells of nodular BCC. DcR2 was also seen in the stroma of both morphoeic and nodular BCC. With regards its subcellular localization DcR2 was seen in the nucleus and cytoplasm of both BCC subtypes.

Results of visual analogue scoring of DcR2 staining of these tumours were analysed (**as mentioned in chapter 2 section 2.3.2**) by plotting the mean staining results (with 95% confidence interval) by subtype. Visual analogue scoring between nodular and morphoeic BCC (**see Figure 3.6E**) shows that there was no significant difference in staining intensity between nodular and morphoeic BCC, but there was significant difference between BCC and normal skin ($P<0.05$) indicating a significant up regulation of DcR2 in BCC compared to normal skin.

In addition to the comparison between nodular and morphoeic BCC and normal skin I also compared by visual analogue scoring nuclear and cytoplasmic expression of DcR2 (**see Figure 3.7A**) and epithelial versus stroma expression in morphoeic BCC (**see Figure 3.7B**) and in nodular BCC (**see Figure 3.8A and 3.8B respectively**). **Figure 3.7** shows that in morphoeic BCC there was no significant difference between nuclear and cytoplasmic DcR2 staining. However, when epithelial versus stromal expression was analysed there was a significantly higher level of DcR2 expression ($P<0.05$) in the stroma of morphoeic BCC compared to epithelial expression. In the nodular BCC there was no significant difference between nuclear and cytoplasmic expression of DcR2 (**see Figure 3.8A**) or between epithelial and stromal expression (**see Figure 3.8B**). These data therefore, indicate up-regulation of DcR2 in the stroma of morpheic BCC.

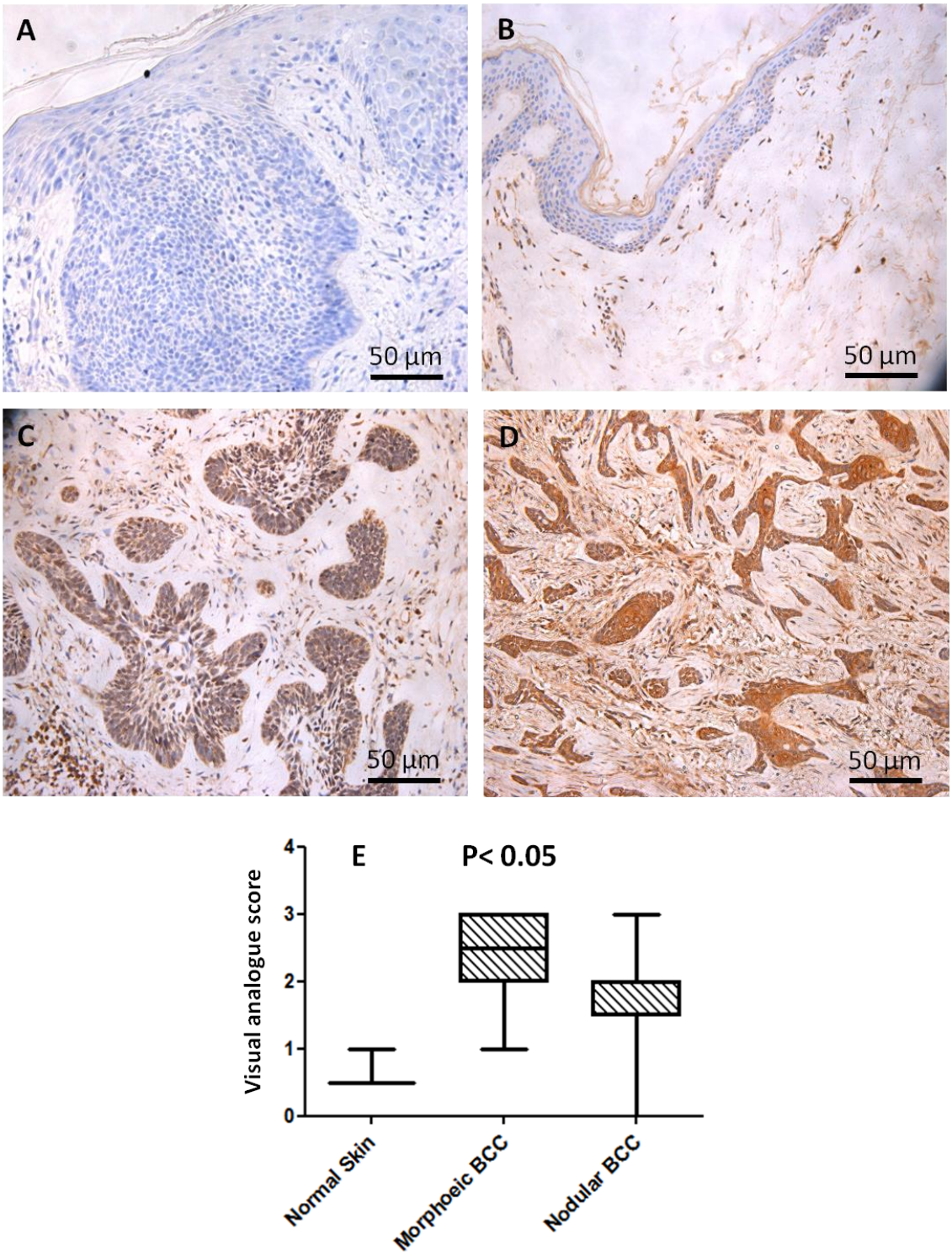

Figure 3.6: Representative images showing DcR2 expression in (A) Negative control (B) Normal Skin (C) Nodular and (D) Morphoeic BCC. Visual analogue (E) scoring of total staining between nodular and morphoeic BCC showed no significant difference of DcR2 expression, but there was a clear difference between normal skin and BCC types. Visual analogue scoring was carried out n=7 normal skin, n=15 nodular and n=15 morphoeic BCC. Statistical analysis was carried out using Two-way Analysis of Variance ANOVA.

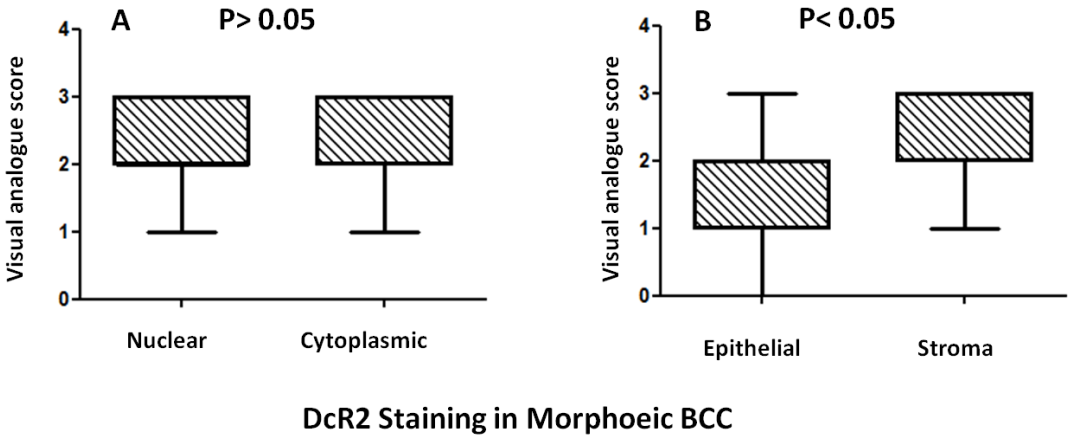

Figure 3.7: DcR2 visual analogue scoring comparing (A) Nuclear versus Cytoplasm and (B) Epithelial versus Stroma DcR2 expression in Morphoeic BCC. The analysis shows no significant difference between nuclear and cytoplasmic but there is a significant increase in stroma DcR2 when compared with epithelia expression. Statistical analysis was carried out using student's t-test.

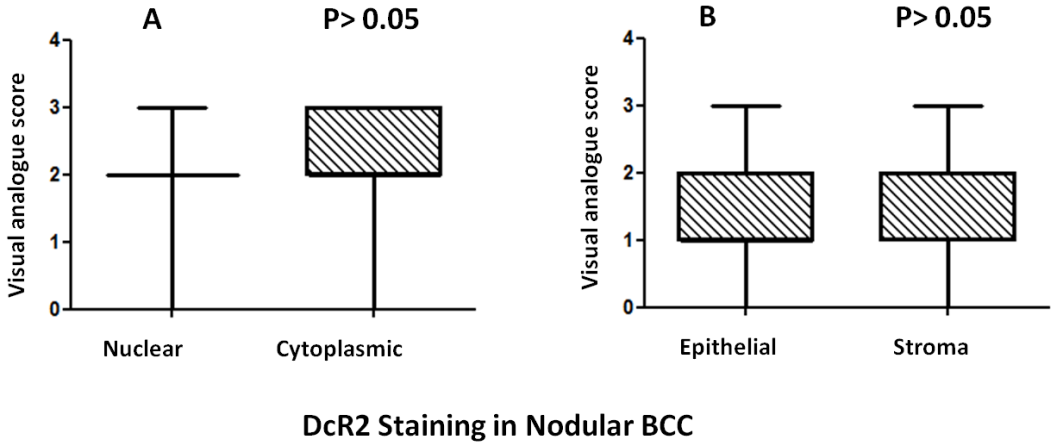

Figure 3.8: DcR2 visual analogue scoring comparing (A) Nuclear versus Cytoplasm and (B) Epithelial versus Stromal DcR2 expression in Nodular BCC. The analysis shows no significant difference between them. Statistical analysis was carried out using student's t-test.

3.2.3 Expression of DEC1 in normal skin and BCC

DEC1 stained positive on all BCC tissue sections of nodular and morphoeic BCC (**see Figure 3.9 C and D**) when compared with normal skin and negative control (**see Figure 3.9 A and B**). In both nodular and morphoeic BCC DEC1 staining is quite clearly seen in the both tumour epithelium of morphoeic BCC and in particular the palisading cells of nodular BCC. DEC1 was also seen in the stroma of both morphoeic and nodular BCC. With regards its subcellular localization DEC1 was seen in the nucleus and cytoplasm of both BCC subtypes.

Results of visual analogue scoring of DEC1 staining of these tumours were analysed (**as mentioned in chapter 2**) by plotting the mean staining results (with 95% confidence interval) by subtype. Visual analogue scoring between nodular and morphoeic BCC (**see Figure 3.9E**) shows that there was no significant difference in staining intensity between nodular and morphoeic BCC, but there was significant difference between BCC and normal skin ($P<0.05$) indicating a significant up regulation of DcR2 in BCC compared to normal skin.

In addition to the comparison between nodular and morphoeic BCC and normal skin I also compared by visual analogue scoring nuclear and cytoplasmic expression of DEC1 (**see Figure 3.10A**) and epithelial versus stroma expression in morphoeic BCC (**see Figure 3.10B**) and in nodular BCC **(see Figure 3.11A and 3.11B respectively**). **Figure 3.10** shows that in morphoeic BCC there was no significant difference between nuclear and cytoplasmic DEC1 staining. However, when epithelial versus stromal expression was analysed there was a significantly higher level of DEC1 expression ($P<0.05$) in the stroma of morphoeic BCC compared to epithelial expression. In the nodular BCC there was no significant difference between nuclear and cytoplasmic expression of DEC1 (**see Figure 3.11A**) or between epithelial and stromal expression (**see Figure 3.11B**). These data therefore, indicate and up-regulation of DEC1 in the stroma of morpheic BCC.

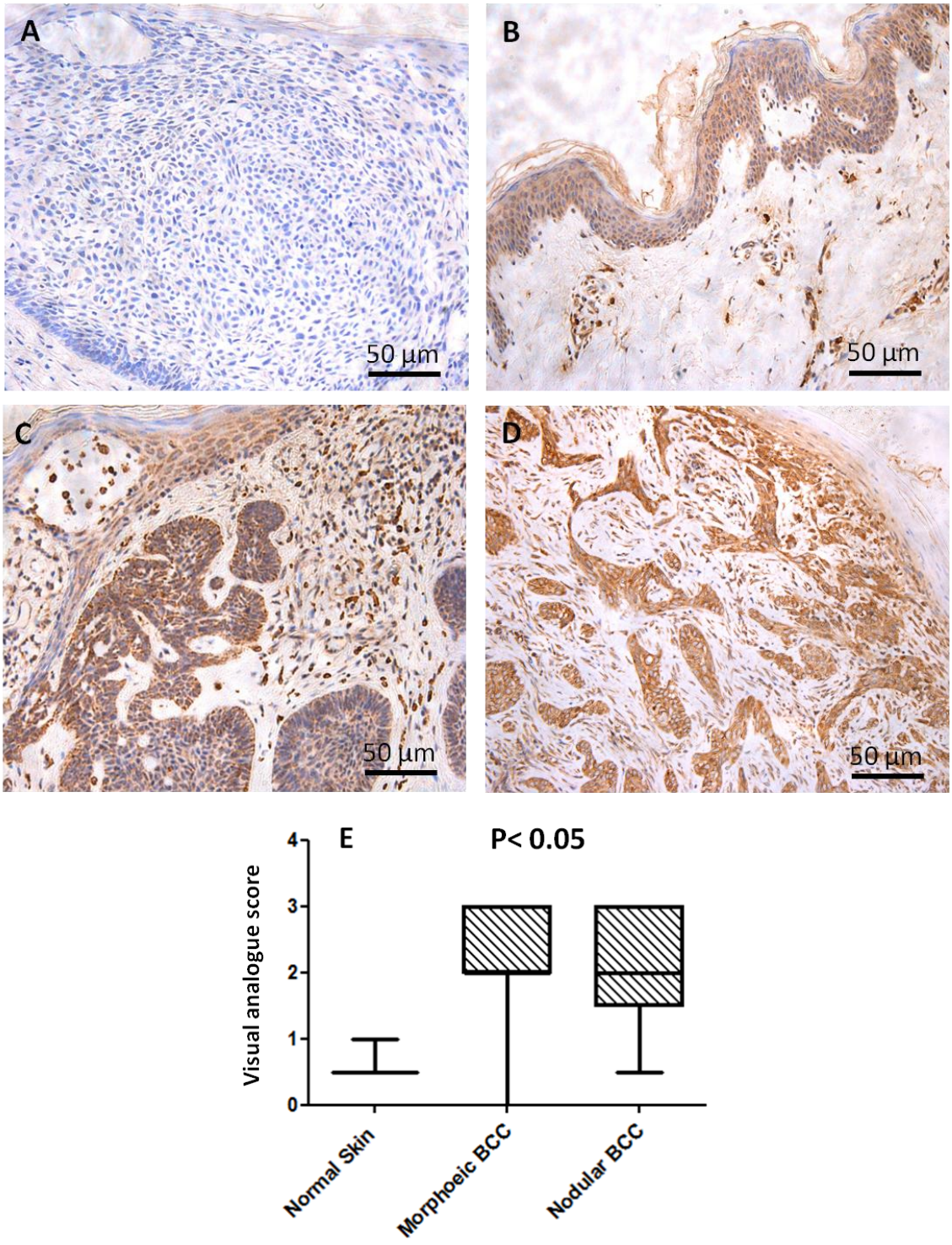

Figure 3.9: Representative images showing DEC1 expression in (A) Negative control (B) Normal Skin (C) Nodular (D) Morphoeic BCC and (E) Visual analogue. Visual analogue scoring of total staining between nodular and morphoeic BCC showed no significant difference in DcR2 expression, but there was a clear difference with normal skin when comparing with BCC types. Visual analogue scoring was carried out n=7 normal skin, n=15 nodular and n=15 morphoeic BCC. Statistical analysis was carried out using Two-way Analysis of Variance ANOVA.

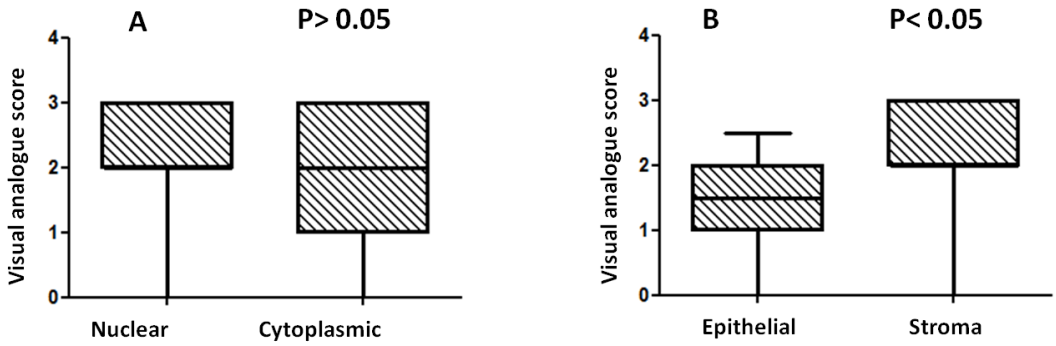

Figure 3.10: DEC1 visual analogue scoring comparing (A) Nuclear versus Cytoplasm and (B) Epithelial versus Stroma expression of DEC1 in Morphoeic BCC. The analysis shows no significant difference between nuclear and cytoplasmic expression but there is a significant increase in stromal DEC1 expression when compared to epithelial expression. Statistical analysis was carried out using student's t-test.

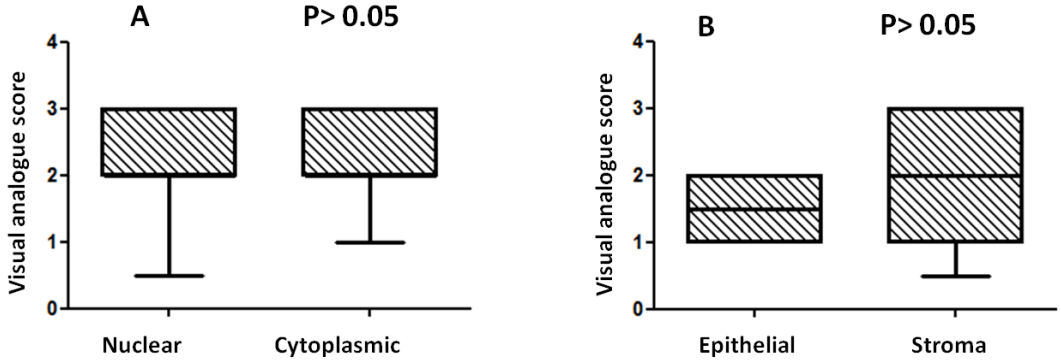

Figure 3.11: DEC1 visual analogue scoring comparing (A) Nuclear versus Cytoplasm and (B) Epithelial versus Stroma DEC1 expression in Nodular BCC. The analysis shows no significant difference between them. Statistical analysis was carried out using student's t-test.

3.2.3 Expression of $p16^{INK4a}$ in normal skin and BCC

$p16^{INK4a}$ stained positive on all BCC tissue sections of nodular and morphoeic BCC (**see Figure 3.12 C and D**) when compared with normal skin and negative control (**see Figure 3.12 A and B**). In both nodular and morphoeic BCC. $p16^{INK4a}$ staining is quite clearly seen in the both tumour epithelium of morphoeic BCC and in particular the palisading cells of nodular BCC. $p16^{INK4a}$ was also seen in the stroma of both morphoeic and nodular BCC. With regards its subcellular localization $p16^{INK4a}$ was seen in the nucleus and cytoplasm of both BCC subtypes.

Results of visual analogue scoring of $p16^{INK4a}$ staining of these tumours were analysed (**as mentioned in chapter 2**) by plotting the mean staining results (with 95% confidence interval) by subtype. Visual analogue scoring between nodular and morphoeic BCC (**see Figure 3.12E**) shows that there was no significant difference in staining intensity between nodular and morphoeic BCC, but there was significant difference between BCC and normal skin ($P<0.05$) indicating a significant up regulation of $p16^{INK4a}$ in BCC compared to normal skin.

In addition to the comparison between nodular and morphoeic BCC and normal skin I also compared by visual analogue scoring nuclear and cytoplasmic expression of $p16^{INK4a}$ (**see Figure 3.13A**) and epithelial versus stroma expression in morphoeic BCC (**see Figure 3.13B**) and in nodular BCC (**see Figure 3.14A and 3.14B respectively**). **Figure 3.13** shows that in morphoeic BCC there was no significant difference between nuclear and cytoplasmic $p16^{INK4a}$ staining and also there was no difference between epithelial versus stromal expression. In the nodular BCC there was no significant difference between nuclear and cytoplasmic expression of $p16^{INK4a}$ (**see Figure 3.14A**). However, when epithelial versus stromal expression was analysed there was a significantly higher level of $p16^{INK4a}$ expression ($P<0.05$) in the stroma of nodular BCC compared to epithelial expression (**see Figure 3.14B**). These data therefore, indicate and up-regulation of $p16^{INK4a}$ in the stroma of nodular BCC.

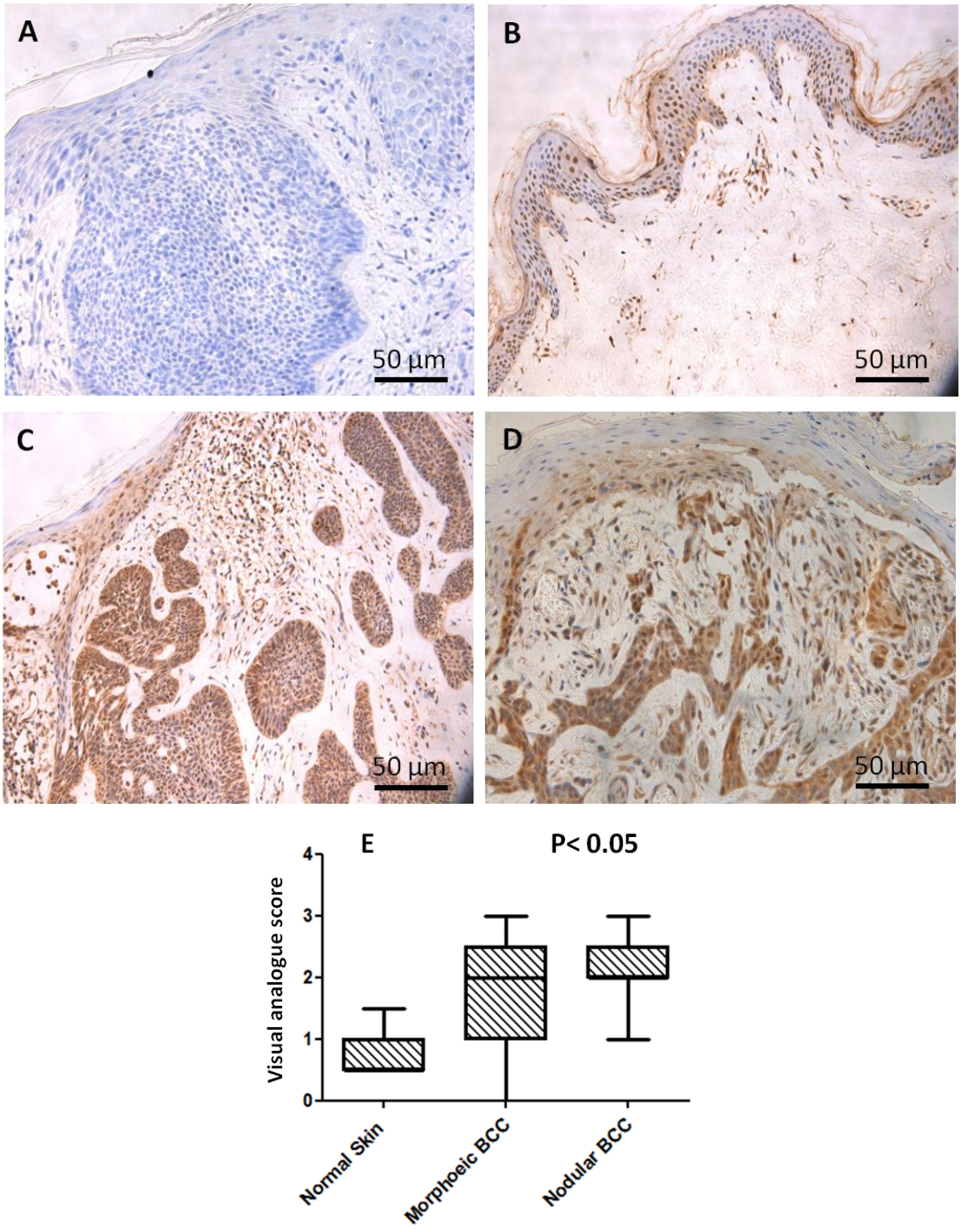

Figure 3.12: Representative images showing p16^{INK4a} expression in (A) Negative control (B) Normal Skin (C) Nodular and (D) Morphoeic BCC. Visual analogue (E) scoring of total staining between nodular and morphoeic BCC showed no significant difference in p16^{INK4a} expression, but there was a clear difference when comparing BCC subtypes with normal skin. Visual analogue scoring was carried out n=7 normal skin n=15 nodular and n=15 morphoeic BCC. Statistical analysis was carried out using Two-way Analysis of Variance ANOVA.

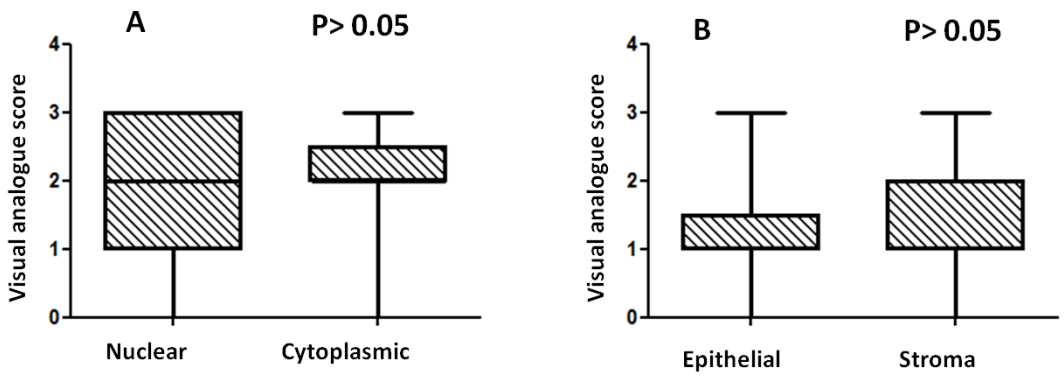

Figure 3.13: p16^{INK4a} visual analogue scoring comparing (A) Nuclear versus Cytoplasm and (B) Epithelial versus Stroma p16^{INK4a} expression in Morphoeic BCC. The analysis shows no significant difference between them. Statistical analysis was carried out using student's t-test.

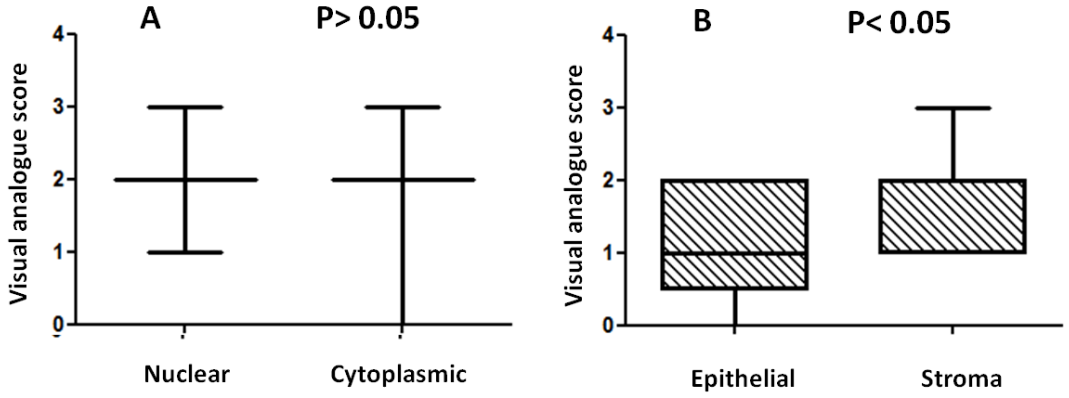

Figure 3.14: p16^{INK4a} means of visual analogue scoring comparing (A) Nuclear versus Cytoplasm and (B) Epithelial versus Stroma p16^{INK4a} expression in Nodular BCC. The analysis shows no significant difference between nuclear and cytoplasmic p16^{INK4a} expression but there is a significant increase in stromal p16^{INK4a} when compared to epithelial expression. Statistical analysis was carried out using student's t-test.

3.2.4 Expression of p15 ^{INK4b} in normal skin and BCC

p15^{INK4b} stained positive on all BCC tissue sections of nodular and morphoeic BCC (**see Figure 3.15 C and D**) when compared with normal skin and negative control (**see Figure 3.15 A and B**). In both nodular and morphoeic BCC p15^{INK4b} staining is quite clearly seen in the both tumour epithelium of morphoeic and nodular BCC and in particular the palisading cells of nodular BCC. p15^{INK4b} was also seen in the stroma of both morphoeic and nodular BCC. With regards its subcellular localization p15^{INK4b} was seen in the nucleus and cytoplasm of both BCC subtypes.

Results of visual analogue scoring of p15^{INK4b} staining of these tumours were analysed (**as mentioned in chapter 2**) by plotting the mean staining results (with 95% confidence interval) by subtype. Visual analogue scoring between nodular and morphoeic BCC (**see Figure 3.15E**) shows that there was no significant difference in staining intensity between nodular and morphoeic BCC, but there was a significant difference between BCC and normal skin ($P<0.05$) indicating a significant up regulation of p15^{INK4b} in BCC compared to normal skin.

In addition to the comparison between nodular and morphoeic BCC and normal skin I also compared by visual analogue scoring nuclear and cytoplasmic expression of p15^{INK4b} (**see Figure 3.16A**) and epithelial versus stroma expression in morphoeic BCC (**see Figure 3.16B**) and in nodular BCC (**see Figure 3.17A and 3.17B respectively**). **Figure 3.16** shows that in morphoeic BCC there was no significant difference between nuclear and cytoplasmic p15^{INK4b} staining. However, when epithelial versus stromal expression was analysed there was a significantly higher level of p15^{INK4b} expression ($P<0.05$) in the stroma of morphoeic BCC compared to epithelial expression. In the nodular BCC there was no significant difference between nuclear and cytoplasmic expression of p15^{INK4b} (**see Figure 3.17A**). However, when epithelial versus stromal expression was analysed there was a significantly higher level of p15^{INK4b} expression ($P<0.05$) in the stroma of nodular BCC compared to epithelial expression (**see Figure 3.17B**). These data therefore, indicate and up-regulation of p15^{INK4b} in the stroma of morpheic BCC.

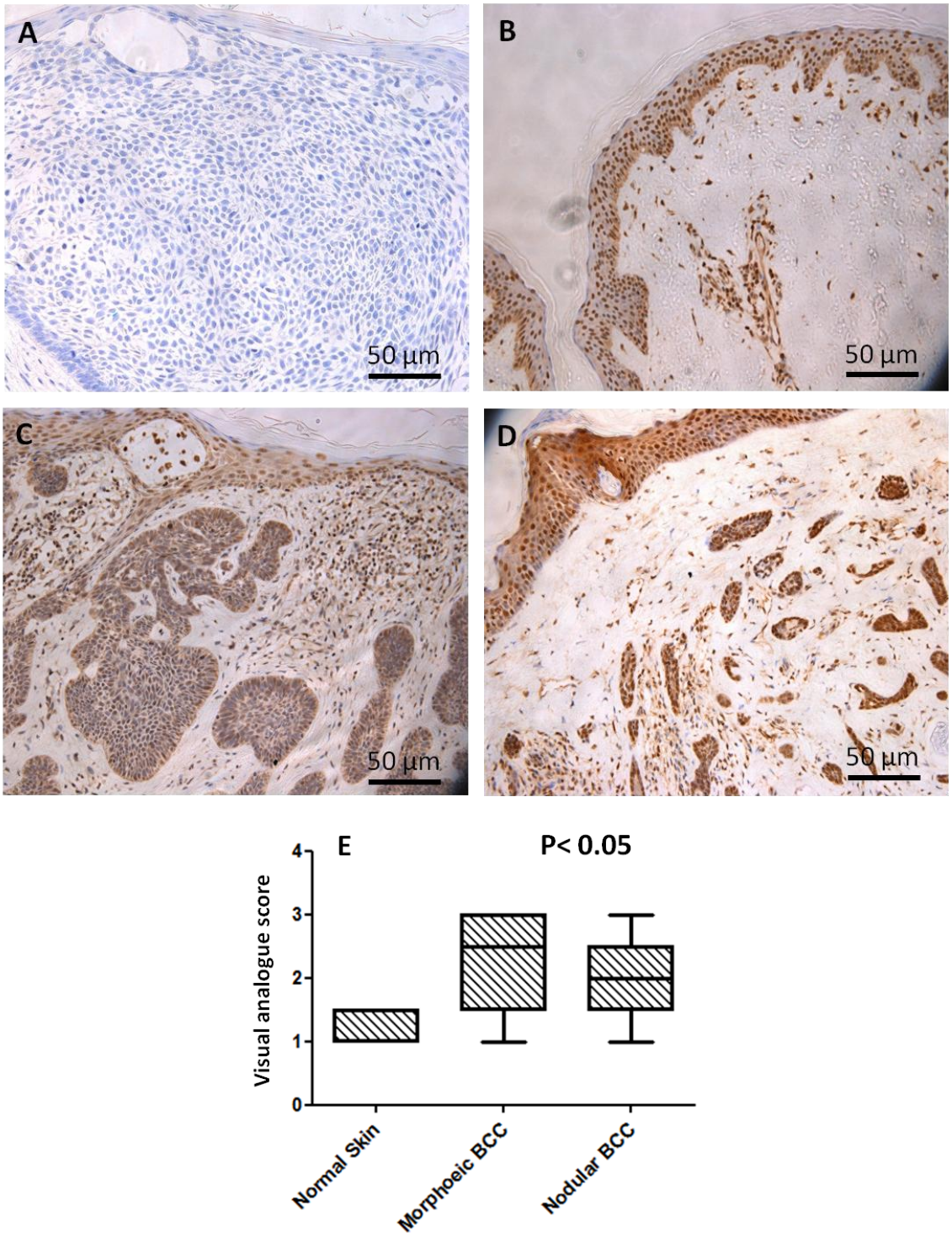

Figure 3.15: Representative images showing p15^{INK4b} expression in (A) Negative control (B) Normal Skin (C) Nodular and (D) Morphoeic BCC. Visual analogue (E) scoring of total staining between nodular and morphoeic BCC showed no significant difference in p15^{INK4b} expression, but there was a significant difference when comparing BCC types with normal skin. Visual analogue scoring was carried out on n=7 normal skin, n=15 nodular and n=15 morphoeic BCC. Statistical analysis was carried out using Two-way Analysis of Variance ANOVA.

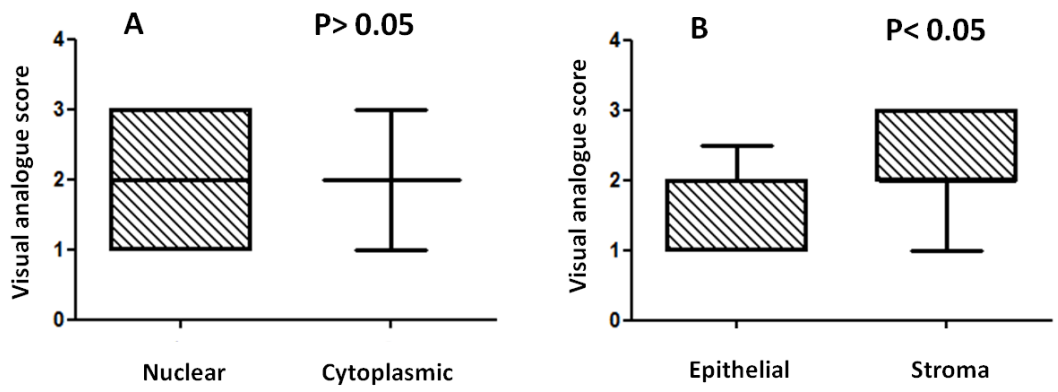

Figure 3.16: $p15^{INK4b}$ visual analogue scoring comparing (A) Nuclear versus Cytoplasm and (B) Epithelial versus Stroma $p15^{INK4b}$ expression in Morphoeic BCC. The analysis shows no significant difference between nuclear and cytoplasmic $p15^{INK4b}$ but there is a significant increase in stromal $p15^{INK4b}$ when compared to epithelial expression. Statistical analysis was carried out using student's t-test.

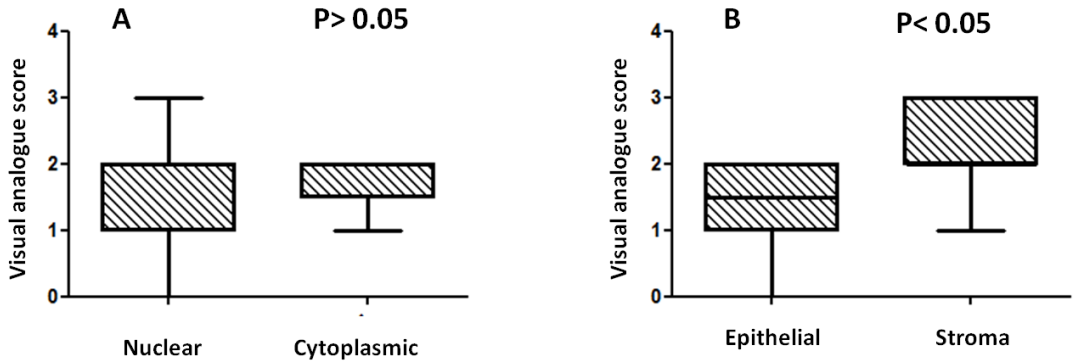

Figure 3.17: $p15^{INK4b}$ visual analogue scoring comparing (A) Nuclear versus Cytoplasm and (B) Epithelial versus Stroma $p15^{INK4b}$ expression in Nodular BCC. The analysis shows no significant difference between nuclear and cytoplasmic $p15^{INK4b}$ but there is a significant increase in stromal $p15^{INK4b}$ when compared to epithelial expression. Statistical analysis was carried out using student's t-test.

3.2.5 Expression of p53 in normal skin and BCC

p53 stained positive on all BCC tissue sections of nodular and morphoeic BCC (**see Figure 3.18 C and D**) when compared with normal skin and negative control (**see Figure 3.18 A and B**). In both nodular and morphoeic BCC p53 staining is quite clearly seen epithelium of morphoeic nodular BCC. p53 was also seen in the stroma of both morphoeic and nodular BCC. With regards its subcellular localization p53 was mostly seen in the nucleus when compared with cytoplasm of both BCC subtypes.

Results of visual analogue scoring of p53 staining of these tumours were analysed (as mentioned in chapter 2) by plotting the mean staining results (with 95% confidence interval) by subtype. Visual analogue scoring between nodular and morphoeic BCC (**see Figure 3.18E**) shows that there was no significant difference in staining intensity between nodular and morphoeic BCC, but there was significant difference between BCC and normal skin ($P<0.05$) indicating a significant up regulation of p53 in BCC compared to normal skin.

In addition to the comparison between nodular and morphoeic BCC and normal skin I also compared by visual analogue scoring nuclear and cytoplasmic expression of p53 (**see Figure3.19A**) and epithelial versus stroma expression in morphoeic BCC (**see Figure 3.19B**) and in nodular BCC (**see Figure 3.20A and 3.20B respectively**). **Figure 3.19** shows that in morphoeic BCC there was a increase expression of p53 in nucleus when compared with cytoplasmic p53 staining ($P<0.05$). However, when epithelial versus stromal expression was analysed there was a significantly higher level of p53 expression ($P<0.05$) in the epithelia of morphoeic BCC compared to stroma expression. In the nodular BCC there was a increase level of p53 in nucleus when compared with cytoplasmic expression of p53 (**see Figure 3.20A**) and also increase of p53 in epithelia when compared with stromal expression (**see Figure 3.20B**) ($p<0.05$). These data therefore, indicate and up-regulation of p53 in the epithelia of both morpheic and nodular BCC.

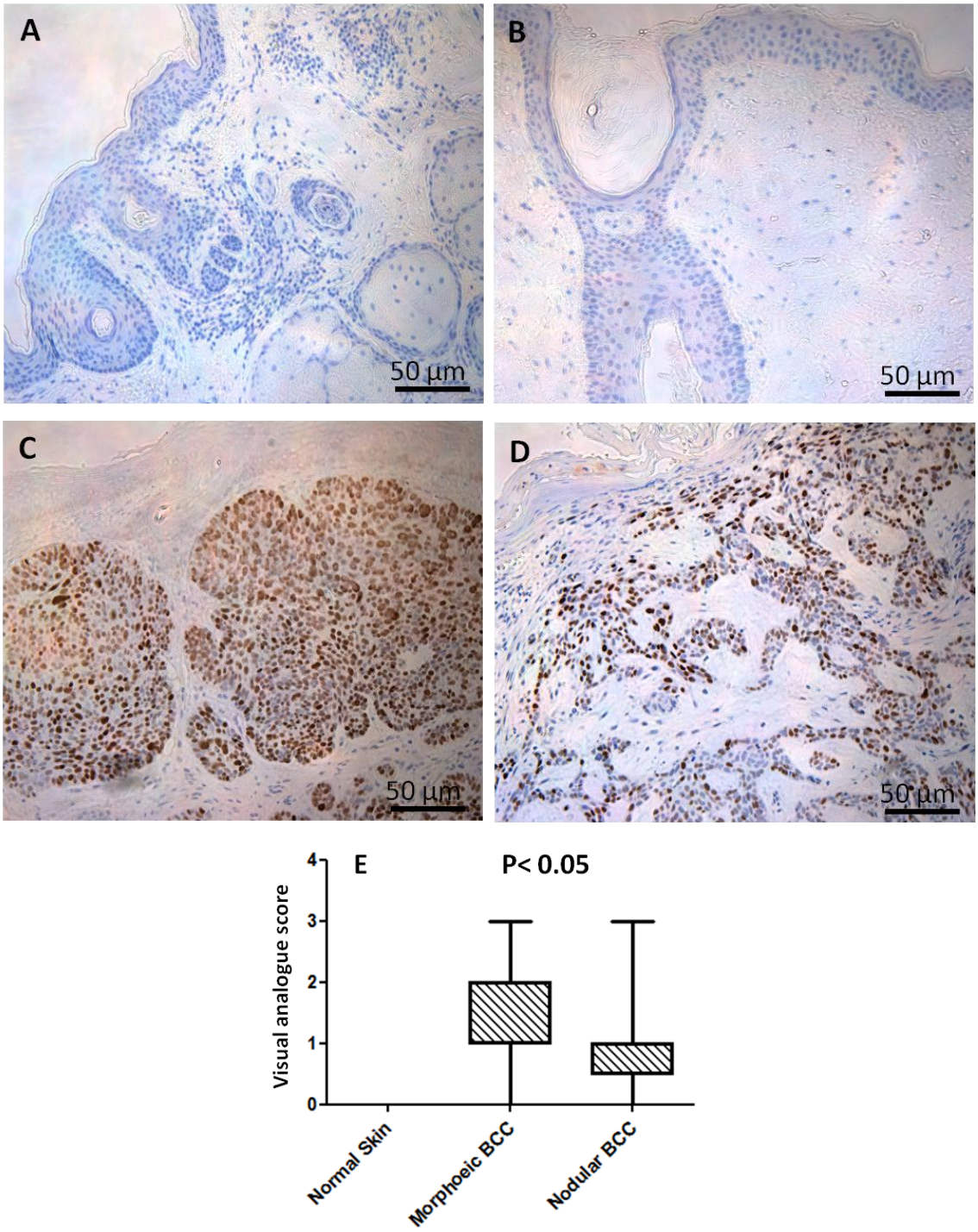

Figure 3.18: Representative images showing p53 expression in (A) Negative control (B) Normal Skin (C) Nodular and (D) Morphoeic BCC. Visual analogue (E) scoring of total staining between nodular and morphoeic BCC showed no significant difference of p53 expression, but there was a clear difference with normal skin when compared with BCC types. Visual analogue scoring was carried out on n=7 normal skin, n=15 nodular and n=15 morphoeic BCC. Statistical analysis was carried out using Two-way Analysis of Variance ANOVA.

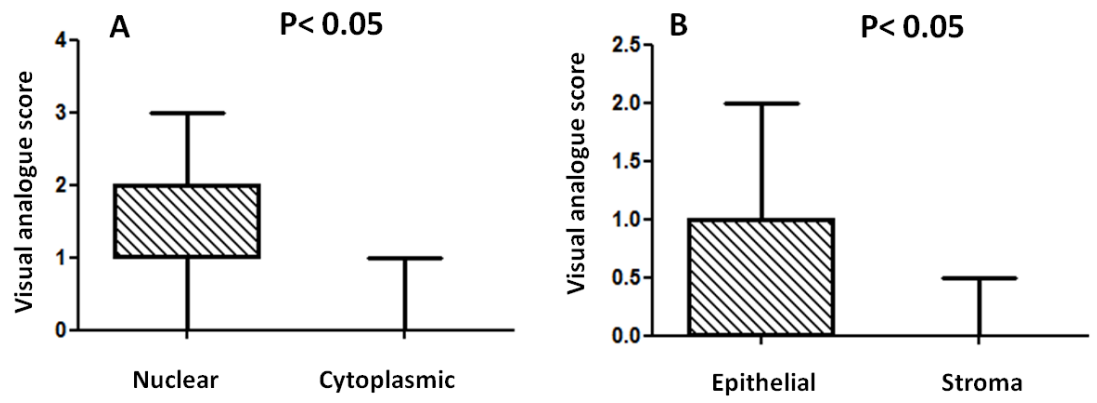

Figure 3.19: p53 visual analogue scoring comparing (A) Nuclear versus Cytoplasm and (B) Epithelial versus Stroma p53 expression in Morphoeic BCC. The analysis shows significant difference between nuclear and cytoplasmic and also between epithelial and stromal p53 expression. Statistical analysis was carried out using student's t-test.

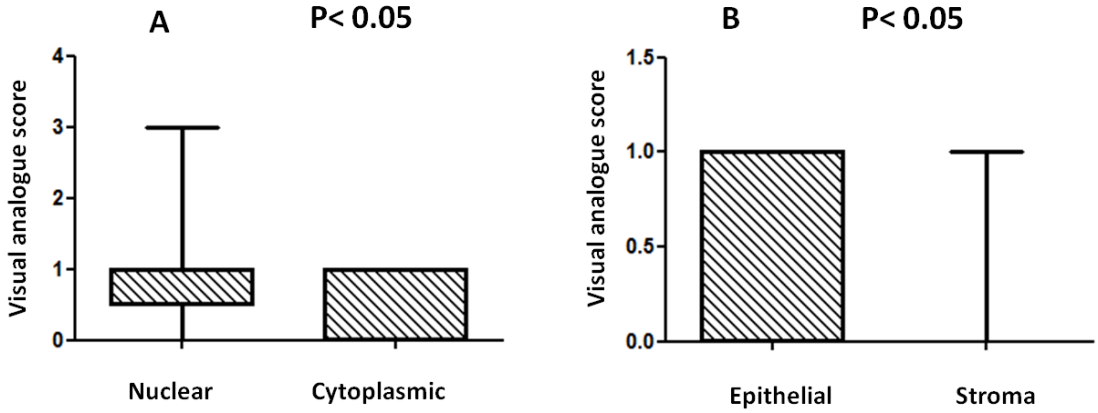

Figure 3.20: p53 visual analogue scoring comparing (A) Nuclear versus Cytoplasm and (B) Epithelial versus Stroma p53 expression in Nodular BCC. The analysis shows significant difference between nuclear and cytoplasmic and also between epithelial and stromal p53 expression. Statistical analysis was carried out using student's t-test.

3.2.5 Expression of p21^{WAF1} in normal skin and BCC

p21^{WAF1} staining is negative on all nodular and morphoeic types of BCC (see figure 3.16 C, D) as compared with normal skin. (see figure 3.16 A, B).There is only some staining in sweat gland in normal skin.

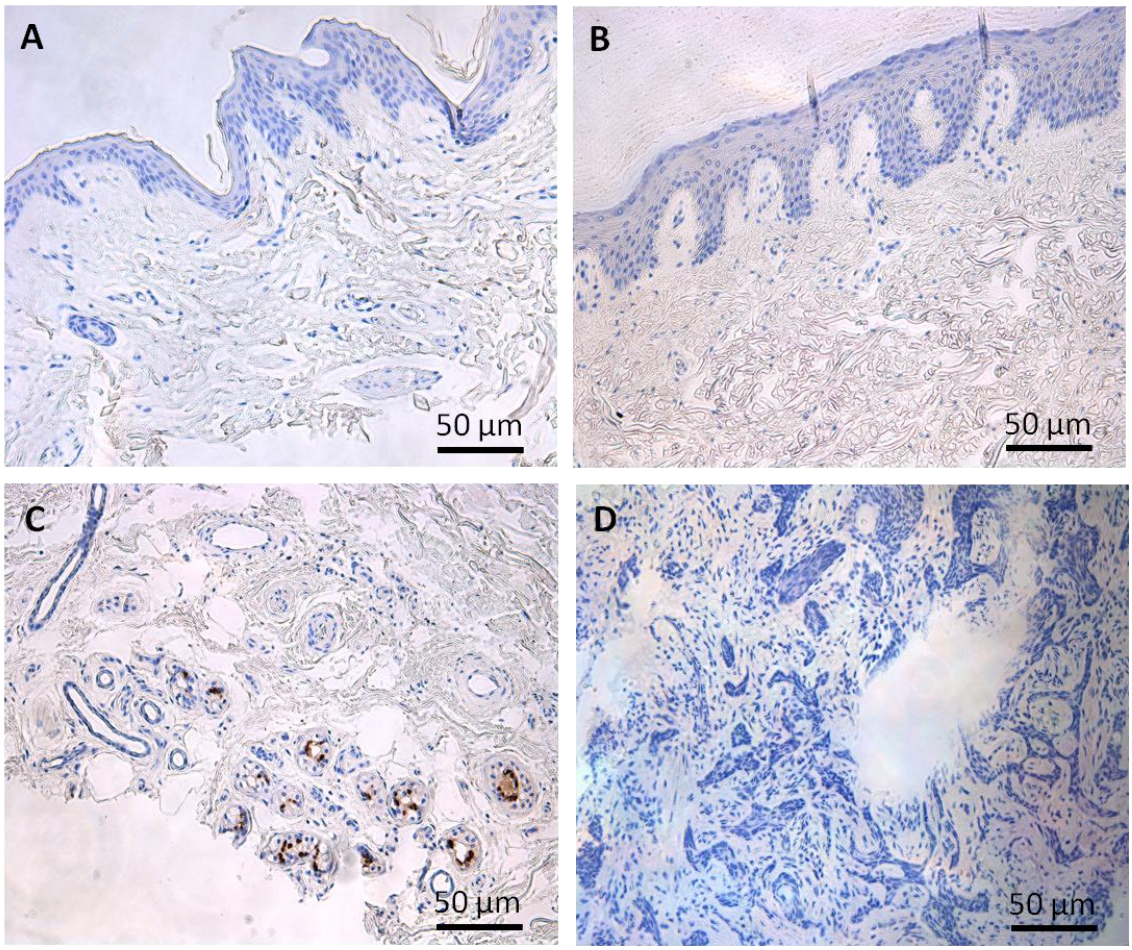

Figure 3.21: Representative images showing p21^{WAF1} expression in (A) Negative control (B) Normal Skin (C) Normal skin showing eccrine sweat glands and (D) Nodular BCC

Discussion

The concept of senescence was first applied to the irreversible growth arrest of cells after prolonged proliferation under *in vitro*, non-physiological conditions (Hayflick, 1965). Now this concept is applied in general to the irreversible arrest of cell proliferation caused by various stresses, including oxidative damage, telomere dysfunction, DNA damage and several chemotherapeutic drugs such as doxorubicin or cisplatin, which affect DNA structure, or taxol and vincristine, which target microtubules (Serrano and Blasco, 2001, Chang et al., 1999).

Recent studies have shown that oncogene-induced senescence (OIS) occurs during the early stages of tumorigenesis (Braig et al., 2005, Chen et al., 2005). These studies show that senescent tumour cells are abundant within premalignant neoplastic lesions such as adenomas, but not in malignant tumours (Collado et al., 2005). This association of senescence cells with the premalignant stages of tumour progression opens up the possibility of using senescence markers as diagnostic and prognostic tools. As some chemotherapeutic treatment such as retinoids induce senescence in tumour cells (Roninson, 2003). Senescence markers could help to monitor treatment response.

There is a lot known about BCC with regards to their histopathological structure, clinical features and to an extent their underlying cause, however much remains undefined with regards the mechanism of development and especially with regards different BCC subtypes e.g. benign versus more aggressive BCC. In the work presented in this chapter I have investigated senescence markers on formalin-fixed paraffin-embedded sections of BCC using standard immunohistochemistry techniques. The work presented in this chapter shows clearly that senescence is characteristic of human BCC. In particular the data presented in this chapter has shown that a number of senescence markers identified in other tumours (Collado et al., 2005, Zhang et al., 2006) are also expressed in BCC. These markers include the cyclin-dependent kinase inhibitor $p15^{INK4b}$, the decoy receptor (DcR2) and the transcription factor differentiated embryo-chondrocyte expressed (DEC1). In the study of Collado et al (2005) these markers showed an increased level of expression specifically in premalignant neoplastic lesions of the skin, lung and pancreas, but not in malignant tumours. The

high levels of these markers correlated well with the presence of SA-β-Gal activity, which confirms their value in identifying the occurrence of OIS *in vivo*.

Senescence associated β-Gal (SA-β-Gal) is widely used as an assay for senescence both *in vitro* and *in vivo* tissue sections(Dimri et al., 1995a). The assay involves the cytochemical detection of β-galactosidase activity at pH 6.0, termed senescence-associated β-galactosidase (SA-β-Gal). Senescence associated β-Gal activity is derived from the increased lysosomal content of senescent cells, which enables the detection of lysosomal β-galactosidase at a suboptimal pH, pH 6.0 (pH 4.0 is optimal). The β-Galactosidase assay has been accepted as a marker of senescence both *in vitro* and *in vivo*, although its biochemical basis is still unknown (Dimri et al., 1995a). SA-β-Gal activity is normally assayed in cultured cells or tissue sections using the chromogenic substrate 5-bromo-4-chloro-3-indolyl β-D-galactopyranoside (X-Gal), or the fluorescent analogue fluorescein-di-β-D-galactopyranoside (FDG). In this chapter I observed that human BCC shows positive staining for SA-β-Gal in both the epithelial tumour mass and in the stroma (**see Figure 3.2**). This may be important as tumorigenesis is a multistep process, whereby genetic changes lead to growth advantage in a subset of cells paving way to progression from normal to malignant cells (Axelrod et al., 2006). Tumour progression is not achieved solely by the evolving cancer cells, but stromal components or the microenvironment of the tumour play a key role. The knowledge that stromal cells have the ability to stimulate oncogenenesis has been taken a step further by recent data showing that stromal fibroblasts present in invasive human breast carcinomas promote tumour growth and angiogenesis through elevated Sdf1 secretion (Orimo et al., 2005). In another study, it has been shown that extensive gene expression changes occur in all breast cell types, including fibroblasts (Allinen et al., 2004). Kiaris et al. have shown an association between TP53 mutations in the stromal component of epithelial tumours and carcinogenesis (Kiaris et al., 2005). Together, these findings indicate that stroma influence the initiation and tumour progression of carcinomas and most of the cells present in stroma are fibroblasts and they have an active role in tumorigenesis (Mueller and Fusenig, 2004, Beacham and Cukierman, 2005). In fact, several findings from different laboratories have suggested that cancer

cells themselves can alter their adjacent stroma to form a permissive and supportive environment for tumour progression (Bhowmick and Moses, 2005).

In addition to human BCC I also carried out staining for SA-β-Gal in normal human skin. The staining for β-galactosidase was observed in most of skin samples investigated mainly in hair follicles and especially in outer root sheath (ORS) and hair germ. The staining for β-galactosidase was also observed in the sebaceous and eccrine sweat glands. The significance of β-galactosidase expression in the ORS and hair germ is unclear. Both the ORS and hair germ contain stem cells (Tumbar et al., 2004) however, it is very unlikely they are truly senescent as these population of cells undergo marked cell proliferation during the hair cycle (Morrison and Spradling, 2008). However, it is also important to note that while β-galactosidase is considered a good marker for cell senescence the basis for this is not fully understood. Therefore, it is very likely that cells that are not senescent may also be positive for β-galactosidase.

Investigation of the signalling pathways leading to OIS has shown that two main pathways are involved, $p16^{INK4a}$-RB (retinoblastoma) and ARF-P53, which are responsible for the execution of the proliferative arrest that characterizes senescence (Campisi, 2005). These two pathways are thought to be crucial for tumour suppression and are often mutated in tumours (Hollstein et al., 1991, Ruas and Peters, 1998a, Sharpless and DePinho, 1999b).

Having shown by SA-β-Gal staining that both tumour epithelium and stroma may be senescent in human BCC. I decided to carry out further analysis of my BCC samples using a panel of senescent markers previously reported to be involved in OIS including p53, DcR2, DEC1, $p16^{INK4a}$, $p15^{INK4b}$ and $P21^{WAF1}$. In order to investigate in more detail expression of these markers I have looked at both benign nodular BCC and aggressive morphoeic BCC. I have quantified immunostaining using a standard analogue scoring system (Hsu and Raine, 1981). DcR2 has not been reported in BCC before. In my study I observed DcR2 was expressed in both nodular and morphoeic BCC (**see Figures 3.6, C, D**) although based on visual analogue scoring system there was no significant difference between nodular and morphoeic BCC. However, in comparison with normal skin I did observed a significant difference between normal skin and BCC subtypes (**see**

Figure 3.6 E). These data shows that compared to normal skin DcR2 is significantly higher in BCC. I have shown a significant increase in stroma staining compared to epithelia expression for DcR2 in morphoeic BCC (**see Figure 3.7 B**) but no difference in nodular BCC (**see Figure 3.8B**). The reason for this difference is unclear without access to cell cultures that would allow further downstream signalling to be investigated. However, increased expression of DcR2 in the stroma of morphoeic BCC may reflect increased stromal resistance to apoptosis. Also there was no significant difference between nuclear and cytoplasmic expression in both nodular and morphoeic BCC subtypes (**see Figure 3.7A,3.8A**). DcR2 is the member of tumour necrosis factor (TNF)-related apoptosis-inducing ligand (TRAIL) receptor family and is also known as TRIAL-R4. DcR2 is classical type 1 transmembrane protein with an extracellular domain, which shows 58-70%homology with TRAIL-R1/R2, and itself has a truncated non-functional death domain. Consequently, these decoy receptors are able to compete for binding with the activators DR4 & DR5, thereby negatively regulating TRAIL-induced apoptosis. DcR2 expression has reported to protect cells from trail induced apoptosis and is regulated by p53. There is also a functional cytoplasmic signalling region which is believed to be involved in the activation of NF-kB, which leads to the induction of protective genes and increase the anti-apoptotic threshold of the cells.

DEC1 has not been reported in BCC before and indeed does not appear to have been investigated in skin cancer. In my study DEC1 was expressed in nodular and morphoeic BCC (**see figures 3.9 C, D**). There was no difference between nodular and morphoeic BCC but there was a significant difference between normal skin and BCC tumor types (**see Figure 3.9 E**). Therefore, in BCC there is an increase in DEC1 expression compared to normal skin. I have also shown significant difference between nuclear to cytoplasmic and epithelial to stroma in nodular and morphoeic BCC. There was an increase in stromal DEC1 expression in morphoeic BCC (**see Figure 3.10 B**) but no difference in nodular BCC (**see Figure 3.11B**). The reason for this difference is not clear as it may be expected that as nodular BCC are less aggressive than morphoeic BCC and as the stroma is known to play a role in tumour development that more senescence would be associated with the stroma of less aggressive BCC. However, it must also be remembered that senescence cells are still very active metabolically and can secrete a

wide range of growth regulatory factors (Coppe et al., 2010). Therefore, it is possible that the senescence stroma of morphoeic BCC may in fact be involve in promoting the more aggressive nature of these BCC. This could be investigated by culturing the stroma from nodular and BCC and investigating their influence on keratinocyte invasion in three-dimensional organotypic models. There was no significant difference between nuclear to cytoplasmic in nodular and morphoeic BCC (**see Figure 3.10 A, 3.11 A**). DEC1 is a basic helix-loop helix protein (bHLH). DEC1 is also known as, enhancer of split and hairy related protein 2 (SHARP2) in rats, or stimulated with retinoic acid 13 (SRA13) in the mouse. This transcription factor is involved in a variety of cellular processes such as cell differentiation, lipid metabolism, proliferation and regulation of the molecular clock. DEC1 is widely expressed in normal tissues such as testis, lymph node, endothelial cells placenta, spleen, thymus, cervix, and ovary but is abundant in various carcinomas in breast cancer, colorectal, pancreatic and non-small cell lung cancer (Turley et al., 2004). Hypoxia a state where tissue is deprived of normal oxygen levels is associated with microenvironment of a tumour. There is little known about how DEC1 mediates cell proliferation, it does initiates G1 cell cycle arrest and it has been shown that DEC1 is a target of tumour suppressor p53 which binds to the promoter on the DEC1 gene.

Mutations in the $p16^{INK4a}$ gene have been previously identified in sporadic melanomas and NMSC resulting in a breakdown of tumour suppression mechanisms (Wagner et al., 1998). Under conditions of stress, and oncogenic stimuli, expression of $p16^{INK4a}$ increases as does $p15^{INK4b}$ expression (Malumbres et al., 2000). $p15^{INK4b}$ has a structural and functional homology with $p16^{INK4a}$ and is transcriptionally activated by transforming growth factor-beta (TGF-β) (Hannon and Beach, 1994). Many cells constitutively express $p15^{INK4b}$ and with the loss $p16^{INK4a}$, $p15^{INK4b}$ will maintain inhibition of CDK4. $p15^{INK4b}$ has been previously described as being involved in the growth arrest that is imposed during Ras-induced senescence (Malumbres et al., 2000). In cancer the influence of $p15^{INK4b}$ is not clear and work with $p15^{INK4b}$ deficient mice has only shown a subtle predisposition to tumours whereas loss of $p16^{INK4a}$ causes a wide range of tumors. The increased expression of these genes results in the suspension of the cell cycle and counteracts the excessive proliferation or the

replication of damaged DNA. Under normal physiological conditions $p16^{INK4a}$ is expressed in low levels but if cells are under stress such as oncogenic stress $p16^{INK4a}$ levels increase. This protein is usually inactive in cancers such as melanoma, leukemia and head and neck cancer, whether by mutation, methylation or deletion which results in the inactivation of the tumour suppressor system. $p16^{INK4a}$ has been previously shown to be expressed in BCC before and stained positive but not as senescence marker. In my study p16 along with $p15^{INK4b}$ was expressed in both BCC subtypes (**see Figures 3.12 C, D and 3.15 C, D**). There was no significant difference between BCC subtypes but there was significant difference between normal skin and BCC tumor types (**see Figure 3.12 E and 3.15 E**). I have also shown difference between nuclear and cytoplasmic and epithelial to stroma in nodular and morphoeic BCC. There was increase in stroma then epithelia in $p16^{INK4a}$ in nodular BCC (**see Figure 3.14 B**) but no difference in morphoeic BCC (**see Figure 3.13 B**) along with nuclear to cytoplasm in nodular and morphoeic BCC (**see Figure 3.13 A, 3.14 A**). For $p15^{INK4b}$ there was increase in stroma then epithelia in both nodular and morphoeic BCC (**see Figure 3.16 B, 3.15 B**), but no difference between nuclear to cytoplasmic (**see Figure 3.16 A, 3.15 A**). Eshkoor et al. (2008) found significant expression of $p16^{INK4a}$ protein and mRNA expression in BCC cells when compared with normal skin tissue and staining was in the nucleus and cytoplasm (Eshkoor et al., 2008). This data supports my results showing that there is clear difference in $p16^{INK4a}$ expression between BCC and normal skin (**see Figure 3.12E**). Svensson et al. (2003), did not observe any difference in the expression of $p16^{INK4a}$ among different histological types of carcinoma suggesting that $p16^{INK4a}$ expression does not correlate with malignancy or proliferation (Svensson et al., 2003). My data confirms the observations of Sevensson et al (2003) as I also did not observe any significant difference in the expression of $p16^{INK4a}$ between benign nodular and aggressive morphoeic BCC.

p53 has been previously reported as senescence marker (Barbareschi et al., 1992, Suzuki et al., 2001). In my study p53 was expressed in both nodular and morphoeic BCC (see figures 3.18 C, D), but not in normal skin. I have also shown difference between nuclear to cytoplasmic and epithelial to stromal expression in nodular and morphoeic BCC. There was a significant increase of p53 in nuclear and epithelial

compartments when compared with cytoplasmic and stromal expression (**see figure 3.19 and 3.20 A,B**). p53 protein is encode by the gene TP53 on the short arm of chromosome 17 (17p3) and is mediated response to DNA damage, telomere shortening, oxidants, hypoxia and a variety of stresses. There are four major functions of p53 1) promotes transient arrest and repair of DNA, 2) defective repair, the repair attempt fails there by promoting the development of cancer, 3) apoptosis, in the case of severe damage p53 up regulates effectors of apoptosis and 4) senescence, initiation of cellular senescence (Vogelstein et al., 2000). In senescence it functions through increasing the expression of CDK inhibitor p21 and there by halting cell progression at G1 (Kramer et al., 2001). P53 expression is often associated with oncogenic RAS and is often seen alongside $p16^{INK4a}$ expression. P53 is the most commonly altered gene in cancer through its loss or mutation which results in an inability to bind target genes (Hanahan and Weinberg, 2000). Barrett et al (1997) shows p53 expression in BCC, also show nuclear staining of p53 this correlates with my study as well (Barrett et al., 1997).

I have also stained for $p21^{WAF1}$ but observed no expression in BCC. In normal human skin there is some staining in sweat glands (**see figure 3.21**). In previous studies also $p21^{WAF1}$ was also negative in BCC (Ahmed et al., 1997). $p21^{WAF1}$, encoded by CDKN1a, was first identified in normal human fibroblasts (Herbig et al., 2003, Roninson, 2002). Expression of $p21^{WAF1}$ can be induced by a number of cell growth regulatory signals including; DNA damage, tumour suppressor p53 and TGFB to affect cellular senescence and cell differentiation (Roninson, 2002). Of all the mechanisms that p53 is involved in $p21^{WAF1}$ only plays a role in cell cycle regulation and senescence (Levine, 1997). Ultimately $p21^{WAF1}$, like $p16^{INK4a}$, maintain pRB in a hypophoshorylated state preventing its inactivation in G1 phase by binding to CDK2/cyclin E (Stein et al., 1999).

In my study β-galactosidase staining along with DcR2, DEC1, $p15^{INK4b}$, $p16^{INK4a}$ and p53 were observed in both tumour epithelium and tumour stroma. The stroma has been shown to play very important role in tumour formation and constitutes the microenvironment of the tumour (Mueller and Fusenig, 2004). Normal stroma consists of a wide range of molecules that act as a supportive framework for tissues and organs. Among all the stromal components, fibroblasts are essential for the synthesis and deposition of the extracellular matrix (ECM) by producing a variety of collagens

and fibronectin (Blankenstein, 2005). Fibroblasts not only maintain the integrity of the ECM and basement membrane, in some cases, they also contribute to the ECM remoulding by secreting proteases such as matrix metalloproteinase (MMPs) which effectively degrade ECM (Orimo and Weinberg, 2006, Östman and Augsten, 2009). Another important role of fibroblasts is wound healing. During wound healing, fibroblasts are activated and become a specialized type of fibroblast, myofibroblast, which is endowed with a higher capability of ECM synthesis (Schaffer and Nanney, 1996, Marsh et al.). Along with fibroblasts, other types of cells such as inflammatory cells and endothelium also contribute to the integrity and homeostasis of the stroma. Among the components of the stromal cells, an increasing number of Cancer associated fibroblasts (CAFs) which share a similar morphology with myofibroblasts observed in wound healing are often found in the cancer (Cirri and Chiarugi, 2012). CAFs are believed to actively participate in the growth and invasion of the tumour cells by providing a unique tumour microenvironment (Cirri and Chiarugi, 2012). CAFs found in different cancers are highly heterogeneous, and they are possibly derived from resident fibroblasts, epithelial cells, endothelial cells or mesenchymal cells (Pietras and Östman, 2010). The results of several in vitro and in vivo experiments indicate that CAFs promote cancer (Shekhar et al., 2001, Chung et al., 2003). In breast cancer, cells of the stromal-epithelial component are able to confer tumourgenic properties (Shekhar et al., 2001). The stromal-epithelial interaction is also important to the normal development of the mammary gland and it has been reported that adjacent cancer cells can alter the stroma to provide a more supportive environment (Shekhar et al., 2001).

In vivo, senescent cells have been observed in association with aging but also with the early phases of tumourgenesis (Beausejour and Campisi, 2006, Collado et al., 2005). Cells in premalignant tumours undertake OIS, but cells of malignant tumours do not, due to the loss of senescence effectors such as p16. BCC is a malignant cancer but it very rarely metastasizes and it also doesn't have premalignant type. The presence of these senescence cells in BCC might have role in restricting BCC and preventing metastasize.

In conclusion, in this chapter I have shown that cell senescence is seen in both the tumour epithelium and stroma of human BCC. However, I did not observe any significant difference between non aggressive nodular BCC and more aggressive BCC types. This suggests that while up-regulation of senescence in BCC is characteristic of this tumour and may explain why they rarely metastasise; cell senescence does not explain difference between subtypes.

Chapter 4: Expression of senescence markers in an *in vitro* BCC model.

Introduction

In Chapter 3 of this thesis I investigated the expression of cell senescence in nodular and morphoeic BCC. I showed that while markers of cell senescence were significantly up-regulated in nodular and morphoeic BCC compared to normal human skin there was no significant difference between BCC sub types. From this data I concluded that cell senescence is involved in human BCC but this does not explain different BCC subtypes.

However, although I have shown up-regulation of senescence markers in BCC, these data do not tell me whether their expression is a direct or indirect result of dysregulation of the Hedgehog signalling pathway and therefore, whether they arise as a direct effect of up-regulation of GLI-1. To investigate this further I decided to use an *in vitro* model. Currently keratinocytes from BCC have proven very difficult to culture. In the introduction to this thesis I have described how Hedgehog signalling is crucial to the development of BCCs, and that irrespective of the site of the upstream genetic mutation, up-regulation of the GLI-1 transcription factor gene and protein is characteristic of BCC. Transgenic experiments in mice have shown us that GLI proteins may have differing roles in both the early stages of tumour development and the later stages of tumour persistence and survival. Clearly the initiation of BCC formation and persistence of the tumour relies on both of the molecules to an extent. However, as described in the introduction to this thesis. There is limited knowledge of what happens downstream of these GLI proteins. Regl et al (2002) have previously used a keratinocyte culture model to examine the interaction of GLI-1 and GLI-2 and have also examined the expression of both GLI-1 and GLI-2 factors in human BCCs. They demonstrated a degree of inter dependence between the two genes, suggesting that the expression of these genes were mutually controlled.

A Medline search for cell culture in basal cell carcinoma provides only seven published reports where the culture of BCC cells has been successfully achieved and has yielded results in the investigation of BCC cell biology. Of note, Asada mentioned that there were only some cellular characteristics of the BCC tumours preserved in culture (Asada *et al.*, 1992). This, and the small number of reports of BCC cell culture being successful

implies that the difficulty in culturing these cells is due to the fact that the cells require a milieu such as the stroma to grow efficiently, and that without it, growth is limited. As a result of such difficulties, many of these reports state that the cultures were short term only, and that although a small number of passages may have been possible, few of these studies go beyond the technical aspects of cell culture to derive useful information from the cell analysis.

It is well accepted that cell culture techniques have been of limited use in terms of culturing keratinocytes from BCC. Although it is not clear why keratinocytes from BCC have been difficult to culture it is possible that growth of BCC is dependent upon its stroma. Therefore, culture of keratinocytes from BCC may require fibroblasts from the tumour stroma to act a feeder layer. However, there have been no reports to data of the use of stromal cells from BCC and indeed in my own group it was observed that fibroblasts from BCC were also difficult to culture in vitro (Jane Elliott PhD thesis). Therefore, a cell culture system that gives insight to the molecular mechanisms of BCC would be a significant development in the investigation of BCC pathogenesis.

To get around this difficulty of growing and manipulating BCCs cells for the purpose of molecular biology investigation, a model system using keratinocytes has been used in the laboratory in which I performed this work. Given the importance of GLI-1 expression in the development of BCC, the group I have worked with has developed a model in which keratinocytes are retrovirally transduced to over-express GLI-1 transcription factor. However, a potential limitation of this model is that while it replicates the up-regulation of GLI-1 seen in BCC normal human keratinocytes have wild-type *PTCH*. *PTCH* is well established as a downstream target of GLI-1 and a consequence when GLI-1 is over-expressed in cells with wild-type *PTCH* the subsequent up-regulation of *PTCH* results in down-regulation of GLI-1 and damping down of these GLI-1 signals. In contrast in BCC *PTCH* is mutated GLI-1 is up-regulated but because *PTCH* is mutated negative feedback cannot happen. Therefore, *PTCH* knockdown in human keratinocytes may be a better model representative of BCC.
In this chapter I have made use of both retroviral expression of GLI-1 in human NEB1 keratinocytes (GLI-1 NEB1) as well as an *in vitro* model of BCC currently being develop

by Mr. Muhammad Rahman. Using a small hairpin RNA (shRNA) sequence that target *PTCH*1, NEB1 immortalised keratinocytes have been retrovirally transduced in order to knockdown *PTCH*1 expression (NEB1 189A). **Figure 4.1A** shows qPCR for *PTCH*1 and confirms strong suppression in NEB1-189A cells and as a result, GLI-1 expression was increased (**Figure 4.1B**). A non-targeting scrambled control (shCON) sequence was used as control. Both the retrovirally over expressing GLI-1 NEB1 cells and NEB1-189A cells were then used to investigate changes in expression of senescence markers investigated in chapter 3.

Therefore, the aim of this chapter is to investigate the expression of cell senescence markers in *in vitro* models of BCC (*PTCH*1 knockdown Cells and GLI-1 over expressing cells) to determine whether over-expression of GLI-1 up-regulates the expression of cell senescence markers identified in chapter 1 of this thesis.

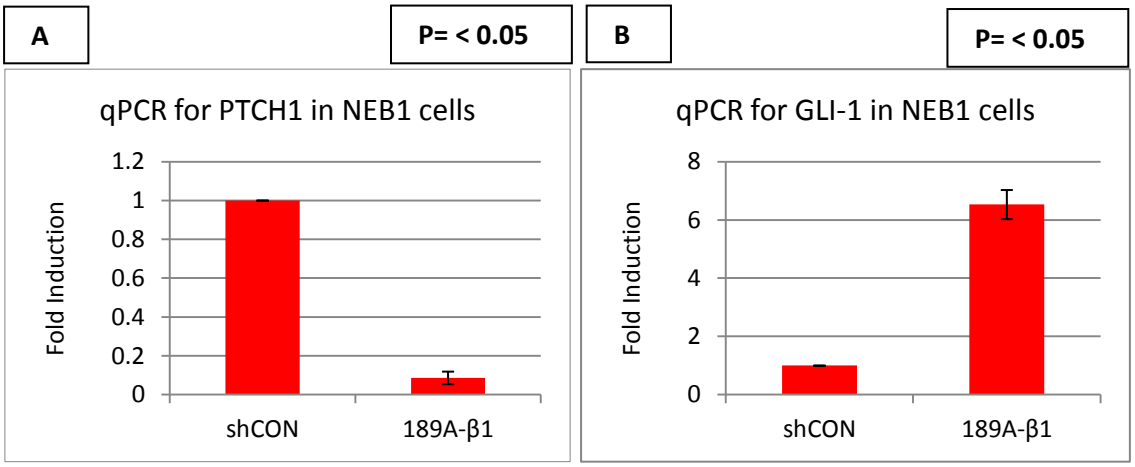

Figure 4.1: qPCR for PTCH1 and GLI-1 in NEB1-shCON and NEB1-189A cells. (A) shows level of PTCH mRNA expression in both control (shCON) NEB1 keratinocytes and in the NEB1 189-A-β1 showing that PTCH was significantly reduced in the NEB1 cells (B) shows that as a result of PTCH knockdown there was an over 6 fold increase in GLI-1 expression in the NEB1 189A-β1 cell line. Results are mean +/- SEM, n=3 separate experiments. Statistical analysis was carried out using Student's t-test.

4.1 Immunofluorescence staining and Quantitative Real Time-Polymerase Chain Reaction (qPCR) of GLI-1 in an *in vitro* model of BCC

In order to investigate GLI-1 regulation of cell senescence markers seen in BCC and reported in **Chapter 3**, immunofluorescence staining was carried out on NEB1 keratinocytes retrovirally over expressing GLI-1 and on NEB1 keratinocytes in which PTCH has been knockdown using shRNA technology resulting in up-regulation of GLI-1. Immunofluorescence staining was carried out for known markers of senescence (Collado and Serrano, 2006) as investigated in chapter 3. Staining was quantified by ImageJ software and each experiment was repeated three times. Along with this Quantitative Polymerase Chain Reaction (qPCR) was also performed to quantify levels of mRNA expression for senescence markers in these cells.

GLI-1 stained positive on all *in vitro* models of BCC including NEB1 GLI-1 cells and NEB-1 189A cells along with NEB1-pBP vector control cells and NEB1 shCON cells as control. GLI-1 immunofluorescence staining was generally more apparent in the cytoplasm of both our NEB1 GLI-1 over expressing and NEB1 189A cells although faint staining can also be seen when looking at nucleus of the cell although when seen against the DAPI stained nuclei this appears as pale blue dots **(see Figure 4.2 A and B)**. In **Figure 4.2A** there is small increase in fluorescence in the NEB1 GLI-1 over expressing cells when compared to control cells in the top panel. However, the difference in GLI-1 immunofluorescence staining is more apparent in **Figure 4.2B** in the NEB1 189A cells when the top control panels are compared with bottom panel it can be seen that in PTCH knockdown cells (bottom panels) there is an increase in GLI-1 staining.

In order to quantify changes in GLI-1 expression I also analysed GLI-1 immunofluorescence staining of both GLI-1 over-expressing cells (NEB1 GLI-1) and PTCH1 knockdown (NEB1 189A) cells using by ImageJ software as discussed in chapter 2. The fluorescence levels for GLI-1 was significantly higher in NEB1 GLI-1 cells **(see Figure 4.2C)** compared to NEB1 pBP control cells ($P<0.05$) and in NEB1 189A cells **(see Figure 4.2C)**, GLI-1 immunofluorescence was significantly higher ($P<0.05$) when compared with NEB1 shCON vector control cells **(see Figure 4.2C)**.

In addition to quantifying immunofluorescence levels I also carried out GLI-1 qPCR (Figure 4.2D). The expression of GLI-1 mRNA level was significantly increased ($P<0.05$) in NEB1 GLI-1 cells **(see Figure 4.2D)** and NEB1 189A cells ($P<0.05$) **(see Figure 4.2D)**, when compared with NEB1 pBP vector control cells **(see Figure 4.2D)** and NEB1 shCON cells **(see Figure 4.2D)**. This data confirms the up-regulation of GLI-1 at protein and mRNA level in both our NEB1 GLI-1 cells and NEB1 189A cells. These cells were then further analysed for expression of cell senescence markers in investigated in chapter three.

GLI-1 Expression in NEB1 GLI-1 over expressing and *PTCH-1* Knockdowns cells

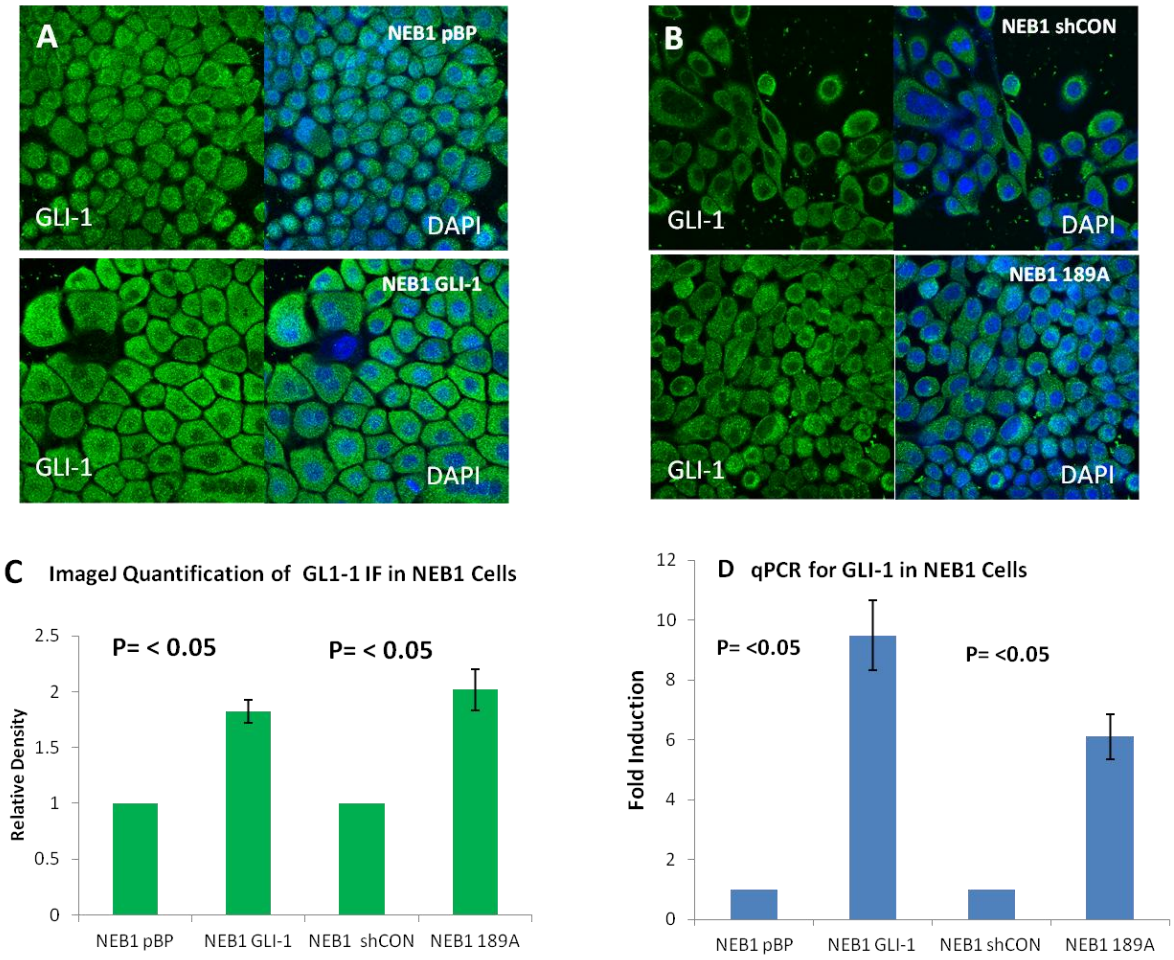

Figure 4.2: Immunofluorescence staining for GLI-1 on *in vitro* BCC models (A) NEB1 pBP vector Control Cells top panels showing GLI-1 immunofluorescence staining and then image merged with DAPI stained cells to show nuclei and NEB1 GLI-1 cells in bottom panel showing GLI-1 immunofluorescence staining and then image merge with DAPI stained cells to show nuclei (B) NEB1 shCON Control cells top panels showing GLI-1 immunofluorescence staining and then image merged with DAPI stained cells to show nuclei and NEB1 189A cells bottom panel showing GLI-1 immunofluorescence staining and then image merge with DAPI stained cells to show nuclei (C) ImageJ quantification of GLI-1 immunofluorescence in both NEB1 GLI-1 and NEB1 189A and NEB1 controls cells (D) Quantitative polymerase chain reaction (qPCR) expression of GLI-1 in NEB1 Cells**.** Results are mean +/- SEM, n=3 separate experiments. Statistical analysis was carried out using Student's t-test.

4.2 Immunofluorescence staining and Quantitative Real Time-Polymerase Chain Reaction (qPCR) of DcR2 in an *in vitro* model of BCC.

DcR2 (Decoy Receptor 2) immunofluorescence was detected in both the NEB1 GLI-1 cells and NEB-1 189A cells along with NEB1-pBP vector control and NEB1 shCON control cells. As I observed with GLI-1, Immunofluorescence staining for DcR2 was generally more apparent in the cytoplasm of both our NEB1 GLI-1 and NEB1 189A cells although weak staining can also be seen when looking at nucleus of the cell although when seen against the DAPI stained nuclei this appears as pale blue **(see Figure 4.3 A and B)**. In **Figure 4.3A** it is possible to see an increase in fluorescence in the NEB1 GLI-1 cells bottom panel when compared to control cells in the top panel. However, there were no apparent differences in DcR2 immunofluorescence staining in the NEB1 189A cells (**Figure 4.3B**) as can be seen when comparing the top panels (shCON) with the bottom panels (NEB1 189A).

In order to quantify DcR2 expression I also analysed DcR2 immunofluorescence staining by ImageJ software as discussed in chapter 2. The immunofluorescence staining for DcR2 in the NEB1 GLI-1 cells **(see Figure 4.3C)**, was significantly higher ($P<0.05$) when compared with NEB1 pBP vector control cells (**Figure 4.3C**). However, there was no significant difference between NEB1 189A cells **(see Figure 4.3C)** when compared with NEB-1 shCON cells **(see Figure 4.3C)** for DcR2.

In addition to quantifying immunofluorescence I also carried out carried out qPCR to quantify the expression of DcR2 mRNA level, there was no significant difference between NEB1 GLI-1 cells **(see Figure 4.3D)** when compared with NEB1 pBP vector control cells **(see Figure 4.D)**. However, there was a significant difference ($P<0.05$) between NEB1 189A cells **(see Figure 4.3D)**, when compared with NEB1 shCON cells **(see Figure 4.3D)**. This data indicates an up-regulation of DcR2 in NEB1 GLI-1 cells at protein level and NEB1 189A cell at mRNA level.

DcR2 Expression in GLI-1 over expressing and *PTCH-1* Knockdowns cells

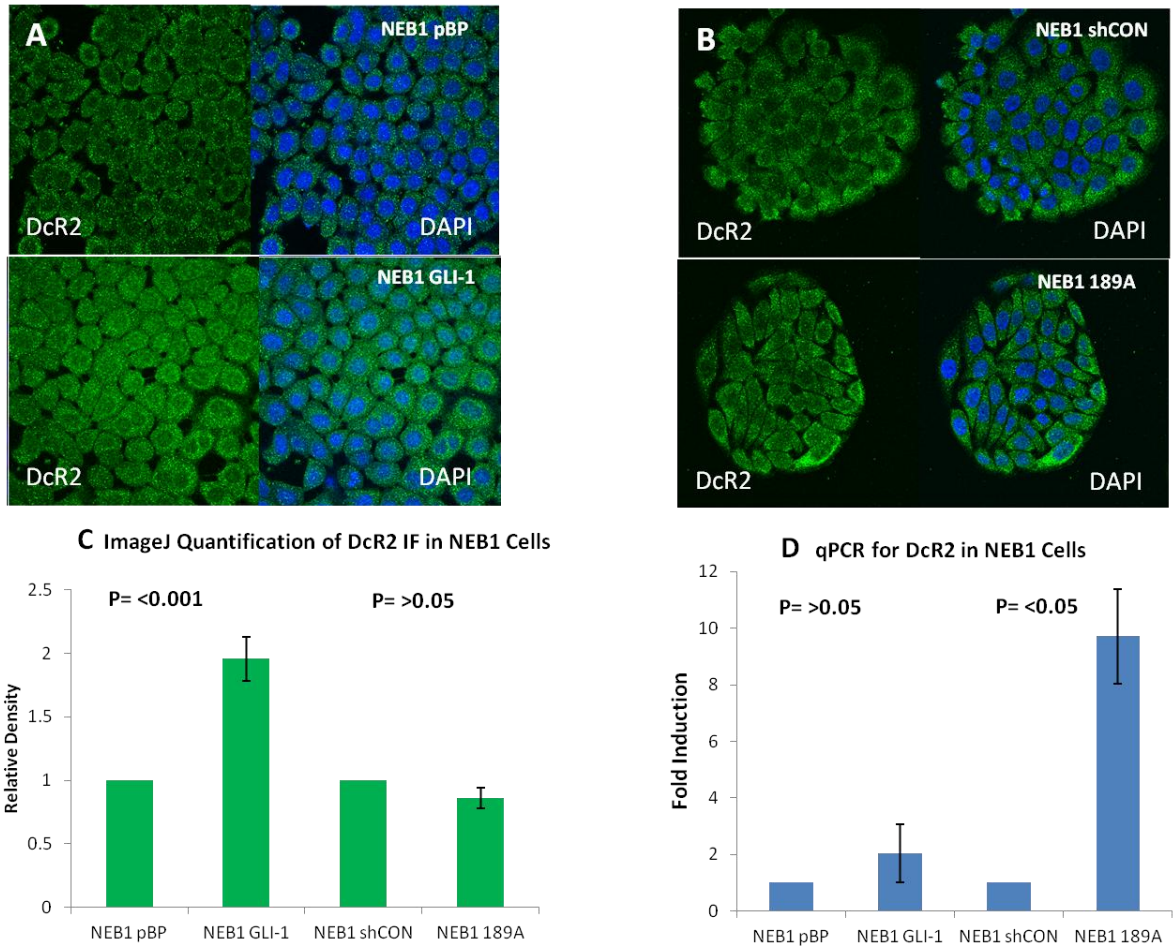

Figure 4.3: Immunofluorescence staining for DcR2 on *in vitro* BCC models. (A) top panels showing DcR2 immunofluorescence staining and then image merged with DAPI stained cells to show nuclei for NEB1 pBP vector Control Cells and in bottom panel showing DcR2 immunofluorescence staining and then image merged with DAPI stained cells to show nuclei in NEB1 GLI-1 cells (B) top panels showing DcR2 immunofluorescence staining and then image merged with DAPI stained cells to show nuclei for NEB1 shCON Control cells and in bottom panel showing DcR2 immunofluorescence staining and then image merged with DAPI stained cells to show nuclei in NEB1 189A cells (C) ImageJ quantification of DcR2 immunofluorescence in both NEB1 GLI-1 over expressing and NEB1 189A Cells and controls (D) Quantitative polymerase chain reaction (qPCR) analysis of DcR2 mRNA expression in NEB-1 Cells. Results are mean +/- SEM, n=3 separate experiments . Statistical analysis was carried out using Student's t-test.

4.3 Immunofluorescence staining and Quantitative Real Time-Polymerase Chain Reaction (qPCR) of DEC1 in an *in vitro* model of BCC.

DEC1 immunofluorescence was detected in both the NEB1 GLI-1 cells and NEB1 189A cells along with NEB1 pBP vector control and NEB1 shCON control cells as control. As I observed with GLI-1, Immunofluorescence staining for DEC1 was generally more apparent in the cytoplasm of both our NEB1 GLI-1 and NEB1 189A cells although weak staining can also be seen when looking at nucleus of the cell although when seen against the DAPI stained nuclei this appears as pale blue **(see Figure 4.4 A and B)**. In **Figure 4.4A** it is possible to see a marked decrease in fluorescence in the GLI-1 over expressing cells bottom panel when compared to control cells in the top panel. However, in contrast there was a marked increase in DEC1 immunofluorescence staining in the NEB1 189A cells (**Figure 4.3B**) as can be seen when comparing the top panels (shCON) with the bottom panels (NEB1 189A).

In order to quantify DEC1 expression I also analysed DEC1 immunofluorescence staining by ImageJ software as discussed in chapter 2. There was a significant difference of the staining of DEC1 in NEB1 GLI-1 cells **(see Figure 4.4C)**, when compared with NEB1 pBP vector control cells **(see Figure 4.4C).** The staining was increased in control cells than in NEB1 GLI-1 cells. However, there was no significant difference between NEB1 189A cells **(see Figure 4.4C)** when compared with NEB1 shCON cells **(see Figure 4.4C)** for DEC1.

In addition to quantifying immunofluorescence I also carried out carried out qPCR to quantify the expression of DEC1 mRNA level, there was a significant difference between NEB1 GLI-1 cells **(see Figure 4.4D)** when compared with NEB1 pBP vector control cells **(see Figure 4.D)**. The mRNA level was more prominent in control cells than in NEB1 GLI-1 cells. However, a significant difference ($P<0.05$) was seen in NEB1 189A PTCH knockdown cells **(see Figure 4.4D)**, when compared with control NEB1 shCON cells **(see Figure 4.4D)**. This data indicates an up-regulation of DEC1 in PTCH cells at mRNA level but this was not reflected in protein expression as determined by immunofluorescence staining.

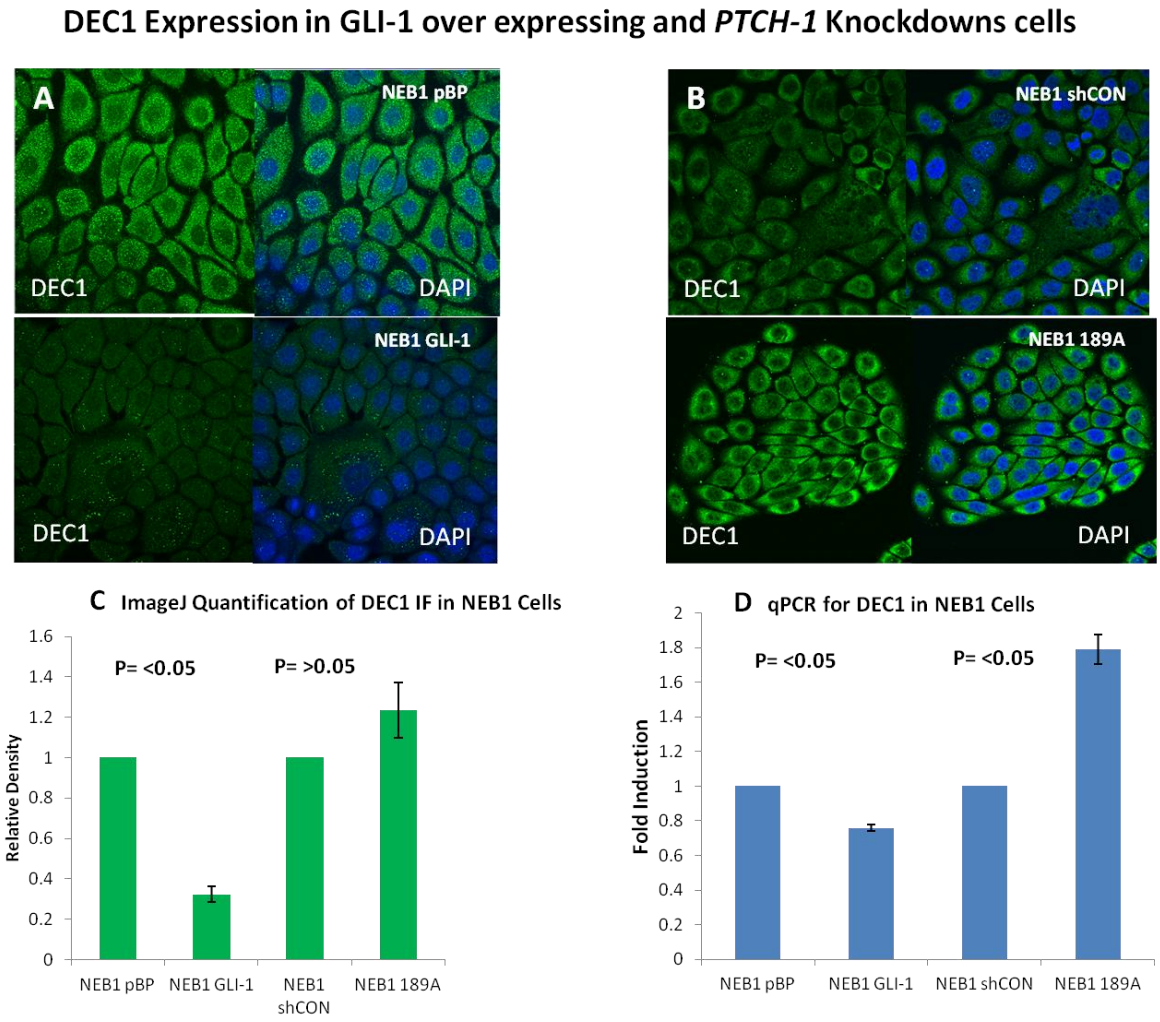

Figure 4.4: Immunofluorescence staining for DEC1 on *in vitro* BCC models (A) Top panels showing immunofluorescence staining and then image merged with DAPI stained cells to show nuclei for NEB1 pBP vector Control Cells and in bottom panel showing DEC1 immunofluorescence staining and then image merged with DAPI stained cells to show nuclei in NEB1 GLI-1 cells (B) top panels showing DEC1 immunofluorescence staining and then image merged with DAPI stained cells to show nuclei for NEB1 shCON cells and in bottom panel showing DEC1 immunofluorescence staining and then image merged with DAPI stained cells to show nuclei in NEB 189A cells (C) ImageJ quantification of DEC1 immunofluorescence in both NEB1 GLI-1 and NEB1 189A cells and controls (D) Quantitative polymerase chain reaction (qPCR) analysis of DEC1 mRNA expression in NEB1 Cells. Statistical analysis was carried out using Student's t-test on 3 separate experiments.

4.4 Immunofluorescence staining and Quantitative Real Time-Polymerase Chain Reaction (qPCR) of $p16^{INK4a}$ in an *in vitro* model of BCC.

$p16^{INK4a}$ immunofluorescence was detected in both NEB1 GLI-1 cells and NEB1 189A cells along with NEB1 pBP vector control and NEB1 shCON control cells. As with previous immunofluorescence staining carried out in this chapter staining was more prominent in the cytoplasm of all cells when compared to the nucleus of the cell **(see Figure 4.5 A and B)**. However, from looking at fluorescent images there were no clear differences between cell types.

In order to quantify $p16^{INK4a}$ expression and determine whether there were any significant differences in immunofluorescence that could not be seen by eye I also analysed $p16^{INK4a}$ immunofluorescence staining by ImageJ software as discussed in chapter 2. There was no significant difference in immunofluorescence staining for $p16^{INK4}$ in either NEB1 GLI-1 cells **(see Figure 4.5C)**, when compared with NEB1 pBP vector control cells **(see Figure 4.5E)**. There was also a significant difference between NEB1 189A cells **(see Figure 4.5C)** when compared with NEB1 shCON cells **(see Figure 4.5C)** for p16. The staining was more in control cells than in NEB1 189A cells.

In addition to quantifying immunofluorescence I also carried out carried out qPCR to analyse the expression of $p16^{INK4a}$ mRNA level. There was no significant difference between NEB1 GLI-1 cells **(see Figure 4.5D)** when compared with NEB1 pBP vector control cells **(see Figure 4.D)**. However, there was a significant difference between NEB1 189A cells **(see Figure 4.5D)**, when compared with control NEB1 shCON cells **(see Figure 4.5D)**. This data indicates an up-regulation of p16 level in NEB1 189A cells at the mRNA level but not in NEB GLI-1 cells. These changes in mRNA expression were not however, reflected at the protein level with regards to immunofluorescence staining.

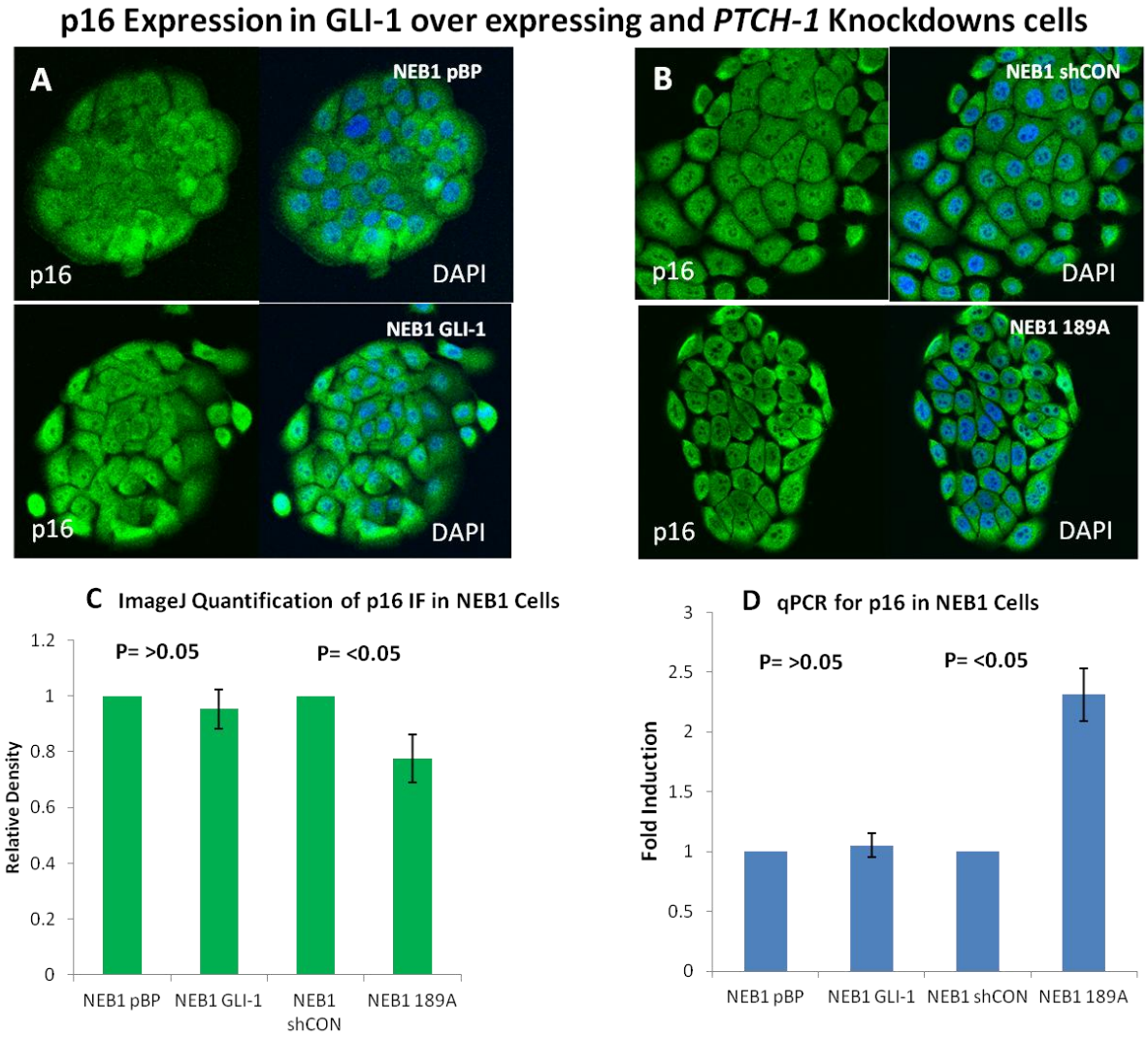

Figure 4.5: Immunofluorescence staining for p16^{INK4a} on *in vitro* BCC models (A) Top panels showing immunofluorescence staining and then image merged with DAPI stained cells to show nuclei for NEB1 pBP vector Control Cells and in bottom panel showing p16^{INK4a} immunofluorescence staining and then image merged with DAPI stained cells to show nuclei in NEB1 GLI-1 cells (B) top panels showing p16^{INK4a} immunofluorescence staining and then image merged with DAPI stained cells to show nuclei for NEB1 shCON cells and in bottom panel showing p16^{INK4a} immunofluorescence staining and then image merged with DAPI stained cells to show nuclei in NEB1 189A cells (C) ImageJ quantification of p16^{INK4a} immunofluorescence in both NEB1 GLI-1, NEB1 189A cells and controls (D) Quantitative polymerase chain reaction (qPCR) analysis of p16^{INK4a} mRNA expression in NEB1 Cells. Statistical analysis was carried out using Student's t-test on 3 separate experiments.

4.5 Immunofluorescence staining and Quantitative Real Time-Polymerase Chain Reaction (qPCR) of p53 in an *in vitro* model of BCC.

p53 stained positive on NEB1 GLI-1 cells and NEB1 189A cells along with NEB1 pBP vector control and NEB1 shCON cells as control. The staining was seen in both the cytoplasm and in the nucleus of the cells **(see Figure 4.6 A and B)**.

ImageJ software was used to analyse immunofluorescence as above and as discussed in chapter 2. There was no significant difference in the immunofluorescence staining for p53 in NEB1 GLI-1 cells **(see Figure 4.6C)**, when compared with NEB1 pBP vector control cells **(see Figure 4.6C)**. However, there was a significant difference ($P<0.05$) between NEB1 189A cells **(see Figure 3.6C)** when compared with their NEB1 shCON cells **(see Figure 4.6C)**.

In addition to quantifying immunofluorescence I also carried out carried out qPCR to analyse the expression of p53 mRNA level, there was a significant difference between NEB1 GLI-1 cells **(see Figure 4.6D)** when compared with NEB1 pBP vector control cells **(see Figure 4.6D)**. The mRNA level was more prominent in control cells compared to NEB1 GLI-1 cells However, the significant difference was seen in NEB1 189A cells **(see Figure 4.6D)**, when compared with NEB1 shCON cells **(see Figure 4.6D)** in p53. This data indicates in up-regulation of p53 level in NEB1 189A cell at mRNA level.

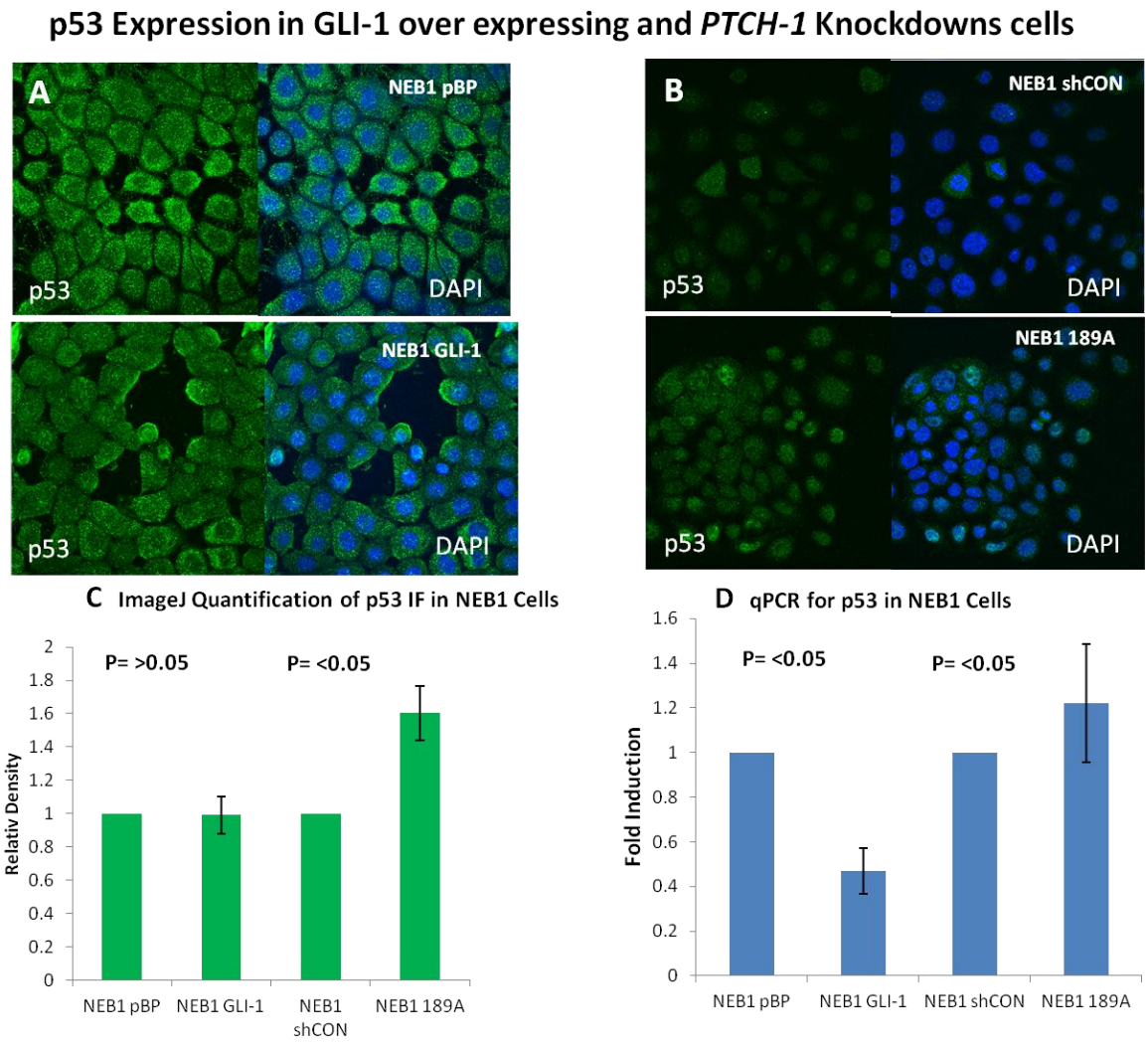

Figure 4.6: Immunofluorescence staining for p53 on in *vitro* BCC models (A) Top panels showing immunofluorescence staining and then image merged with DAPI stained cells to show nuclei for NEB1 pBP vector Control Cells and in bottom panel showing p53 immunofluorescence staining and then image merged with DAPI stained cells to show nuclei in GLI-1 cells (B) top panels showing p53 immunofluorescence staining and then image merged with DAPI stained cells to show nuclei for NEB1 shCON cells and in bottom panel showing p53 immunofluorescence staining and then image merged with DAPI stained cells to show nuclei in NEB1 189A cells (C) ImageJ quantification of p53 immunofluorescence in both NEB1 GLI-1 and NEB1 189A cells and controls (D) Quantitative polymerase chain reaction (qPCR) analysis of p53 mRNA expression in NEB1 Cells. Statistical analysis was carried out using Student's t-test on 3 separate experiments.

4.6 Immunofluorescence staining and Quantitative Real Time-Polymerase Chain Reaction (qPCR) of $p21^{WAF1}$ in an *in vitro* model of BCC.

$p21^{WAF1}$ stained positive on NEB1 GLI-1 cells and NEB1 189A cells along with NEB1 pBP vector control and NEB1 shCON cells as control. Immunofluorescence staining for NEB1 GLI-1 cells and their NEB1 pBP controls were higher than for the NEB1 189A cells and their control. In NEB1 GLI-1 cells immunofluorescence appeared to be higher in the NEB1 GLI-1 cells compared to control cells. However, in the control cells immunofluorescence appeared more localised in the nucleus as determined by pale blue dots. NEB1 189A cells display weak immunofluorescence for $p21^{WAF1}$ detected in the cytoplasm of control cells and this appeared higher in NEB1 189 cells **(see Figure 4.7 A and B)**.

ImageJ software was used as discussed in chapter 2 to quantify immunofluorescence staining. There was no significant difference in immunofluorescence staining for $p21^{WAF1}$ in NEB1 GLI-1 cells **(Figure 4.7C)**, when compared with NEB1 pBP vector control cells **(Figure 4.7C)**. However, there was a significant difference ($P<0.05$) between NEB1 189A cells **(see Figure 3.7C)** when compared with NEB1 shCON cells **(see Figure 4.7C)** for $p21^{WAF1}$.

I also carried out qPCR to quantify the expression of $p21^{WAF1}$ mRNA level, there was no significant difference between NEB1 Gli-1 cells **(see Figure 4.7D)** when compared with NEB1 pBP vector control cells **(Figure 4.7D)**. However, there was a significant difference ($P<0.05$) in NEB1 189A cells **(4.7D)**, when compared with NEB1 shCON cells **(Figure 4.7D)** in $p21^{WAF1}$.

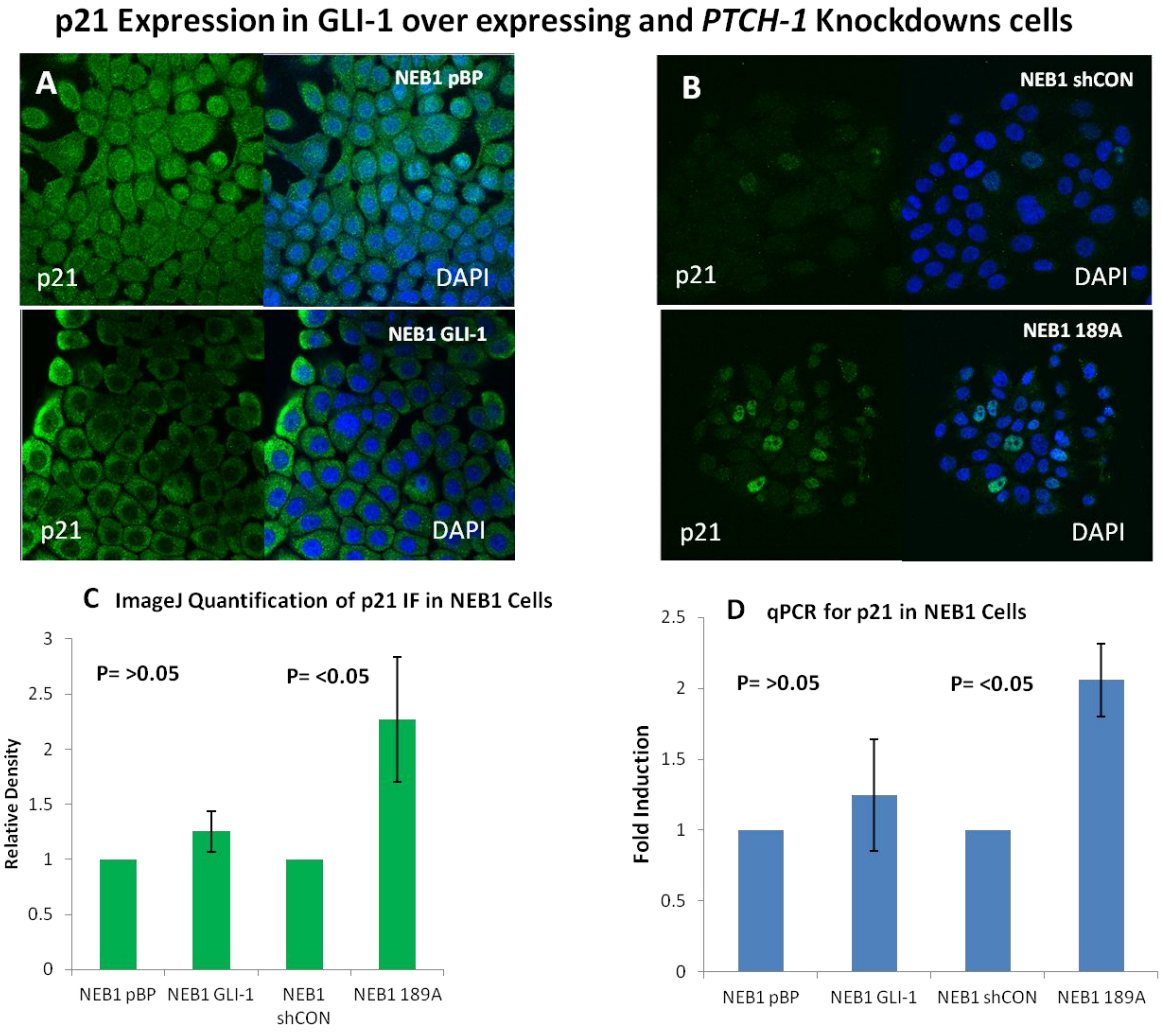

Figure 4.7: Immunofluorescence staining for $p21^{WAF1}$ Antibody on *in vitro* BCC models (A) Top panels showing immunofluorescence staining and then image merged with DAPI stained cells to show nuclei for NEB1 pBP vector Control Cells and in bottom panel showing $p21^{WAF1}$ immunofluorescence staining and then image merged with DAPI stained cells to show nuclei in NEB1 GLI-1 cells (B) top panels showing $p21^{WAF1}$ immunofluorescence staining and then image merged with DAPI stained cells to show nuclei for NEB1 shCON cells and in bottom panel showing $p21^{WAF1}$ immunofluorescence staining and then image merged with DAPI stained cells to show nuclei in NEB1 189A cells (C) ImageJ quantification of $p21^{WAF1}$ immunofluorescence in both NEB1 GLI-1 and NEB1 189A and control cells (D) Quantitative polymerase chain reaction (qPCR) analysis of $p21^{WAF1}$ mRNA expression in NEB1 Cells. Statistical analysis was carried out using Student's t-test on 3 separate experiments.

Discussion

There has been much debate about the physiological relevance of senescence *in vivo*, particularly as this response was originally identified as an *in vitro* phenomenon. Ultimately, much data have emerged that demonstrate the relevance of cellular senescence *in vivo* in both mouse and human tumours (Collado et al., 2007, Collado et al., 2005, Michaloglou et al., 2005, Itahana et al., 2004). In recent years the understanding of the pathology of cancer has highlighted the relevance and role of senescence as a physiological barrier against tumour initiation and progression (Prieur and Peeper, 2008, Decottignies and d'Adda di Fagagna, 2011). The first description of 'cellular senescence' dates to 1965 when Leonard Hayflick observed that cells undergo a replicative senescence in culture (Hayflick, 1965, Hayflick and Moorhead, 1961). It is now well established that premature forms of cellular senescence can be triggered through either the activation of oncogenes (a type of senescence that is termed oncogene-induced senescence (OIS)) or the loss of tumour suppressor genes (Nardella et al., 2011, Saretzki, 2010). This phenomenon can also be observed in response to other stimuli, such as oncogenic stress, DNA damage or cytotoxic drugs (Maruyama et al., 2009, Dimri, 2005). Cells displaying senescent characteristics have not only been observed in cell culture but also in their maternal tissue environment. A number of reports have been related to reduced cellular lifespan with metabolic disease, stress sensitivity, progeria syndromes, and impaired healing, indicating that entry into cellular senescence may contribute to human disease (Vergel et al., 2011, Smith et al., 2005). It has been suggested now that cellular senescence is in part responsible for the pathogenesis of a number of human diseases, such as atherosclerosis, osteoarthritis, muscular degeneration, ulcer formation, Alzheimer's dementia, diabetes and immune exhaustion (Vergel et al., 2011).

In chapter 3 of this thesis I confirmed the expression of senescence markers in human BCC this suggests that senescence may play an important role in BCC. In this chapter I wanted to further investigate these markers in BCC cells and to determine whether these markers were direct targets of hedgehog signalling and GLI-1. Because there are virtually no BCC cell lines I have employed a cell model in which GLI-1 is retrovirally over expressed in human keratinocyte cell lines and as such has been widely published

by my group (Gore et al., 2009) and a second model involving shRNA to knockdown PTCH in keratinocytes.. The reason I used two separate in vitro models is that although retroviral over expression of GLI-1 has been widely used in hedgehog research (Ruiz i Altaba et al., 2002b) the major limitation with this model is keratinocytes express wild-type PTCH. Because PTCH is a downstream target and a negative regulator of GLI-1 (Mancuso et al., 2004) the consequence of over expressing GLI-1 is up-regulation of PTCH and potential down-regulation of GLI-1 this damping down any GLI-1 response. Because of this I have also used a new model being developed by Muhammed Rahman a PhD student in the Centre in which he uses shRNA to knockdown PTCH expression. This model is thought to be a closer replication of BCC in which PTCH mutations are the common mutation (Kim et al., 2002, Reifenberger et al., 2005) and as a result of PTCH knockdown GLI-1 is up regulated in BCC (Mancuso et al., 2004).

I have confirmed that the loss of PTCH1 in NEB1 189A cells leads to the increase of GLI-1 protein and mRNA expression compared to NEB1 shCON cells (**Figure 4.1**). This is as expected as GLI-1 is downstream of PTCH1 in the pathway and also, BCCs have been shown to have increased levels of GLI-1 (Hatta et al., 2005).

I used both the retroviral GLI-1 over-expression and PTCH knockdown models to investigate expression of senescence markers using immunofluorescence staining and qPCR analysis where up regulation of $p16^{INK4a}$, p53, $p21^{WAF1}$, DcR2 and DEC1 was observed. Data from these experiments showed variation between protein expression as determined by immunofluorescence staining and qPCR. However, overall the experiments carried out in this chapter showed especially at the mRNA level that there was an increase in senescence marker expression in response to increased GLI-1 expression. The cells did not changed their morphology as seen in typically senescence cells, however, change in morphology is most likely a late event in cell senescence and had I maintained my cells in culture for longer I may have seen the classical 'fried egg' morphology associated with senescence and which describes the appearance of senescent cells as they become flattened and enlarge (Chen and Goligorsky, 2006). However, maintaining cells for longer may have resulted in down-regulation of the markers of interest. The presence of senescence has been previously described in other diseases as well, such as venous ulcers (Braig et al., 2005, Collado et al., 2005,

Michaloglou et al., 2005, Mendez et al., 1998). Cells cultured from venous ulcers have been shown to have a reduced replicative life span with increased β-gal compared to cells form unaffected areas (Mendez et al., 1998).

Decoy receptor 2 (DcR2) is a member of the tumour necrosis factor (TNF)-related apoptosis-inducing ligand (TRAIL) receptor family and is also known as TRAIL-R4. DcR2 is bound by the TRAIL ligand which is an inducer of apoptosis in cells and acts through binding to the TRAIL receptor family which consists of two death domain receptors, DR4 (TRAIL-R1) and DR5 (TRAIL-R2) (Degli-Esposti et al., 1997, Johnstone et al., 2008). The other two receptors, DcR1 (TRAIL-R3) and DcR2, are referred to as decoys as although they bind to the TRAIL ligand they do not signal downstream. DcR2 itself has a truncated non functional death domain (Liu et al., 2005). Consequently, these decoy receptors are able to compete for binding with the activators DR4 & DR5, thereby negatively regulating TRAIL-induced apoptosis. DcR2 expression has been reported to protect cells from TRAIL-induced apoptosis and is regulated by p53 (Liu et al., 2005). p53 is the most commonly altered gene in cancer through its loss (Liu et al., 2005).

In my study I have seen an increase in expression of DcR2 showing a strong positive stain in the cytoplasm of the cells. This has also been reported in melanoma cell lines and it is suggested that the expression of this receptor may involve regulated movement from the intracellular compartments to the membrane (Zhang et al., 2000, Qian et al., 2008). In some studies, DcR2 was seen in the nucleus but then sub cellular localisation to the cytoplasm was seen in the melanoma cells on their exposure to the TRAIL ligand (Zhang et al., 2000). In this study I have shown by qPCR up regulation of DcR2 mRNA in the NEB1 189A cells and a slight but not significant increase in DcR2 mRNA in the NEB1 GLI-1 cells. I also saw an increase at the protein level in NEB1 GLI-1 cells but not in the NEB1 189A cells. The reason for these differences is difficult to explain. However, they may reflect differences in the cell model with GLI-1 cells having wild type active PTCH whereas in NEB1 189A cells this has been knocked down. These differences may reflect complexity in the Hedgehog signalling pathway in these two cells types and also may reflect differences in the degree of cell senescence brought about by over-expression of GLI-1 versus up-regulation of GLI-1 in PTCH null cells. In addition it is increasingly accepted that mRNA and protein levels do not always

correlate (Ideker et al., 2001, Nishizuka et al., 2003). However, these data do suggest that DcR2 is regulated by GLI-1 expression in human keratinocytes and supports the data in chapter 3 showing increased DcR2 expression in BCC. Moreover, the expression of DcR2 in cells that over express GLI-1 as well as the well established up regulation of Bcl-2 (Regl et al., 2004, Yoon et al., 2002) may also explain why these cells are more resistant to apoptosis in vitro (Harrison, 2013).

Human Differentially Expressed in Chondrocytes (DEC1) is a basic helix-loop-helix protein (bHLH). DEC1 is also known as, enhancer of split and hairy related protein 2 (SHARP2) in rats, or stimulated with retinoic acid 13 (STRA13) in the mouse (Qian et al., 2008). This transcription factor is involved in a variety of cellular processes such as cell differentiation, lipid metabolism, proliferation and regulation of the molecular clock (Li et al., 2006). The mouse homologue STRA13 is involved in cell growth arrest and is a transcriptional repressor promoting neuronal differentiation (Yoon et al., 2001). DEC1 expression is abundant in carcinomas but not in the adjacent tissues. Hypoxia, a state where tissue is deprived of normal oxygen levels, is associated with the microenvironment of a tumour. DEC1 expression has been found in response to the hypoxic state (Li et al., 2006, Yoon et al., 2001). Furthermore, over expression of DEC1 in the mouse fibroblast cell line NIH3T3 inhibited cell proliferation (Qian et al., 2008). Although little is known about how DEC1 mediates cell proliferation, it does initiate G1 cell cycle arrest and it has been shown that DEC1 is a target of the tumour suppressor p53 which binds to the promoter on the DEC1 gene (Qian et al., 2008).

DEC1 has been shown to be over expressed in carcinomas and is usually expressed when cells are in a hypoxic state (Qian et al., 2012, Collado et al., 2005). It has been previously demonstrated that DEC1 transcriptionally activates a gene called survivin which is a member of the Inhibitor of the Apoptosis family (IAF) and inhibits caspase and therefore negatively regulates apoptosis (Li et al., 2002b). In this chapter I have shown an increase in DEC1 mRNA and protein expression in NEB1 189A cells. In NEB1 GLI-1 cells there was a significant down-regulation of DEC1 protein as determined by immunofluorescence staining and a slight but not significant decrease in mRNA. These differences between GLI-1 and PTCH knockdown cells may again reflect differences in the models used and perhaps in GLI-1 over-expressing cells the influence of wild type

PTCH. However, the data in PTCH knockdown cells would suggest that DEC1 is a target of GLI-1. There is a correlation between DEC1 expression and tumour grade and prevention of apoptosis in mouse mammary epithelial cells (Ehata et al., 2007). Like DcR2, DEC1 has an anti apoptotic role in senescence and cancer (Qian et al., 2008, Qian and Chen, 2008). This expression of DEC1 might reflect non aggressiveness of cancers. It has been previously published that DEC1 was expressed in premalignant tumours and is involved in senescence.

Although senescence cells are no longer able to proliferate, they are still metabolically active and can survive for extensive periods of time in this state (Kuilman et al., 2010). The inactivation of more than one pathway is normally required to bypass senescence. In keratinocytes the inhibition of both $p16^{INK4a}$ and p53 is required for the replicative lifespan of the keratinocytes to increase (Kiyono et al., 1998, Rheinwald et al., 2002). $p16^{INK4a}$ is very important in determining the lifespan of keratinocytes, but also mammary epithelial and urothelial cells, increasing serially with passage and preventing the immortalisation of cells (Dickson et al., 2000). In contrast Rheinwald et al. (2002) showed that senescence in fibroblasts was not necessarily dependent on the inhibition of $p16^{INK4a}$ and p53 and that mutant p53 in fibroblast was sufficient to extend their lifespan. Fibroblasts normally maintain senescence through two pathways, p53 and/or $p16^{INK4a}$, depending on whether $p16^{INK4a}$ is present and that it is presence of $p16^{INK4a}$ that determines the irreversible nature of the senescence (Campisi, 2005, Sharpless and DePinho, 2004). Senescence caused by telomere dysfunction and maintained by p53 is a reversible state; however $p16^{INK4a}$ expression in this scenario is a dominant irreversible effect that forms a second barrier against cell proliferation (Bond et al., 2004, Beausejour et al., 2003, Chin et al., 1999). Although $p16^{INK4a}$ upregulation can be seen at the same time as p53 and $p21^{WAF1}$, it is triggered and acts independently (Zindy et al., 1998). If one pathway is up regulated (i.e. $p16^{INK4a}$) this does not prevent the cells from responding to the other pathways (i.e. $p53/p21^{WAF1}$) at a subsequent time (Ben-Porath and Weinberg, 2005).

In this chapter I observed a significant increase in $p16^{INK4a}$ expression in NEB1 189A cells although saw no significant difference in protein level and saw no significant

effect at either protein or mRNA level in NEB1 GLI-1 cells. This data suggests that $p16^{INK4a}$ is most likely a target of GLI-1 in PTCH null cells.

The role of p53 can vary depending on the cell type; sometimes it is important in initiating senescence whilst in others it is important in maintaining senescence. Previously in our group Jane Elliott a PhD student investigating senescence in BCC derived fibroblasts showed that expression of p53 was not increased in BCC derived fibroblasts compared to normal dermal fibroblasts at either early or late passage. This suggests that p53 was not significant in either the establishment or maintenance of the senescence. Nevertheless, $p16^{INK4a}$ expression was increased in BCC derived fibroblast, suggesting that in these cells $p16^{INK4a}$ is playing a dominant role and would account for the irreversible nature of senescence in the cells despite low passage numbers and access to nutrients and good culture conditions. In my experiments p53 mRNA and protein was up-regulated in NEB1 189A cells but not in GLI-1 cells although GLI-1 mRNA was significantly down-regulated. My data showing an increase in p53 in the NEB1 189A cells suggests that this protein is a target of GLI-1 and is involved in senescence in BCC *in vivo*. Moreover, it is well established that p53 is mutated in between 30-70% of BCC (Reifenberger et al., 2005, Lacour, 2002).

Since senescence is characterised by a permanent cell-cycle block, significant emphasis has been placed on the p53 targets that mediate cell-cycle arrest and especially on the CDK inhibitor $p21^{WAF1}$ (Castro et al., 2004). The protein levels of $p21^{WAF1}$ are elevated at senescence in several cellular systems and, indeed, the $p21^{WAF1}$ gene was found in a screening for senescence-inducing genes by one of the groups that first identified p21 (Ruan et al., 2012). Nevertheless, the question of whether $p21^{WAF1}$ is essential or not for the establishment of senescence has yet to be unambiguously answered. Activation of p53 induces the up regulation of the cyclin-dependent kinase (CDK) inhibitor $p21^{WAF1}$, which has a direct inhibitory action on the cell-cycle machinery and correlates well with the declining growth rate observed in senescing cultures (Vergel et al., 2011). In mouse embryo fibroblasts, however, the absence of $p21^{WAF1}$ does not overcome senescence (Castro et al., 2004). This suggests that at least one additional downstream effector is needed for p53-induced growth arrest in senescence. In contrast, elimination of $p21^{WAF1}$ by a double round of homologous recombination is sufficient to

bypass senescence in human cells. In my experiments $p21^{WAF1}$ was up-regulated in PTCH knockdown cells at both the mRNA and protein level. In contrast in GLI-1 over-expressing cells I saw no significant difference. However, *in vivo* (chapter 3) I saw no staining of $p21^{WAF1}$ in BCC suggesting that this protein is not up-regulated in BCC. Therefore, the up regulation of $p21^{WAF1}$ in PTCH1 null cells does not appear to reflect the expression patterns seen in BCC *in vivo.* The reason for this difference is not clear however, it might reflect the complexity of sonic hedgehog signalling in BCC and the involvement of other signalling pathways such as TGF-β and involvement of the stroma (Taipale and Beachy, 2001, Lange et al., 1999). Indeed it has recently been reported that BCC has one of the highest mutation rates of all human cancers (Jayaraman et al., 2013) and that because of this they are unlikely to be homogenous and that it is very unlikely that one pathway alone is contributory although clearly mutation plays a central role.

Mutations in the $p16^{INK4a}$ gene have been previously identified in sporadic melanomas and NMSC resulting in breakdown of tumour suppression mechanisms (De Zwaan and Haass, 2010). Under conditions of stress, and oncogenic stimuli, expression of both $p16^{INK4a}$ and $p15^{INK4b}$ increases (Kim et al., 2010, Serrano et al., 1997). The increase expression of these genes results in the suspension of cell cycle and counteracts excessive cell proliferation or the replication of damaged DNA. Work by Rheinwald et al, (2002) has shown that normal keratinocyte proliferation is limited by $p16^{INK4a}$ regardless of culture conditions or telomerase expression. There are number of possible reasons for the up regulation of $p16^{INK4a}$ and $p15^{INK4b}$ seen in these cell lines (Rheinwald et al., 2002).

As mentioned in earlier studies telomere initiated senescence and DNA damaged senescence depend on p53 expression which is accompanied by $p21^{WAF1}$ expression (Roninson, 2003). However $p16^{INK4a}$ expression can be induced by DNA damaged albeit delayed as a second barrier to prevent the growth of damaged cells. Moreover, treatment of normal human fibroblasts with various DNA damaging agents including ionizing radiation result in the rapid activation of p53 and long term induction of $p21^{WAF1}$ (Di Leonardo et al., 1994).

The signaling pathways of $p16^{INK4a}$ and $p15^{INK4b}$ both differ but each acts on cyclin D which is involved in G1/S phase regulation (Maddika et al., 2007). The SHH pathway, a key player in BCC development has also been noted as a potential regulator of the cyclin D family and ultimately is important in G1/S phase regulation (Daya-Grosjean and Couvé-Privat, 2005). These observations were made in the cerebellum of mice but it has also been reported that SHH signaling opposes epithelial cell cycle arrest by $p21^{WAF1}$ in human keratinocytes transduced with SHH and $p21^{WAF1}$ (Fan and Khavari, 1999). Furthermore, Bishop et al. (2010), saw depression and modulation of $p16^{INK4a}$ by the SHH and IHH genes and the HH signaling pathway. The downstream target of HH signaling, GL1-2 accumulated in the nucleus and directly binds to the promoter of $p16^{INK4a}$. Examination of p16 promoter revealed a previously unreported GL1 binding site and only differs by one base mismatch from the recognised GLI binding site.

In vivo, senescent cells have been observed in association with aging but also with the early phases of tumourgenesis (Pardue and DeBaryshe, 2001). Cells in premalignant tumours undergo OIS, in contrast cells of malignant tumours have overcome senescence due to loss of senescence effectors such as $p16^{INK4a}$ (Nardella et al., 2011, Collado et al., 2005).

In this study I have shown increased level of senescence markers in both NEB1 GLI-1 cells and NEB1 189A cells. Overall there was a greater correlation between expression of senescence markers and GLI-1 in the PTCH knockdown model compared to GLI-1 over expressed cells. The reason for this is most likely the fact that wild type PTCH is present in the GLI-1 over expressed model and via negative feedback can dampen down the GLI-1 effect. In contrast in the PTCH knockdown model we observe an increase in the GLI-1 but as PTCH has been knockdown negative feedback cannot happen. Therefore, the PTCH knockdown model may be a better model representative of BCC.

I did observe variability in response to PTCH knockdown with regards protein and mRNA expression. These differences are always difficult to explain but most likely reflect the effects of cell culture condition, timing of expression. It is also important to emphasise that protein was quantified in cells by fluorescence and the relative density

measurement are much less sensitive than measuring fold changes in mRNA. This is clearly seen in Figure 4.2 with regard GLI protein and mRNA expression. Therefore, our qPCR data may be more reliable as a measurement of effects of GLI-1 on senescence markers. Based on these data but also considering protein expression. I conclude that DcR2, DEC1, $p16^{INK4a}$, p53 and $p21^{WAF1}$ are probably early targets of GLI activation.

Chapter 5: Investigation of senescence in a mouse model of BCC

Introduction

In the **chapter 3** of this thesis I showed that senescence is associated with human BCC and in **chapter 4** I showed up-regulation of senescence at both the mRNA and protein level in human keratinocytes over expressing GLI-1. These data therefore, suggested that the senescence seen in human BCC may be associated with activation of the HH pathway.

Mouse models of BCC are widely used to investigate the role of HH signalling in BCC (**see Chapter 2; section 1:10**). However, it is not known whether cell senescence plays a role in mouse BCC. The principal aim of this chapter was to investigate the expression of senescence markers in a mouse model of basal cell carcinoma and to determine whether OIS was also observed in mouse BCC. BCC is a disease of ageing (over 40 years) and rare in younger people. The main cause of this disease is UV radiation. I have already described the expression of a well characterised panel of senescence markers in human BCC (**Chapter 3**) and also in an *in-vitro* model of BCC (**Chapter 4**). The expression of senescence markers in mouse basal cell carcinoma has not previously been described in the medical or scientific literature. The markers to be used are those described in **Chapter 3** and **Chapter 4** and include p53, $p16^{INK4a}$, $p15^{INK4b}$, $p21^{WAF1}$, DEC1 and DcR2. Although some of these markers have been described previously not all have been investigated in mouse skin and not in relationship to a possible role in senescence (Zhang et al., 2005, Mitsunaga et al., 1995). In this chapter I have examined the expression of both β-galactosidase as well as p53, $p16^{INK4a}$, $p15^{INK4b}$, $p21^{WAF1}$, DEC1 and DcR2 in a murine model of BCC. The murine model I have used is that developed by Mariateresa Mancuso from Biotechnology Unit and Radiation Protection Unit, ENEA-Ente per le Nuove Tecnologie, l'Energia e l'Ambiente, Centro Ricerche, Casaccia, Rome, Italy (Mancuso et al., 2004). In this model the mice lack one *Ptch*1 allele (+/-) and have previously been shown to be susceptible to x-ray (ionizing radiation) induced BCC (Pazzaglia et al., 2004, Mancuso et al., 2009). Moreover, these mice have been shown to develop both a nodular type BCC as well as more aggressive variant BCC. I have therefore, used this model to determine whether mouse BCC also undergo senescence and also whether differences in cell senescence can be detected between Nodular and variant murine BCC's. The

expression of senescence markers were assessed by visual analogue scoring as described in the **Chapter 2**.

5.1 Expression of β-Galactosidase in *Ptch*1 wild-type (+/+) mouse skin and mouse skin lacking one *Ptch*1 Allele (+/-) and in mouse BCC derived from x-ray irradiated *Ptch*1 +/- Mice.

β-galactosidase staining was carried out on the frozen tissue sections of mouse basal cell carcinoma given by the Mariateresa Mancuso from Biotechnology Unit and Radiation Protection Unit, ENEA-Ente per le Nuove Tecnologie, l'Energia e l'Ambiente, Centro Ricerche, Casaccia, Rome, Italy . When cells undergo senescence they normally change their morphology and show β-galactosidase staining, which is recognized as marker of senescent cells (Dimri et al., 1995a). The tissues used by me in this study includes homozygous wild-type *Ptch*1 mouse skin (+/+), mouse skin lacking one *Ptch*1 allele (+/-) and mouse BCC derived from x-ray irradiated *Ptch*1 +/- mice. I have investigated β-galactosidase staining on these different types of mouse tissues to determine whether senescence is characteristic of all these tissues types or perhaps only restricted to specific groups and whether senescence is related to ionising radiation.

To carry out this study I have used a panel of murine skin biopsies as described above. Details of the mouse skin and BCC samples are shown in **Table 5.1**. The staining took 24 hours to develop. Results of these experiments are shown in **Figure 5.1 and 5.2. Figure 5.1A and B** shows that in *Ptch*1 homozygous (+/+) mouse skin β-galactosidase was mostly in the sebaceous glands with very faint probably non-specific staining in the supra basal layers of the epidermis. In *Ptch*1 +/- mouse skin (**see Figure 5.1C and D**) β-galactosidase was again restricted to the sebaceous glands. In mouse BCC derived from *Ptch*1 +/- irradiated mice (**see Figure 5.2**) no staining for β-galactosidase was detected in any of the tumour islands or stroma. The staining protocol was same for all BCC sample.

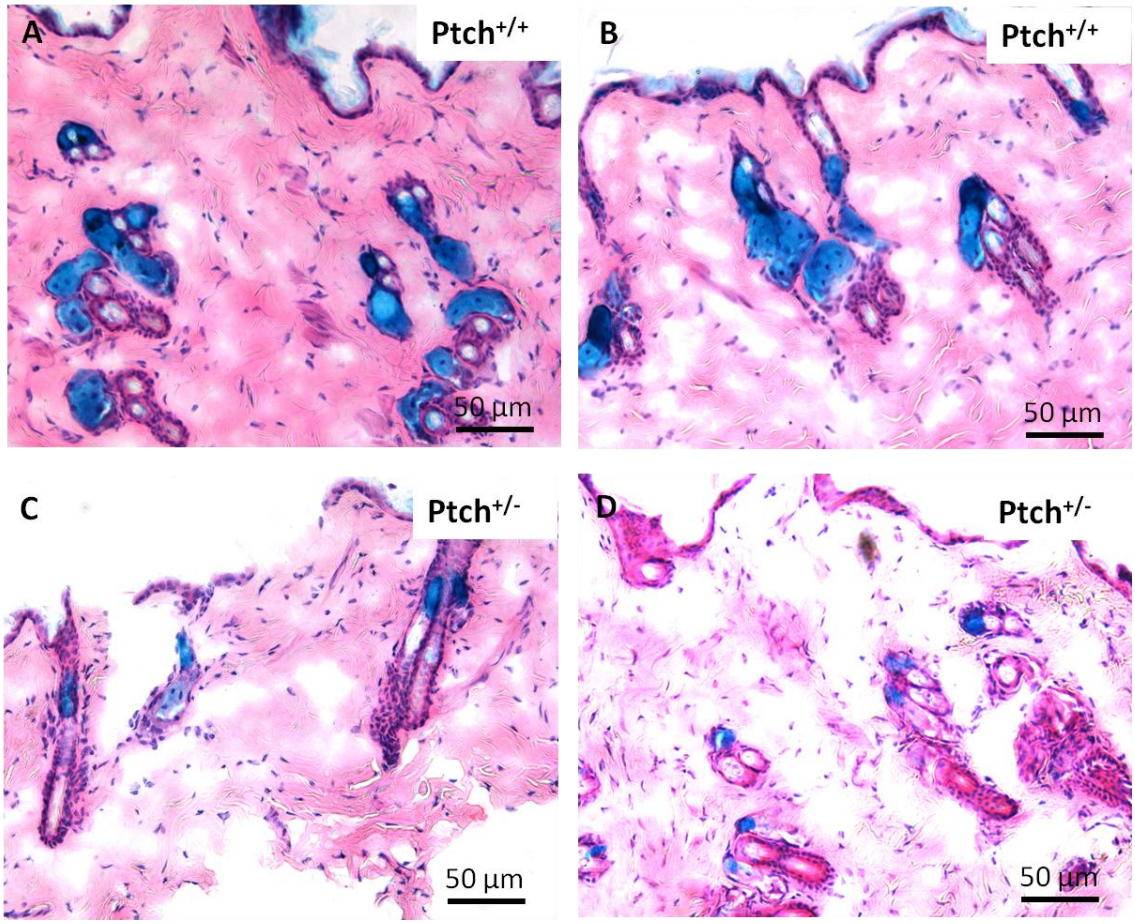

Figure 5.1: Representative images showing β-Galactosidase expression in mouse tissues (A and B) *Ptch*1 wild-type (+/+) Mouse skin (C and D) Mouse skin lacking one *Ptch*1 allele (+/-). The staining was mostly seen in the sebaceous glands.

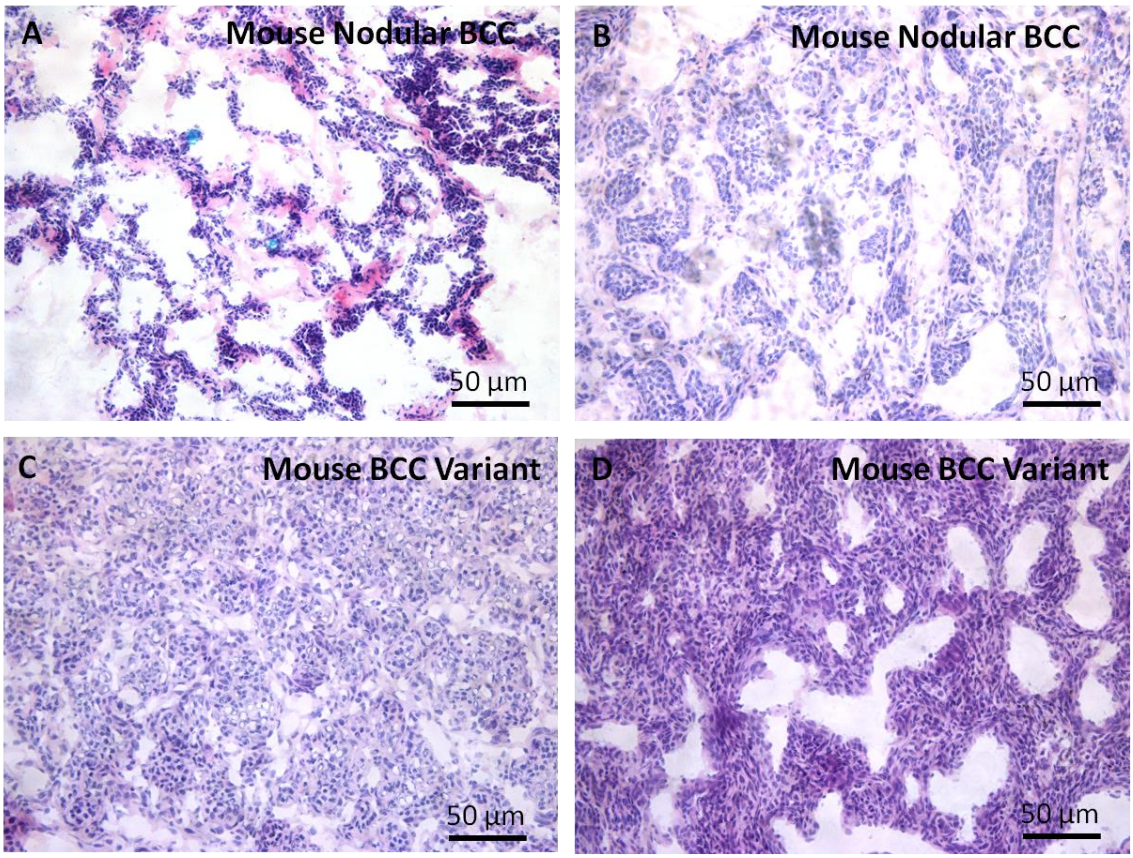

Figure 5.2: Representative images showing β-galactosidase expression in Mouse BCC derived from x-ray irradiated *Ptch* +/- Mice (A and B) Mouse BCC like tumours (C and D) Mouse BCC variants. β-galactosidase staining was negative in all samples investigated.

5.2 Expression of p53 in *Ptch*1 wild-type (+/+) and Mouse skin lacking one *Ptch*1 allele (+/-) and in Mouse BCC derived from x-ray irradiated *Ptch*1 +/- Mice

A panel of mouse skin and mouse BCC were stained for p53. The tissues included both *Ptch*1 wild-type (+/+) and *Ptch*1 null (+/-) skin as well as nodular BCC and BCC variant tumours derived from the *Ptch*1 null mice following irradiation, (**see Figure 5.3 and 5.4**). The intensity of staining was assessed by visual analogue scoring.

In both the *Ptch*1 wild-type (+/+) mice and *Ptch*1 null (+/-) mice p53 in non-irradiated skin (**Figure 5.3**) was strongly expressed in the cytoplasm of both the epidermis and in the hair follicles and sebaceous glands of both wild-type (**Figure 5.3B**) and *Ptch*1 null (**Figure 5.3C**) mice.

In irradiated mouse skin p53 stained positive and was very strong on all nodular mouse BCC tissue sections (**see Figure 5.4 A, B and C**), however in mouse BCC variant tumours the staining was very weak (**see Figure 5.4 D**). In nodular mouse BCC p53 staining is quite clearly seen in the epithelial compartment of tumours when compared with the stroma. With regards its subcellular localization p53 was mostly seen in the nucleus of the nodular BCC when compared to expression in the cytoplasm. For the variant BCC types p53 was weakly cytoplasmic and was not observed in the nucleus. Results of visual analogue scoring of staining of these tumours were analysed (**as shown in Table 5.1**).

Table 5.1: Showing Visual Analogue Scoring of Senescence Markers.

Sample Number	p53	$p16^{INK4a}$	$p21^{WAF1}$	$p15^{INK4b}$	DEC1	DcR2
Mouse skin wild type *Ptch*1 +/+ (sample 1)	3	1	0	2	1	1
Mouse skin wild type *Ptch*1 +/+ (sample 2)	3	1	2	2	1	1
Mouse skin wild type *Ptch*1 +/+ (sample 3)	3	1	0	2	1	1
Mouse Skin *Ptch*1 +/- (sample 1)	3	1	0	2	1	1
Mouse Skin *Ptch*1 +/- (sample 2)	3	1	0	2	1	1
Mouse Skin *Ptch*1 +/- (sample 3)	3	1	0	2	1	1
Mouse Nodular BCC (sample 7)	3	3	0	2	2	2
Mouse Nodular BCC (sample 8)	3	3	0	2	2	2
Mouse Nodular BCC (sample 9)	3	3	0	2	2	2
Mouse BCC Variant (sample 3)	1	0	0	1	1	0
Mouse BCC Variant (sample 4)	1	0	0	1	1	0
Mouse BCC Variant (sample 5)	1	0	0	1	1	0

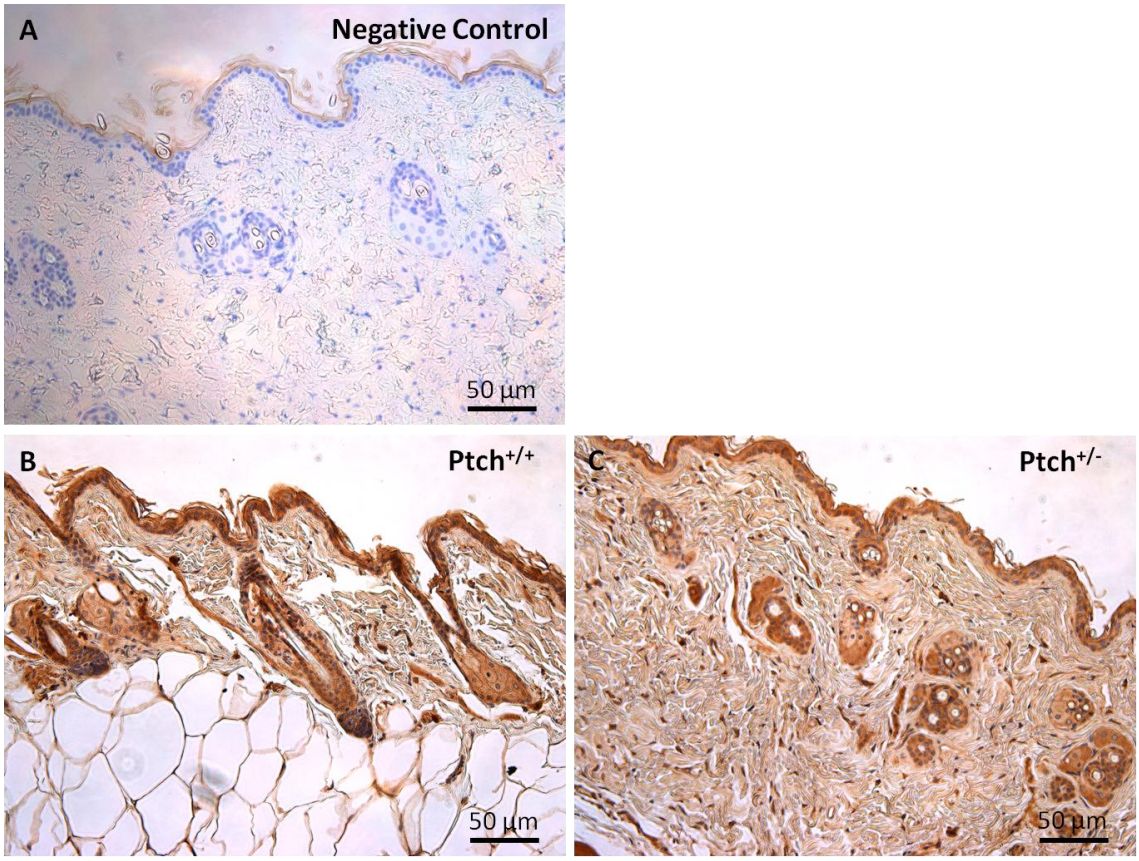

Figure 5.3: Representative images showing p53 expression in Mouse tissues (A) Mouse skin negative control (B) *Ptch*1 wild-type (+/+) Mouse skin (C) Mouse skin lacking one *Ptch*1 allele (+/-). p53 protein expression was mostly seen in epidermis, sebaceous glands and hair follicles in all investigated samples.

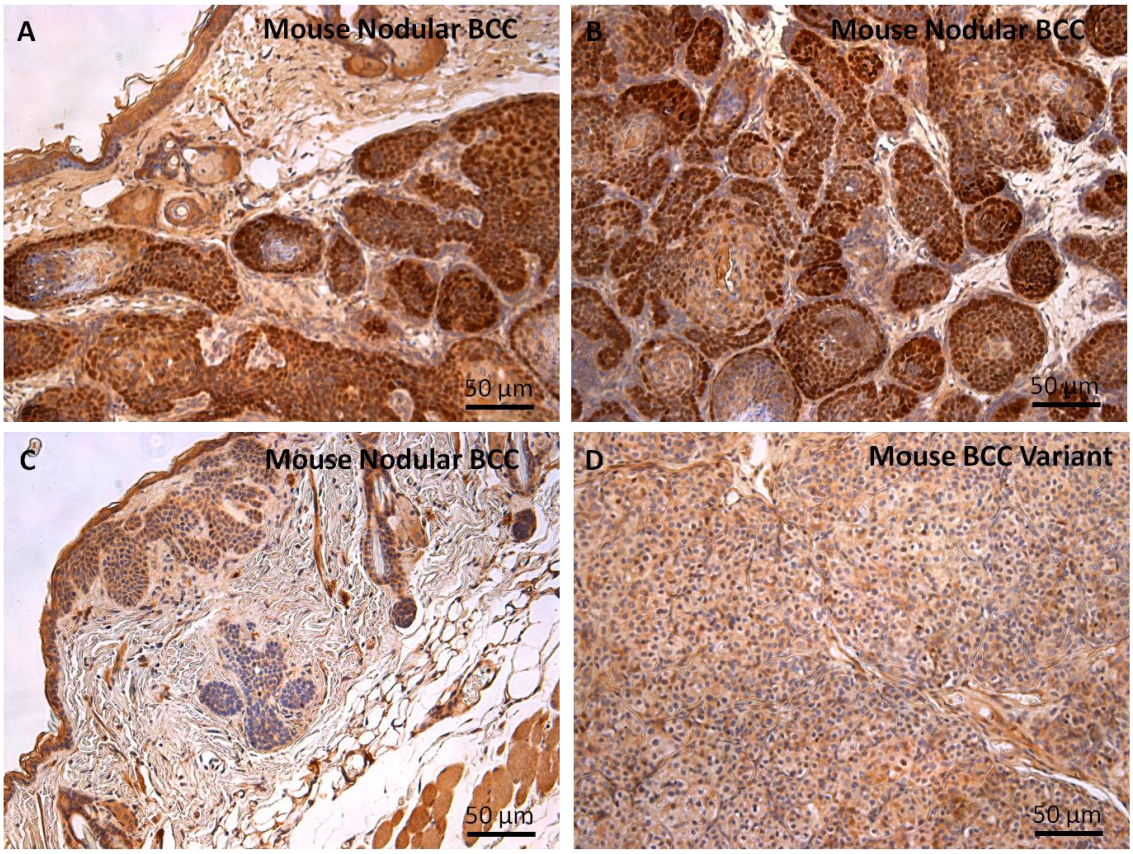

Figure 5.4: Representative images showing p53 expression in Mouse BCC derived from irradiated *Ptch*1 +/- Mice (A, B and C) Mouse Nodular BCC (D) Mouse BCC variant. The p53 staining was very strong on all tissues samples of mouse nodular BCC but not on mouse BCC variant. The staining was mostly seen in epithelial region, hair follicles and on epidermis. The cellular localization of staining was mostly seen in nucleus of nodular BCC but weakly cytoplasmic in the variant tumours.

5.3 Expression of DcR2 in *Ptch*1 wild-type (+/+) and mouse skin lacking one *Ptch*1 allele (+/-) and in mouse BCC derived from x-ray irradiated *Ptch*1 +/- Mice.

A panel of mouse skin and mouse BCC were stained for DcR2. The tissues included both *Ptch*1 wild-type (+/+) and *Ptch*1 null (+/-) skin as well as nodular BCC and BCC variant tumours derived from the *Ptch*1 null mice following irradiation, (**see Figure 5.5 and 5.6**). The intensity of staining was assessed by visual analogue scoring.

In both the *Ptch*1 wild-type (+/+) mice and *Ptch*1 null (+/-) mice DcR2 in non-irradiated skin (**Figure 5.5**) was weakly expressed in the cytoplasm of both the epidermis and in the hair follicles and sebaceous glands of both wild-type (**Figure 5.3B**) and *Ptch*1 null (**Figure 5.5C**) mice.

In irradiated mouse skin DcR2 stained positive and was of moderate in intensity on all nodular mouse BCC tissue sections (**see Figure 5.6 A, B and C**), however in mouse BCC variant the staining was negative (**see Figure 5.6 D**). In nodular mouse BCC staining is quite clearly seen in epithelial compartment and also in the stroma of tumour. With regards its subcellular localization DcR2 was mostly seen in the cytoplasm of the nodular BCC when compared to expression in the nucleus. For the variant BCC types DcR2 weakly positive in the cytoplasm. Results of visual analogue scoring of staining of these tumours were analysed (**as shown in Table 5.1**).

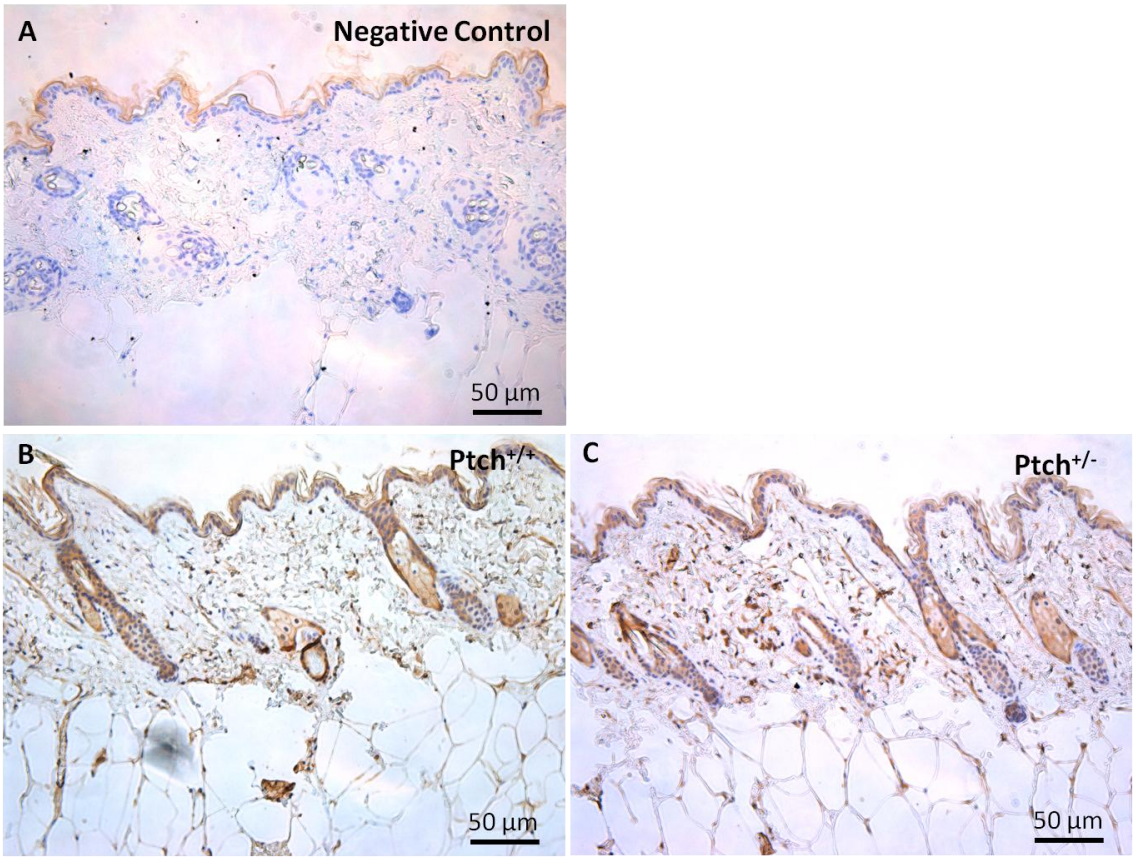

Figure 5.5 Representative images showing DcR2 expression in Mouse skin tissues (A) Mouse skin negative control (B) *Ptch*1 wild-type (+/+) Mouse skin (C) Mouse skin lacking one *Ptch*1 allele (+/-). The staining was very weak and cytoplasmic on all tissues of mouse skin samples.

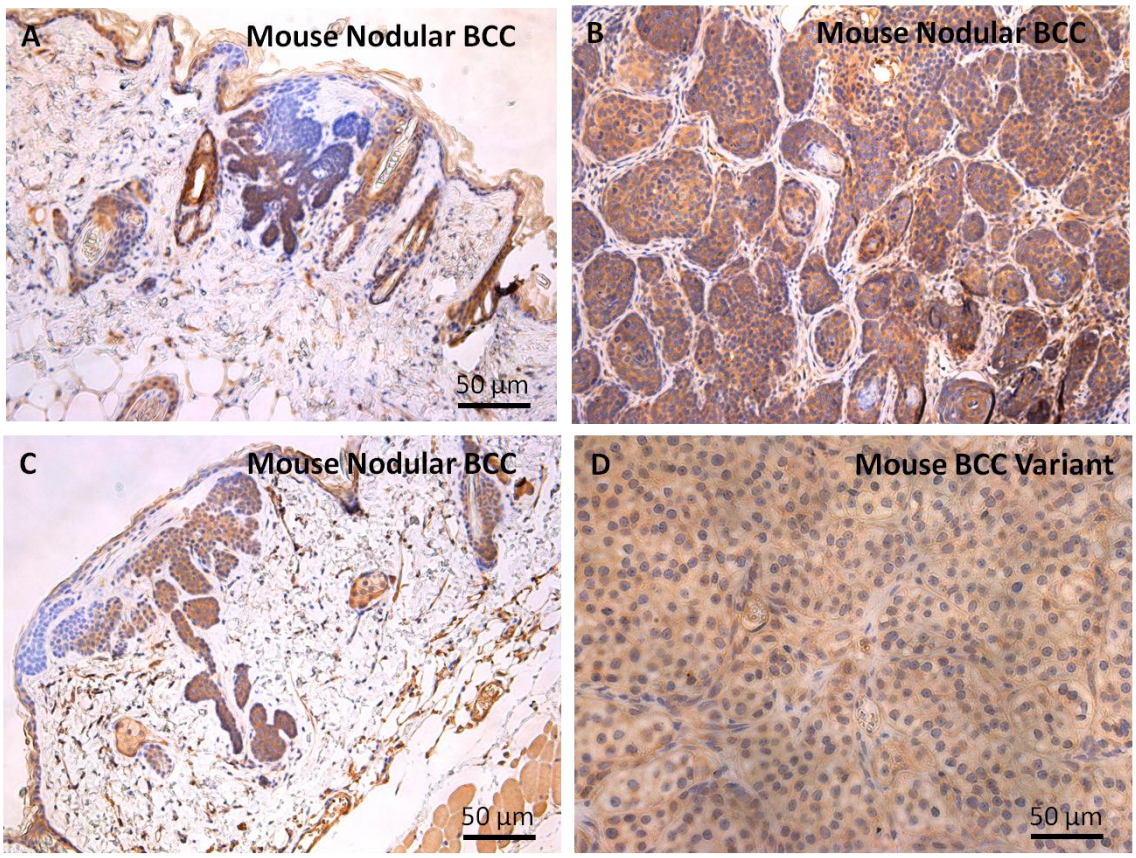

Figure 5.6: Representative images showing DcR2 expression in Mouse BCC derived from irradiated *Ptch*1 +/- Mice (A, B and C) Mouse Nodular BCC (D) Mouse BCC variant. DcR2 expression was seen in mouse nodular BCC and was seen as moderate in intensity, but on mouse BCC variant it was weakly positive. The cellular localization of staining was mostly seen in cytoplasm.

5.4 Expression of DEC1 in *Ptch*1 wild-type (+/+) and Mouse skin lacking one *Ptch*1 allele (+/-) and in Mouse BCC derived from x-ray irradiated *Ptch*1 +/- Mice.

A panel of mouse skin and mouse BCC were stained for DEC1. The tissues included both *Ptch*1 wild-type (+/+) and *Ptch*1 null (+/-) skin as well as nodular BCC and BCC variant tumours derived from the *Ptch*1 null mice following irradiation, (**see Figure 5.7 and 5.8**). The intensity of staining was assessed by visual analogue scoring.

In both the *Ptch*1 wild-type (+/+) mice and *Ptch*1 null (+/-) mice DEC1 in non-irradiated skin (**Figure 5.7**) was weakly expressed in the cytoplasm of both the epidermis and in the hair follicles and sebaceous glands of both *Ptch*1 wild-type (**Figure 5.7B**) and *Ptch*1 null (**Figure 5.7C**) mice.

In irradiated mouse skin DEC1 stained positive and was moderate in intensity on all nodular mouse BCC tissue sections (**see Figure 5.8 A, B and C**), however in mouse BCC variant tumours the staining was very weak (**see Figure 5.8 D**). In nodular mouse BCC staining is quite clearly seen in epithelial compartment when compared with the stroma. With regards its subcellular localization DEC1 was mostly seen in the cytoplasm of the nodular BCC when compared to expression in the nucleus. For the variant BCC types DEC1 remained weakly cytoplasmic and was not observed in the nucleus. Results of visual analogue scoring of staining of these tumours were analysed (**as shown in Table 5.1**).

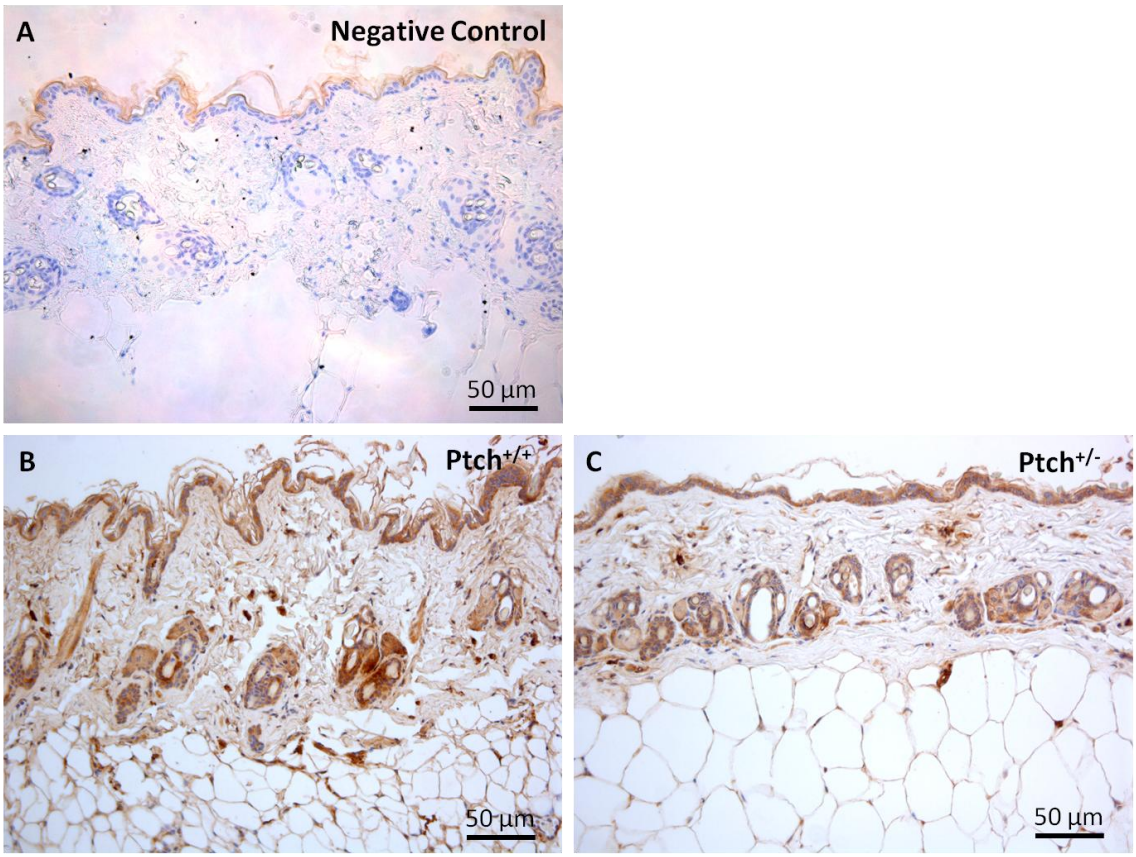

Figure 5.7: Representative images showing DEC1 expression in Mouse skin tissues (A) Mouse skin negative control (B) *Ptch*1 wild-type (+/+) Mouse skin (C) Mouse skin lacking one *Ptch*1 allele (+/-). The staining was very weak on these samples of mouse skin. The staining was seen mostly seen in epidermis and hair follicles.

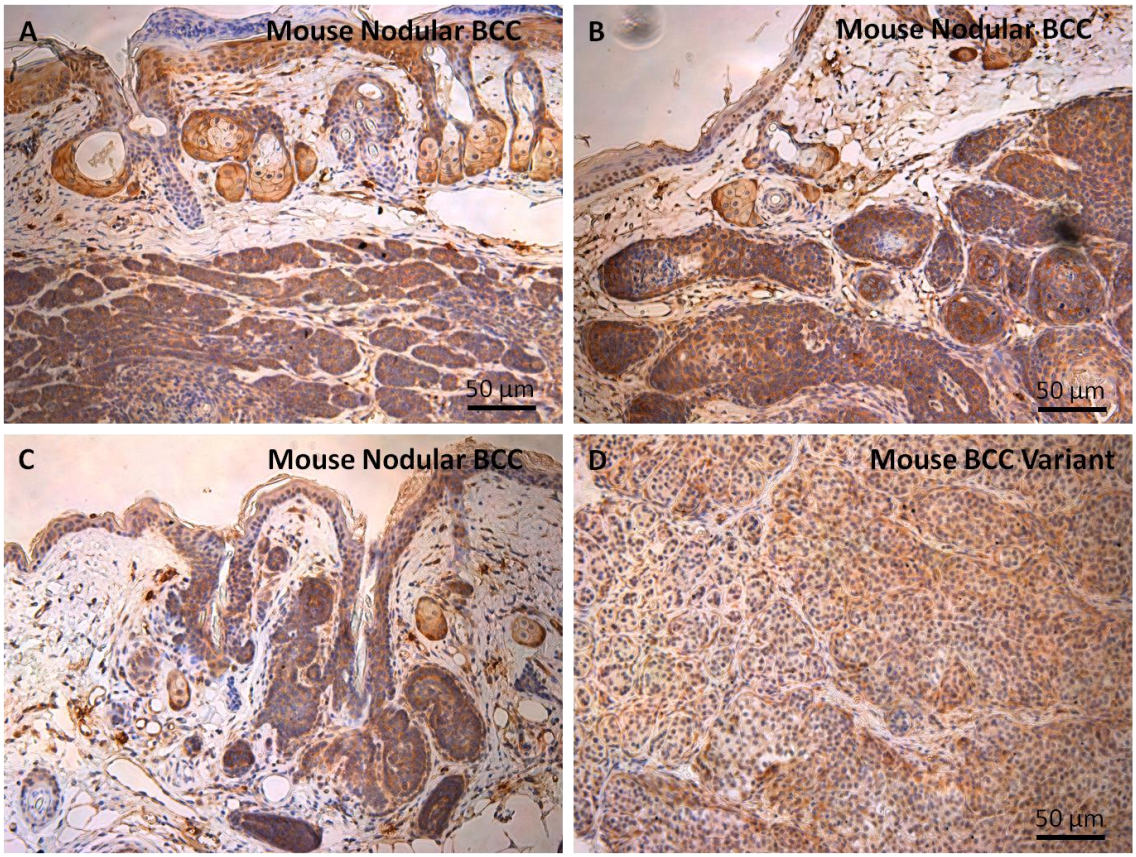

Figure 5.8: Representative images showing DEC1 expression in Mouse BCC derived from irradiated *Ptch*1 +/- Mice (A, B and C) Mouse Nodular BCC (D) Mouse BCC variant. DEC1 expression was more strongly seen in nodular mouse BCC when compared with mouse BCC variant tumours. In both nodular and variant tumours expression was cytoplasmic.

5.5 Expression of $p16^{INK4a}$ in *Ptch*1 wild-type (+/+) and Mouse skin lacking one *Ptch*1 allele (+/-) and in Mouse BCC derived from x-ray irradiated *Ptch*1 +/- Mice.

A panel of mouse skin and mouse BCC were stained for $p16^{INK4a}$. The tissues included both *Ptch*1 wild-type (+/+) and *Ptch*1 null (+/-) skin as well as nodular BCC and BCC variant tumours derived from the *Ptch*1 null mice following irradiation, (**see Figure 5.9 and 5.10**). The intensity of staining was assessed by visual analogue scoring.

In both the *Ptch*1 wild-type (+/+) mice and *Ptch*1 null (+/-) mice, $p16^{INK4a}$ in non-irradiated skin (**Figure 5.9**) was weakly expressed in the cytoplasm of both the epidermis and in the hair follicles and sebaceous glands of both wild-type (**Figure 5.9B**) and *Ptch*1 null (**Figure 5.9C**) mice.

In irradiated mouse skin $p16^{INK4a}$ stained positive and was very strong on all nodular mouse BCC tissue sections (**see Figure 5.10 A, B and C**), however in mouse BCC variant the staining was negative (**see Figure 5.10 D**). In nodular mouse BCC staining is quite clearly seen in epithelial compartment when compared with the stroma of tumour type. With regards its subcellular localization $p16^{INK4a}$ was mostly seen in the cytoplasm of the nodular BCC when compared to expression in the nucleus. Results of visual analogue scoring of staining of these tumours were analysed (**as shown in Table 5.1**).

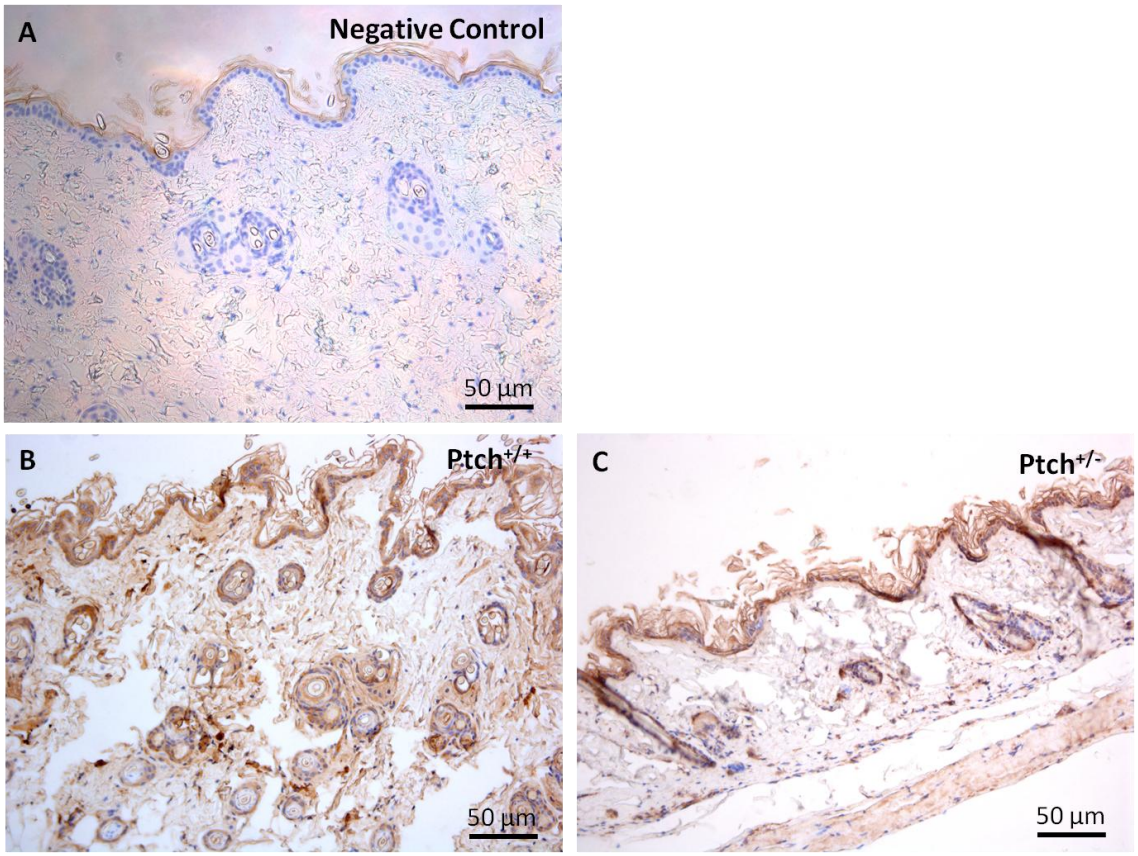

Figure 5.9 Representative images showing $p16^{INK4a}$ expression in Mouse skin tissues (A) Mouse skin negative control (B) *Ptch*1 wild-type (+/+) Mouse skin (C) Mouse skin lacking one *Ptch*1 allele (+/-). The $p16^{INK4a}$ expression was very weak on all tissues investigated.

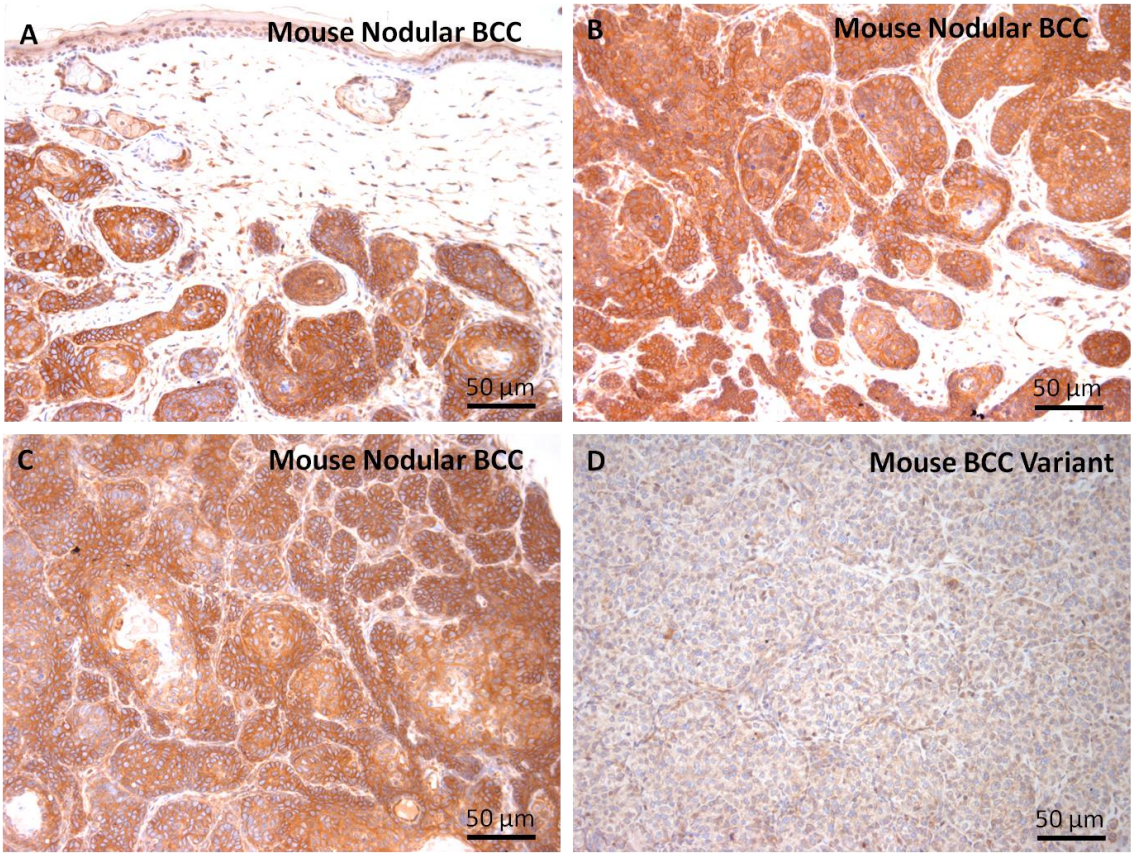

Figure 5.10: Representative images showing p16^{INK4a} expression in Mouse BCC derived from irradiated *Ptch* +/- Mice (A, B and C) Mouse Nodular BCC (D) Mouse BCC variant. p16^{INK4a} staining was seen in nodular mouse BCC but staining was absent in the mouse BCC variant apart from some weak possibly stromal staining. The cellular localization of p16 ^{INK4a} was seen in cytoplasm of nodular mouse BCC.

5.6 Expression of p15^{INK4b} in *Ptch*1 wild-type (+/+) and Mouse skin lacking one *Ptch*1 allele (+/-) and in Mouse BCC derived from x-ray irradiated *Ptch*1 +/- Mice.

A panel of mouse skin and mouse BCC were stained for p15^{INK4b}. The tissues included both *Ptch*1 wild-type (+/+) and *Ptch*1 null (+/-) skin as well as nodular BCC and BCC variant tumours derived from the *Ptch*1 null mice following irradiation, (**see Figure 5.11 and 5.12**). The intensity of staining was assessed by visual analogue scoring.

In both the *Ptch*1 wild-type (+/+) mice and *Ptch*1 null (+/-) mice p15^{INK4b} in non-irradiated skin (**Figure 5.11**) was expressed in the cytoplasm of both the epidermis and in the hair follicles and sebaceous glands of both wild-type (**Figure 5.11B**) and *Ptch*1 null (**Figure 5.11C**) mice.

In irradiated mouse skin p15^{INK4b} stained positive and was very strong on all nodular mouse BCC tissue sections (**see Figure 5.12 A, B and C**), however in mouse BCC variant the staining was very weak (**see Figure 5.12 D**). In nodular mouse BCC staining is quite clearly seen in epithelial compartment when compared with the stroma of tumour type. With regards its subcellular localization p15^{INK4b} was mostly seen in the cytoplasm of the nodular BCC when compared to expression in the nucleus. For the variant BCC types p15^{INK4b} remained weakly cytoplasmic and was not observed in the nucleus. Results of visual analogue scoring of staining of these tumours were analysed (**as shown in Table 5.1**).

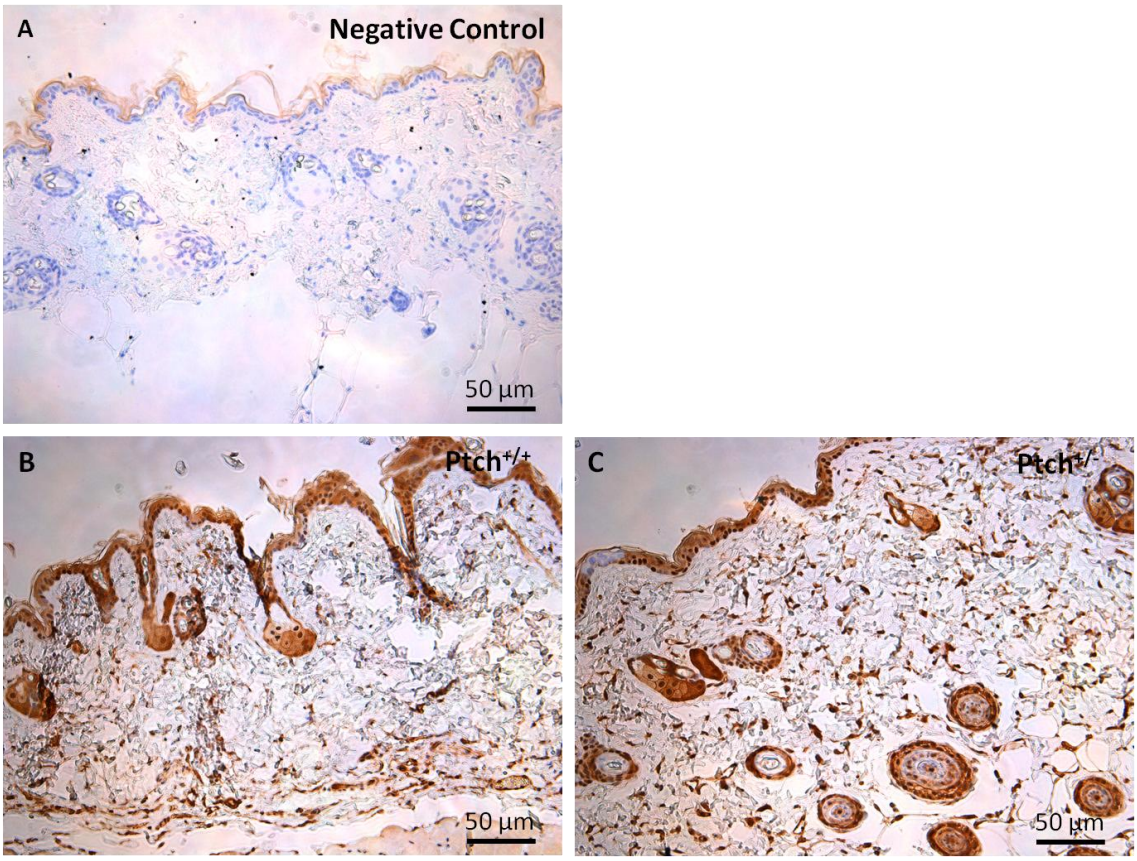

Figure 5.11: Representative images showing $p15^{INK4b}$ expression in Mouse skin (A) Mouse skin negative control (B) *Ptch*1 wild-type (+/+) Mouse skin (C) Mouse skin lacking one *Ptch*1 allele (+/-). The staining of $p15^{INK4b}$ was seen in all samples of skin sample investigated. The staining was mostly seen epidermis and hair follicles.

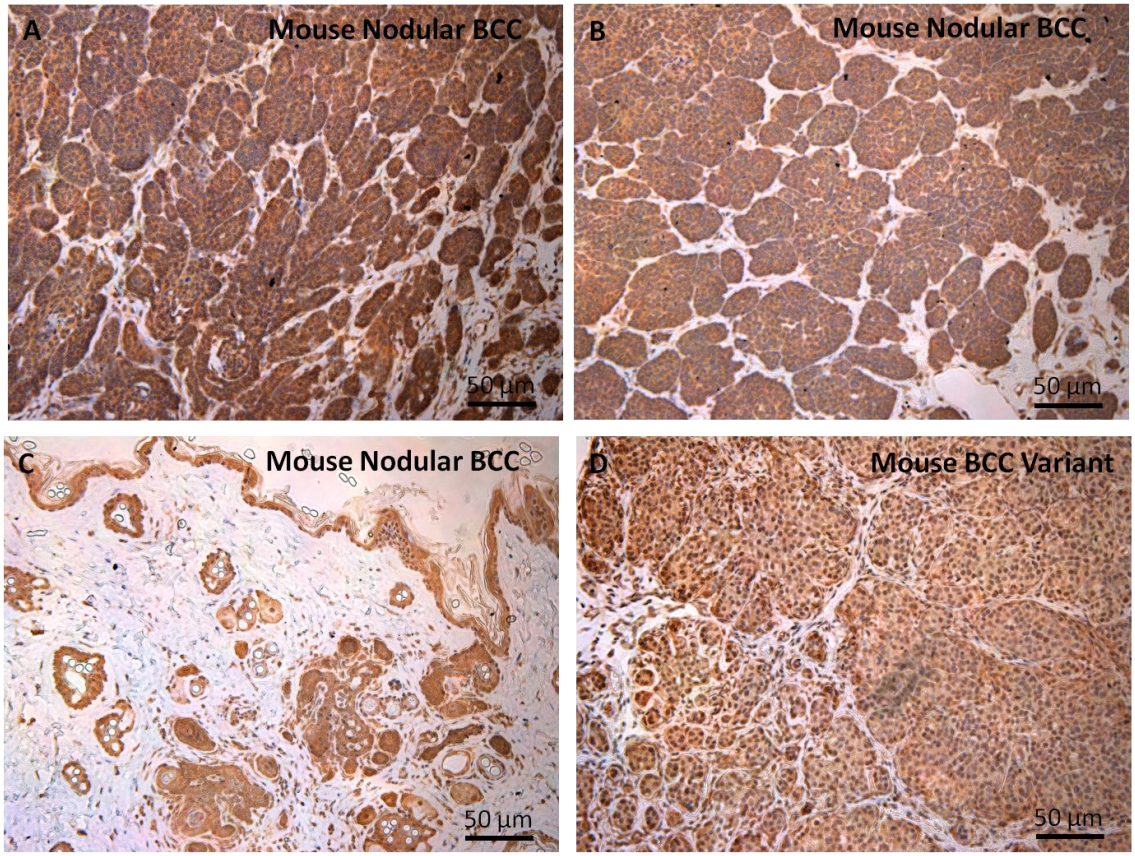

Figure 5.12: Representative images showing $p15^{INK4b}$ expression in Mouse BCC derived from irradiated *Ptch* +/- Mice (A, B and C) Mouse Nodular BCC (D) Mouse BCC variant. $p15^{INK4b}$ expression was seen in all nodular mouse BCC and also very weak staining was seen in mouse variant BCC.

5.7 Expression of p21^{WAF1} in *Ptch*1 wild-type (+/-) and Mouse skin lacking one *Ptch*1 allele (+/-) and in Mouse BCC derived from x-ray irradiated *Ptch*1 +/- Mice.

Multiple tissues of mouse BCC and mouse skin were stained for p21^{WAF1}. The tissues includes nodular BCC, BCC variants, *Ptch*1 Wild type Mouse skin (+/+) and Mouse skin lacking on *Ptch*1 allele (+/-) (**see Figure 5.13**). The intensity of staining was assessed by visual analogue scoring.

There was no staining of p21^{WAF1} on all nodular mouse BCC tissue sections and also no staining in mosue BCC variant along with *Ptch*1 Wild type Mouse skin (+/+) and Mouse skin lacking on *Ptch*1 allele (+/-)(**see Figure 5.13 C & D**). I have used mouse colon tissues as positive control for p21^{WAF1} and it shows staining in nucleus (**see Figure 5.13 B**) These data therefore, indicate no staining of p21^{WAF1} in the mouse BCCs and mouse skin. Results of visual analogue scoring of staining of these tumours were analysed (**as shown in Table 5.1**).

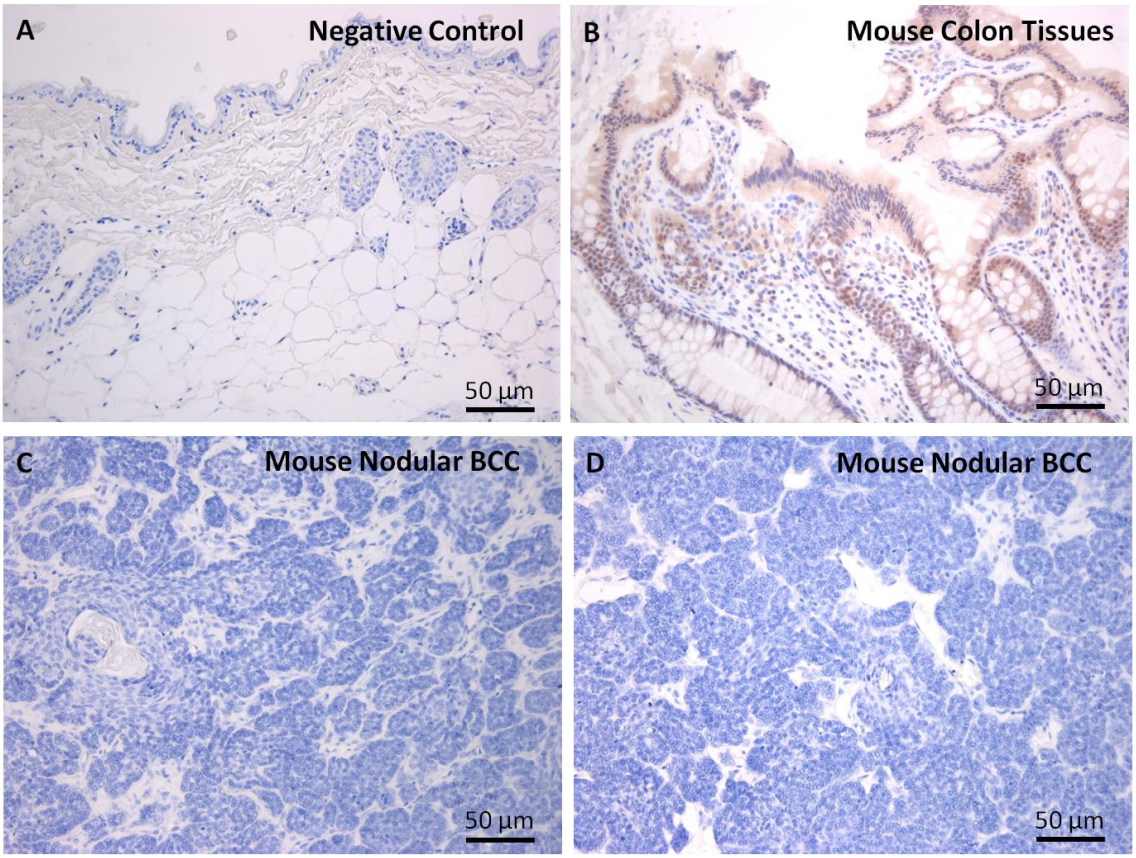

Figure 5.13: Representative images showing $p21^{WAF1}$ expression in Mouse skin and BCC tissues (A) Negative control (B) Mouse colon tissues as positive control (C) Mouse Nodular BCC (D) Mouse BCC variant. The staining of $p21^{WAF1}$ was negative on all samples investigated apart from the positive control which showed staining for $p21^{WAF1}$ in the colon and thus confirming the antibody staining was working.

Discussion

The aim of this study was to examine the presence of senescence markers in mouse BCC and mouse skin to determine whether senescence is also a characteristic of these mouse tumours. The immunohistochemical expression and localization of senescence markers was investigated in wild type *Ptch* +/+ mouse skin, *Ptch* +/- mouse skin and mouse BCC derived from irradiated *Ptch* +/- mouse skin (Mancuso et al., 2004). My experiments shows marked increased in cell senescence markers in mouse BCC when compared to control wild type *Ptch* +/+, *Ptch* +/- mouse skin. It was interesting to note however, that in general more intense staining for senescence markers was observed in the nodular mouse BCCs compared to the more aggressive variant BCCs. This may suggest that in the variant BCCs the tumour cells have been able to escape senescence or have not undergone senescence.

Cellular senescence is an age-related process where cells remain metabolically active but in a growth-arrested state at the G1 phase. p53, $p21^{WAF1}$, $p15^{INK4b}$ and $p16^{INK4a}$, which are known to regulate G1 cell cycle arrest, and the tumour necrosis factor receptor super family member decoy receptor 2 (DCR2) and DEC1 have been recently identified as senescence markers (Xu et al., 2012).

Overall in this study the expression of senescence markers were higher in mouse nodular BCC (benign type of BCC) compared to mouse BCC variants (aggressive type of BCC). This data suggests that senescence is a feature of the benign mouse tumours but not in the more aggressive or malignant type. This data is different to that observed in human BCC where similar levels of senescence markers were observed in both benign nodular and more aggressive morphoeic BCC. Although senescence in mouse models of BCC have not been previously reported senescence has been demonstrated in chemically induced skin papillomas in mice which have H-ras oncogenic mutations (Collado et al., 2005). Senescence has also been reported in mouse lung and colorectal tumours (Serrano and Blasco, 2001, Serrano et al., 1997, Floyd et al., 2005, Bennecke et al., 2010).

With regards p53 this has previously been shown to be expressed in BCC before and cellular localization was mostly in the nucleus (Eshkoor et al., 2008). Also in my study p53 is mostly expressed nucleus of mouse BCC. This data correlates with previous data. p53 has also been reported in mouse basal cell carcinomas in mice over expressing GLI-1 (Nilsson et al., 2000a) and also in *Ptch*1 deficient mice (Mancuso et al., 2004). Bolshakov et al. (2003) in his study on human BCC also showed no difference in staining for p53 in aggressive and non aggressive BCC (Bolshakov et al., 2003) which supports my data. Inactivating mutations in p53 are found in most tumour types, and so contribute to the complex network of molecular events leading to tumour formation (Levine, 1997). The p53 gene exerts anti-proliferative effect in response to a variety of different stimuli, such as DNA damage telomere shortening, oxidants, hypoxia and a variety of stresses. Loss of functional p53 may also inhibit apoptotic pathways and hence enhance survival of abnormal cells (Levine, 1997).

In this study I observed $p16^{INK4a}$ and $p15^{INK4b}$ expression in mouse BCC that was predominately localised in the cytoplasm. It has been reported that there is structural and functional homology between $p15^{INK4b}$ and $p16^{INK4a}$ and that $p15^{INK4b}$ is transcriptionally activated by transforming growth factor-B (TGF-β) (Rahimi and Leof, 2007, Hannon and Beach, 1994). Human BCCs have previously been reported to express $p16^{INK4a}$ in human BCC and has been reported as a senescence markers in adenoma and adenocarcinoma (Collado et al., 2005, Eshkoor et al., 2008). The expression of $p16^{INK4a}$ is reported to be induced in response to DNA damage, oncogenic Ras expression and by other cellular stresses. Under normal physiological conditions $p16^{INK4a}$ is expressed in low levels but if cells are under stress such as oncogenic stress $p16^{INK4a}$ levels increase. The $p16^{INK4a}$ protein is often highly expressed in senescent cells in culture and inactivated in a variety of human cancers (Eshkoor et al., 2008, Michaloglou et al., 2005, Serrano et al., 1997). In cancer the influence of $p15^{INK4b}$ is not clear and work with $p15^{INK4b}$ deficient mice has only shown a subtle predisposition to tumours whereas loss of $p16^{INK4a}$ causes a wide range of tumours (Eshkoor et al., 2008). Staining for $p15^{INK4b}$ has been reported in human premalignant lung tumors, nodular hyperplasia and PIN tissues (Zhang et al., 2006). Therefore expression of $p15^{INK4b}$ in mouse BCC may not play important role in senescence.

However, the fact that these tumours also express $p16^{INK4a}$ suggest a role for the protein in BCC senescence.

DcR2 expression has been reported to protect cells from trail induced apoptosis and is regulated by p53 (Liu et al., 2005). DcR2 expression is often silenced or down-regulated by promoter hypermethylation in multiple cancer types, including cervical cancer, breast cancer, neuroblastoma, malignant mesothelioma, and prostate cancer (Liu et al., 2005). The expression of the DcR2 has been previously reported in adenomas and carcinomas. Both adenomas and carcinomas exhibited cytoplasmic staining for DcR2. Meng *et al* (2000) found DCR2 overexpression in human colon cancer cells and studies have shown that some chemotherapy agents caused DCR2 over expression in a human lung cancer cell lines (Meng et al., 2000). However, my current study is the first time this has been reported in either human or mouse BCC.

DEC1 expression is reported to be induced in response to hypoxia (Chakrabarti et al., 2004). The expression of DEC1 has been reported in the nuclei of a number of human tumours including breast, colon, lung, and head and neck cancers (Ehata et al., 2007). The expression pattern in tumour cells was much stronger than that in surrounding non-neoplastic tissue or that seen previously in normal tissues. However, there are no reports so far of DEC1 expression in either mouse or human BCC.

In summary, my study demonstrated that there is an increased protein expression of senescence-associated molecular markers indicating that cellular senescence might play a role in mouse BCC cancer. In particular my data showed that in the more aggressive mouse BCCs p53, DcR2, DEC1, $p16^{INK4a}$ and $p15^{INK4b}$ were only weakly expressed when compared to nodular BCC types. These data suggest that the more aggressive mouse BCC may have overcome cell senescence and this may explain the more aggressive nature of these tumours. This is however, different from human BCCs in which I observed similar levels of expression of senescent markers in both the benign nodular BCCs and in more aggressive morphoeic tumours. The mechanism by which the variant mouse BCCs overcome senescence is not clear from my studies however, understanding how cancer cells are able to evade senescence is of considerable interest but poorly understood. In general there are two possible

mechanisms of tumour reversion or avoidance involving either reversal of senescence involving inactivating mutations of essential senescence-maintenance genes or avoidance of senescence through low levels of oncogene expression (McDuff and Turner, 2011).

My data may indicate that in the variant mouse BCC senescence avoidance is achieved via low levels of expression of proteins associated with senescence. However, for my studies the mechanism of action is not clear.

Chapter 6: Discussion

Discussion

BCC is the most common skin cancer in humans which accounts for approximately 80% of all NMSC with incidence of BCC increase by 10% annually. Although BCC very rarely metastasise they can be locally very destructive of surrounding tissue and can be divided into two groups. The first group of BCC include less aggressive (superficial and nodular BCC) and second group includes the more aggressive BCC subtypes such as morphoeic and infiltrative. Cellular senescence is an important tumour suppressor, limiting cell lifespan and removing damaged cells from a proliferative state preventing the formation of clonal tumours. The aim of the work carried out in this thesis was to investigate senescence in human BCC. I hypothesised that senescence may be a characteristic the more benign nodular and superficial BCC subtypes and that there may be down regulation of senescence in the more aggressive morphoeic and infiltrative types of BCC. Cellular senescence is an important tumour suppressor, limiting cell lifespan and removing damaged cells from a proliferative state preventing the formation of clonal tumours. To study this I have used a number of models and have investigated cell senescence in human BCC tissues, in an in-vitro model BCC developed in my laboratory by another PhD student Muhammad Rahman (Rahman, 2013) and in mouse BCCs. To characterise senescence in these models I have used a number of well known and well characterised markers of cell senescence. The major well defined markers include senescence associated β-galactosidase assay, DcR2 (Decoy Receptor 2), DEC1 (differentially embryo-chondrocyte expressed gene), p53, $p16^{INK4a}$ and $p21^{WAF1}$ genes. . Overall the techniques I have used in this thesis have been straightforward and with the exception of immunohistochemistry using the $p21^{WAF1}$ antibody I have experienced very few problems.

In **Chapter 3** of this thesis I carried out β-galactosidase staining on the frozen tissue sections of basal cell carcinoma and also looked at the expression of DcR2, DEC1, $p16^{INK4a}$, p53, $p21^{WAF1}$ and $p15^{INK4b}$ in formalin fixed BCC from the archives of the Royal London Hospital. These experiments were carried out in formalin fixed sections as morphoeic BCCs are not very common and therefore, would have taken considerable time to collect fresh morphoeic tumours. I therefore, carried out the β-galactosidase

assay on fresh frozen samples as the β-galactosidase assay will not work on formalin fixed sections for the reasons described in Chapter 2. The senescence markers used in my study have previously been in a number of pathological conditions, includes chronic ulcers, benign prostate hypertrophy, atherosclerotic plaques, osteoarthritis, and tissue damage by radiation or chemotherapy (Campisi, 2005, Jeyapalan and Sedivy, Kahlem et al., 2004). In my study β-galactosidase staining was in all human BCC samples investigated, however, expression was mainly restricted to the stromal cells of the tumour and only occasional epithelium cells showed positive β-galactosidase staining. In contrast DcR2, DEC1, $p16^{INK4a}$, p53, $p21^{WAF1}$ and $p15^{INK4b}$ were detected in both the stroma and epithelium of BCCs. The reason why the epithelium of BCC did not stain for β-galactosidase when it was positive for the other senescence markers is not clear. However, although β-galactosidase is widely used and accepted as a marker of senescence there was some reservation about its use. Dimri *et al.,* (Dimri et al., 1995a) in experiments with cultured fibroblasts, first described lysosomal beta-galactosidase activity, which is expressed ubiquitously in most cells when assayed at a pH of 4.0 as a marker for senescent cells which stain positively for beta-galactosidase when assayed at a pH of 6.0. This novel staining capacity was ultimately referred to as senescence-active beta-galactosidase (SA-β-gal) activity. Although, SA-β-Gal is widely used as a marker of senescence in some human cells (Choi et al., 2000). We do not yet know the origin or function of SA-β-Gal. Moreover, it is not known whether this is a distinct enzyme active at pH 6, and differentially expressed in senescence, or reflects an increase in the classic acid lysosomal β-galactosidase. The specificity and selectivity of this assay have been disputed by other groups (Kurz et al., 2000). β-galactosidase activity at pH 6 has been shown in immortalised cell lines following either serum starvation or phorbol ester-induced macrophage-like differentiation (Yegorov et al., 1998), or have detected pH 6 activity, using a sensitive high-pressure liquid chromatography assay, in various proliferating cell lines and in liver homogenates (Krishna et al., 1999). However, despite the reservations senescence-associated β-galactosidase (SA-β-gal) is still the most widely used biomarker for senescent or ageing cells. However, it is advisable to use this marker in parallel with established markers. Therefore, in my thesis as well as using senescence-associated β-galactosidase (SA-β-

gal) I have also used the panel of senescence markers described by (Collado et al., 2005).

In my research I observed that there was no significant difference in the expression of senescence markers between different BCC types as I had originally hypothesised. This suggests that while senescence is a characteristic of BCC the difference between benign and aggressive BCC does not appear to be due to differences in the level of senescence i.e. aggressive BCC do not appear to be any less senescent than benign BCC. Perhaps this is not totally surprising as it has recently been reported that human BCC have one of the highest rates of mutations in any human tumour (Jayaraman et al., 2013). Therefore, while PTCH may be the initial driver mutation the subsequent biology of BCC may be influenced by many other pathways.

In Chapter 4 of my thesis I went on to investigate whether the senescence markers detected in BCC in Chapter 3 were direct targets of HH signalling. To investigate this I used two different *in vitro* models of BCC developed by my group. The first of these models was NEB-1 keratinocytes transduced by retrovirus to over express GLI-1. The second model was NEB-1 keratinocytes in which the PTCH1 receptor has been knocked down by shRNA. As outlined in Chapter 4 the disadvantage of using cells over expressing GLI1 is that although this reflects the increase in GLI1 seen in BCC these cells have wild type PTCH1. In these keratinocytes over expression of GLI1 will activate a negative feedback loop in which GLI1 up-regulates its target gene PTCH1 and then PTCH1 then is able to repress the GLI1 response. This may result in damping down of any possible effect of GLI1. In contrast PTCH1 knockdown recapitulates the events seen in BCC in which PTCH1 is mutated and as a result GLI1 is up regulated. Because I used shRNA this also results in a stable heritable knockdown of the target gene. In Chapter 4 I showed that at both the mRNA and protein level that there is increase in senescence markers in my *in-vitro* model at protein and mRNA level. However, I did observe marked differences in levels of expression both at the mRNA and protein level between the PTCH knockdown and GLI overexpressing cells. The reason for this variation can most probably be explained by the fact that in the NEB1 GLI-1 cells, GLI-1 is overexpressed in cells containing the wild type PTCH1 gene. As PTCH1 is a direct target of GLI-1 and act as a negative feedback loop it is highly likely that in these cells

PTCH1 is able to damp down the effects of GLI-1 overexpression. In contrast in the NEB1-189A cells in which PTCH1 has been knocked down using shRNA the subsequent increase in GLI1 expression may be a better reflection of what happens in BCC. However, for the reasons explained above and the high burden of mutations in BCC the PTCH knockdown cells may only reflect early events in BCC development. However, such models are essential for understanding early events in BCC development and Harrison et al (2013) have used human keratinocytes to over express GLI1 and GLI2 and shown that these cells are resistant to apoptosis but do not form colonies in soft agar indicating that they are not transformed. However, on treatment with known mutagens colonies of cells survive and grow in soft agar suggesting cellular transformation. It would be important to see if similar changes occur with PTCH1 knockdown cells and whether exposure to UV or carcinogens can then be used to model subsequent events in BCC tumour development. Finally, it is also important to highlight that BCC is associated with an extensive stroma and that this stroma is likely to play an important role in growth and development of the BCC. Further working using PTCH1 knockdown cells and BCC derived stroma would be important although as mentioned in Chapter 3 these cells are also senescent and have proven difficult to maintain *in vitro*.

Finally in Chapter 5 I have investigated whether the cell senescence I observed in human BCC in Chapter 3 and which I showed in Chapter 4 is associated with HH signalling can also be observed in mouse BCCs. This is important as murine models of BCC are widely used to investigate BCC biology (See Section Chapter 1). The mouse model of BCC I used was that developed by Mariateresa Mancuso from Biotechnology Unit and Radiation Protection Unit, ENEA-Ente per le Nuove Tecnologie, l'Energia e l'Ambiente, Centro Ricerche, Casaccia, Rome, Italy. This group have generated Mice lacking one *Ptch*1 allele, through targeted disruption of exons 6 and 7 in 129/SV ES cells and maintained on CD1 background (Mancuso et al., 2004). Mancuso et al performed X-ray irradiation **(HVL _ 1.6 mmCu)** on these mice using a Gilardoni CHF 320G X-ray generator (Gilardoni S.p.A.; Mandello de Lario Lecco, Italy) operated at 250 kVp, 15 mA, with filters of 2.0 mm of A1 and 0.5 mm of Cu. *PTCH*1$^{neo67/+}$ mice and wild-type littermates of both sexes were whole-body irradiated with 3 Gy of X-rays as

newborns (4 days of age) or adults (90 days of age). In addition, 2-month-old mice were subjected to local irradiation of the dorsal skin with a single dose of 4 Gy of X-rays. I carried out staining for β-galactosidase as well as DcR2, DEC1, $p16^{INK4a}$, p53, $p21^{WAF1}$ and $p15^{INK4b}$ on *Ptch1* Wild-type (+/+) and *Ptch1* (+/-) mouse skin as well as on BCC derived from irradiated *Ptch1* +/- Mice. Although I did not detect β-galactosidase in any mouse tumours the staining for most markers was moderate in intensity in all nodular BCC except for p53 which was very strong on nodular mouse BCC (non aggressive type). In contrast I only observed very weak or no staining for these markers on mouse BCC variant (aggressive type). These data suggest that mouse nodular BCC are similar to human nodular BCC and are highly senescent. In contrast the aggressive mouse variant BCC have much lower levels of senescence and this is in direct contrast with the situation in human morphoeic BCC. The data from the mouse variant BCCs suggest that these mice have either overcome senescence or perhaps levels of senescence were lower to start with and which may explain why these variant tumours develop.

Lack of senescence associated β-galactosidase activity in mouse tumours is not clear. However, it may be related to the early stages of BCC development with the mouse tumours harbouring fewer mutations. It has also been shown in a mouse model of bladder tumorigenesis that up-regulation of senescence associated molecules including Dec1 and DcR2 was not associated with senescence associated β-galactosidase activity (Mo et al., 2007). Lack of senescence associated β-galactosidase activity may also be linked to lack of expression of p21 as this protein has been associated with cell senescence and decreased senescence associated β-galactosidase activity has been reported in v-Ha-ras transduced keratinocytes cells lacking p21 (Weinberg and Denning 2002 for review). Finally senescence associated β-galactosidase activity is associated with the lysosome but is itself not essential for senescence to occur (Lee et al., 2002)

Although much is known about BCC in regards to their histopathological structure, clinical features and to an extent their cause, much remains undefined with regards the molecular mechanisms that regulate BCC development and in particular the differences between benign and aggressive BCC. It is also worth noting that in most

other tumours aberrant HH pathway activation is associated with highly aggressive and metastatic tumours (Kasper et al., 2006a). It is therefore striking that in skin aberrant HH pathway activation is rarely associated with metastasis. While mouse models of skin carcinogenesis have been very informative and a number of murine models for BCC have been developed these mouse BCC models may be more indicative of hyper proliferation of the epidermis resulting in tumour formation. It would be very useful to carry out exome sequencing of some of these mouse BCC to see how closely they resemble human BCC.

Understanding the molecular mechanisms that regulate BCC development has been difficult in part due to the fact that culture of primary human BCC and its cell types in vitro has proven very difficult, thereby making the study of this cancer and its molecular changes challenging. There are few papers in the literature that report success in culturing BCC keratinocytes usually with fibroblasts derived from the same tissue sample (Dicker et al., 2002, Lacina et al., 2007). However, currently there are no commercially available BCC cell lines and BCC keratinocyte cell culture is still generally regarded by workers in the field as extremely complicated. My data showing that BCC epithelium and stroma express senescence markers and hence my conclusion that BCC are a highly senescent tumour may well explain why BCC cells are difficult to culture in vitro and hence why there are no cell lines. Indeed a previous PhD student Jane Elliot (Elliot, 2011) in my supervisor Professor Philpotts group attempted to culture BCC keratinocytes from BCC using fibroblasts derived from the same BCC as feeder layers. However, she observed that while it was possible to explant some keratinocytes from BCC these rapidly senesced in vitro. Moreover, she also showed that fibroblasts from BCC also grew very slowly and also senesced as determined by expression of β-galactosidase, DEC1, DcR2 and $p16^{INK4a}$.

Inactivation of more than one pathway is required to bypass senescence. Senescence caused by telomere dysfunction and maintained by p53 is a reversible state, however $p16^{INK4a}$ expression in this scenario is a dominant irreversible effect that forms a second barrier against cell proliferation (Beausejour and Campisi, 2006). Although $p16^{INK4a}$ up regulation can be seen at the same time as p53 and $p21^{WAF1}$, it is triggered and acts independently. If one pathway is up regulated (i.e. $p16^{INK4a}$) this doesn't

prevent the cells from responding to the other pathways (i.e. p53/$p21^{WAF1}$) at a subsequent time (Herbig and Sedivy, 2006). Therefore, my observation that BCC expressed both $p16^{INK4a}$ as well as p53 supports my hypothesis that BCC has high levels of senescence and supports both the data from Jane Elliots PhD thesis but also probably explains why BCC keratinocytes have been so difficult to culture. To overcome this senescence would presumably involve both $p16^{INK4a}$ and p53 being mutated.

Mutation in the $p16^{INK4a}$ gene have been previously identified in sporadic melanomas and NMSC resulting in breakdown of tumour suppression mechanisms. Under conditions of stress, and oncogenic stimuli, expression of $p16^{INK4a}$ increases and does $p15^{INK4b}$ expression. The increase expression of these genes results in the suspension of cell cycle and counteracts the excessive proliferation or the replication of damaged DNA. It would be of great interest to know whether rare metastatic BCC have mutations in $p16^{INK4a}$ and or p53 which allows them to overcome senescence. However, these tumours are very rare and were not available for this current study. It would also have been interesting to have been able to look at the basal-squamous skin tumours to see whether they expressed components of the HH pathway and if so whether they also expressed senescence markers.

As previously described the presence of DcR2 BCC cells may protect them from the actions of TRAIL induced apoptosis. In my study immunocytological investigation for the receptor DcR2 showed a strong positive stain in human BCC , in my *in vitro* model of BCC and in mouse BCC. This has also been reported in melanoma cell lines and it is suggested that the expression of this receptor may involve regulated movement from the intracellular compartments to the membrane. In that study by Zhang et al, 2000, DcR2 was shown to be localized to the nucleus but then sub cellular localization to the cytoplasm was seen in the melanoma cells on their exposure to the TRAIL ligand (Zhang et al., 2000). Apoptotic cells have been observed in BCC (Erb et al., 2005, Orlandi et al., 2004, Harrison, 2013) however, this is at a relatively low level. Moreover, GLI1 and GLI2 expressing cells have been shown to have up-regulated Bcl-2 an important anti apoptotic protein and to be resistant to apoptosis (Pantazi, 2010, Harrison, 2013).

Senescent cells, whilst also acquiring altered gene expression, often become resistant to cell death signals and therefore apoptosis. Another senescence associated marker observed in this initial study was DEC1. DEC1 is abundant in carcinomas and usually expressed when cells are in a hypoxic state. It has been previously demonstrated that DEC1 transcriptionally activates a gene called survivin which is a member of the Inhibitor of the Apoptosis family (IAF) and inhibits caspase and therefore negatively regulates apoptosis (Chakrabarti et al., 2004). In my study DEC1 has also shown increase level in human BCC, in my *in vitro* model of BCC and in mouse BCC. There is a correlation between DEC1 expression and tumour grade and prevention of apoptosis in mouse mammary epithelial cells. Like DcR2, DEC1 has an anti apoptotic role in senescence and cancer.

The hypothesis of my thesis was that cell senescence may explain the more benign BCC subtypes and that more aggressive BCCs may either escape senescence or have lower levels of senescence markers. This does not appear to be the case and similar levels of cell senescence were observed in both nodular and morphoeic BCC

In conclusion I have shown that cell senescence is seen in human BCC as well as in a mouse model of BCC although in the mouse model used in my study aggressive variant BCCs had much lower levels of senescence than nodular BCC and this contrast with human BCC. I also showed in an in-vitro model of BCC that the senescence markers used in my study are up regulated by GLI1 and hence I conclude are targets of HH signalling. My data suggests that while up-regulation of senescence in BCC is characteristic of this tumour and may explain why they rarely metastasise; cell senescence does not explain difference between BCC subtypes.

6.2 Future work

This research presented in this thesis forms the foundations for future study of senescence in BCC and its role in BCC biology. As such there is a wide scope of future experiments that can be performed across a range of topics. Initially, some of the data presented here needs to be confirmed by doing some other experiments. Key among these would be to knockdown GLI-1 in the PTCH null cell line using shRNA to confirm that the increase in cell senescence markers is directly associated with Gli1. By knocking down GLI-1 we would expect to see down regulation of DcR2, DEC1, $p16^{INK4a}$, p53, $p21^{WAF1}$ and $p15^{INK4b}$ thus further confirming that DcR2, DEC1, $p16^{INK4a}$, p53, $p21^{WAF1}$ and $p15^{INK4b}$ are targets of HH signalling.

One of the key questions remaining from my work relates to the mechanism by which BCC may overcome senescence to allow tumor growth. It is known that p53 is mutated in many BCCs and therefore, it would be interesting to knockdown p53 in our PTCH null cell line and indeed in the GLI1 over-expressing cells, again using shRNA and see if this overcomes cell senescence. However, it is also likely that the local tumour environment plays a crucial role in the growth of BCC tumours and the balance between proliferation and senescence and therefore investigating the role of the stroma in BCC formation would also be important (see below).

Although I have shown no apparent quantifiable differences in senescence between benign and aggressive BCC it would be interesting to further investigate senescence in metastatic BCCs as it would be expected that these tumors would not be senescent. However, metastatic BCC are very rare and I am not aware of any having been seen at the Royal London Hospital in the past 5 years. However, it may be possible by collaborating with other groups to collect a small sample of these tumors from pathology archives. As all of our antibodies work on formalin fixed tissues we could carry out a retrospective study. It would also be interesting to look at senescence in basosquamous tumors as these BCC also have the ability to metastasise. basosquamous tumours have an incidence rate of between 1.2 to 2.7% (Garcia et al 2009) and so it is more likely we could obtain sufficient samples from pathology archives for a retrospective study. It is not known whether these tumors express

components of the HH pathway and so this could be investigated along with senescence.

Gene arrays on epithelial and stromal tissue from nodular and morphoeic BCC should also be carried out to try and identify differences that may explain more aggressive nature of morphoeic BCC. Two approaches could be used the first would be to carry out gene arrays on cultured cells from these tumours. However, while this would be possible on early passage BCC derived fibroblasts it would represent a major challenge with BCC keratinocytes. However, comparing fibroblasts would be a very valuable approach and may help identify stromal differences that may explain some differences between BCC subtypes. It would also be useful to carry out Exome sequencing of human morphoeic BCC and to compare these data with Exome sequencing of nodular BCC. In addition Exome sequencing of mouse BCC would provide valuable information with regards similarities and differences between the human disease and mouse models.

It is well established that the local tumour environment plays an important role in tumour growth and indeed it is known that senescent cells although they no longer proliferate are metabolically active and secrete a range of cytokines. Fibroblasts could be cultured from nodular and morphoeic BCC to investigate the kind of cytokines they secrete. However, as already mentioned in this thesis previous workers in my supervisors laboratory have also found these cells difficult to culture. However, they were able to maintain fibroblasts over several passages and were able to measure TGF-β and SHH secretion using ELISA and a SHH activity in tissue culture serum using a cell based reporter assay (Elliott 2011). Therefore, it is possible to measure cytokines produced by BCC derived fibroblasts by ELISA.

The data generated by Elliott (2011) also suggested that the BCC keratinocytes were required for optimum BCC fibroblast culture and that BCC keratinocytes were required for optimum fibroblast culture. This data was based on explant culture. An additional approach would be to make organotypic models with early passage before senescent but also possibly senescent fibroblasts from nodular and morphoeic BCC and investigate effects on both normal keratinocytes but also the GLI-1 and GLI-2

expressing cells and the PTCH1 knockdown cells. This would allow us to investigate the influences of the stroma and in particular fibroblasts on BCC formation as keratinocytes expressing GLI1 and GLI2 are widely used in BCC research in the absence of suitable BCC keratinocyte cell lines. Recently Dr Wesley Harrison a postdoctoral scientist in my group has published a paper in Oncogene (Harrison et al 2013) showing that both GLI1 and GLI2 confer apoptosis resistance on human keratinocytes and that when exposed to known carcinogens this promotes cellular transformation and cell invasion in collagen gels. Cell invasion can be quantified using ImageJ software both in terms of depth of invasion but also average number of detached invasions per field of view (Harrison et al 2013).

Currently there are no BCC cells lines and this may be for the reasons identified in this thesis. However, not all cells in the BCC can be senescent and the work carried out in my group by a previous PhD student, Jane Elliott showed that both BCC keratinocytes and fibroblasts could be grown as explant culture although on passage they rapidly senesce (Elliott 2011). It would be worth trying to make immortalised cell lines from BCC keratinocytes and fibroblasts while in explant culture or following early passage. My supervisors group has considerable experience in making immortalised cell lines from human hair follicles using either the catalytic subunit of human telomerase (hTERT) or the HPV E6/E7 proteins and indeed have recently made an immortalised line for the secretory coil of human eccrine sweat glands (unpublished data). Both hTERT and HPV E6/E7 are accepted methods of immortalisation (Storey and Banks 1993; Dickson et al 2000).

The experiments outlined above would help further understand the differences between benign and aggressive BCC and the role of senescence and as proof of principle all of the approaches suggested have been shown to be viable although as outlined above some are much more technically challenging than others.

BIBLOGRAPHY

http://www.theage.com.au/news/Business/Peplins-skin-cancer-trial-a-success/2006/05/01/1146335660056.html [Online]. [Accessed].

ADOLPHE, C., HETHERINGTON, R., ELLIS, T. & WAINWRIGHT, B. 2006. Patched1 Functions as a Gatekeeper by Promoting Cell Cycle Progression. *Cancer Research,* 66**,** 2081-2088.

AHMED, N. U., UEDA, M. & ICHIHASHI, M. 1997. p21 WAF1/cip1expression in non-melanoma skin tumors. *Journal of Cutaneous Pathology,* 24**,** 223-227.

ALCEDO, J., AYZENZON, M., VON OHLEN, T., NOLL, M. & HOOPER, J. E. 1996. The Drosophila smoothened Gene Encodes a Seven-Pass Membrane Protein, a Putative Receptor for the Hedgehog Signal. *Cell,* 86**,** 221-232.

ALLINEN, M., BEROUKHIM, R., CAI, L., BRENNAN, C., LAHTI-DOMENICI, J., HUANG, H., PORTER, D., HU, M., CHIN, L., RICHARDSON, A., SCHNITT, S., SELLERS, W. R. & POLYAK, K. 2004. Molecular characterization of the tumor microenvironment in breast cancer. *Cancer Cell,* 6**,** 17-32.

ALONSO, L. & FUCHS, E. 2003. Stem cells of the skin epithelium. *Proceedings of the National Academy of Sciences of the United States of America,* 100**,** 11830-11835.

ANDER, M., ANTONIO, M., PETER, K., IGNACIO, F., ISABEL, G.-C., CONSUELO, B., JUANA, M. F., JOSE, V., A, MARIA, A. B. & MANUEL, S. 2007. Delayed ageing through damage protection by the Arf/p53 pathway. *Nature,* 448**,** 375-379.

ASPLUND, A., GRY BJORKLUND, M., SUNDQUIST, C., STROMBERG, S., EDLUND, K., OSTMAN, A., NILSSON, P., PONTEN, F. & LUNDEBERG, J. 2008. Expression profiling of microdissected cell populations selected from basal cells in normal epidermis and basal cell carcinoma. *The British journal of dermatology,* 158**,** 527-38.

ASZTERBAUM, M., EPSTEIN, J., ORO, A., DOUGLAS, V., LEBOIT, P. E., SCOTT, M. P. & EPSTEIN, E. H. 1999. Ultraviolet and ionizing radiation enhance the growth of BCCs and trichoblastomas in patched heterozygous knockout mice. *Nat Med,* 5**,** 1285-1291.

AXELROD, R., AXELROD, D. E. & PIENTA, K. J. 2006. Evolution of cooperation among tumor cells. *Proceedings of the National Academy of Sciences,* 103**,** 13474-13479.

BARBARESCHI, M., GIRLANDO, S., CRISTOFOLINI, P., CRISTOFOLINI, M., TOGNI, R. & BOI, S. 1992. p53 protein expression in basal cell carcinomas. *Histopathology,* 21**,** 579-581.

BARR, B. B. B., MCLAREN, K., SMITH, I. W., BENTON, E. C., BUNNEY, M. H., BLESSING, K. & HUNTER, J. A. A. 1989. HUMAN PAPILLOMA VIRUS INFECTION AND SKIN CANCER IN RENAL ALLOGRAFT RECIPIENTS. *The Lancet,* 333**,** 124-129.

BARRETT, T. L., SMITH, K. J., HODGE, J. J., BUTLER, R., HALL, F. W. & SKELTON, H. G. 1997. Immunohistochemical nuclear staining for p53, PCNA, and Ki-67 in different histologic variants of basal cell carcinoma. *Journal of the American Academy of Dermatology,* 37**,** 430-437.

BASTIAENS, M. T., HOEFNAGEL, J. J., BRUIJN, J. A., WESTENDORP, R. G. J., VERMEER, B. J. & BAVINCK, J. N. B. 1998. Differences in Age, Site Distribution, and Sex Between Nodular and Superficial Basal Cell Carcinomas Indicate Different Types of Tumors. 110**,** 880-884.

BEACHAM, D. A. & CUKIERMAN, E. 2005. Stromagenesis: The changing face of fibroblastic microenvironments during tumor progression. *Seminars in Cancer Biology,* 15**,** 329-341.

BEACHY, P. A., KARHADKAR, S. S. & BERMAN, D. M. 2004. Tissue repair and stem cell renewal in carcinogenesis. *Nature,* 432**,** 324-31.

BEAUSEJOUR, C. M. & CAMPISI, J. 2006. Ageing - Balancing regeneration and cancer. *Nature,* 443**,** 404-405.

BEAUSEJOUR, C. M., KRTOLICA, A., GALIMI, F., NARITA, M., LOWE, S. W., YASWEN, P. & CAMPISI, J. 2003. Reversal of human cellular senescence: roles of the p53 and p16 pathways. *EMBO J,* 22**,** 4212-4222.

BECKMANN, H., SU, L. K. & KADESCH, T. 1990. TFE3: a helix-loop-helix protein that activates transcription through the immunoglobulin enhancer muE3 motif. *Genes & Development,* 4**,** 167-179.

BEN-PORATH, I. & WEINBERG, R. A. 2005. The signals and pathways activating cellular senescence. *The International Journal of Biochemistry & Cell Biology,* 37**,** 961-976.

BENNECKE, M., KRIEGL, L., BAJBOUJ, M., RETZLAFF, K., ROBINE, S., JUNG, A., ARKAN, M. C., KIRCHNER, T. & GRETEN, F. R. 2010. Ink4a/Arf and Oncogene-Induced Senescence Prevent Tumor Progression during Alternative Colorectal Tumorigenesis. *Cancer Cell,* 18**,** 135-146.

BHOWMICK, N. A. & MOSES, H. L. 2005. Tumor–stroma interactions. *Current Opinion in Genetics & Development,* 15**,** 97-101.

BISHOP, C. L., BERGIN, A. M., FESSART, D., BORGDORFF, V., HATZIMASOURA, E., GARBE, J. C., STAMPFER, M. R., KOH, J. & BEACH, D. H. 2010. Primary cilium-dependent and -independent Hedgehog signaling inhibits p16(INK4A). *Molecular cell,* 40**,** 533-47.

BLANKENSTEIN, T. 2005. The role of tumor stroma in the interaction between tumor and immune system. *Current Opinion in Immunology,* 17**,** 180-186.

BLANPAIN, C. & FUCHS, E. 2006. Epidermal Stem Cells of the Skin. *Annual Review of Cell and Developmental Biology,* 22**,** 339-373.

BLANPAIN, C. & FUCHS, E. 2009. Epidermal homeostasis: a balancing act of stem cells in the skin. *Nat Rev Mol Cell Biol,* 10**,** 207-217.

BOLSHAKOV, S., WALKER, C. M., STROM, S. S., SELVAN, M. S., CLAYMAN, G. L., EL-NAGGAR, A., LIPPMAN, S. M., KRIPKE, M. L. & ANANTHASWAMY, H. N. 2003. p53 Mutations in Human Aggressive and Nonaggressive Basal and Squamous Cell Carcinomas. *Clinical Cancer Research,* 9**,** 228-234.

BOND, J., JONES, C., HAUGHTON, M., DEMICCO, C., KIPLING, D. & WYNFORD-THOMAS, D. 2004. Direct evidence from siRNA-directed "knock down" that p16INK4a is required for human fibroblast senescence and for limiting ras-induced epithelial cell proliferation. *Experimental Cell Research,* 292**,** 151-156.

BONIFAS, J. M., PENNYPACKER, S., CHUANG, P. T., MCMAHON, A. P., WILLIAMS, M., ROSENTHAL, A., DE SAUVAGE, F. J. & EPSTEIN, E. H., JR. 2001. Activation of expression of hedgehog target genes in basal cell carcinomas. *The Journal of investigative dermatology,* 116**,** 739-42.

BORG, Å., SANDBERG, T., NILSSON, K., JOHANNSSON, O., KLINKER, M., MÅSBÄCK, A., WESTERDAHL, J., OLSSON, H. & INGVAR, C. 2000. High Frequency of Multiple Melanomas and Breast and Pancreas Carcinomas in CDKN2A Mutation-Positive Melanoma Families. *Journal of the National Cancer Institute,* 92**,** 1260-1266.

BOUKAMP, P. 2005. UV-induced Skin Cancer: Similarities – Variations. *JDDG: Journal der Deutschen Dermatologischen Gesellschaft,* 3**,** 493-503.

BRAIG, M., LEE, S., LODDENKEMPER, C., RUDOLPH, C., PETERS, A. H. F. M., SCHLEGELBERGER, B., STEIN, H., DORKEN, B., JENUWEIN, T. & SCHMITT, C. A. 2005. Oncogene-induced senescence as an initial barrier in lymphoma development. *Nature,* 436**,** 660-665.

BREMNES, R. M., DØNNEM, T., AL-SAAD, S., AL-SHIBLI, K., ANDERSEN, S., SIRERA, R., CAMPS, C., MARINEZ, I. & BUSUND, L.-T. 2011. The Role of Tumor Stroma in Cancer Progression and Prognosis: Emphasis on Carcinoma-Associated Fibroblasts and Non-small Cell Lung Cancer. *Journal of Thoracic Oncology,* 6**,** 209-217 10.1097/JTO.0b013e3181f8a1bd.

CAMPISI, J. 2005. Senescent Cells, Tumor Suppression, and Organismal Aging: Good Citizens, Bad Neighbors. *Cell,* 120**,** 513-522.

CANDI, E., KNIGHT, R. A. & MELINO, G. 2001. Cornification of the Skin: A Non-apoptotic Cell Death Mechanism. *eLS.* John Wiley & Sons, Ltd.

CARPENTER, D., STONE, D. M., BRUSH, J., RYAN, A., ARMANINI, M., FRANTZ, G., ROSENTHAL, A. & DE SAUVAGE, F. J. 1998. Characterization of two patched receptors for the vertebrate hedgehog protein family. *Proceedings of the National Academy of Sciences,* 95**,** 13630-13634.

CASTRO, M. E., GUIJARRO, M. D. V., MONEO, V. & CARNERO, A. 2004. Cellular senescence induced by p53-ras cooperation is independent of p21waf1 in murine embryo fibroblasts. *Journal of Cellular Biochemistry,* 92**,** 514-524.

CHAKRABARTI, J., TURLEY, H., CAMPO, L., HAN, C., HARRIS, A. L., GATTER, K. C. & FOX, S. B. 2004. The transcription factor DEC1 (stra13, SHARP2) is associated with the hypoxic response and high tumour grade in human breast cancers. *British Journal of Cancer,* 91**,** 954-958.

CHANG, B.-D., BROUDE, E. V., DOKMANOVIC, M., ZHU, H., RUTH, A., XUAN, Y., KANDEL, E. S., LAUSCH, E., CHRISTOV, K. & RONINSON, I. B. 1999. A Senescence-like Phenotype Distinguishes Tumor Cells That Undergo Terminal Proliferation Arrest after Exposure to Anticancer Agents. *Cancer Research,* 59**,** 3761-3767.

CHEN, J. & GOLIGORSKY, M. S. 2006. Premature senescence of endothelial cells: Methusaleh's dilemma. *American Journal of Physiology - Heart and Circulatory Physiology,* 290**,** H1729-H1739.

CHEN, W., TANG, T., EASTHAM-ANDERSON, J., DUNLAP, D., ALICKE, B., NANNINI, M., GOULD, S., YAUCH, R., MODRUSAN, Z., DUPREE, K. J., DARBONNE, W. C., PLOWMAN, G., DE SAUVAGE, F. J. & CALLAHAN, C. A. 2011. Canonical hedgehog signaling augments tumor angiogenesis by induction of VEGF-A in stromal perivascular cells. *Proceedings of the National Academy of Sciences of the United States of America,* 108**,** 9589-94.

CHEN, Z., TROTMAN, L. C., SHAFFER, D., LIN, H.-K., DOTAN, Z. A., NIKI, M., KOUTCHER, J. A., SCHER, H. I., LUDWIG, T., GERALD, W., CORDON-CARDO, C. & PAOLO PANDOLFI, P. 2005. Crucial role of p53-dependent cellular senescence in suppression of Pten-deficient tumorigenesis. *Nature,* 436**,** 725-730.

CHIN, L., ARTANDI, S. E., SHEN, Q., TAM, A., LEE, S.-L., GOTTLIEB, G. J., GREIDER, C. W. & DEPINHO, R. A. 1999. p53 Deficiency Rescues the Adverse Effects of Telomere Loss and Cooperates with Telomere Dysfunction to Accelerate Carcinogenesis. *Cell,* 97**,** 527-538.

CHOI, J., SHENDRIK, I., PEACOCKE, M., PEEHL, D., BUTTYAN, R., IKEGUCHI, E. F., KATZ, A. E. & BENSON, M. C. 2000. Expression of senescence-associated beta-galactosidase in enlarged prostates from men with benign prostatic hyperplasia. *Urology,* 56**,** 160-166.

CHUNG, L. W. K., HSIEH, C.-L., LAW, A., SUNG, S.-Y., GARDNER, T. A., EGAWA, M., MATSUBARA, S. & ZHAU, H. E. 2003. New targets for therapy in prostate cancer: modulation of stromal–epithelial interactions. *Urology,* 62**,** 44-54.

CIRRI, P. & CHIARUGI, P. 2012. Cancer-associated-fibroblasts and tumour cells: a diabolic liaison driving cancer progression. *Cancer and Metastasis Reviews,* 31**,** 195-208.

COLLADO, M., BLASCO, M. A. & SERRANO, M. 2007. Cellular Senescence in Cancer and Aging. *Cell,* 130**,** 223-233.

COLLADO, M., GIL, J., EFEYAN, A., GUERRA, C., SCHUHMACHER, A. J., BARRADAS, M., BENGURIA, A., ZABALLOS, A., FLORES, J. M., BARBACID, M., BEACH, D. & SERRANO, M. 2005. Tumour biology: Senescence in premalignant tumours. *Nature,* 436**,** 642-642.

COLLADO, M. & SERRANO, M. 2006. The power and the promise of oncogene-induced senescence markers. *Nat Rev Cancer,* 6**,** 472-476.

COPPE, J. P., DESPREZ, P. Y., KRTOLICA, A. & CAMPISI, J. 2010. The Senescence-Associated Secretory Phenotype: The Dark Side of Tumor Suppression. *Annual Review of Pathology-Mechanisms of Disease.* Palo Alto: Annual Reviews.

COUVE-PRIVAT, S., LE BRET, M., TRAIFFORT, E., QUEILLE, S., COULOMBE, J., BOUADJAR, B., AVRIL, M. F., RUAT, M., SARASIN, A. & DAYA-GROSJEAN, L. 2004. Functional analysis of novel sonic hedgehog gene mutations identified in basal cell carcinomas from xeroderma pigmentosum patients. *Cancer research,* 64**,** 3559-65.

CRONMILLER, C., SCHEDL, P. & CLINE, T. W. 1988. Molecular characterization of daughterless, a Drosophila sex determination gene with multiple roles in development. *Genes & Development,* 2**,** 1666-1676.

CROWSON, A. N. 2006. Basal cell carcinoma: biology, morphology and clinical implications. *Mod Pathol,* 19 Suppl 2**,** S127-47.

CZARNECKI, D., O'BRIEN, T. & MEEHAN, C. 1994. NONMELANOMA SKIN CANCER: NUMBER OF CANCERS AND THEIR DISTRIBUTION IN OUTPATIENTS. *International Journal of Dermatology,* 33**,** 416-417.

D'ADDA DI FAGAGNA, F., TEO, S.-H. & JACKSON, S. P. 2004. Functional links between telomeres and proteins of the DNA-damage response. *Genes & Development,* 18**,** 1781-1799.

DATTA, S. & DATTA, M. 2006. Sonic Hedgehog signaling in advanced prostate cancer. *Cellular and Molecular Life Sciences,* 63**,** 435-448.

DAYA-GROSJEAN, L. & COUVÉ-PRIVAT, S. 2005. Sonic hedgehog signaling in basal cell carcinomas. *Cancer letters,* 225**,** 181-192.

DE ZWAAN, S. E. & HAASS, N. K. 2010. Genetics of basal cell carcinoma. *Australasian Journal of Dermatology,* 51**,** 81-92.

DECOTTIGNIES, A. & D'ADDA DI FAGAGNA, F. 2011. Epigenetic alterations associated with cellular senescence: A barrier against tumorigenesis or a red carpet for cancer? *Seminars in Cancer Biology,* 21**,** 360-366.

DEGLI-ESPOSTI, M. A., DOUGALL, W. C., SMOLAK, P. J., WAUGH, J. Y., SMITH, C. A. & GOODWIN, R. G. 1997. The Novel Receptor TRAIL-R4 Induces NF-ºB and Protects against TRAIL-Mediated Apoptosis, yet Retains an Incomplete Death Domain. *Immunity,* 7**,** 813-820.

DENEF, N., NEUBÜSER, D., PEREZ, L. & COHEN, S. M. 2000. Hedgehog Induces Opposite Changes in Turnover and Subcellular Localization of Patched and Smoothened. *Cell,* 102**,** 521-531.

DENNLER, S., ANDRE, J., ALEXAKI, I., LI, A., MAGNALDO, T., TEN DIJKE, P., WANG, X. J., VERRECCHIA, F. & MAUVIEL, A. 2007. Induction of sonic hedgehog mediators by transforming growth factor-beta: Smad3-dependent activation of Gli2 and Gli1 expression in vitro and in vivo. *Cancer research,* 67**,** 6981-6.

DI LEONARDO, A., LINKE, S. P., CLARKIN, K. & WAHL, G. M. 1994. DNA damage triggers a prolonged p53-dependent G1 arrest and long-term induction of Cip1 in normal human fibroblasts. *Genes & Development,* 8**,** 2540-2551.

DI MAGLIANO, M. P. & HEBROK, M. 2003. Hedgehog signalling in cancer formation and maintenance. *Nat Rev Cancer,* 3**,** 903-911.

DICKER, A. J., SEREWKO, M. M., RUSSELL, T., ROTHNAGEL, J. A., STRUTTON, G. M., DAHLER, A. L. & SAUNDERS, N. A. 2002. Isolation (from a basal cell carcinoma) of a functionally distinct fibroblast-like cell type that overexpresses Ptch. *J Invest Dermatol,* 118**,** 859-865.

DICKSON, M. A., HAHN, W. C., INO, Y., RONFARD, V., WU, J. Y., WEINBERG, R. A., LOUIS, D. N., LI, F. P. & RHEINWALD, J. G. 2000. Human Keratinocytes That Express hTERT and Also

Bypass a p16INK4a-Enforced Mechanism That Limits Life Span Become Immortal yet Retain Normal Growth and Differentiation Characteristics. *Molecular and Cellular Biology,* 20**,** 1436-1447.

DIEPGEN, T. L. & MAHLER, V. 2002. The epidemiology of skin cancer. *British Journal of Dermatology,* 146**,** 1-6.

DIMRI, G. P. 2005. What has senescence got to do with cancer? *Cancer Cell,* 7**,** 505-512.

DIMRI, G. P., LEE, X., BASILE, G., ACOSTA, M., SCOTT, G., ROSKELLEY, C., MEDRANO, E. E., LINSKENS, M., RUBELJ, I. & PEREIRA-SMITH, O. 1995a. A biomarker that identifies senescent human cells in culture and in aging skin in vivo. *Proceedings of the National Academy of Sciences,* 92**,** 9363-9367.

DIMRI, G. P., LEE, X., BASILE, G., ACOSTA, M., SCOTT, G., ROSKELLEY, C., MEDRANO, E. E., LINSKENS, M., RUBELJ, I. & PEREIRA-SMITH, O. 1995b. A biomarker that identifies senescent human cells in culture and in aging skin in vivo. *Proceedings of the National Academy of Sciences of the United States of America,* 92**,** 9363-9367.

DOMARUS, H. V. & STEVENS, P. J. 1984. Metastatic basal cell carcinoma: Report of five cases and review of 170 cases in the literature. *Journal of the American Academy of Dermatology,* 10**,** 1043-1060.

DONOVAN, J. 2009. Review of the Hair Follicle Origin Hypothesis for Basal Cell Carcinoma. *Dermatologic Surgery,* 35**,** 1311-1323.

EHATA, S., HANYU, A., HAYASHI, M., ABURATANI, H., KATO, Y., FUJIME, M., SAITOH, M., MIYAZAWA, K., IMAMURA, T. & MIYAZONO, K. 2007. Transforming Growth Factor-β Promotes Survival of Mammary Carcinoma Cells through Induction of Antiapoptotic Transcription Factor DEC1. *Cancer Research,* 67**,** 9694-9703.

ELLIOT, J. A. 2011. *An In Vitro study of the potential stromal role in Basal Cell Carcinoma development.* PhD, Queen Mary University of London.

EPSTEIN, E. H. 2008. Basal cell carcinomas: attack of the hedgehog. *Nat Rev Cancer,* 8**,** 743-54.

ERB, P., JI, J., WERNLI, M., KUMP, E., GLASER, A. & BÜCHNER, S. A. 2005. Role of apoptosis in basal cell and squamous cell carcinoma formation. *Immunology Letters,* 100**,** 68-72.

ESHKOOR, S. A., ISMAIL, P., RAHMAN, S. A. & OSHKOUR, S. A. 2008. p16 Gene Expression in Basal Cell Carcinoma. *Archives of medical research,* 39**,** 668-673.

FAN, H. & KHAVARI, P. A. 1999. Sonic Hedgehog Opposes Epithelial Cell Cycle Arrest. *The Journal of Cell Biology,* 147**,** 71-76.

FARAGE, M., MILLER, K. & MAIBACH, H. 2010. Degenerative Changes in Aging Skin. *In:* FARAGE, M., MILLER, K. & MAIBACH, H. (eds.) *Textbook of Aging Skin.* Springer Berlin Heidelberg.

FARHI, D., DUPIN, N., PALANGIÉ, A., CARLOTTI, A. & AVRIL, M. F. 2007. Incomplete Excision of Basal Cell Carcinoma: Rate and Associated Factors among 362 Consecutive Cases. *Dermatologic Surgery,* 33**,** 1207-1214.

FELLOUS, T. G., MCDONALD, S. A. C., BURKERT, J., HUMPHRIES, A., ISLAM, S., DE-ALWIS, N. M. W., GUTIERREZ-GONZALEZ, L., TADROUS, P. J., ELIA, G., KOCHER, H. M., BHATTACHARYA, S., MEARS, L., EL-BAHRAWY, M., TURNBULL, D. M., TAYLOR, R. W., GREAVES, L. C., CHINNERY, P. F., DAY, C. P., WRIGHT, N. A. & ALISON, M. R. 2009. A Methodological Approach to Tracing Cell Lineage in Human Epithelial Tissues. *STEM CELLS,* 27**,** 1410-1420.

FENDERSON, B. A. 2008. Molecular Biology of the Cell, 5Th Edition. *Shock,* 30**,** 100 10.1097/01.shk.0000286288.33338.f6.

FENDRICH, V., OH, E., BANG, S., KARIKARI, C., OTTENHOF, N., BISHT, S., LAUTH, M., BROSSART, P., KATSANIS, N., MAITRA, A. & FELDMANN, G. 2011. Ectopic overexpression of sonic hedgehog (shh) induces stromal expansion and metaplasia in the adult murine pancreas. *Neoplasia,* 13**,** 923-30.

FERNANDEZ-ZAPICO, M. E. 2008. Primers on molecular pathways GLI: more than just Hedgehog? *Pancreatology : official journal of the International Association of Pancreatology,* 8**,** 227-9.

FISCHER, U., MÜLLER, H. W., SATTLER, H. P., ZANG, K. D., MEESE, E. & FEIDEN, K. 1995. Amplification of the met gene in glioma. *Genes, Chromosomes and Cancer,* 12**,** 63-65.

FLOYD, H. S., FARNSWORTH, C. L., KOCK, N. D., MIZESKO, M. C., LITTLE, J. L., DANCE, S. T., EVERITT, J., TICHELAAR, J., WHITSETT, J. A. & MILLER, M. S. 2005. Conditional expression of the mutant Ki-rasG12C allele results in formation of benign lung adenomas: development of a novel mouse lung tumor model. *Carcinogenesis,* 26**,** 2196-2206.

FUCHS, E. 1990. Epidermal differentiation: the bare essentials. *The Journal of Cell Biology,* 111**,** 2807-2814.

FUCHS, E. & RAGHAVAN, S. 2002. Getting under the skin of epidermal morphogenesis. *Nat Rev Genet,* 3**,** 199-209.

FUJIMOTO, K., SHEN, M., NOSHIRO, M., MATSUBARA, K., SHINGU, S., HONDA, K., YOSHIDA, E., SUARDITA, K., MATSUDA, Y. & KATO, Y. 2001. Molecular Cloning and Characterization of DEC2, a New Member of Basic Helix-Loop-Helix Proteins. *Biochemical and Biophysical Research Communications,* 280**,** 164-171.

GAILANI, M. R. & BALE, A. E. 1997. Developmental Genes and Cancer: Role of Patched in Basal Cell Carcinoma of the Skin. *Journal of the National Cancer Institute,* 89**,** 1103-1109.

GAILANI, M. R., STAHLE-BACKDAHL, M., LEFFELL, D. J., GLYN, M., ZAPHIROPOULOS, P. G., UNDEN, A. B., DEAN, M., BRASH, D. E., BALE, A. E. & TOFTGARD, R. 1996. The role of the human homologue of Drosophila patched in sporadic basal cell carcinomas. *Nat Genet,* 14**,** 78-81.

GARCIA C, POLETTI E, CROWSON AN. Basosquamous carcinoma. J Am Acad Dermatol. 2009 60(1):137-43.

GAWKRODGER, D. J. 2002. *Dermatology : An Illustrated Colour Text*, Churchill Livingstone.

GORE, S. M., KASPER, M., WILLIAMS, T., REGL, G., ABERGER, F., CERIO, R., NEILL, G. W. & PHILPOTT, M. P. 2009. Neuronal differentiation in basal cell carcinoma: possible relationship to Hedgehog pathway activation? *The Journal of Pathology,* 219**,** 61-68.

GORLIN, R. J. 1995. NEVOID BASAL-CELL CARCINOMA SYNDROME. *Dermatologic Clinics,* 13**,** 113-125.

GRACHTCHOUK, M., MO, R., YU, S., ZHANG, X., SASAKI, H., HUI, C.-C. & DLUGOSZ, A. A. 2000. Basal cell carcinomas in mice overexpressing Gli2 in skin. *Nat Genet,* 24**,** 216-217.

HAHN, H., WICKING, C., ZAPHIROPOULOS, P. G., GAILANI, M. R., SHANLEY, S., CHIDAMBARAM, A., VORECHOVSKY, I., HOLMBERG, E., UNDEN, A. B., GILLIES, S., NEGUS, K., SMYTH, I., PRESSMAN, C., LEFFELL, D. J., GERRARD, B., GOLDSTEIN, A. M., DEAN, M., TOFTGARD, R., CHENEVIX-TRENCH, G., WAINWRIGHT, B. & BALE, A. E. 1996. Mutations of the Human Homolog of Drosophila patched in the Nevoid Basal Cell Carcinoma Syndrome. *Cell,* 85**,** 841-851.

HANAHAN, D. & WEINBERG, R. A. 2000. The Hallmarks of Cancer. *Cell,* 100**,** 57-70.

HANNON, G. J. & BEACH, D. 1994. pl5INK4B is a potentia| effector of TGF-[beta]-induced cell cycle arrest. *Nature,* 371**,** 257-261.

HARRISON, B. C., G NEILL, M PHILPOTT 2013. The oncogenic GLI transcription factors facilitate keratinocyte survival and transformation upon exposure to genotoxic agents. *Oncogene,* 1-9.

HARTEVELT, M. M., BAVINCK, J. N. B., KOOTTE, A. M. M., VERMEER, B. J. & VANDENBROUCKE, J. P. 1990. INCIDENCE OF SKIN-CANCER AFTER RENAL-TRANSPLANTATION IN THE NETHERLANDS. *Transplantation,* 49**,** 506-509.

HARVEY, J. M., CLARK, G. M., OSBORNE, C. K. & ALLRED, D. C. 1999. Estrogen Receptor Status by Immunohistochemistry Is Superior to the Ligand-Binding Assay for Predicting Response to Adjuvant Endocrine Therapy in Breast Cancer. *Journal of Clinical Oncology,* 17**,** 1474.

HATSELL, S. & FROST, A. 2007. Hedgehog Signaling in Mammary Gland Development and Breast Cancer. *Journal of Mammary Gland Biology and Neoplasia,* 12**,** 163-173.

HATTA, N., HIRANO, T., KIMURA, T., HASHIMOTO, K., MEHREGAN, D. R., ANSAI, S., TAKEHARA, K. & TAKATA, M. 2005. Molecular diagnosis of basal cell carcinoma and other basaloid cell neoplasms of the skin by the quantification of Gli1 transcript levels. *Journal of Cutaneous Pathology,* 32**,** 131-136.

HAYFLICK, L. 1965. The limited in vitro lifetime of human diploid cell strains. *Experimental Cell Research,* 37**,** 614-636.

HAYFLICK, L. & MOORHEAD, P. S. 1961. The serial cultivation of human diploid cell strains. *Experimental Cell Research,* 25**,** 585-621.

HEBERLEIN, U., WOLFF, T. & RUBIN, G. M. 1993. The TGF[beta] homolog dpp and the segment polarity gene hedgehog are required for propagation of a morphogenetic wave in the Drosophila retina. *Cell,* 75**,** 913-926.

HERBIG, U. & SEDIVY, J. M. 2006. Regulation of growth arrest in senescence: Telomere damage is not the end of the story. *Mechanisms of Ageing and Development,* 127**,** 16-24.

HERBIG, U., WEI, W., DUTRIAUX, A., JOBLING, W. A. & SEDIVY, J. M. 2003. Real-time imaging of transcriptional activation in live cells reveals rapid up-regulation of the cyclin-dependent kinase inhibitor gene CDKN1A in replicative cellular senescence. *Aging Cell,* 2**,** 295-304.

HIROSE, K., MORITA, M., EMA, M., MIMURA, J., HAMADA, H., FUJII, H., SAIJO, Y., GOTOH, O., SOGAWA, K. & FUJII-KURIYAMA, Y. 1996. cDNA cloning and tissue-specific expression of a novel basic helix-loop- helix/PAS factor (Arnt2) with close sequence similarity to the aryl hydrocarbon receptor nuclear translocator (Arnt). *Mol. Cell. Biol.,* 16**,** 1706-1713.

HOEY, D. A., DOWNS, M. E. & JACOBS, C. R. 2011. The mechanics of the primary cilium: An intricate structure with complex function. *Journal of biomechanics*.

HOLLSTEIN, M., SIDRANSKY, D., VOGELSTEIN, B. & HARRIS, C. 1991. p53 mutations in human cancers. *Science,* 253**,** 49-53.

HOOPER, J. E. & SCOTT, M. P. 1989. The Drosophila patched gene encodes a putative membrane protein required for segmental patterning. *Cell,* 59**,** 751-765.

HOOPER, J. E. & SCOTT, M. P. 2005. Communicating with Hedgehogs. *Nature reviews. Molecular cell biology,* 6**,** 306-17.

HSU, S. M. & RAINE, L. 1981. Protein A, avidin, and biotin in immunohistochemistry. *Journal of Histochemistry & Cytochemistry,* 29**,** 1349-53.

HUANG, S., YANG, L., AN, Y., MA, X., ZHANG, C., XIE, G., CHEN, Z.-Y., XIE, J. & ZHANG, H. 2011. Expression of hedgehog signaling molecules in lung cancer. *Acta Histochemica,* 113**,** 564-569.

HUANGFU, D. & ANDERSON, K. V. 2006. Signaling from Smo to Ci/Gli: conservation and divergence of Hedgehog pathways from Drosophila to vertebrates. *Development,* 133**,** 3-14.

IDEKER, T., THORSSON, V., RANISH, J. A., CHRISTMAS, R., BUHLER, J., ENG, J. K., BUMGARNER, R., GOODLETT, D. R., AEBERSOLD, R. & HOOD, L. 2001. Integrated Genomic and Proteomic Analyses of a Systematically Perturbed Metabolic Network. *Science,* 292**,** 929-934.

ITAHANA, K., CAMPISI, J. & DIMRI, G. 2004. Mechanisms of cellular senescence in human and mouse cells. *Biogerontology,* 5**,** 1-10.

IVANOVA, A. V., IVANOV, S. V., DANILKOVITCH-MIAGKOVA, A. & LERMAN, M. I. 2001. Regulation of STRA13 by the von Hippel-Lindau Tumor Suppressor Protein, Hypoxia,

and the UBC9/Ubiquitin Proteasome Degradation Pathway. *Journal of Biological Chemistry,* 276**,** 15306-15315.

JACOBS, G. H., RIPPEY, J. J. & ALTINI, M. 1982. Prediction of aggressive behavior in basal cell carcinoma. *Cancer,* 49**,** 533-537.

JAVELAUD, D., ALEXAKI, V. I., DENNLER, S., MOHAMMAD, K. S., GUISE, T. A. & MAUVIEL, A. 2011. TGF-β/SMAD/GLI2 Signaling Axis in Cancer Progression and Metastasis. *Cancer Research,* 71**,** 5606-5610.

JAYARAMAN, S. S., RAYHAN, D. J., HAZANY, S. & KOLODNEY, M. S. 2013. Mutational Landscape of Basal Cell Carcinomas by Whole Exome Sequencing. *J Invest Dermatol*.

JEMAL, A., DEVESA, S. S., HARTGE, P. & TUCKER, M. A. 2001. Recent Trends in Cutaneous Melanoma Incidence Among Whites in the United States. *Journal of the National Cancer Institute,* 93**,** 678-683.

JES, S, G. & GORDON, P. 2006. Regulation of the INK4b|[ndash]|ARF|[ndash]|INK4a tumour suppressor locus: all for one or one for all. *Nature Reviews Molecular Cell Biology,* 7**,** 667-677.

JEYAPALAN, J. C. & SEDIVY, J. M. Cellular senescence and organismal aging. *Mechanisms of Ageing and Development,* 129**,** 467-474.

JOHNSON, R. L., ROTHMAN, A. L., XIE, J., GOODRICH, L. V., BARE, J. W., BONIFAS, J. M., QUINN, A. G., MYERS, R. M., COX, D. R., EPSTEIN, E. H. & SCOTT, M. P. 1996. Human Homolog of patched, a Candidate Gene for the Basal Cell Nevus Syndrome. *Science,* 272**,** 1668-1671.

JOHNSTONE, R. W., FREW, A. J. & SMYTH, M. J. 2008. The TRAIL apoptotic pathway in cancer onset, progression and therapy. *Nat Rev Cancer,* 8**,** 782-798.

KAHLEM, P., DÖRKEN, B. & SCHMITT, C. A. 2004. Cellular senescence in cancer treatment: friend or foe? *The Journal of Clinical Investigation,* 113**,** 169-174.

KARHADKAR, S. S., STEVEN BOVA, G., ABDALLAH, N., DHARA, S., GARDNER, D., MAITRA, A., ISAACS, J. T., BERMAN, D. M. & BEACHY, P. A. 2004. Hedgehog signalling in prostate regeneration, neoplasia and metastasis. *Nature,* 431**,** 707-712.

KASPER, M., JAKS, V., FIASCHI, M. & TOFTGARD, R. 2009. Hedgehog signalling in breast cancer. *Carcinogenesis,* 30**,** 903-11.

KASPER, M., REGL, G., FRISCHAUF, A.-M. & ABERGER, F. 2006a. GLI transcription factors: Mediators of oncogenic Hedgehog signalling. *European Journal of Cancer,* 42**,** 437-445.

KASPER, M., REGL, G., FRISCHAUF, A. M. & ABERGER, F. 2006b. GLI transcription factors: mediators of oncogenic Hedgehog signalling. *European journal of cancer,* 42**,** 437-45.

KATOH, Y. & KATOH, M. 2008. Integrative genomic analyses on GLI2: mechanism of Hedgehog priming through basal GLI2 expression, and interaction map of stem cell signaling network with P53. *International journal of oncology,* 33**,** 881-6.

KEATING, G. M. 2012. Vismodegib: In Locally Advanced or Metastatic Basal Cell Carcinoma. *Drugs,* 72**,** 1535-1541 10.2165/11209590-000000000-00000.

KIARIS, H., CHATZISTAMOU, I., TRIMIS, G., FRANGOU-PLEMMENOU, M., PAFITI-KONDI, A. & KALOFOUTIS, A. 2005. Evidence for Nonautonomous Effect of p53 Tumor Suppressor in Carcinogenesis. *Cancer Research,* 65**,** 1627-1630.

KIM, M.-Y., PARK, H. J., BAEK, S.-C., BYUN, D. G. & HOUH, D. 2002. Mutations of the p53 and PTCH gene in basal cell carcinomas: UV mutation signature and strand bias. *Journal of Dermatological Science,* 29**,** 1-9.

KIM, Y.-J., JUNG, J. K., LEE, S. Y. & JANG, K. L. 2010. Hepatitis B virus X protein overcomes stress-induced premature senescence by repressing p16INK4a expression via DNA methylation. *Cancer letters,* 288**,** 226-235.

KIYONO, T., FOSTER, S. A., KOOP, J. I., MCDOUGALL, J. K., GALLOWAY, D. A. & KLINGELHUTZ, A. J. 1998. Both Rb/p16INK4a inactivation and telomerase activity are required to immortalize human epithelial cells. *Nature,* 396**,** 84-88.

KO, L. J. & PRIVES, C. 1996. p53: puzzle and paradigm. *Genes & Development,* 10**,** 1054-1072.

KRAMER, D. L., CHANG, B.-D., CHEN, Y., DIEGELMAN, P., ALM, K., BLACK, A. R., RONINSON, I. B. & PORTER, C. W. 2001. Polyamine Depletion in Human Melanoma Cells Leads to G1 Arrest Associated with Induction of p21WAF1/CIP1/SDI1, Changes in the Expression of p21-regulated Genes, and a Senescence-like Phenotype. *Cancer Research,* 61**,** 7754-7762.

KRICKER, A., ARMSTRONG, B. K., ENGLISH, D. R. & HEENAN, P. J. 1995. Does intermittent sun exposure cause basal cell carcinoma? a case-control study in Western Australia. *International Journal of Cancer,* 60**,** 489-494.

KRISHNA, D. R., SPERKER, B., FRITZ, P. & KLOTZ, U. 1999. Does pH 6 β-galactosidase activity indicate cell senescence? *Mechanisms of Ageing and Development,* 109**,** 113-123.

KUILMAN, T., MICHALOGLOU, C., MOOI, W. J. & PEEPER, D. S. 2010. The essence of senescence. *Genes & Development,* 24**,** 2463-2479.

KURZ, D. J., DECARY, S., HONG, Y. & ERUSALIMSKY, J. D. 2000. Senescence-associated (beta)-galactosidase reflects an increase in lysosomal mass during replicative ageing of human endothelial cells. *Journal of Cell Science,* 113**,** 3613-3622.

LACINA, L., SMETANA, K., DVOŘÁNKOVÁ, B., PYTLÍK, R., KIDERYOVÁ, L., KUČEROVÁ, L., PLZÁKOVÁ, Z., ŠTORK, J., GABIUS, H. J. & ANDRÉ, S. 2007. Stromal fibroblasts from basal cell carcinoma affect phenotype of normal keratinocytes. *British Journal of Dermatology,* 156**,** 819-829.

LACOUR, J. P. 2002. Carcinogenesis of basal cell carcinomas: genetics and molecular mechanisms. *British Journal of Dermatology,* 146**,** 17-19.

LANGE, D., PERSSON, U., WOLLINA, U., TEN DIJKE, P., CASTELLI, E., HELDIN, C. H. & FUNA, K. 1999. Expression of TGF-beta related Smad proteins in human epithelial skin tumors. *International journal of oncology,* 14**,** 1049-1056.

LAUTH, M. & TOFTGARD, R. 2007. Non-canonical activation of GLI transcription factors: implications for targeted anti-cancer therapy. *Cell cycle,* 6**,** 2458-63.

LEAR, J., TAN, B., SMITH, A., BOWERS, W., JONES, P., HEAGERTY, A., STRANGE, R. & FRYER, A. 1997. Risk factors for basal cell carcinoma in the UK: case-control study in 806 patients. *J R Soc Med,* 90**,** 371-374.

LEE, L. R. & FREDERIC, J. D. S. 2006. Targeting the Hedgehog pathway in cancer. *Nature Reviews Drug Discovery,* 5**,** 1026-1033.

LEOVIC, D., SABOL, M., OZRETIC, P., MUSANI, V., CAR, D., MARJANOVIC, K., ZUBCIC, V., SABOL, I., SIKORA, M., GRCE, M., GLAVAS-OBROVAC, L. & LEVANAT, S. 2011. Hh-Gli signaling pathway activity in oral and oropharyngeal squamous cell carcinoma. *Head & neck*.

LEVINE, A. J. 1997. p53, the Cellular Gatekeeper for Growth and Division. *Cell,* 88**,** 323-331.

LI, C., CHI, S. & XIE, J. 2011. Hedgehog signaling in skin cancers. *Cellular Signalling,* 23**,** 1235-1243.

LI, Y., XIE, M., SONG, X., GRAGEN, S., SACHDEVA, K., WAN, Y. & YAN, B. 2003. DEC1 Negatively Regulates the Expression of DEC2 through Binding to the E-box in the Proximal Promoter. *Journal of Biological Chemistry,* 278**,** 16899-16907.

LI, Y., XIE, M., YANG, J., YANG, D., DENG, R., WAN, Y. & YAN, B. 2006. The expression of antiapoptotic protein survivin is transcriptionally upregulated by DEC1 primarily through multiple sp1 binding sites in the proximal promoter. *Oncogene,* 25**,** 3296-3306.

LI, Y., ZHANG, H., XIE, M., HU, M., GE, S., YANG, D., WAN, Y. & YAN, B. 2002a. Abundant expression of Dec1/stra13/sharp2 in colon carcinoma: its antagonizing role in serum deprivation-induced apoptosis and selective inhibition of procaspase activation. *Biochem. J.,* 367**,** 413-422.

LI, Y. X., ZHANG, H., XIE, M. X., HU, M. W., GE, S. J., YANG, D. F., WAN, Y. S. & YAN, B. F. 2002b. Abundant expression of Dec1/stra13/sharp2 in colon carcinoma: its antagonizing role in serum deprivation-induced apoptosis and selective inhibition of procaspase activation. *Biochemical Journal,* 367**,** 413-422.

LIU, X., YUE, P., KHURI, F. R. & SUN, S.-Y. 2005. Decoy Receptor 2 (DcR2) Is a p53 Target Gene and Regulates Chemosensitivity. *Cancer Research,* 65**,** 9169-9175.

LO, J. S., SNOW, S. N., REIZNER, G. T., MOHS, F. E., LARSON, P. O. & HRUZA, G. J. 1991. METASTATIC BASAL-CELL CARCINOMA - REPORT OF 12 CASES WITH A REVIEW OF THE LITERATURE. *Journal of the American Academy of Dermatology,* 24**,** 715-719.

LOVE W, B. J. D. B. J. S. 2009. Topical imiquimod or fluorouracil therapy for basal and squamous cell carcinoma: A systematic review. *Archives of Dermatology,* 145**,** 1431-1438.

LOWE, S. W., CEPERO, E. & EVAN, G. 2004. Intrinsic tumour suppression. *Nature,* 432**,** 307-315.

LUM, L. & BEACHY, P. A. 2004. The Hedgehog Response Network: Sensors, Switches, and Routers. *Science,* 304**,** 1755-1759.

MADDIKA, S., ANDE, S. R., PANIGRAHI, S., PARANJOTHY, T., WEGLARCZYK, K., ZUSE, A., ESHRAGHI, M., MANDA, K. D., WIECHEC, E. & LOS, M. 2007. Cell survival, cell death and cell cycle pathways are interconnected: Implications for cancer therapy. *Drug Resistance Updates,* 10**,** 13-29.

MALONEY, M. E. 1996. Arsenic in dermatology. *Dermatologic Surgery,* 22**,** 301-304.

MALUMBRES, M., PÉREZ DE CASTRO, I., HERNÁNDEZ, M. I., JIMÉNEZ, M., CORRAL, T. & PELLICER, A. 2000. Cellular Response to Oncogenic Ras Involves Induction of the Cdk4 and Cdk6 Inhibitor p15 INK4b. *Molecular and Cellular Biology,* 20**,** 2915-2925.

MANCUSO, M., GALLO, D., LEONARDI, S., PIERDOMENICO, M., PASQUALI, E., DE STEFANO, I., REBESSI, S., TANORI, M., SCAMBIA, G., DI MAJO, V., COVELLI, V., PAZZAGLIA, S. & SARAN, A. 2009. Modulation of basal and squamous cell carcinoma by endogenous estrogen in mouse models of skin cancer. *Carcinogenesis,* 30**,** 340-347.

MANCUSO, M., PAZZAGLIA, S., TANORI, M., HAHN, H., MEROLA, P., REBESSI, S., ATKINSON, M. J., DI MAJO, V., COVELLI, V. & SARAN, A. 2004. Basal Cell Carcinoma and Its Development. *Cancer Research,* 64**,** 934-941.

MARIGO, V., DAVEY, R. A., ZUO, Y., CUNNINGHAM, J. M. & TABIN, C. J. 1996. Biochemical evidence that patched is the Hedgehog receptor. *Nature,* 384**,** 176-179.

MARKS, R., STAPLES, M. & GILES, G. G. 1993. TRENDS IN NON-MELANOCYTIC SKIN-CANCER TREATED IN AUSTRALIA - THE 2ND NATIONAL SURVEY. *International Journal of Cancer,* 53**,** 585-590.

MARSH, T., PIETRAS, K. & MCALLISTER, S. S. Fibroblasts as architects of cancer pathogenesis. *Biochimica et Biophysica Acta (BBA) - Molecular Basis of Disease*.

MARUYAMA, J., NAGURO, I., TAKEDA, K. & ICHIJO, H. 2009. Stress-Activated MAP Kinase Cascades in Cellular Senescence. *Current Medicinal Chemistry,* 16**,** 1229-1235.

MATHEU, A., MARAVER, A. & SERRANO, M. 2008. The Arf/p53 Pathway in Cancer and Aging. *Cancer Research,* 68**,** 6031-6034.

MCDUFF, F. K. E. & TURNER, S. D. 2011. Jailbreak: Oncogene-induced senescence and its evasion. *Cellular Signalling,* 23**,** 6-13.

MCGRATH, J. A., EADY, R. A. J. & POPE, F. M. 2008. Anatomy and Organization of Human Skin. *Rook's Textbook of Dermatology.* Blackwell Publishing, Inc.

MENDEZ, M. V., STANLEY, A., PARK, H.-Y., SHON, K., PHILLIPS, T. & MENZOIAN, J. O. 1998. Fibroblasts cultured from venous ulcers display cellular characteristics of senescence. *Journal of Vascular Surgery,* 28**,** 876-883.

MENG, R. D., MCDONALD, E. R., SHEIKH, M. S., FORNACE, A. J. & EL-DEIRY, W. S. 2000. The TRAIL Decoy Receptor TRUNDD (DcR2, TRAIL-R4) Is Induced by Adenovirus-p53

Overexpression and Can Delay TRAIL-, p53-, and KILLER/DR5-Dependent Colon Cancer Apoptosis. *Mol Ther,* 1**,** 130-144.

MICHALOGLOU, C., VREDEVELD, L. C. W., SOENGAS, M. S., DENOYELLE, C., KUILMAN, T., VAN DER HORST, C. M. A. M., MAJOOR, D. M., SHAY, J. W., MOOI, W. J. & PEEPER, D. S. 2005. BRAFE600-associated senescence-like cell cycle arrest of human naevi. *Nature,* 436**,** 720-724.

MICHAUD, E. J. & YODER, B. K. 2006. The primary cilium in cell signaling and cancer. *Cancer research,* 66**,** 6463-7.

MICKE, P., KAPPERT, K., OHSHIMA, M., SUNDQUIST, C., SCHEIDL, S., LINDAHL, P., HELDIN, C. H., BOTLING, J., PONTEN, F. & OSTMAN, A. 2007. In situ identification of genes regulated specifically in fibroblasts of human basal cell carcinoma. *J Invest Dermatol,* 127**,** 1516-23.

MITHOEFER, A. B., SUPRAN, S. & FREEMAN, R. B. 2002. Risk factors associated with the development of skin cancer after liver transplantation. *Liver Transplantation,* 8**,** 939-944.

MITSUNAGA, S. I., ZHANG, S. Y., RUGGERI, B. A., GIMENEZ-CONTI, I., ROBLES, A. I., CONTI, C. J. & KLEIN-SZANTO, A. J. P. 1995. Positive immunohistochemical staining of p53 and cyclin D in advanced mouse skin tumors, but not in precancerous lesions produced by benzo[a]pyrene. *Carcinogenesis,* 16**,** 1629-1635.

MORLEY, S. M., D'ALESSANDRO, M., SEXTON, C., RUGG, E. L., NAVSARIA, H., SHEMANKO, C. S., HUBER, M., HOHL, D., HEAGERTY, A. I., LEIGH, I. M. & LANE, E. B. 2003. Generation and characterization of epidermolysis bullosa simplex cell lines: scratch assays show faster migration with disruptive keratin mutations. *British Journal of Dermatology,* 149**,** 46-58.

MORRISON, S. J. & SPRADLING, A. C. 2008. Stem Cells and Niches: Mechanisms That Promote Stem Cell Maintenance throughout Life. *Cell,* 132**,** 598-611.

MUELLER, M. M. & FUSENIG, N. E. 2004. Friends or foes [mdash] bipolar effects of the tumour stroma in cancer. *Nat Rev Cancer,* 4**,** 839-849.

MURONE, M., ROSENTHAL, A. & DE SAUVAGE, F. J. 1999. Sonic hedgehog signaling by the Patched–Smoothened receptor complex. *Current Biology,* 9**,** 76-84.

NAKANO, Y., GUERRERO, I., HIDALGO, A., TAYLOR, A., WHITTLE, J. R. S. & INGHAM, P. W. 1989. A protein with several possible membrane-spanning domains encoded by the Drosophila segment polarity gene patched. *Nature,* 341**,** 508-513.

NARDELLA, C., CLOHESSY, J. G., ALIMONTI, A. & PANDOLFI, P. P. 2011. Pro-senescence therapy for cancer treatment. *Nat Rev Cancer,* 11**,** 503-511.

NIKOLOFF, D. M., MCGRAW, P. & HENRY, S. A. 1992. The INO2 gene of Saccharomyces cerevisiae encodes a helix-loop-helix protein that is required for activation of phospholipid synthesis. *Nucleic Acids Research,* 20**,** 3253.

NILSSON, M., UNDÈN, A. B., KRAUSE, D., MALMQWIST, U., RAZA, K., ZAPHIROPOULOS, P. G. & TOFTGÅRD, R. 2000a. Induction of basal cell carcinomas and trichoepitheliomas in mice overexpressing GLI-1. *Proceedings of the National Academy of Sciences,* 97**,** 3438-3443.

NILSSON, M., UNDÈN, A. B., KRAUSE, D., MALMQWIST, U., RAZA, K., ZAPHIROPOULOS, P. G. & TOFTGÅRD, R. 2000b. Induction of basal cell carcinomas and trichoepitheliomas in mice overexpressing GLI-1. *Proceedings of the National Academy of Sciences of the United States of America,* 97**,** 3438-3443.

NISHIZUKA, S., CHARBONEAU, L., YOUNG, L., MAJOR, S., REINHOLD, W. C., WALTHAM, M., KOUROS-MEHR, H., BUSSEY, K. J., LEE, J. K., ESPINA, V., MUNSON, P. J., PETRICOIN, E., LIOTTA, L. A. & WEINSTEIN, J. N. 2003. Proteomic profiling of the NCI-60 cancer cell lines using new high-density reverse-phase lysate microarrays. *Proceedings of the National Academy of Sciences,* 100**,** 14229-14234.

OHTANI, N., YAMAKOSHI, K., TAKAHASHI, A. & HARA, E. 2004. The p16^{INK4a}-RB pathway : molecular link between cellular senescence and tumor suppression. *The Journal of Medical Investigation,* 51**,** 146-153.

ORIMO, A., GUPTA, P. B., SGROI, D. C., ARENZANA-SEISDEDOS, F., DELAUNAY, T., NAEEM, R., CAREY, V. J., RICHARDSON, A. L. & WEINBERG, R. A. 2005. Stromal Fibroblasts Present in Invasive Human Breast Carcinomas Promote Tumor Growth and Angiogenesis through Elevated SDF-1/CXCL12 Secretion. *Cell,* 121**,** 335-348.

ORIMO, A. & WEINBERG, R. A. 2006. Stromal Fibroblasts in Cancer: A Novel Tumor-Promoting Cell Type. *Cell Cycle,* 5**,** 1597-1601.

ORLANDI, A., BIANCHI, L., COSTANZO, A., CAMPIONE, E., SPAGNOLI, L. G. & CHIMENTI, S. 2004. Evidence of Increased Apoptosis and Reduced Proliferation in Basal Cell Carcinomas Treated with Tazarotene. *J Investig Dermatol,* 122**,** 1037-1041.

ÖSTMAN, A. & AUGSTEN, M. 2009. Cancer-associated fibroblasts and tumor growth – bystanders turning into key players. *Current Opinion in Genetics & Development,* 19**,** 67-73.

OWENS, D. M. & WATT, F. M. 2003. Contribution of stem cells and differentiated cells to epidermal tumours. *Nat Rev Cancer,* 3**,** 444-451.

PAN, Y., BAI, C. B., JOYNER, A. L. & WANG, B. 2006. Sonic hedgehog Signaling Regulates Gli2 Transcriptional Activity by Suppressing Its Processing and Degradation. *Mol. Cell. Biol.,* 26**,** 3365-3377.

PANTAZI, E. 2010. *The role of GLI2 in human Basal Cell Carcinoma tumerogenesis.* PhD, Queen Mary University of London.

PARDUE, M.-L. & DEBARYSHE, G. 2001. Telomeres in Cell Function: Cancer and Ageing. *eLS.* John Wiley & Sons, Ltd.

PAZZAGLIA, S., MANCUSO, M., TANORI, M., ATKINSON, M. J., MEROLA, P., REBESSI, S., DI MAJO, V., COVELLI, V., HAHN, H. & SARAN, A. 2004. Modulation of Patched-Associated

Susceptibility to Radiation Induced Tumorigenesis by Genetic Background. *Cancer Research,* 64**,** 3798-3806.

PFISTER, H. & SCHEGGET, J. T. Role of HPV in cutaneous premalignant and malignant tumors. *Clinics in Dermatology,* 15**,** 335-347.

PIETRAS, K. & ÖSTMAN, A. 2010. Hallmarks of cancer: Interactions with the tumor stroma. *Experimental Cell Research,* 316**,** 1324-1331.

POTTEN, C. S. & BOOTH, C. 2002. Keratinocyte Stem Cells: a Commentary1. 119**,** 888-899.

PRESCOTT, J. C. & BLACKBURN, E. H. 1999. Telomerase: Dr Jekyll or Mr Hyde? *Current Opinion in Genetics & Development,* 9**,** 368-373.

PRIEUR, A. & PEEPER, D. S. 2008. Cellular senescence in vivo: a barrier to tumorigenesis. *Current Opinion in Cell Biology,* 20**,** 150-155.

PRIVES, C. & HALL, P. A. 1999. The P53 pathway. *Journal of Pathology,* 187**,** 112-126.

QIAN, Y. & CHEN, X. 2008. ID1, Inhibitor of Differentiation/DNA Binding, Is an Effector of the p53-dependent DNA Damage Response Pathway. *Journal of Biological Chemistry,* 283**,** 22410-22416.

QIAN, Y., JUNG, Y.-S. & CHEN, X. 2012. Differentiated embryo-chondrocyte expressed gene 1 regulates p53-dependent cell survival versus cell death through macrophage inhibitory cytokine-1. *Proceedings of the National Academy of Sciences,* 109**,** 11300-11305.

QIAN, Y., ZHANG, J., YAN, B. & CHEN, X. 2008. DEC1, a Basic Helix-Loop-Helix Transcription Factor and a Novel Target Gene of the p53 Family, Mediates p53-dependent Premature Senescence. *Journal of Biological Chemistry,* 283**,** 2896-2905.

RAHIMI, R. A. & LEOF, E. B. 2007. TGF-β signaling: A tale of two responses. *Journal of Cellular Biochemistry,* 102**,** 593-608.

RAHMAN, M. M. 2013. *Characterisation of a novel in vitro model of Basal cell carcinoma (BCC) through stable PTCH1 suppression in immortalised human keratinocytes.* PhD Thesis, Queen Mary University of London.

REGL, G., KASPER, M., SCHNIDAR, H., EICHBERGER, T., NEILL, G. W., PHILPOTT, M. P., ESTERBAUER, H., HAUSER-KRONBERGER, C., FRISCHAUF, A.-M. & ABERGER, F. 2004. Activation of the BCL2 Promoter in Response to Hedgehog/GLI Signal Transduction Is Predominantly Mediated by GLI2. *Cancer Research,* 64**,** 7724-7731.

REIFENBERGER, J., WOLTER, M., KNOBBE, C. B., KÖHLER, B., SCHÖNICKE, A., SCHARWÄCHTER, C., KUMAR, K., BLASCHKE, B., RUZICKA, T. & REIFENBERGER, G. 2005. Somatic mutations in the PTCH, SMOH, SUFUH and TP53 genes in sporadic basal cell carcinomas. *British Journal of Dermatology,* 152**,** 43-51.

RHEINWALD, J. G., HAHN, W. C., RAMSEY, M. R., WU, J. Y., GUO, Z., TSAO, H., DE LUCA, M., CATRICALÀ, C. & O'TOOLE, K. M. 2002. A Two-Stage, p16INK4A- and p53-Dependent Keratinocyte Senescence Mechanism That Limits Replicative Potential Independent of Telomere Status. *Molecular and Cellular Biology,* 22**,** 5157-5172.

RINN, J. L., BONDRE, C., GLADSTONE, H. B., BROWN, P. O. & CHANG, H. Y. 2006. Anatomic Demarcation by Positional Variation in Fibroblast Gene Expression Programs. *PLoS Genet,* 2**,** e119.

RIPPEY 1998. Why classify basal cell carcinomas? *Histopathology,* 32**,** 393-398.

ROHATGI, R., MILENKOVIC, L. & SCOTT, M. P. 2007a. Patched1 Regulates Hedgehog Signaling at the Primary Cilium. *Science,* 317**,** 372-376.

ROHATGI, R., MILENKOVIC, L. & SCOTT, M. P. 2007b. Patched1 regulates hedgehog signaling at the primary cilium. *Science,* 317**,** 372-6.

ROMAGOSA, R., SAAP, L., GIVENS, M., SALVARREY, A., HE, J. L., HSIA, S. L. & TAYLOR, J. R. 2000. A Pilot Study to Evaluate the Treatment of Basal Cell Carcinoma with 5-Fluorouracil Using Phosphatidyl Choline as a Transepidermal Carrier. *Dermatologic Surgery,* 26**,** 338-340.

RONINSON, I. B. 2002. Oncogenic functions of tumour suppressor p21Waf1/Cip1/Sdi1: association with cell senescence and tumour-promoting activities of stromal fibroblasts. *Cancer letters,* 179**,** 1-14.

RONINSON, I. B. 2003. Tumor Cell Senescence in Cancer Treatment. *Cancer Research,* 63**,** 2705-2715.

ROWE, D. E., CARROLL, R. J. & DAY, C. L. 1989a. LONG-TERM RECURRENCE RATES IN PREVIOUSLY UNTREATED (PRIMARY) BASAL-CELL CARCINOMA - IMPLICATIONS FOR PATIENT FOLLOW-UP. *Journal of Dermatologic Surgery and Oncology,* 15**,** 315-328.

ROWE, D. E., CARROLL, R. J. & DAY, C. L. 1989b. MOHS SURGERY IS THE TREATMENT OF CHOICE FOR RECURRENT (PREVIOUSLY TREATED) BASAL-CELL CARCINOMA. *Journal of Dermatologic Surgery and Oncology,* 15**,** 424-431.

ROZEN, S. & SKALETSKY, H. 1999. Primer3 on the WWW for General Users and for Biologist Programmers

Bioinformatics Methods and Protocols. *In:* MISENER, S. & KRAWETZ, S. A. (eds.). Humana Press.

RUAN, J.-W., LIAO, Y.-C., LUA, I., LI, M.-H., HSU, C.-Y. & CHEN, J.-H. 2012. Human pituitary tumor-transforming gene 1 overexpression reinforces oncogene-induced senescence through CXCR2/p21 signaling in breast cancer cells. *Breast Cancer Research,* 14**,** R106.

RUAS, M. & PETERS, G. 1998a. The p16INK4a/CDKN2A tumor suppressor and its relatives. *Biochimica et Biophysica Acta (BBA) - Reviews on Cancer,* 1378**,** F115-F177.

RUAS, M. & PETERS, G. 1998b. The p16INK4a/CDKN2A tumor suppressor and its relatives. *Biochimica et Biophysica Acta (BBA) - Reviews on Cancer,* 1378**,** 115-177.

RUBIN, A. I., CHEN, E. H. & RATNER, D. 2005. Basal-cell carcinoma. *The New England journal of medicine,* 353**,** 2262-9.

RUIZ I ALTABA, A., PALMA, V. & DAHMANE, N. 2002a. Hedgehog-GLI signaling and the growth of the brain. *Nat Rev Neurosci,* 3**,** 24-33.

RUIZ I ALTABA, A., SANCHEZ, P. & DAHMANE, N. 2002b. Gli and hedgehog in cancer: tumours, embryos and stem cells. *Nat Rev Cancer,* 2**,** 361-372.

RUIZ I ALTABA, A., SANCHEZ, P. & DAHMANE, N. 2002c. Gli and hedgehog in cancer: tumours, embryos and stem cells. *Nat Rev Cancer,* 2**,** 361-72.

RYAN, K. E. & CHIANG, C. 2012. Hedgehog Secretion and Signal Transduction in Vertebrates. *Journal of Biological Chemistry,* 287**,** 17905-17913.

SARAN, A. 2010. Basal cell carcinoma and the carcinogenic role of aberrant Hedgehog signaling. *Future Oncology,* 6**,** 1003-1014.

SARETZKI, G. 2010. Cellular senescence in the development and treatment of cancer. *Current pharmaceutical design,* 16**,** 79-100.

SCHAFFER, C. J. & NANNEY, L. B. 1996. Cell Biology of Wound Healing. *In:* KWANG, W. J. (ed.) *International Review of Cytology.* Academic Press.

SCHMITT, C. A. 2003. Senescence, apoptosis and therapy — cutting the lifelines of cancer. *Nat Rev Cancer,* 3**,** 286-295.

SERRANO, M. & BLASCO, M. A. A. 2001. Putting the stress on senescence. *Current Opinion in Cell Biology,* 13**,** 748-753.

SERRANO, M., LIN, A. W., MCCURRACH, M. E., BEACH, D. & LOWE, S. W. 1997. Oncogenic ras Provokes Premature Cell Senescence Associated with Accumulation of p53 and p16INK4a. *Cell,* 88**,** 593-602.

SEVERINO, J., ALLEN, R. G., BALIN, S., BALIN, A. & CRISTOFALO, V. J. 2000. Is β-Galactosidase Staining a Marker of Senescence in Vitro and in Vivo? *Experimental Cell Research,* 257**,** 162-171.

SHARPLESS, N. E. & DEPINHO, R. A. 1999a. The INK4A/ARF locus and its two gene products. *Current Opinion in Genetics & Development,* 9**,** 22-30.

SHARPLESS, N. E. & DEPINHO, R. A. 1999b. The INK4A/ARF locus and its two gene products. *Current Opinion in Genetics & Development,* 9**,** 22-30.

SHARPLESS, N. E. & DEPINHO, R. A. 2004. Telomeres, stem cells, senescence, and cancer. *The Journal of Clinical Investigation,* 113**,** 160-168.

SHAY, J. W. & WRIGHT, W. E. 2005. Senescence and immortalization: role of telomeres and telomerase. *Carcinogenesis,* 26**,** 867-874.

SHEKHAR, M. P. V., WERDELL, J., SANTNER, S. J., PAULEY, R. J. & TAIT, L. 2001. Breast Stroma Plays a Dominant Regulatory Role in Breast Epithelial Growth and Differentiation: Implications for Tumor Development and Progression. *Cancer Research,* 61**,** 1320-1326.

SHENG, H., GOICH, S., WANG, A., GRACHTCHOUK, M., LOWE, L., MO, R., LIN, K., DE SAUVAGE, F. J., SASAKI, H., HUI, C.-C. & DLUGOSZ, A. A. 2002. Dissecting the Oncogenic Potential of Gli2: Deletion of an NH2-Terminal Fragment Alters Skin Tumor Phenotype. *Cancer Research,* 62**,** 5308-5316.

SIGURDSSON, H. & AGNARSSON, B. A. 1998. Basal cell carcinoma of the eyelid. Risk of recurrence according to adequacy of surgical margins. *Acta Ophthalmologica Scandinavica,* 76**,** 477-480.

SIMPSON, F., KERR, M. C. & WICKING, C. 2009. Trafficking, development and hedgehog. *Mechanisms of development,* 126**,** 279-88.

SMITH, E. D., KUDLOW, B. A., FROCK, R. L. & KENNEDY, B. K. 2005. A-type nuclear lamins, progerias and other degenerative disorders. *Mechanisms of Ageing and Development,* 126**,** 447-460.

SNIJDERS, A. M., HUEY, B., CONNELLY, S. T., ROY, R., JORDAN, R. C., SCHMIDT, B. L. & ALBERTSON, D. G. 2009. Stromal control of oncogenic traits expressed in response to the overexpression of GLI2, a pleiotropic oncogene. *Oncogene,* 28**,** 625-37.

STEIN, G. H., DRULLINGER, L. F., SOULARD, A. & DULIĆ, V. 1999. Differential Roles for Cyclin-Dependent Kinase Inhibitors p21 and p16 in the Mechanisms of Senescence and Differentiation in Human Fibroblasts. *Molecular and Cellular Biology,* 19**,** 2109-2117.

STERN, R. S. & LANGE, R. 1988. NON-MELANOMA SKIN-CANCER OCCURRING IN PATIENTS TREATED WITH PUVA 5 TO 10 YEARS AFTER 1ST TREATMENT. *Journal of Investigative Dermatology,* 91**,** 120-124.

STONE, D. M., HYNES, M., ARMANINI, M., SWANSON, T. A., GU, Q., JOHNSON, R. L., SCOTT, M. P., PENNICA, D., GODDARD, A., PHILLIPS, H., NOLL, M., HOOPER, J. E., DE SAUVAGE, F. & ROSENTHAL, A. 1996. The tumour-suppressor gene patched encodes a candidate receptor for Sonic hedgehog. *Nature,* 384**,** 129-134.

STOREY A, BANKS L.1993. Human papillomavirus type 16 E6 gene cooperates with EJ-ras to immortalize primary mouse cells. *Oncogene*. 8(4):919-24.

SUZUKI, K., MORI, I., NAKAYAMA, Y., MIYAKODA, M., KODAMA, S. & WATANABE, M. 2001. Radiation-Induced Senescence-like Growth Arrest Requires TP53 Function but not Telomere Shortening. *Radiation Research,* 155**,** 248-253.

SVÄRD, J., HENRICSON, K. H., PERSSON-LEK, M., ROZELL, B., LAUTH, M., BERGSTRÖM, Å., ERICSON, J., TOFTGÅRD, R. & TEGLUND, S. 2006. Genetic Elimination of Suppressor of Fused Reveals an Essential Repressor Function in the Mammalian Hedgehog Signaling Pathway. *Developmental cell,* 10**,** 187-197.

SVENSSON, S., NILSSON, K., RINGBERG, A. & LANDBERG, G. 2003. Invade or Proliferate? Two Contrasting Events in Malignant Behavior Governed by p16INK4a and an Intact Rb Pathway Illustrated by a Model System of Basal Cell Carcinoma. *Cancer Research,* 63**,** 1737-1742.

TAIPALE, J. & BEACHY, P. A. 2001. The Hedgehog and Wnt signalling pathways in cancer. *Nature,* 411**,** 349-354.

TAKAHASHI, A. 2007. A Novel Mechanism of Irreversible Cell Cycle Arrest in Cellular Senescence. *Journal of Oral Biosciences,* 49**,** 47-53.

TAKAHASHI, A., OHTANI, N. & HARA, E. 2007. Irreversibility of cellular senescence: dual roles of p16INK4a/Rb-pathway in cell cycle control. *Cell Division,* 2**,** 10.

TOJO, M., KIYOSAWA, H., IWATSUKI, K., NAKAMURA, K. & KANEKO, F. 2003. Expression of the GLI2 oncogene and its isoforms in human basal cell carcinoma. *The British journal of dermatology,* 148**,** 892-7.

TOWERS, M. & TICKLE, C. 2009. Growing models of vertebrate limb development. *Development,* 136**,** 179-190.

TUMBAR, T., GUASCH, G., GRECO, V., BLANPAIN, C., LOWRY, W. E., RENDL, M. & FUCHS, E. 2004. Defining the Epithelial Stem Cell Niche in Skin. *Science,* 303**,** 359-363.

TURLEY, H., WYKOFF, C. C., TROUP, S., WATSON, P. H., GATTER, K. C. & HARRIS, A. L. 2004. The hypoxia-regulated transcription factor DEC1 (Stra13, SHARP-2) and its expression in human tissues and tumours. *The Journal of Pathology,* 203**,** 808-813.

UNDÉN, A. B., ZAPHIROPOULOS, P. G., BRUCE, K., TOFTGÅRD, R. & STÅHLE-BÄCKDAHL, M. 1997. Human patched (PTCH) mRNA Is Overexpressed Consistently in Tumor Cells of Both Familial and Sporadic Basal Cell Carcinoma. *Cancer Research,* 57**,** 2336-2340.

VALIN, A., BARNAY-VERDIER, S., ROBERT, T., RIPOCHE, H., BRELLIER, F., CHEVALLIER-LAGENTE, O., AVRIL, M. F. & MAGNALDO, T. 2009. PTCH1 +/- dermal fibroblasts isolated from healthy skin of Gorlin syndrome patients exhibit features of carcinoma associated fibroblasts. *PLoS One,* 4**,** e4818.

VAN DEN HEUVEL, M. & INGHAM, P. W. 1996. smoothened encodes a receptor-like serpentine protein required for hedgehog signalling. *Nature,* 382**,** 547-551.

VELCHETI, V. & GOVINDAN, R. 2007. Hedgehog Signaling Pathway and Lung Cancer. *Journal of Thoracic Oncology,* 2**,** 7-10 10.1097/JTO.0b013e31802c0276.

VENTURA, A., KIRSCH, D. G., MCLAUGHLIN, M. E., TUVESON, D. A., GRIMM, J., LINTAULT, L., NEWMAN, J., RECZEK, E. E., WEISSLEDER, R. & JACKS, T. 2007. Restoration of p53 function leads to tumour regression in vivo. *Nature,* 445**,** 661-665.

VERGEL, M., MARIN, J. J., ESTEVEZ, P. & CARNERO, A. 2011. Cellular Senescence as a Target in Cancer Control. *Journal of Aging Research,* 2011.

VILLARES, R. & CABRERA, C. V. 1987. The achaete-scute gene complex of D. melanogaster: Conserved Domains in a subset of genes required for neurogenesis and their homology to myc. *Cell,* 50**,** 415-424.

VILLONE, D., FRITSCH, A., KOCH, M., BRUCKNER-TUDERMAN, L., HANSEN, U. & BRUCKNER, P. 2008. Supramolecular interactions in the dermo-epidermal junction zone: anchoring

fibril-collagen VII tightly binds to banded collagen fibrils. *The Journal of biological chemistry,* 283**,** 24506-24513.

VITASA, B. C., TAYLOR, H. R., STRICKLAND, P. T., ROSENTHAL, F. S., WEST, S., ABBEY, H., NG, S. K., MUNOZ, B. & EMMETT, E. A. 1990. ASSOCIATION OF NONMELANOMA SKIN-CANCER AND ACTINIC KERATOSIS WITH CUMULATIVE SOLAR ULTRAVIOLET EXPOSURE IN MARYLAND WATERMEN. *Cancer,* 65**,** 2811-2817.

VOGELSTEIN, B., LANE, D. & LEVINE, A. J. 2000. Surfing the p53 network. *Nature,* 408**,** 307-310.

WAGNER, BRIEDIGKEIT & GOOS 1998. Homozygous deletion of the p16INK4a and the p15INK4b tumour suppressor genes in a subset of human sporadic cutaneous malignant melanoma. *British Journal of Dermatology,* 138**,** 13-21.

WALSH, P. C. 2005. Hedgehog Signalling in Prostate Regeneration, Neoplasia and Metastasis. *The Journal of Urology,* 173**,** 1169.

WALTER, K., OMURA, N., HONG, S. M., GRIFFITH, M., VINCENT, A., BORGES, M. & GOGGINS, M. 2010. Overexpression of smoothened activates the sonic hedgehog signaling pathway in pancreatic cancer-associated fibroblasts. *Clinical cancer research : an official journal of the American Association for Cancer Research,* 16**,** 1781-9.

WANG, B., FALLON, J. F. & BEACHY, P. A. 2000. Hedgehog-Regulated Processing of Gli3 Produces an Anterior/Posterior Repressor Gradient in the Developing Vertebrate Limb. *Cell,* 100**,** 423-434.

WATKINS, D. N., BERMAN, D. M. & BAYLIN, S. B. 2003. Hedgehog Signaling: Progenitor Phenotype in Small-Cell Lung Cancer. *Cell Cycle,* 2**,** 195-197.

WEEDON, M. N., LANGO, H., LINDGREN, C. M., WALLACE, C., EVANS, D. M., MANGINO, M., FREATHY, R. M., PERRY, J. R. B., STEVENS, S., HALL, A. S., SAMANI, N. J., SHIELDS, B., PROKOPENKO, I., FARRALL, M., DOMINICZAK, A., JOHNSON, T., BERGMANN, S., BECKMANN, J. S., VOLLENWEIDER, P., WATERWORTH, D. M., MOOSER, V., PALMER, C. N. A., MORRIS, A. D., OUWEHAND, W. H., CAULFIELD, M., MUNROE, P. B., HATTERSLEY, A. T., MCCARTHY, M. I. & FRAYLING, T. M. 2008. Genome-wide association analysis identifies 20 loci that influence adult height. *Nat Genet,* 40**,** 575-583.

WHITFIELD JAMES, F. & CHAKRAVARTHY, B. 2001. *Calcium: The Grand-Master Cell Signaler*, NRC Research Press.

WIDELITZ, R. B. 2008. Wnt signaling in skin organogenesis. *Organogenesis,* 4**,** 123-133.

WONG, C. S., STRANGE, R. C. & LEAR, J. T. 2003. Basal cell carcinoma. *BMJ,* 327**,** 794-8.

XIE, J., ASZTERBAUM, M., ZHANG, X., BONIFAS, J. M., ZACHARY, C., EPSTEIN, E. & MCCORMICK, F. 2001. A role of PDGFRα in basal cell carcinoma proliferation. *Proceedings of the National Academy of Sciences of the United States of America,* 98**,** 9255-9259.

XIE, J., MURONE, M., LUOH, S.-M., RYAN, A., GU, Q., ZHANG, C., BONIFAS, J. M., LAM, C.-W., HYNES, M., GODDARD, A., ROSENTHAL, A., JR, E. H. E. & DE SAUVAGE, F. J. 1998. Activating Smoothened mutations in sporadic basal-cell carcinoma. *Nature,* 391**,** 90-92.

XU, Q., MA, P., HU, C., CHEN, L., XUE, L., WANG, Z., LIU, M., ZHU, H., XU, N. & LU, N. 2012. Overexpression of the DEC1 Protein Induces Senescence In Vitro and Is Related to Better Survival in Esophageal Squamous Cell Carcinoma. *PLoS ONE,* 7**,** e41862.

YAMADA, K. & MIYAMOTO, K. 2005. Basic helix-loop-helix transcription factors, BHLHB2 and BHLHB3; Their gene expressions are regulated by multiple extracellular stimuli. *Frontiers in Bioscience-Landmark,* 10**,** 3151-3171.

YAMADA, M., KODAMA, K., FUJITA, S., AKAHOSHI, M., YAMADA, S., HIROSE, R. & HORI, M. 1996. Prevalence of skin neoplasms among the atomic bomb survivors. *Radiation Research,* 146**,** 223-226.

YANG, L., XIE, G., FAN, Q. & XIE, J. 2010. Activation of the hedgehog-signaling pathway in human cancer and the clinical implications. *Oncogene,* 29**,** 469-81.

YANG, N.-C. & HU, M.-L. 2004. A fluorimetric method using fluorescein di-β-d-galactopyranoside for quantifying the senescence-associated β-galactosidase activity in human foreskin fibroblast Hs68 cells. *Analytical Biochemistry,* 325**,** 337-343.

YAUCH, R. L., GOULD, S. E., SCALES, S. J., TANG, T., TIAN, H., AHN, C. P., MARSHALL, D., FU, L., JANUARIO, T., KALLOP, D., NANNINI-PEPE, M., KOTKOW, K., MARSTERS, J. C., RUBIN, L. L. & DE SAUVAGE, F. J. 2008. A paracrine requirement for hedgehog signalling in cancer. *Nature,* 455**,** 406-10.

YEGOROV, Y. E., AKIMOV, S. S., HASS, R., ZELENIN, A. V. & PRUDOVSKY, I. A. 1998. Endogenous beta-galactosidase activity in continuously nonproliferating cells. *Experimental Cell Research,* 243**,** 207-211.

YOO, Y. A., KANG, M. H., KIM, J. S. & OH, S. C. 2008. Sonic hedgehog signaling promotes motility and invasiveness of gastric cancer cells through TGF-beta-mediated activation of the ALK5-Smad 3 pathway. *Carcinogenesis,* 29**,** 480-90.

YOON, D. Y., BUCHLER, P., SAARIKOSKI, S. T., HINES, O. J., REBER, H. A. & HANKINSON, O. 2001. Identification of Genes Differentially Induced by Hypoxia in Pancreatic Cancer Cells. *Biochemical and Biophysical Research Communications,* 288**,** 882-886.

YOON, J. W., KITA, Y., FRANK, D. J., MAJEWSKI, R. R., KONICEK, B. A., NOBREGA, M. A., JACOB, H., WALTERHOUSE, D. & IANNACCONE, P. 2002. Gene Expression Profiling Leads to Identification of GLI1-binding Elements in Target Genes and a Role for Multiple Downstream Pathways in GLI1-induced Cell Transformation. *Journal of Biological Chemistry,* 277**,** 5548-5555.

YOUSSEF, K. K., VAN KEYMEULEN, A., LAPOUGE, G., BECK, B., MICHAUX, C., ACHOURI, Y., SOTIROPOULOU, P. A. & BLANPAIN, C. 2010. Identification of the cell lineage at the origin of basal cell carcinoma. *Nat Cell Biol,* 12**,** 299-305.

ZANETTI, R., ROSSO, S., MARTINEZ, C., NAVARRO, C., SCHRAUB, S., SANCHOGARNIER, H., FRANCESCHI, S., GAFA, L., PEREA, E., TORMO, M. J., LAURENT, R., SCHRAMECK, C., CRISTOFOLINI, M., TUMINO, R. & WECHSLER, J. 1996. The multicentre south European study 'Helios' .1. Skin characteristics and sunburns in basal cell and squamous cell carcinomas of the skin. *British Journal of Cancer,* 73**,** 1440-1446.

ZAWEL, L., YU, J., TORRANCE, C. J., MARKOWITZ, S., KINZLER, K. W., VOGELSTEIN, B. & ZHOU, S. 2002. DEC1 is a downstream target of TGF-β with sequence-specific transcriptional repressor activities. *Proceedings of the National Academy of Sciences of the United States of America,* 99**,** 2848-2853.

ZGLINICKI, T. V., SARETZKI, G., LADHOFF, J., FAGAGNA, F. D. A. D. & JACKSON, S. P. 2005. Human cell senescence as a DNA damage response. *Mechanisms of Ageing and Development,* 126**,** 111-117.

ZHANG, X. D., FRANCO, A. V., NGUYEN, T., GRAY, C. P. & HERSEY, P. 2000. Differential Localization and Regulation of Death and Decoy Receptors for TNF-Related Apoptosis-Inducing Ligand (TRAIL) in Human Melanoma Cells. *The Journal of Immunology,* 164**,** 3961-3970.

ZHANG, Z., ROSEN, D. G., YAO, J. L., HUANG, J. & LIU, J. 2006. Expression of p14ARF, p15INK4b, p16INK4a, and DCR2 increases during prostate cancer progression. *Mod Pathol,* 19**,** 1339-1343.

ZHANG, Z., YAO, R., LI, J., WANG, Y., BOONE, C. W., LUBET, R. A. & YOU, M. 2005. Induction of Invasive Mouse Skin Carcinomas in Transgenic Mice with Mutations in Both H-ras and p53. *Molecular Cancer Research,* 3**,** 563-574.

ZIEGLER, A., LEFFELL, D. J., KUNALA, S., SHARMA, H. W., GAILANI, M., SIMON, J. A., HALPERIN, A. J., BADEN, H. P., SHAPIRO, P. E. & BALE, A. E. 1993. Mutation hotspots due to sunlight in the p53 gene of nonmelanoma skin cancers. *Proceedings of the National Academy of Sciences of the United States of America,* 90**,** 4216-4220.

ZINDY, F., EISCHEN, C. M., RANDLE, D. H., KAMIJO, T., CLEVELAND, J. L., SHERR, C. J. & ROUSSEL, M. F. 1998. Myc signaling via the ARF tumor suppressor regulates p53-dependent apoptosis and immortalization. *Genes & Development,* 12**,** 2424-2433.

Appendix

Appendix 1

Details of Patients Demographics (Age and Sex)

Paraffin Tissues

Patients Number	Nodular BCC		Patient Number	Morphoeic BCC	
	Age	Sex		Age	Sex
1	54	M	1	75	M
2	69	M	2	69	M
3	37	M	3	58	F
4	75	F	4	54	M
5	81	F	5	60	F
6	52	M	6	52	M
7	54	F	7	84	F
8	59	F	8	59	F
9	82	F	9	59	F
10	68	F	10	68	F
11	91	M	11	91	M
12	56	M	12	56	M
13	51	F	13	59	F
14	49	M	14	49	M
15	76	F	15	30	F

Appendix 2

Details of Patients Demographics (Age and Sex). Frozen Tissues

Patient Number	Age	Sex	Type BCC
SM 120	54	M	Nodular
SL A01	69	F	Nodular
SW M68	37	M	Nodular
LA 107	75	M	Nodular
EL 652	81	F	Nodular
MA 4BT	52	M	Nodular
GJ 106	54	F	Nodular
BD 641	59	M	Nodular
JW 611	82	M	Nodular
JK 959	68	M	Nodular
WJ 140	91	F	Nodular / Micronodular
MJ 120	56	M	Micronodular
DF 572	51	F	Superficial
HP 115	49	M	Superficial
AC 636	76	F	Superficial
RF M75	75	M	Infiltrative
MN 108	69	F	Infiltrative
MJ F26	58	F	Infiltrative
JS 668	54	M	Morphoeic
JG 138	60	F	Morphoeic
NJ 646	52	F	Morphoeic

Appendix 3

The commercial kit contain the following reagents:-

- 10X Fixative Solution (15ml)
- X-Gal (150mg)
- 10X Staining Solution (15ml)
- 100X Staining Solution Supplement A (1.5ml)
- 100X Staining Solution Supplement B (1.5ml)

Appendix 4

Materials used for β-galactosidase staining made in our own laboratory.

Solution	Stock Concentration	Working Concentration	Volume (to make 10ml)
X-gal	20 mg/ml	1mg/ml	0.5ml
NaCl	5M	150mM	0.3ml
MgCl	1M	2mM	20µL
$K_3Fe(CN)_6$	100mM	5mM	0.5mL
$K_4Fe(CN)6$	100mM	5mM	0.5mL
NaPi pH6.0*	100mM	40mM	4mL
dH_2O			4.18mL

* **NaPi (pH6.0), 100mM, consists of;**

1M Disodium Hydrogen Phosphate (Na2HPO4) 12mL

1M Sodium Dihydrogen Phosphate (NaH2PO4) 88mL

Distilled water (dH_2O) 900mL

Glutaraldehyde 0.2% (v/v) 1ml in 125ml PBS

Appendix 5

KGM Media which is consists of :

AlphaMEM from BioWhittaker/Lonza

Penicillin/Streptomycin

10% Foetal bovine serum (FBS)

L-glutamine

KGM supplement which is made up of:

Adenine

Cholera toxin

Insulin

Hydrocortisone

Epidermal growth factor.

Appendix 6

Trypsin EDTA include;

Trypsin 0.5 mg/ml

EDTA (Titriplex III) 0.22 mg/ml

Solvent PBS, without Ca & Mg

Phosphate Buffer Saline (PBS)(Dulbecco's PBS (1x) PAA Laboratories GmbH)

Appendix 7

Components of qPCR Kit

Component	Volume(µl)
2X (SYBER Green PCR Master Mix)	10
50mM $MgCl_2$ (comes to a final conc. of 7mM in 20µl of total reaction)	1
Primers at 1µM (Forward and Reverse) (comes to final concentration of 100nM per 20 of total reaction)	2+2 (F+R)
Nuclease free water (NF-H_2O) (Ambion)	X (4)
cDNA (0.5µg/µl) (comes to a final of 25ng/µl)	1
X-refers to variable volume of NF-H_2O.	**Total = 20**

Appendix 8

DcR2 (Decoy Receptor)

DcR2 (Decoy Receptor)						
Nodular Basal Cell Carcinoma						
Patient Number	**Nuclear Staining**	**Cytoplasmic Staining**	**Epithelial Staining**	**Stromal Staining**	**Overall Staining**	**Normal Skin DcR2**
1048/2000A	2	2	2	1	1.5	1
1059/2009	2	2	1	2	2	0.5
1092/1999	3	3	1	3	3	0.5
1090/2000	3	3	2	3	3	0.5
1056/1998	2	2	2	2	2	0.5
1156/2009	2	2	1	2	2	0.5
1075/2007	0	2	1	1	1	0.5
1172/2008	0	0	0	0	0	
104/1999	2	2	1	2	2	
1022/1999	1	1	1	1	1	
1073/2007	2	2	2	1	1.5	
1019/2007	2	3	3	2	2	
1003/1999	3	2	1	3	3	
1123/2002	2	2.5	2	1	1.5	
1024/2007	2	3	3	2	2	
Morphoeic Basal Cell Carcinoma						
Patient Number	**Nuclear Staining**	**Cytoplasmic Staining**	**Epithelial Staining**	**Stromal Staining**	**Overall Staining**	
2103/2004	2	2	1	3	2.5	
761/1997	3	3	3	3	3	
118/2000	2	3	2	2	2	
406/1998	2	3	3	3	2.5	
2353/2006	3	3	2	3	3	
696/1997	2	3	2	2	2	
836/1997	2	3	2	2	2	
357/1998	3	3	1	3	3	
307/2001A	1	1	0	1	1	
49/2002	3	3	3	3	3	
391/1996A	2	3	1	3	2.5	
252/1999	3	2	1	3	3	
307/2001B	2	2	2	2	2	
306/2000	1	1	1	1	1	
637/1996	2	2	1	1	2.5	

DEC1 (Differentially Embryo-chondrocyte Expressed Gene)

DEC1 (Differentially Embryo-chondrocyte Expressed Gene)						
Nodular Basal Cell Carcinoma						
Patient Number	**Nuclear Staining**	**Cytoplasmic Staining**	**Epithelial Staining**	**Stromal Staining**	**Overall Staining**	**Normal Skin DEC1**
1048/2000A	2	2	1.5	1	2.5	1.5
1059/2009	3	3	2	3	3	1.5
1092/1999	2	2	1.5	1	1.5	0.5
1090/2000	2	2	1	2	2	1
1056/1998	2	2	1	1	1.5	0.5
1156/2009	0.5	3	2	0.5	0.5	0.5
1075/2007	3	2	2	2	2.5	0.5
1172/2008	3	3	2	3	3	
104/1999	0.5	1	1	0.5	0.5	
1022/1999	2	2	1	2	2	
1073/2007	2	2	1.5	2	2	
1019/2007	3	2	2	3	3	
1003/1999	3	3	1	3	3	
1123/2002	3	3	2	1	2	
1024/2007	3	3	2	3	3	
Morphoeic Basal Cell Carcinoma						
Patient Number	**Nuclear Staining**	**Cytoplasmic Staining**	**Epithelial Staining**	**Stromal Staining**	**Overall Staining**	
2103/2004	2	2	1	2	2	
761/1997	3	3	2	3	3	
118/2000	3	3	2	3	3	
406/1998	2	3	2.5	2	2	
2353/2006	1	1	2	1	1	
696/1997	2	2	1.5	2	2	
836/1997	1	1	0.5	1	1	
357/1998	3	3	0	3	3	
307/2001A	0	0	0	0	0	
49/2002	3	3	2	3	3	
391/1996A	3	3	2	3	3	
252/1999	2	2	2	2	2	
307/2001B	3	2	1	3	3	
306/2000	2	1	1	2	2	
637/1996	2	2	1.5	2	2	

p53

p53						
Nodular Basal Cell Carcinoma						
Patient Number	**Nuclear Staining**	**Cytoplasmic Staining**	**Epithelial Staining**	**Stromal Staining**	**Overall Staining**	**Normal Skin p53**
1048/2000A	1	0	1	0	1	0
1059/2009	3	0	1	0	3	0
1092/1999	3	1	0	0	3	0
1090/2000	1	0	1	0	1	0
1056/1998	0	0	1	0	0.5	0
1156/2009	0	0	0	0	0	0
1075/2007	1	0	0.5	0	0.5	0
1172/2008	1	1	1	0	1	
104/1999	1	1	0	0	1	
1022/1999	0	0	0	0	0	
1073/2007	3	0	1	0	3	
1019/2007	1	0	0	0	0.5	
1003/1999	1	1	0	0	1	
1123/2002	0.5	0	0	0	0.5	
1024/2007	1	0	0	1	1	
Morphoeic Basal Cell Carcinoma						
Patient Number	**Nuclear Staining**	**Cytoplasmic Staining**	**Epithelial Staining**	**Stromal Staining**	**Overall Staining**	
2103/2004	1	0	1	0	1	
761/1997	1	0	1	0	1	
118/2000	2	0	0	0	2	
406/1998	2	0	0	0	2	
2353/2006	0	0	0	0	0	
696/1997	1	0	0	0	1	
836/1997	2	0	0	0	2	
357/1998	3	0	2	0.5	3	
307/2001A	2	1	0	0	2	
49/2002	1	0	1	0	1	
391/1996A	2	0	0	0	2	
252/1999	0	0	0	0	0	
307/2001B	2	0	1	0	2	
306/2000	1	1	0	0	1	
637/1996	3	0	1	0	3	

p16^{INK4a}

p16^{INK4a}						
Nodular Basal Cell Carcinoma						
Patient Number	**Nuclear Staining**	**Cytoplasmic Staining**	**Epithelial Staining**	**Stromal Staining**	**Overall Staining**	**Normal Skin p16^{INK4a}**
1048/2000A	2	1.5	1	1	1.5	1.5
1059/2009	3	2	1.5	2	2.5	0.5
1092/1999	2	2	1	2	2	0.5
1090/2000	2	2	2	2	2	0.5
1056/1998	2	2	1	2	2	0.5
1156/2009	2	3	0.5	1	2	0.5
1075/2007	2	3	2	2	2	1
1172/2008	2	0	0	3	2.5	
104/1999	2	2	0.5	2	2	
1022/1999	1	0.5	0.5	1	1	
1073/2007	1	2	2	1	1	
1019/2007	2	2	2	2	2	
1003/1999	3	3	1	2	2.5	
1123/2002	2	2	1.5	2	2	
1024/2007	3	2	1.5	3	3	
Morphoeic Basal Cell Carcinoma						
Patient Number	**Nuclear Staining**	**Cytoplasmic Staining**	**Epithelial Staining**	**Stromal Staining**	**Overall Staining**	
2103/2004	3	2	1	2	2.5	
761/1997	3	3	1	3	3	
118/2000	1	2.5	1.5	2	1.5	
406/1998	3	2	3	3	3	
2353/2006	3	2	1.5	2	2.5	
696/1997	2	2	1.5	2	2	
836/1997	2	2	2	2	2	
357/1998	1	2.5	0	1	1	
307/2001A	2	0	0	2	2	
49/2002	1	2	2	1	1	
391/1996A	1	2	1	1	1	
252/1999	0	3	0.5	0	0	
307/2001B	2	2	1.5	2	2	
306/2000	2	1	1.5	2	2	
637/1996	2	1	1	2	2	

p15^{INK4b}

p15^{INK4b}						
Nodular Basal Cell Carcinoma						
Patient Number	**Nuclear Staining**	**Cytoplasmic Staining**	**Epithelial Staining**	**Stromal Staining**	**Overall Staining**	**Normal Skin p15^{INK4b}**
1048/2000A	3	2	2	2	2.5	1.5
1059/2009	3	2	1.5	2	2.5	1.5
1092/1999	2	1.5	1.5	3	2.5	1
1090/2000	3	2	2	3	3	1
1056/1998	2	2	1	3	2.5	1.5
1156/2009	1	1	1	2	1.5	1.5
1075/2007	2	2	1.5	3	2.5	1
1172/2008	1	2	1	2	1.5	
104/1999	1	2	2	2	1.5	
1022/1999	0	1	2	2	1	
1073/2007	2	2	0	2	2	
1019/2007	0	1.5	1.5	3	2	
1003/1999	2	2	1	2	2	
1123/2002	1	1.5	1.5	2	1.5	
1024/2007	1	1.5	1.5	1	1	
Morphoeic Basal Cell Carcinoma						
Patient Number	**Nuclear Staining**	**Cytoplasmic Staining**	**Epithelial Staining**	**Stromal Staining**	**Overall Staining**	
2103/2004	3	2	2.5	3	3	
761/1997	3	2	1	3	3	
118/2000	3	2	1.5	3	3	
406/1998	3	2	2	3	3	
2353/2006	3	2	2	2	2.5	
696/1997	1	1.5	1	1	1	
836/1997	2	1	2	2	2	
357/1998	1	2	1	2	1.5	
307/2001A	1	1	1	2	1.5	
49/2002	3	2	2	1	2	
391/1996A	2	3	1	3	2.5	
252/1999	1	2	2	1	1	
307/2001B	2	2	2	3	2.5	
306/2000	3	2	2	3	3	
637/1996	2	2	1.5	2	2	

GLI-1

GLI-1					
Nodular Basal Cell Carcinoma					
Patient Number	**Nuclear Staining**	**Cytoplasmic Staining**	**Epithelial Staining**	**Stromal Staining**	**Overall Staining**
1048/2000A	2	1	0	0	2
1059/2009	2	2	1	1	2
1092/1999	2	1	1	1	2
1090/2000	1	0	1	1	1
1056/1998	3	3	1	0	2
1156/2009	2	1	1	1	1.5
1075/2007	0.5	1	0	0.5	1
1172/2008	3	2	1	1	2
104/1999	2	1	0.5	0	1.5
1022/1999	3	3	2	2	2.5
1073/2007	3	3	2	1	2.5
1019/2007	2	1	1	0	1
1003/1999	2	1	1	1	1.5
1123/2002	0.5	0.5	1	0	0.5
1024/2007	2	1	2	0.5	2
Morphoeic Basal Cell Carcinoma					
Patient Number	**Nuclear Staining**	**Cytoplasmic Staining**	**Epithelial Staining**	**Stromal Staining**	**Overall Staining**
2103/2004	1	1	1	0	1
761/1997	3	2	0.5	0.5	2
118/2000	2	1	0.5	0.5	1
406/1998	3	3	3	1	2.5
2353/2006	1	1	0	0	0.5
696/1997	1	0	0	0.5	0.5
836/1997	2	2	0.5	1	1.5
357/1998	2	1	0	0.5	1
307/2001A	2	2	2	2	2
49/2002	2	2	2	2	2
391/1996A	1	0.5	1	1	1
252/1999	3	3	1	0.5	2
307/2001B	2	1	0.5	0.5	1
306/2000	2	3	1	2	2.5
637/1996	0.5	1	0	1	1